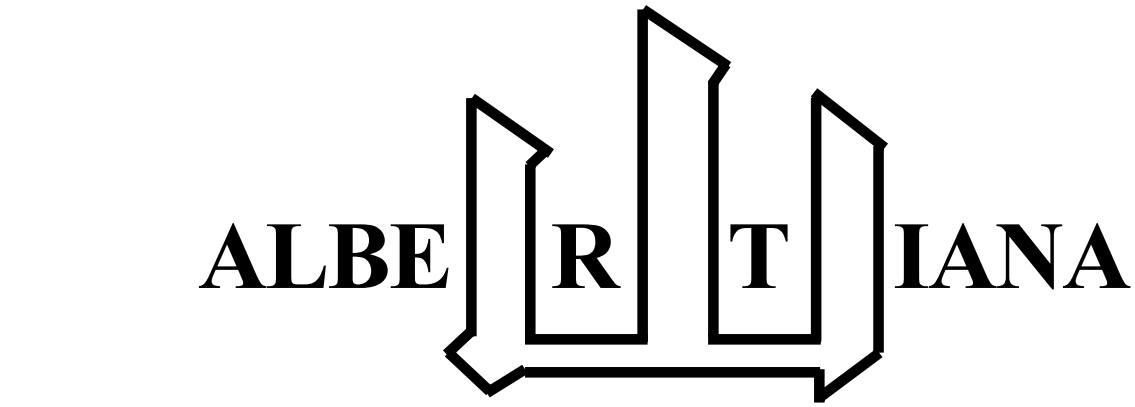

Part I: Program and Abstracts

33

May 2005
ISSN 0619-4324

Contents

The primary aim of ALBERTIANA is to promote the interdisciplinary collaboration and understanding among members of the I.U.G.S. Subcommission on Triassic stratigraphy. Within this scope ALBERTIANA serves as the newsletter for the announcement of general information and as a platform for discussion of developments in the field of Triassic stratigraphy. ALBERTIANA thus encourages the publication of anouncements, literature reviews, progress reports, preliminary notes etc. - i. e. those contributions in which information is presented relevant to current interdisciplinary Triassic research. An electronic version of ALBERTIANA is also available in PDF format at the

ALBERTIANA website

at http://www.bio.uu.nl/~palaeo/Albertiana/Albertiana01.htm.

Editor
Dr. Wolfram M. Kürschner, Palaeoecology, Laboratory of Palaeobotany and Palynology, Utrecht University, Budapestlaan 4, 3584 CD Utrecht, The Netherlands, w.m.kuerschner@bio.uu.nl;

Editorial Commitee
Dr. Aymon Baud, Musee de Geologie, BFSH2-UNIL, 1015 Lausanne, Switzerland, aymon.baud@sst.unil.ch;
Prof. Dr. Hans Kerp, WWU, Abt. Palaeobotanik, Hindenburgplatz 57, 48143 Münster, Germany, kerp@uni-muenster.de;
Dr. Spencer G. Lucas, New Mexico Museum of Natural History, 1801 Mountain Road N. W., Albuquerque, NM 87104, USA, slucas@nmmnh.state.nm.us;
Dr. Mike Orchard, Geological Survey of Canada, 101-605 Robson Street, Vancouver, British Columbia, V6B 5J3, Canada, morchard@nrcan.gc.ca;
Dr. E. T. Tozer, Geological Survey of Canada, 101-605 Robson Street, Vancouver, British Columbia, V6B 5J3, Canada, etozer@nrcan.gc.ca;
Prof. Dr. Henk Visscher, Palaeoecology, Laboratory of Palaeobotany and Palynology, Utrecht University, Budapestlaan 4, 3584 CD Utrecht, The Netherlands, h.visscher@bio.uu.nl.

Program

International Symposium on Triassic Chronostratigraphy and Biotic Recovery
Chaohu, China 23-25th of May 2005

ORGANIZERS

China University of Geosciences
Office of Land and Resources, Anhui Province
Government of Chaohu City, Anhui Province

CO-SPONSORS

China University of Geosciences
ICS Subcommission on Permian Stratigraphy
ICS Subcommission on Triassic Stratigraphy
IGCP-467 (Triassic Time and trans-Panthalassan Correlation)
National Commission of Stratigraphy of China
National Natural Science Foundation of China
NSF-CHRONOS Project
Task Group on Induan-Olenekian Boundary

ORGANIZING COMMITTEE

Chairman:

Orchard, Mike: Chairman of Subcommission on Triassic Stratigraphy, leader of IGCP-467

Vice-chairmen:

Zakharov, Yuri: Leader of Induan-Olenekian Task Force, Vice-Chairman of Subcommission on Triassic Stratigraphy
Yin, Hongfu: Vice-chairman of Subcommission on Triassic Stratigraphy, Vice-Chairman of China National Stratigraphic Commission

Members:

Henderson, Charles: Chairman of Subcommission on Permian Stratigraphy
Lane, Richard: Vice-Chairman of International Commission on Stratigraphy
Ma, Fuchen: Vice-Chairman of National Natural Science Foundation of China
Ogg, Jimes: Secretary General of International Commission on Stratigraphy
Song, Guoquan: Vice-President of Chaohu City, Anhui Province
Yang, Xianjing: Vice-Director of Land and Resources Office of Anhui Province
Wardlaw, Bruce: Co-leader of the CHRONOS Project, NSF

Secretariat:

Tong Jinnan (Correspondence): Professor of China University of Geosciences (Wuhan)
Xia Yan: Director of Land and Resources Office of Anhui Province
Wen Xianhong: Vice-Director of Land and Resources Bureau of Chaohu City

VENUES

Most activities of the symposium will take place at the Tang Shan Hotel in Chaohu City, Anhui Province.

The **Symposium Desk** is in the Hall of the Main Building at the Tang Shan Hotel at 9:00-21:00 on 22 May and 8:00-12:00 and 14:00-18:00 on 23-25 May. It is in Room 2108 of the Main Building at the other time.

The **Main Conference Room**, where the Plenary Session is arranged, is on the third floor in the Main Building at the Tang Shan Hotel.

Conference Room A and **Conference Room B**, where the scientific sessions and workshops will happen, are on the second floor in the Main Building at the Tang Shan Hotel.

The **Ballroom**, where the Poster Displays are shown, is on the second floor in the Main Building at the Tang Shan Hotel.

The **Dining Room**, where meals are provided, is on the first floor in the Main Building at the Tang Shan Hotel.

REGISTRATION

The registration is in the Hall of the Main Building at the Tang Shan Hotel from 9:00 to 21:00 on 22 May. Those who come late register at the symposium desk. After your registration, you will get a symposium bag with all symposium materials and a paper listing all of your data.

ARRIVAL AND DEPARTURE

We will try our best to meet and see you off at the railway stations and airports. Please tell the symposium desk about your return schedule when you register. Those who haven't booked return tickets can ask for help there as well.

ICEBREAKER PARTY AND PRE-SYMPOSIUM RECEPTION

The get-together "Icebreaker Party" will be held in the yard of the Tang Shan Hotel on 22 May, starting at 18:00 h. There will be a buffet with beverages and food.

ADVICE TO SPEAKERS

20 minutes will be allowed for each oral presentation and 30 minutes for keynote address, plus 5 minutes for questions and discussions. One computer projector and one overhead projector will be available in each conference room. Speakers are advised to copy your PPT file(s) onto the conference computers at the symposium desk one day before your talk.

POSTERS

Posters will be presented on two A0 page size panels in the Ballroom on the second floor of the Main Building at the Tang Shan Hotel. Authors are urged to mount their poster displays to the panels during the registration on 22 May and encouraged to stay at their posters at 17:00-18:00 on 23-24 May.

MEALS

Buffet is provided in the Dining Room on the first floor in the Main Building at the Tang Shan Hotel. The breakfast is included in your accommodation fees if you stay at the Tang Shan Hotel but the lunch and dinner are at your own expense.

CITY TOUR AND SHOPPING

The Tang Shan Hotel is in the east of the Chaohu City and 6 km from the downtown. If you want to visit the downtown and do shopping, tell the symposium desk. We will arrange you a car and have some volunteer students to bring you there. You can also take a taxi and it is about RMB 10 yuan from the Tang Shan Hotel to the downtown.

GENERAL PROGRAM

21-22 May 2005 (Saturday-Sunday)

Pre-Symposium Field Excursion from Changxing to Nanjing

22 May 2005 (Sunday)

9:00-21:00: Registration at the Tang Shan Hotel

18:00-21:00: Icebreaker and Reception in the yard of the Tang Shan Hotel

23 May 2005 (Monday)

8:30-12:00: Opening Ceremony and Plenary Session 1 in Main Conference Room

12:00-13:00: Lunch in Dining Room
14:00-17:00: Plenary Sessions 2 and 3 in Main Conference Room
17:00-18:00: Poster Displays in Ballroom
18:00-19:00: Dinner in Dining Room
19:30-21:30: STS and IGCP-467 workshops in Conference Room A

24 May 2005 (Tuesday)

8:00-12:00: Mid-Symposium Field Excursion in Chaohu, Anhui Province
12:00-13:00: Lunch in Dining Room
14:00-17:00: Sessions A1 and A2 in Conference Room A
14:00-17:00: Sessions B1 and B2 in Conference Room B
17:00-18:00: Poster Displays in Ballroom
18:00-19:00: Dinner in Dining Room
19:30-21:30: IOBWG workshop in Conference Room A
19:30-21:30: SPS workshop in Conference Room B

25 May 2005 (Wednesday)

8:00-12:00: Sessions A3 and A4 in Conference Room A
8:00-12:00: Sessions B3 and B4 in Conference Room B
12:00-13:00: Lunch in Dining Room
14:00-17:20: Plenary Sessions 4 and 5 in Main Conference Room
17:30-18:00: Close Remarks in Main Conference Room
18:00-19:00: Dinner in Dining Room
19:30-21:30: CHRONOS workshop in Conference Room A

26-30 May 2005 (Thursday-Monday)

Post-Symposium Field Excursion 1 in Central and Western Guizhou

26-29 May 2005 (Thursday-Sunday)

Post-Symposium Field Excursion 2 in Southern Guizhou

26 May-1 June 2005 (Thursday-Wednesday)

Post-Symposium Field Excursion 3 in Guizhou

Scientific Program

23 May 2005 (Monday)

Opening Ceremony in Main Conference Room
Chairperson: Yin Hongfu

8:30-9:20 *Opening Speeches*
9:20-9:40 *Group photo in the yard of the Tang Shan Hotel*

9:40-10:00 *Morning Tea*

Plenary Session 1 in Main Conference Room
Chairperson: Jim Ogg

10:00-10:35 **Hongfu Yin** (keynote)
A VIEW ON THE LATE PERMIAN-EARLY TRIASSIC REVOLUTION

10:35-11:10 **Bruce R. Wardlaw**, Vladimir I. Davydov and Peter Sadler (keynote)
THE PERMIAN-TRIASSIC TIME SLICE PROJECT OF CHRONOS: A PROGRESS REPORT

11:10-11:35 **Aymon Baud**, Sylvain Richoz and Sara Pruss
THE LOWER TRIASSIC ANACHRONISTIC CARBONATE FACIES IN SPACE AND TIME

11:35-12:00 **Manfred Menning** and M. Szurlies
ORBITAL TUNING OF THE INDUSIAN AND OLENEKIAN STAGES USING SEDIMENTARY CYCLES OF THE GERMANIC TRIAS

Plenary Session 2 in Main Conference Room
Chairpersons: Yuri Zakharov

14:00-14:35 **Mike Orchard** (keynote)
ON THE EXPLOSIVE RADIATION OF LOWER TRIASSIC CONODONTS: A NEW MULTIELEMENT PERSPECTIVE

14:35-15:00 **Charles Henderson**
CORRELATION OF THE PROPOSED BASE-OLENEKIAN GSSP FROM CHAOHU, CHINA TO WESTERN CANADA

15:00-15:25 **Leopold Krystyn**, Om N. Bhargava and Devendra K. Bhatt
MUTH (SPITI, INDIAN HIMALAYA) – A CANDIDATE GLOBAL STRATIGRAPHIC SECTION AND POINT (GSSP) FOR THE BASE OF THE OLENEKIAN STAGE

15:25-15:35 *Afternoon Tea*

Plenary Session 3 in Main Conference Room
Chairperson: Leopold Krystyn

15:35-16:00 **Yuri D. Zakharov**, Alexander M. Popov and Galina I. Buryi
UNIQUE MARINE OLENEKIAN-ANISIAN BOUNDARY SECTION FROM SOUTH PRIMORYE, RUSSIAN FAR EAST

16:00-16:25 **Zhao Laishi**, Mike Orchard and Tong Jinnan
CONODONT SEQUENCES AND ITS GLOBAL CORRELATION OF THE INDUAN-OLENEKIAN BOUNDARY IN WEST PINGDINGSHAN SECTION, CHAOHU, ANHUI PROVINCE

16:25-17:00 **Tong Jinnan**
LOWER TRIASSIC STRATIGRAPHICAL SEQUENCE IN CHAOHU, ANHUI PROVINCE

17:00-18:00 *Poster Displays in Dining Room*

24 May 2005 (Tuesday)

Session A1 in Conference Room A
Chairperson: Charles Henderson

14:00-14:35 **Christopher A. McRoberts** (keynote)
EXTINCTION AND SURVIVAL OF PERMIAN TO EARLY TRIASSIC MARINE MYALINIDAE (BIVALVIA: PTERIOIDA)

14:35-15:00 **Shen Shuzhong**, Cao Changqun, Henderson Charles M., Wang Xiangdong, Shi, G. R. Wang Wei, Wang Yue
END-PERMIAN MASS EXTINCTION PATTERN IN THE NORTHERN PERI-GONDWANAN REGION

15:00-15:25 **Wang Wei**
ISOTOPIC CHEMOSTRATIGRAPHY OF PTB IN SOUTH CHINA

15:25-15:35 *Afternoon Tea*

Session A2 in Conference Room A
Chairperson: Sheng Shuzhong

15:35-16:10 **Ian Metcalfe**, R. S. Nicoll and Wang Xiaofeng (keynote)
1. CHRONOSTRATIGRAPHIC AND BIOSTRATIGRAPHIC CONTROL ON THE PERMIAN-TRIASSIC BOUNDARY IN THE ZHONGZHAI SECTION, GUIZHOU PROVINCE, SOUTHWEST CHINA
2. AGE CONSTRAINTS ON THE *NEOSPATHODUS TRIANGULARIS* ZONE, UPPER SPATHIAN (TRIASSIC), IN THE DALISHAN SECTION, JIANGSU PROVINCE, CHINA

16:10-16:35 **Wang Yue**, Shen Shuzhong, Cao Changqun, Wang Wei, Charles Henderson, Jin Yugan
THE WUCHIAPINGIAN-CHANGHSINGIAN BOUNDARY (UPPER PERMIAN) AT MEISHAN OF CHANGXING COUNTY, SOUTH CHINA

16:35-17:00 **Vladimir I. Davydov** and Bruce Wardlaw
PROGRESS ON THE CISURALIAN (LOWER PERMIAN) TIME-SCALE, SOUTHERN URALS, RUSSIA

Session B1 in Conference Room B
Chairperson: John Marzolf

14:00-14:35 **Michael A. Shishkin** (keynote)
THE PATTERNS OF RECOVERY OF TETRAPOD COMMUNITIES IN THE EARLY TRIASSIC OF EUROPE AND SOUTHERN GONDWANA: A COMPARISON AND IMPLICATIONS

14:35-15:00 **Lars Schmitz**, Jiang Dayong, Ryosuke Motani, Hao Weicheng, Sun Yuanlin
EARLY RADIATION AND GEOGRAPHIC DISPERSAL OF ICHTHYOPTERYGIANS (REPTILIA, DIAPSIDA)

15:00-15:25 Jiang Dayong, **Ryosuke Motani**, Lars Schmitz, Hao Weicheng and Sun Yuanlin
EXPLOSIVE RADIATION OF SHELL-EATING MARINE REPTILES DURING THE POST-PERMIAN RECOVERY

15:25-15:35 *Afternoon Tea*

Session B2 in Conference Room B
Chairperson: Yukio Isozaki

15:35-16:10 **Richard J. Twitchett** (keynote)
THE LILLIPUT EFFECT IN THE AFTERMATH OF THE END-PERMIAN EXTINCTION EVENT

16:10-16:35 **Wang Yongbiao**, Tong Jinnan, Wang Jiasheng and Zhou Xiugao
CALCIMICROBIALITE AFTER END-PERMIAN MASS EXTINCTION IN SOUTH CHINA

16:35-17:00 **Oliver Weidlich**

PTB MASS EXTINCTION AND EARLIEST TRIASSIC RECOVERY OVERLOOKED? A REINTERPRETATION OF EARLIEST TRIASSIC MICROBIAL CARBONATES OF THE CENTRAL EUROPEAN BASIN (GERMANY)

17:00-18:00 *Poster Displays in Dining Room*

25 May 2005 (Wednesday)

Session A3 in Conference Room A
Chairperson: Yao Jiangxin

8:00-8:25 **Adam D. Woods**, David J. Bottjer and Frank A. Corsetti
LOWER TRIASSIC SEAFLOOR PRECIPITATES FROM EAST-CENTRAL CALIFORNIA: SEDIMENTOLOGY AND PALEOBIOLOGICAL SIGNIFICANCE

8:25-8:50 **Margaret L. Fraiser** and David J. Bottjer
THE LATEST PERMIAN-EARLY TRIASSIC BIOCALCIFICATION CRISIS

8:50-9:15 **Yan Jiaxin**
CHEMICAL COMPOSITION OF SEAWATER AND BIOTIC CRISIS AROUND THE PALEOZOIC – MESOZOIC TRANSITION (PMT)

9:15-9:40 **Thomas J. Algeo** and Brooks Ellwood
PRELIMINARY GEOCHEMICAL ANALYSIS OF THE CAO BANG PERMIAN-TRIASSIC BOUNDARY SECTION IN NORTHEASTERN VIETNAM

9:40-10:05 **Pedro J. Marenco**, Frank A. Corsetti, David J. Bottjer, Aymon Baud, Alan Jay Kaufman
SULFUR ISOTOPIC ANOMALIES ACROSS THE PERMO-TRIASSIC BOUNDARY AND THROUGH THE EARLY TRIASSIC

10:05-10:20 *Morning Tea*

Session A4 in Conference Room A
Chairperson: Manfred Menning

10:20-10:45 **John E. Marzolf**
THE TRIASSIC OF THE SOUTHWESTERN UNITED STATES AND NORTH-WESTERN MEXICO: AGE CONSTRAINTS ON SEQUENCE BOUNDARIES OF CORRELATIVE NON-MARINE AND MARINE SEQUENCES

10:45-11:10 **Yao Jianxin**, Ji Zhansheng, Wang Yanbin, Liu Dunyi, Wang Liting, Wu Guichun
RESEARCH ON CONODONT BIOSTRATIGRAPHY AND AGE DETERMINATION OF THE LOWER-MIDDLE TRIASSIC BOUNDARY IN SOUTHERN PART OF GUIZHOU PROVINCE, CHINA

11:10-1135 **U. Kagan Tekin**
NEW EARLY TO MIDDLE NORIAN RADIOLARIAN TAXA FROM ALAKIRCAY NAPPE OF ANTALYA NAPPES, ANTALYA, SW TURKEY

11:35-12:00 **Michaela Bernecker**
CARNIAN TO RHAETIAN ISOLATED PLATFORM AND REEF DEVELOPMENT IN THE NEO-TETHYS (OMAN)

Session B3 in Conference Room B
Chairperson: Robert Nicoll

8:00-8:25 **Chen Zhongqiang**
EXTINCTION-SURVIVAL-RECOVERY OF BRACHIOPOD FAUNAS DURING THE PERMIAN-TRIASSIC TRANSITION

8:25-8:50 **Tyler W. Beatty**, John-Paul Zonneveld and Charles M. Henderson
LATE PERMIAN AND EARLY TRIASSIC ICHNOFOSSIL ASSEMBLAGES FROM THE NORTHWEST MARGIN OF PANGEA

8:50-9:15 **He Weihong**

BRACHIOPOD MINIATURIZATION IN THE PERMIAN-TRIASSIC LIFE CRISIS IN SOUTH CHINA

9:15-9:40 **Demir Altiner**, John R. Groves, Sevinç Özkan-Altiner
CALCAREOUS FORAMINIFERAL RECOVERY FROM THE END-PERMIAN MASS EXTINCTION, SOUTHERN TURKEY

9:40-10:05 **Wu Yasheng**
CONODONT EVOLUTION DURING PERMIAN-TRIASSIC TRANSITION IN MID-LOW LATITUDES: A CLOSE-UP VIEW

10:05-10:20 *Morning Tea*

Session B4 in Conference Room B
Chairperson: Oliver Weidlich

10:20-10:45 **Tea Kolar-Jurkovsek** and Bogdan Jurkovsek
ISARCICELLA POPULATION IN THE LOWERMOST TRIASSIC OF SLOVENIA

10:45-11:10 **Robert S. Nicoll** and Ian Metcalfe
EARLY TRIASSIC CONODONTS OF THE GENUS *ISARCICELLA*

11:10-1135 **Ji Zhansheng**, Yao Jianxin, Yukio Isuzaki, Tetsuo Matsuda, Wu Guichun
CONODONT BIOSTRATIGRAPHY ACROSS THE PERMIAN-TRIASSIC BOUNDARY AT CHAOTIAN SECTION, NORTHERN SICHUAN, CHINA

11:35-12:00 **Valery Ja. Vuks**
OLENEKIAN FORAMINIFERS OF THE GORNY MANGYSHLAK, EASTERN PRECAUCASUS AND WESTERN CAUCASUS: CORRELATION, PALEOECOLOGICAL AND PALEOBIOGEOGRAPHICAL ASPECTS

Plenary Session 4 in Main Conference Room
Chairperson: Bruce Wardlaw

14:00-14:35 **David J. Bottjer** (keynote)
BIOTURBATION AND EARLY TRIASSIC ENVIRONMENTAL CRISES

14:35-15:10 **Jin Yugan** (keynote)

15:10-15:35 **Yukio Isozaki**
DEEP-SEA CHERT AND SHALLOW-SEA CARBONATE FROM THE END-PERMIAN MID-PANTHALASSA

15:35-15:45 *Afternoon Tea*

Plenary Session 5 in Main Conference Room
Chairperson: Mike Orchard

15:45-16:20 **Vladimir I**. **Davydov,** B. R. Wardlaw, T. Taylor, M. D. Schmitz, J. R. Groves, T. A. Schiappa and W. S. Snyder (keynote)
A STRATIGRAPHIC, BIOSTRATIGRAPHIC, PALEOBIOLOGIC DIGITAL INFORMATION SYSTEM: PALEOSTRAT AND THE CHRONOS SYSTEM

16:20-16:45 **Peng Yuanqiao**, Yin Hongfu, Gao Yongqun, Yang Fengqing and Yu Jianxin
ALIGNING MARINE AND NON-MARINE PERMIAN-TRIASSIC BOUNDARY SECTIONS USING BIOSTRATIGRAPHY AND HIGH-RESOLUTION EVENTOSTRATIGRAPHY: AN EXAMPLE FROM WESTERN GUIZHOU AND EASTERN YUNNAN, SOUTHWESTERN CHINA

16:45-17:20 **Daniel J. Lehrmann**, Jonathan L. Payne, Paul Enos, Jiayong Wei, Youyi Yu, Samuel A. Bowring, Jahandar Ramezani, Michael J. Orchard, Paul Montgomery, Daniel P. Schrag and Andrew H. Knoll
END-PERMIAN EXTINCTION AND BIOTIC RECOVERY: A COMPLETE RECORD FROM AN ISOLATED CARBONATE PLATFORM, THE GREAT BANK OF GUIZHOU, SOUTH CHINA

17:30-18:00 *Close Remarks*

Abstracts

Preliminary Geochemical Analysis of the Cao Bang Permian-Triassic Boundary Section in Northeastern Vietnam

Thomas J. Algeo[1] and Brooks Ellwood[2]

[1] Department of Geology, University of Cincinnati, USA; thomas.Algeo@uc.edu

[2] Dept. of Geological Sciences, Louisiana State University, USA; ellwood@lsu.edu

Recent biostratigraphic and magnetic susceptibility event correlation (MSEC) studies have resulted in recognition of the Permian-Triassic boundary in carbonate platform successions of northeastern Vietnam (Nguyen, Ellwood, et al., 2002, 2004). The boundary is associated with a transition from packstone containing a diverse, open-marine Permian fauna to calcimicrobial framestones lacking Permian macrofossils as well as with a ~100-fold increase in magnetic susceptibility. In the Cao Bang (Nhi Tao) section, biostratigraphic data place the boundary within bed 11, while MSEC data place it about 35 cm lower, between beds 9 and 10. The present study analyzed TOC, TIC, and major- and trace-element concentrations in the Cao Bang section with the goals of (1) general characterization of the geochemistry of the P-T boundary event in a carbonate succession, and (2) resolution of discrepancies in the biostratigraphic versus MSEC placement of the boundary.

The 7.5-m-thick section at Cao Bang analyzed in this study consists entirely of weakly argillaceous carbonate (<5% clay minerals) deposited under fully oxic conditions during the Late Permian and Early Triassic. However, an abrupt change in elemental chemistry is evident midway through the section, represented by (1) a decrease in TOC from 0.2-1.1% to values uniformly <0.1%, (2) an increase in total sulfur from <0.05% to 0.1-0.3%, (3) substantial increases in Fe, Mn, and P, with strong covariation (r^2>0.99) between Fe and Mn, and (4) modest decreases in redox-sensitive trace metals (e.g., Mo, U, V, and Cu). The decline in TOC may reflect reduced primary productivity during the P-T boundary event, and lower trace-metal concentrations are probably due to the lesser availability of sedimentary organic host phases. More significantly, large increases in Fe, Mn, and P may reflect concurrent changes in redox conditions and aqueous-phase chemistry elsewhere in the global ocean, e.g., increased concentrations of these elements in seawater due to remobilization from the sediment as a consequence of a shift from suboxic to anoxic conditions, possibly over large areas of seafloor. The associated increase in S may reflect greater availability of reactive Fe in the sediment for fixation of small quantities of bacterial H_2S. This geochemical transition commences in bed 8, about 15 cm below the MSEC placement of the P-T boundary and 50 cm below the main extinction horizon. This suggests that changes in ocean chemistry preceded changes in climate (as proxied by MSEC) and marine biotas during the P-T boundary event, an indication of the complexity and duration of this important stratigraphic interval. This reflects the fact that significant events in Earth history generally are not instantaneous, resulting in timing inconsistencies among event tracers.

Thoa, N. T. K., Ellwood, B. B., Ngan, P. K., Nam, V. H., Lan, L. T. P., 2002. Determination of the Devonian-Carboniferous boundary in limestone formations from Cat Ba and Nui Voi using the MSEC Method. Journal of Sciences of the Earth (in Vietnamese with an English abstract), 24: 56-66.

Thoa, N. T. K., Huyen, D. T., Ellwood, B. B., Lan, L. T. P., Truong, D. N., 2004. Determination of Permian-Triassic boundary in limestone formations from Northeast of Vietnam by paleontological and MSEC methods, Journal of Sciences of the Earth (in Vietnamese with an English abstract), 26: 222-232.

Lithofacies and Conodont Based Chronostratigraphy of the Lower Triassic Shallow Marine Succession in the Gorski Kotar region – Croatia

Dunja Aljinovic[1], Tea Kolar-Jurkovsek[2] and Bogdan Jurkovsek[2]

[1] University of Zagreb, Faculty of Mining, Geology and Petroleum Engineering, HR-10 000 Zagreb, Pierottijeva 6, Croatia; daljin@rgn.hr

[2] Geological Survey of Slovenia, Dimiceva 14, SLO-1000 Ljubljana, Slovenia

The investigated area of the Lower Triassic sedimentary complex in the Gorski Kotar region – Croatia, is located in the External Dinarides between the Alps and the Velebit Mt. The Lower Triassic depositional environment is envisaged as shallow marine realm of a passive continental margin. Sedimentary complex differentiates in predominantly carbonate sedimentation that characterise the beginning of deposition with upward increasing trend of terrigeneous influx. Five Lower Triassic sections (Homer, Skolski Brijeg, Zelin Crnoluski, Kramarcin Potok and Dobra) have been investigated. They were lithofacially defined, but their chronostratigraphical position was uncertain due to lack of fossils or their inadequate preservation.

A facial assemblage investigated in central part of Gorski Kotar region (Homer, Skolski Brijeg and Zelin Crnoluski sections) differs from those appeared in marginal parts (Kramarcin Potok and Dobra sections). In central part the shallow water carbonate facies predominate and reflect the shallow marine sedimentation of the stable rimmed shelf. Basal ca. 10 m thick cross-bedded interval of ooid grainstones (Homer and Skolski Brijeg sections) was interpreted as ooid bars that possibly formed subaqueous oolithic barrier with the landward laying lagoon. Thus the overlaying predominantly thin or medium-bedded grey

dolomicrites, sandy dolomites and calcarenaceous sandstones were interpreted as lagoonal sediments. Storms and post-storm tidal reworked processes influenced the deposition of ooid bars. Ooid grainstones were late diagenetically dolomitised, while the lagoon facies reflects the early diagenetic processes. The widening of the lagoon has been conceived through overall transgressive trend. The rapid transgression caused in-place drowning of the ooid bars and formation of a new seaward oriented coast that is represented by facies (dolomites, sandy dolomites and rarely siltites) organized in typical storm sequences of Crnoluski Zelin section deposited near fair weather wave base of unrestricted shelf. The intense influx of a dominantly red siliciclastic terrigenous material has been recorded in the Lower Triassic sediments of the marginal, western and eastern parts of Gorski Kotar region (Kramarcin Potok and Dobra sections). The thick-bedded ooid barrier bars as well as overlaying lagoon dolomicrites and sandy dolomites are missing in those sections. Vertical facies successions are characterised by the interbedded oolithic limestone/dolostone, red siltite and sandstone beds with occasional appearance of flat pebble conglomerates. Beds vary in thickness from few decimetres up to 1 m and are organised in fining upward sequences that represent shifting of a laterally existed facies deposited in ooid/sandy shoals and restricted muddy bays. The lithofacies present in Kramarcin Potok and Dobra sections resemble red clastic sediments i. e. Seiser beds of the Southern Alps that make them compatible to the wide area of the External Dinarides. The different lateral facies distribution was interpreted as the result of transgression that transformed narrow rimmed shelf with ooid bars and lagoon facies to unrestricted shelf and finally to the wide epicontinental sea with its ooid/sandy shoals and restricted muddy bays. This interpretation has never been proved while the precise chronostratigraphic dating of the investigated sections were missing in previous investigations. Therefore the lithofacial investigations were supplemented by conodont studies at each of five localities.

Twenty-five rock samples, with minimum weight of 3.5 kg were investigated by means of conodonts, but only fourteen samples proved to yield conodont elements. In general, the recovered conodonts are rare, except for the *Pachycladina* elements, but their preservation is commonly fragmented. The CAI (Color Alteration Index) of the conodonts is above 5, implying post-depositional temperatures varying between temperature ranges 300-480°C and 490-720°C (Epstein et al. 1977, Rejebian et al. 1987).

The oldest investigated strata are marked by the presence of *Hindeodus parvus* in the Skolski Brijeg section. The first appearance datum (FAD) of this taxon has been approved to define the base of the Triassic system (Yin et al. 2001). The biostratigraphical data allow recognition of the *parvus-isarcicella* Zone, *obliqua* Zone and *Platyvillosus* Subzone. The conodont zonation and lithofacial definition contribute to the definition of the Lower Triassic depositional realm of the External Dinarides and prove the correlative elements for comparison with some other parts of the Western Tethys.

Epstein, A. G., Epstein, J. B, Harris, L. D., 1977. Conodont Alteration Index - and Index to Organic Metamorphism. Geol. Surv. Prof. Pap., 995, 27p., Washington.

Rejebian, V. A., Harris, A. G., Huebner, J. S., 1987. Conodont color and textural alteration: An index to regional metamorphism, contact metamorphism and hydrothermal alteration. Geol. Soc. Am. Bull., 99: 471-497.

Yin, H., Zhang, K., Tong, J., Yang, Z., Wu, S., 2001. The Global Stratotype Section and Point (GSSP) of the Permian-Triassic Boundary. Episodes, 24: 102-114.

Calcareous Foraminiferal Recovery from the End-Permian Mass Extinction, Southern Turkey

Demir Altiner[1], John R. Groves[2] and Sevinç Özkan-Altiner[1]

[1] Department of Geological Engineering, Middle East Technical University, 06531 Ankara, Turkey; demir@metu.edu.tr

[2] Department of Earth Science, University of Northern Iowa, Cedar Falls 50614-0335, USA

As shown by Altiner et al. (2000) the Permian-Triassic boundary beds are well-exposed in the Taurides and Arabian Platform region of southern Turkey (Fig. 1). In most outcrops, assigned to the Southern Biofacies Belt (Altiner et al., 2000), the Lopingian Series is characterized by monotonous shallow-marine and micritic carbonate deposits rich in algae and smaller foraminifera but poor in fusulines. A Changhxingian age is assigned to the upper part of these carbonates on the basis of the foraminifer *Paradagmarita monodi* (Altiner et al., 2000; Altiner ve Özgül, 2001; Groves et al., in press), and to a lesser extent, ostracodes (Crasquin-Soleau et al., 2002).

The uppermost Permian beds in many localities of the southern Turkey are characterized by thin (<1 m) oolitic grainstones or high energy rudstones. The upper layer of these rippled oolitic grainstones or rudstones are sharply truncated by an unconformity and overlain by stratiform stromatolites (Groves et al., in press). An Induan age was assigned to these beds by Crasquin-Soleau et al. (2002) based on conodonts and the foraminiferal taxon, *Rectocornusipira kalhori*, also suggests an Induan age (Altiner and Özgül, 2001; Groves et al., in press). The Induan stromatolites, widely exposed in the Taurides and the Arabian Platform, are overlain by thick sequences of cross-bedded oolitic grainstones and then varicolored edgewise conglomerates, calcareous shales and thin-bedded, yellowish, molluscan packstones of later Induan age.

The Permian-Triassic boundary beds in southern Turkey have been studied at four localities (Fig. 1). These are Çürük Dag (locality 1; Marcoux and Baud, 1986; Crasquin-Soleau et al., 2002) and Demirtali (locality 3;

Groves et al., in press) both in the Antalya Nappes and Takent (locality 2; Groves et al., in press) and Aygörmez Dag (locality 4; Altiner and Zaninetti, 1981; Altiner et al., 1980) in the Aladag Nappe. Calcareous foraminifers are an excellent fossil group for detecting the Permian-Triassic extinction and the early phases of the survival interval at the base of the Triassic. Later stages of the survival interval and the following recovery interval in the Triassic have been compiled from various calcareous foraminiferal data obtained in Turkey.

Extinction, survival and recovery of calcareous foraminifera

In nearly all outcrops of the Southern Biofacies Belt the Permian-Triassic boundary is easily marked by the net decline of calcareous foraminifera in the orders Fusulinida, Miliolida and Lagenida.

Order Fusulinida**:** In southern Turkey, the Lopingian Series is characterized by the presence of several families in the order Fusulinida including Schubertellidae, Ozawainellidae, Staffellidae, Pseudovidalinidae, Lasiodiscidae, Palaeotextulariidae, Tetrataxidae, Biseriamminidae and Endothyridae. Among these families, Pseudovidalinidae became extinct in the Wuchiapingian and the schubertellid genus *Codonofusiella* made its last appearance below the Wuchiapingian-Changhxingian boundary. In the

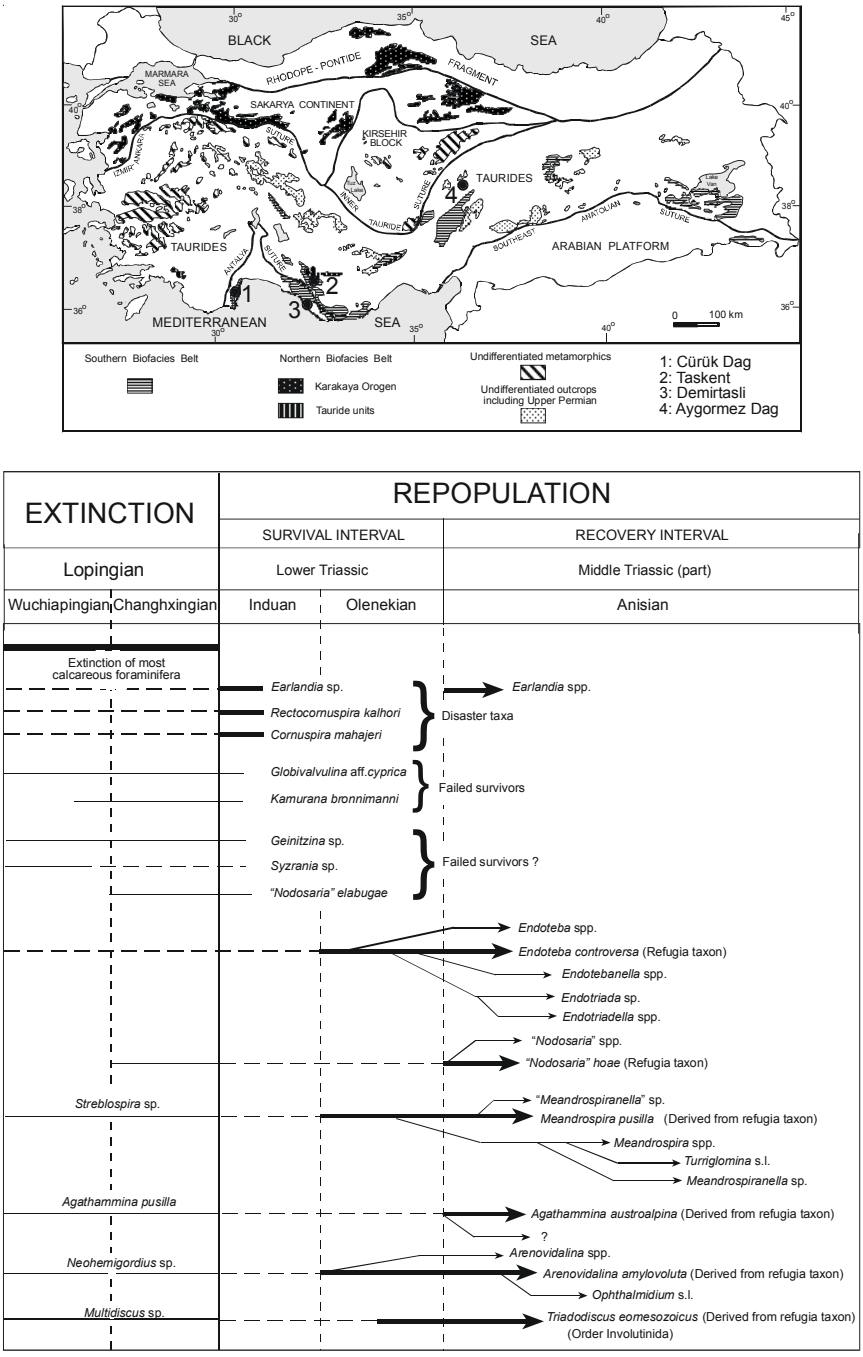

Figure 1. Locations of major sections (1-4) in the southern biofacies belt of Turkey and occurrences of calcareous foraminifera across the Permian-Triassic boundary

Changhxingian of southern Turkey, most tetrataxids (*Tetrataxis*), schubertelllids (*Boultonia*, *Paleofusulina*), ozawainellids (*Reichelina*), palaeotextulariids (*Palaeotextularia*, *Deckerella*, *Climacammina*) and endothyrids (*Neoendothyra*, *Postendothyra*) occur sporadically, so that their value in determining the Permian-Triassic boundary is diminished. However, staffellids (*Staffella*, *Nankinella*, *Sphaerulina*) are more frequently occurring taxa. The biseriamminids, *Dagmarita*, *Louisettita*, *Paradagmarita*, *Septoglobivalvulina*, although they declined in abundance, are present even in the uppermost Permian oolitic grainstones.

Basal Triassic deposits are generally devoid of fusulinide foraminifers, although one genus of biseriamminids occurs at the base of Triassic as a failed survivor (Fig. 1). Specifically, the specimens found belong probably to *Globivalvulina cyprica*.

The morphologically simple, long ranging, bilocular foraminifera, *Earlandia* occurs in large numbers in the Lower Induan of Turkey (Altiner et al., 1980; Altiner and Özgül, 2001; Groves et al., in press). Its presence in the microbialite facies or in close proximity of microbialites strongly suggests the interpretation of *Earlandia* as a disaster taxon, as first noted by Hallam and Wignall (1997).

Endoteba is regarded as a Lazarus taxon (Groves and Altiner, in press). The type species *Endoteba contraversa* occurs in the Capitanian strata in Turkey, but not in higher levels of the Permian or in the Lower Triassic. It reappears in the Olenekian stage suggesting prolonged residence in refugia. (Fig. 1). We favor the hypothesis that the other endotebid *Endotebanella* and the endotriadids including *Endotriada* and *Endotriadella* evolved in the Triassic from an *Endoteba* ancestor.

Order Lagenida**:** Lopingian lagenides are quite diverse and abundant in southern Turkey. *Geinitzina*, *Pachyphloia*, *Frondina*, *Ichthyofrondina*, *Nodosinelloides* and *Robuloides* were quite widespread and present in the uppermost levels of the Permian. Most dissappeared at the Permian-Triassic boundary.

In the Turkish sections, the Induan and Olenekian stages contain very few lagenides (Fig. 1). *Geinitzina* sp., *Syzrania* sp. and '*Nodosaria' elabugae* are possibly failed survivors in the Induan stage. Rare lagenides are joined in the Lower Triassic by *Tezaquina*? *luperti*.

'*Nodosaria*' *hoae* is known from the Changhxingian and the Middle Triassic and thus is regarded as a Lazarus taxon. This form is probably the root-stock of several later Triassic lagenides.

Order Miliolida**:** In the Lopingian Series of southern Turkey, the order Miliolida is represented by cornuspirids, hemigordiopsids and baisalinids. Genera in these families exhibit stable and roughly equal diversity throughout the Lopingian, except for the appearance of *Kamurana* in the Changhxingian. The extinction of the order was not complete at the Permian-Triassic boundary athough almost all hemigordiopsids and baisalinids disappeared.

The cornuspirins *Cornuspira mahajeri* and *Rectocornuspira kalhori* occur just above the Permian-Triassic boundary and they are short-lived disaster taxa (Fig. 1). The Permian genus *Kamurana*, survived in the Early Triassic as a failed survivor. *Meandrospira* is a Lazarus taxon whose occurrence in the Olenekian Stage probably represents the phyletic continuation of the Permian form assigned to *Streblospira*.. The earliest appearance in the Early Triassic is represented by *Meandrospira pusilla* from which progressive appearances of taxa in the Olenekian and the Anisian indicate species-level diversification (Groves and Altiner, in press). Similarly Triassic *Agathammina* and *Arenovidalina* could be regarded as Lazarus taxa (Fig. 1). As previously suggested the latter appeared within the *Neohemigordius-Arenovidalina* lineage in the Olenekian and gave rise to the appearance of ophthalmidids in the Anisian.

Order Involutinida**:** We favor the hypothesis that the hemigordiopsid *Multidiscus* could have given rise to involutinids. The *Multidiscus-Triadodiscus* transition could have occurred in the Induan by the transformation of the wall mineralogy from high-Mg calcite to aragonite. However, the great difference between mechanisms of wall secretion in the orders of Miliolida and Involutinida and recent rDNA analyses suggest that the phylogenetic link between the orders Miliolida and Involutinida is at best distant (Groves and Altiner, in press).

Conclusions

Based on Turkish data, most Lopingian calcareous foraminifera (more than %90 at the generic level) became extinct at or just before the Permian-Triassic boundary. Survivors can be categorized into three major groups. Disaster taxa consisting of *Earlandia*, *Rectocornuspira* and *Cornuspira* populations bloomed at the base of Triassic. Failed survivors (*Globivalvulina*, *Kamurana* and possibly others) became extinct diachronously in the survival interval. The main bulk of later Triassic foraminifera (ophthalmidids, involutinids, lagenides, endotebids and endotriadids) seem to have been derived progressively from the Olenekian onwards, either directly from refugia taxa ('*Nodosaria*' *hoae*, *Endoteba controversa*) or from the derivatives (*Meandrospira pusilla*, *Agathammina austroalpina*, *Arenovidalina amylovoluta*, *Triadodiscus eomesozoicus*) of Permian refugia taxa.

Altiner, D., Baud, A., Guex, J., Stampfli, G., 1980. La limite Permien-Trias dans quelques localité du Moyen-Orient: recherches stratigraphiques et micropaléontologiques. Riv. Ital. Paleont., 85: 683-714.

Altiner, D., Özkan-Altiner, S., Kocyigit A., 2000. Late Permian foraminiferal biofacies belts in Turkey: paleogeographic and tectonic implications. *in* Bozkurt, E., Winchester, J. A., Piper, J. D. A. (eds) Tectonics and magmatism in Turkey and the surrounding area. Geological Society, London, Special Publications, 173: 83-96.

Altiner, D., Özgül, N., 2001. Carboniferous and Permian of the allochthonous terranes of the central Tauride Belt,

southern Turkey. PaleoForams 2001, International Conference of Paleozoic Benthic Foraminifera (Ankara), Guidebook, 35p.

Altiner, D., Zaninetti L., 1981. Le Trias dans la région de Pinarbasi, Taurus oriental, Turquie: unités lithologiques, micropaléontologie, milieux dépôt. Riv. Ital. Paleont., 86: 705-760.

Crasquin-Soleau, S., Richoz, S., Marcoux, J., Angiolini, L., Nicora, A., Baud, A., 2002. Les événement de la limite Permien-Trias: derniers survivants et/ou premiers colonisateurs parmi les ostracodes du Taurus (sud-ouest de la Turquie). C. R. Geoscience, 334: 489-495.

Groves, J. R., Altiner, D., in press. Survival and recovery of calcareous foraminifera pursuant to the end-Permian mass extinction. C. R. Palevol.

Groves, J. R., Altiner, D., Rettori, R., in press. Decline and recovery of lagenide foraminifers in the Permian-Triassic boundary interval (Central Taurides, Turkey). Paleontological Society of Memoir, Supplement to J. Paleont.

Hallam, A., Wignall, P. B., 1997. Mass extinctions and their aftermath. Oxford University Press, Oxford, New York, Tokyo.

Marcoux, J., Baud, A., 1986. The Permo-Triassic boundary in the Antalya Nappes (western Taurides, Turkey). *in* Cassinis, G. (ed) Permian and Permian-Triassic boundary in the south-Alpine segment of the western Tethys, and additional regional reports. Mem. Soc. Geol. It., 34: 243-252.

The Lower Triassic Anachronistic Carbonate Facies in Space and Time

Aymon Baud[1], Sylvain Richoz[1] and Sara Pruss[2]

[1] Geological Museum, UNIL_BFSH2, CH-1015 Lausanne, Switzerland; aymon.baud@unil.ch

[2] Department of Organismic and Evolutionary Biology, Harvard University, 26 Oxford Street, Cambridge, MA 02138, USA

In the aftermath of the end-Permian mass extinction, a major crisis occurred in Phanerozoic carbonate systems that involved a whole scale change in oceanic geochemistry. The prolific upper Paleozoic skeletal carbonate factory was abruptly replaced by a non-skeletal carbonate factory (Baud, 1998). When preserved between the two carbonate systems, the boundary is marked by a post extinction clay (boundary clay) of latest Permian age (*Preparvus-Meishanensis* zone). Microbial communities affected sedimentation in a variety of normal marine areas (Baud et al., 1997).

The first microbial episode took place during latest Permian-earliest Triassic time as part of the main step of a very rapid and large-scale flooding of the giant carbonate platforms of the Cimmerian blocks (N margin of the Neotethys and S margin of the Paleotethys) and of N Gondwana (Arabian margin of the Neotethys). We note this also in the shallow, low energy post-extinction carbonate ramp of the N Gondwana margin (Bukk Montains (Hips, 2004), Hungary, S Alps, Italy and Slovenia, Taurus (Baud et al. in press), S Turkey, Zagros and N Oman). Massive thrombolitic mounds and/or stromatolites represent this microbial episode. The same microbial episode is also present in Central and E Elburz (S Paleotethyan margin, N Iran). On the more distal open marine ramp (S Armenia (Baud et al., 1997), NW and Central Iran) the microbial episode is expressed as digitate thrombolites (dendrolites), large stromatolitic mounds and oncoids. In addition to the widespread microbialites described here, seafloor precipitates were deposited in Lower Triassic strata of W Taurus (Baud et al. in press), S. Armenia and Central Iran. When environmental conditions changed from low to high-energy, oolitic deposition replaced stromatolites and thrombolites. The basal Triassic microbial cap carbonate (Baud et al. in press) was then terminated by a sudden input of terrigenous sediment (the multi-colored *Claraia* shales), dated as late Griesbachian to Dienerian in age. In eastern Tethys, a latest Permian—basal Triassic calcimicrobial framestone has been reported from large carbonate banks that occurred in the Nanpanjiang basin (Guizhou, S China) south of the giant Yangtze carbonate platform (Lehrmann et al., 2003). The high-energy crest of the bank is built by oolitical shoals. A microbial? carbonate crust of similar age to those reported above has been described in S Sichuan (Kershaw et al. 2002).

Due to widespread terrigenous sediment deposition and erosion, basal Triassic microbialites are absent or have not been found on the western Pangean margin. In the boreal seas, stromatolitic limestone lenses ~4 m are recorded within the Wordie Creek shaly unit of Jameson Land in SE Greenland (Wignall et al. 2002). Microbial buildups have not yet been observed at high southern latitudes (Indian margin, Australian and New-Zeeland margins). The Panthalassa Permian-Triassic seamount that crops out within the Chichibu Jurassic accretionary complex of S Japan exposes Griesbachian calcimicrobial bindstone overlying Changhsingian skeletal limestones (Sano et al., 1997).

The second microbial episode appears in the late Griesbachian to Dienerian cyclic limestone that contains calcimicrobial mounds from the carbonate banks rimed by oolites of the Nanpanjiang basin, South China (Lehrmann et al. 2003). This, and the following third episode are present in “the massive algal limestones” with stromatolites and oncoids (Nazarevitch et al., 1986) from the Pre-Caucasus margin of Paleotethys (Azerbaidjan).

The third microbial episode (lower Olenekian) is mainly recorded by oolitic shoals, accessory stromatolites, and edge-wise conglomerates on the carbonate ramps of both N and S Neotethys margins (S Turkey, N and central Iran).

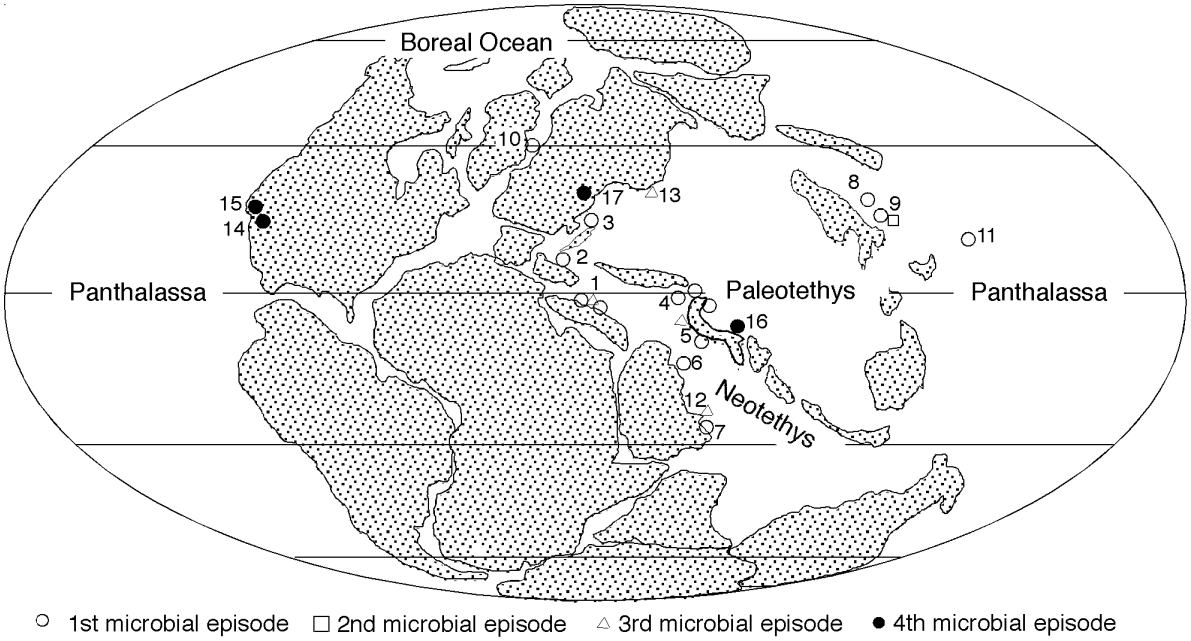

Figure 1. Paleogeographic sketch during the Permo-Triassic transition. Approximate position of microbial episodes: 1- Taurus (Turkey), 2-S Alps, 3- Bukk Mts (Hungary), 4- Armenia and NW Iran 5- Central Iran, 6- Zagros (S Iran), 7- Oman shelf, 8- S Sichuan (China), 9- Guizhou (China), 10- Jameson Land (Greenland), 11- Chichibu terrane (Japan), 12- Sumeini slope and Baid exotic (Oman), 13- Pre-Caucasus (Azerbaidjan), 14- Virgin Member (SW Nevada), 15- Union Wash Formation (SE California), 16- Aghdarband (E Iran), 17- Dobrogea (E Romania).

Oncoids and stromatolites occur on the carbonate platform of the Arabian margin in Oman. The proximal shallow carbonate platform exports a huge amount of microbial micrite, microbial clasts and ooids in the adjacent Sumeini slope depocenter (Richoz et al., 2005).

Red coloured calcimicrobial build-ups and black calcium carbonate fans grow up within a red ammonoid limestone (Baud et al., 2005) and these occur on a seamount of the distal Gondwana margin in Oman (Baid tilted block).

On the West Pangea coast, the Union Wash Formation (S California) deposited during the Olenekinan-Anisian, contains the third and the fourth microbial episodes with black precipitated concretions and fine laminated black lime mudstone (Woods, 1998).

The fourth microbial episode is recorded during Late Spathian time. Here this microbial episode is represented by thrombolites, stromatolites and seafloor precipitates (Virgin Limestone and Union Wash Formations (Pruss et al., 2004; Woods et al., 1999).

On the Paleotethys complex of NE Iran (Aghdarband), late Spathian calcimicrobial mounds contain the first reef-dwelling calcareous algae (Baud et al. 1991).

On the Dobrogea rift (E Romania), late Spathian to basal Anisian ammonoid-bearing white and red limestones exhibit thrombolitic textures with internal cavities and peloidal coccoids (Atudorei et al., 1997).

Atudorei, V., Baud, A., Crasquin-Soleau, S. Galbrun, B., Gradinaru, E., Mirauta, E., Renard, M., Zerrari, S., 1997. Extended scientific report of the Peri-Tethys Project, C. *in* Baud, A. (ed.) The Triassic of North Dobrogea, Lausanne, Geological Museum., 64 p.

Baud, A., 1998. Marine carbonate and siliceous factories: global Change after the end of Permian Mass Extinction. *in* Abstract book, 15th International Sedimentological Congress: Alicante (Spain), p. 180.

Baud, A., Atudorei, V., Richoz, S., 2005. Sea-floor carbonate cement and calcimicrobial mound in the lower Triassic red limestone of the Alwa Formation, Baid Exotic, Eastern Oman Mountains. 24th IAS Meeting of Sedimentology, Muscat, Jan. 10-13, 2005, Oman, Abstract book, p. 31.

Baud, A., Brandner, R., Donofrio, D. A., 1991. The Sefid Kuh Limestone - A late Lower Triassic Carbonate Ramp (Aghdarband, NE - Iran). Abhandlungen der Geologisches Bundes-Anstalt in Wien, 38: 111-123.

Baud, A., Cirilli, S., Marcoux, J., 1997. Biotic response to mass extinction: the Lowermost Triassic microbialites. Facies, 36: 238-242.

Baud, A., Richoz, S., Marcoux, J., in press. Post-extinction calcimicrobial cap rocks: examples from the basal Triassic carbonate platform of the Taurus (SW Turkey).

Hips, 2005. Calcmicrobial stromatolites at the Permian-Triassic boundary in a western Tethyan section (Bükk Mountain, Hungary). *in* 24th IAS Meeting in Sedimentology, Muscat, Jan. 10-13, 2005, Abstract book, p. 80.

Kershaw, S., Guo, L., Swift, A., Fan, J. S., 2002. Microbialites in the Permian-Triassic boundary interval in Central China: Structure, age and distribution. Facies, 47: 83-89.

Lehrmann, D. J., Payne, J. L., Felix, S. V., Dillett, P. M., Wang, H., Yu, Y. Y., Wei, J. Y., 2003. Permian-Triassic boundary sections from shallow-marine carbonate platforms of the Nanpanjiang Basin, south China: Implications for oceanic conditions associated with the end-Permian extinction and its aftermath. Palaios, 18: 138-152.

Nazarevitch, B. P., Nazarevitch, I. A., Boiko N. I., 1986. *in* Sokolov B. S. (eds.) URSS Phanerozoic Reefs and Corals, Akademia Nauk SSSR, 161-166.

Pruss, S., Bottjer, D. J., 2004. Late Early Triassic microbial reefs of the western United States:a description and model for their deposition in the aftermath of the end-Permian mass extinction. Palaeogeography, Palaeoclimatology, Palaeoecology, 211: 127-137.

Richoz, S., Baud, A., Krystyn, L., Twitchett, R., 2005. Permo-Triassic Deposits of the Oman Mountains: from Basin and Slope to the shallow Platform. Post-Conference Field Guidebook A13, Jan. 14-17, 2005, 24th IAS Meeting of Sedimentology, Muscat, Oman, 65 p.

Sano, H., Nakashima, K., 1997. Lowermost Triassic (Griesbachian) microbial bindstone-cementstone facies, Southwest Japan. Facies, 36: 1-24.

Wignall, P. B., Twitchett, R. J., 2002. Permian-Triassic sedimentology of Jameson Land, East Greenland: incised submarine channels in an anoxic basin. Journal of the Geological Society, 159: 691-703.

Woods, A. D., 1998. Paleoenvironmental analysis of the Union Wash Formation, east-central California: Evidence for unique Early Triassic paleoceanographic conditions: Los Angeles, USC, p. 270.

Woods, A. D., Bottjer, D. J., Mutti, M., Morrison, J., 1999. Lower Triassic large sea-floor carbonate cements: Their origin and a mechanism for the prolonged biotic recovery from the end-Permian mass extinction. Geology, 27: 645-648.

Late Permian and Early Triassic Ichnofossil Assemblages from The Northwest Margin of Pangea

Tyler W. Beatty[1], John-Paul Zonneveld[2] and Charles M. Henderson [1]

[1] Applied Stratigraphy Research Group, Department of Geology and Geophysics, University of Calgary, Calgary, AB T2N 1N4, Canada; tbeatty@ucalgary.ca

[2] Geological Survey of Canada, 3303-33rd Street NW, Calgary, AB T2L 2A7, Canada

Late Permian and Early Triassic ichnofossil assemblages from the northwest margin of Pangea provide a proxy record of benthic community composition across the Permian–Triassic boundary interval. These assemblages document variable recovery along the margin. To better understand the paleogeographic arrangement of both diverse and depauperate assemblages, Upper Permian and Lower Triassic strata representing a range of depositional environments were examined in the Canadian Arctic, Canadian Rockies, the Western Canadian Sedimentary Basin subsurface, and the southwest United States. From these investigations the following conclusions can be drawn: 1) moderately diverse Early Triassic ichnofossil assemblages are not restricted to mid-high paleolatitudes; 2) instead these appear restricted to shoreface environments during the Griesbachian and Dienerian; 3) depauperate assemblages occupy shale and siltstone facies associated with the end-Permian transgression; 4) only some of the Late Permian ichnotaxa reappear in the early Griesbachian, but this may in part be due to a change in lithology across the boundary. Case studies from the Canadian Arctic, Canadian Rockies, and the southwest United States are presented below.

The Permian–Triassic boundary interval is well recorded in the Sverdrup Basin of the Canadian Arctic Islands. Here, the end-Permian transgression onlaps Late Permian strata with increasing disconformity from basin centre to basin margin. At Confederation Point, where the unconformity is minimal (Beauchamp, pers. comm. 2004), ichnotaxa such as *Kouphichnium*, *Asteriacites*, *Haentzschelinia*, *Acanthoraphe*, and *Lockeia* are present within the first 20m of strata above the boundary. The ichnofossil assemblage occurs in distal fan sandstones interbedded with distal shelf siltstones, the trace makers were likely transported although well-developed fodichnia imply somewhat suitable living conditions. Rare, diminutive (2-4mm diameter) *Planolites* characterize the first 40m of siltstone beds, but are larger and more common up-section and occur with *Helminthopsis*. At this section conodont data places the top of the Griesbachian some 250m above the base of the transgression. Below, a 20m thick succession of silicified siltstone and chert of the Van Hauen Formation is devoid of trace fossils, but underlying hummocky cross-stratified spiculitic chert of the Lindstrom Formation contains *Cylindrichnus*, cf. *Schaubcylindrichnus*, *Teichichnus*, *Phycosiphon* and *Zoophycos*. At Lindstrom Creek, a more proximal section, *Skolithos*, *Spongeliomorpha*, *Cruziana*?, *Planolites*, and *Rhizocorallium* occur with *Claraia* in offshore transition sandstone 80m above the end-Permian transgression. Here, basal shale and siltstone beds are recessive and poorly exposed, but the underlying bedded chert of the Lindstrom Formation contains *Cylindrichnus*, *Teichichnus*, *Phycosiphon* and *Zoophycos*. At Buchanan Lake, the most distal section studied in the arctic, trace fossils are not present in shales underlying or overlying the end Permian event, but rare *Bergaueria* were observed 45m above this boundary in Griesbachian siltstone.

On Williston Lake, in the Canadian Rockies, two sections that span basinal strata of the P-T boundary include chert of the Fantasque Formation overlain by silicified shale and siltstone representing the end-Permian transgression. Ichnotaxa in the chert include *Bergaueria*, *Teichichnus*, *Phycosiphon*, and *Zoophycus*. Above the boundary, shale and dolomitic siltstone beds of the Grayling Formation

are devoid of trace fossils; Wignall and Newton (2003) indicate these strata were deposited under anoxic conditions. Griesbachian shoreface successions in the subsurface contain anomalously diverse ichnofossil assemblages. In the Kananaskis region of southwest Alberta, exposures of the Lower Sulphur Mountain Formation record shoaling upward offshore transition and lower shoreface successions through the Griesbachian and Dienerian. Upper Griesbachian fine-grained hummocky cross-stratified sandstone beds contain *Planolites* and rare *Diplocraterion.* In addition, Dienerian sandstone beds also contain abundant *Lockeia* on some bedding planes. Ichnotaxa present in the Lower Montney Formation in the subsurface of the northern Alberta – BC border region include *Diplocraterion*, *Halopoa*, *Helminthopis*, *Planolites*, *Skolithos*, and *Treptichnus* in heterolithic interbedded shale and silty sandstone and isolated specimens of *Cruziana*, *Diplichnites*, *Rhizocorallium*, *Rusophycus*, *Spongeliomorpha* and *Thalassinoides* (Zonneveld *et al.*, 2004). Other subcrop exposures of Lower Montney Formation shoreface successions, however, preserve only rare occurrences of trace fossils (*i.e*. Panek, 2000). The factors controlling such dissimilarities in ichnofossil assemblages occurring within comparable depositional environments are currently being studied.

Near Bear Lake, southeast Idaho, the Dinwoody Formation unconformably overlies the Permian Rex Chert. Trace fossils observed in the Rex Chert are limited to *Planolites*, *Teichichnus*, and *Conichnus*?, but the condition of the rock made identifications difficult. The duration of the sub-Triassic unconformity is uncertain, but from available conodont data it spans at least the Upper Permian. The basal Dinwoody comprises planar laminated shale and dolomitic siltstone that includes rare diminutive *Planolites* that first appear 30m from the base. Above a covered interval, lime-packstones are interbedded with fine-grained, ripple cross-laminated calcareous sandstone. The packstones contain abundant *Claraia* and disarticulated lingulid brachiopods; several specimens of *Hindeodus* sp. have been recovered from this outcrop. Sandstone beds contain diverse ichnotaxa including *Diplocraterion*, *Planolites*, *Thalassinoides*, *Bergaueria*, *Lockeia*, *Lingulichnus*?, *Phycodes*?, and *Gyrochorte.*

Evidence for complex ethologies, previously unreported from Griesbachian and Dienerian strata, has been documented in shoreface successions from higher, middle, and lower paleolatitudes along the northwest margin of Pangea. These ichnotaxa, with the exception of transported individuals, appear restricted to offshore transition or shallower environments. Conditions preclusive to extended occupation of benthic environments must then have existed below these depths. If stress from anoxia played an important role during the Early Triassic as previously suggested (Twitchett and Wignall, 1996), then perhaps wave action (normal and storm) acted to mitigate this stress in shallower environments.

Panek, R., 2000. The sedimentology and stratigraphy of the Lower Triassic Montney Formation in the subsurface of the Peace River Area, Northwestern Alberta. Unpublished MSc Thesis, University of Calgary, 275p.

Twitchett, R. J., Wignall, P. B., 1996. Trace fossils and the aftermath of the Permo–Triassic mass extinction: evidence from northern Italy. Palaeogeography, Palaeoclimatology, Palaeoecology, 124: 137-151.

Wignall, P. B., Newton, R., 2003. Contrasting deep-water records from the Upper Permian and Lower Triassic of South Tibet and British Columbia: Evidence for a Diachronous Mass Extinction. Palaios, 18: 153-167.

Zonneveld, J.-P., Henderson, C. M., Macnaughton, R., Beatty, T. W., 2004. Diverse ichnofossil assemblages from the Lower Triassic of northeastern British Columbia, Canada: Evidence for a shallow marine refugium on the northwestern coast of Pangea. Geological Society of America Annual Meeting, Nov., 2004, Denver, Colorado.

Carnian to Rhaetian Isolated Platform and Reef Development in the Neo-Tethys (Oman)

Michaela Bernecker

Institute of Paleontology, Loewenichstr. 28, D-91054 Erlangen, Germany; bernecker@pal.uni.erlangen.de

The time interval spanning the shallow-water facies of Triassic isolated platforms is under discussion. At Jebel Misfah, the Ladinian-Carnian Sudayb Formation, which forms the base of Misfah Formation, comprises a succession from mafic volcanics to dark nodular limestones (Pillevuit 1993; Pillevuit et al. 1997) and is regarded as the lowermost unit of this Neo-Tethyan isolated carbonate platform. Basal limestones found at Jebel Kawr are shallow-water platform carbonates of the Misfah Formation and no evidence of the Sudayb Formation exists. Based on the present data, shallow-water carbonates of the isolated Kawr platform belong to the Misfah Formation and comprise platform rim as well as bedded inner platform facies. Although platform rim facies has only been found in the section near Sint (Bernecker 1996), a margin with varying amounts of reefs and cross-bedded oolite and/or skeletal-peloid packstone can be assumed from comparisons with other Triassic isolated platforms known from the Dolomites (e.g. Bosellini 1984; Blendinger et al. 2004) and South China (e.g. Guizhou bank, South China, Lehrmann et al. 1998, 2001).

Correlation of three measured sections of the Misfah Formation points to a platform architecture with composite sequences MF1-MF4 (Weidlich & Bernecker 2003). Basal sequence MF1 lacks biostratigraphic microfossils. The occurrence of the calcareous algae *Poikyloporella duplicata*, *Clypeina besici*, and the foraminifer *Aulotortus*

praegaschei at the base of sequence MF2 points to a Carnian age. Sequence MF4 at the top of section yields the foraminifer *Triassina hantkeni* indicative of Rhaetian age. The termination of the shallow-water platform sedimentation is indicated by platform drowning during the Lower Jurassic (Fatah Formation, Section Ma'Wa: Pillevuit 1993). A debris flow, not reported in previous studies, is separated from the bedded facies by normal faults. It is obviously younger than the bedded facies of the Misfah Formation, because the gravity flow deposit contains clasts of the Misfah Formation and older than post-drowning sediments, which are not represented in the debris flows. Summarizing these data, a Carnian to Rhaetian age is backed by own biostratigraphic determinations and a Ladinian to Early Jurassic age has been assumed in literature (Pillevuit 1993; Baud et al. 2001).

Transgressive systems tract facies variation

The TST facies of the inner platform of Misfah Formation is dominated by fully marine megalodont-rich floatstone containing diverse biota. The sediment between the large bivalves is often bioturbated and points to good oxygenation of the uppermost layer. In addition, gastropods, calcareous algae, and smaller foraminifera are ubiquitous skeletal grains. Subtidal mud- and wackestone and sub- to intertidal algal stromatolite occur rarely. Subaerial unconformities are absent during the TST facies.

Facies patterns and sediment composition of TST facies at the platform margin can be best described using the data of the Sint section. Composite sequence MF1 is not exposed near Sint, but dominance of sub- to intertidal stromatolites of the inner platform facies suggests moderate lateral depth gradients during this phase. During MF2-TST, the inner platform facies of Jebel Kawr laterally passes from subtidal megalodont floatstone towards the rim in multi-colored bioturbated bioclastic wackestone, laminated wackestone, bivalve floatstone, and rare grainstone with dasycladacean algae or oncoids. MF3-TST differs in its biotic composition significantly from MF2-TST and is dominated by crinoid float- and rudstone. From base to top, crinoid ossicles are increasingly disarticulated, but not transported. These crinoid-rich sediments laterally correlate with a dark, bituminous coral/chaetetid floatstone. This coral bank facies yields chaetetids (*Blastochaetetes dolomiticus*) and corals (*Retiophyllia norica*) and is unique in its composition throughout the isolated Kawr platform. This facies represents the only occurrence of coral/chaetetid level-bottom communities on the inner platform and is conspicuously dark and bituminous. It is the maximum flooding surface of the platform and can be correlated with a similar zone of the Mahil Formation of the Gondwana shelf (Weidlich & Bernecker 2003). MF4-TST is characterized by fully marine bedded platform facies with megalodonts. Comparable to composite sequence MF1, a differentiation between TST and HST is too arbitrary owing to the absence of significant facies changes and therefore not practized. Tempestites are an ubiquitous phenomenon of the platform and are striking in the prograding platform facies above the coral reef.

Highstand systems tract facies variation and platform drowning

The inner platform facies of the HST is dominated by bedded Lofer cyclothems and sub- to intertidal algal stromatolite as well as mudstone are more common than subtidal megalodont-rich floatstone. Subaerial exposure horizons are frequent. The greatest facies variation of the isolated Kawr platform occurs at the platform rim. The HST commenced with coral reef facies evolving from boundstone to floatstone and finally to lithoclastic rudstone due to decreasing water depth and increasing turbulence. Composite sequence MF3 is terminated by prograding platform facies with heterogeneous composition including abundant bivalve tempestites, oolites, and wacke/packstone. Occasional subaerial exposure horizons point to short-lived, punctuated sea level lowstands as a result of decreasing accommodation space. The youngest platform sediments have been eroded and platform termination remains therefore enigmatic. Matrix-rich debris flow deposits with onlapping geometries point either to a lowstand wedge with long-lasting platform exposure at the end of Triassic or to a rifting event related to extension of the Neo-Tethys (e.g. Glennie et al. 1974; Robertson and Searle 1990; Loosveld et al. 1996). The youngest carbonates of the isolated platform are thin-bedded deep-water limestones, which record platform drowning subsequent to erosion.

Interpretation

Composite sequences MF1 - MF4 are characterized by a variation of internal architecture. Differentiation of TST and HST units is only possible near the platform rim due to a pronounced facies differentiation in ooid shoal, reef, and bedded platform facies. In addition, composite sequence MF3 is the only unit, which can be correlated on a platform-wide scale owing to a significant facies change. The other TSTs and HSTs platform sequences are indistinct and, therefore, their differentiation would be too arbitrary. This is due to the fact that inner platform is characterized by stacked high-frequency cycles comparable to the Lofer cyclothems with subtidal megalodont-rich floatstone, shallow-subtidal to intertidal birdseye-bearing mudstone, and laminated stromatolite terminated by subaerial exposure horizons (e.g. Fischer 1964; Goldhammer et al. 1990; Samankassou et al. 2001).

The change in the architectural style from bank to platform rimmed by reefs took place during MF2. Until MF2-TST, the depositional system corresponds to a low-relief bank with indistinct lateral gradients. Facies differentiation is obvious during MF2-HST comprising ooid shoals at the platform rim and megalodont mudstones on the platform. During MF3-HST, coral reef facies aggraded at sea level showing no evidence for subaerial exposure. When the reef catch up sea level, percentage of float- and rudstone increased and platform aggradation switched to progradation. Reef development therefore reflects shallowing with changes in biotic composition and preservation of framework.

The debris flow probably may indicate either subaerial

exposure of the isolated platform prior to drowning or drowning of the platform related to rifting and opening of the Neo-Tethys. On one hand, subaerial exposures is backed by the sea-level curve for the Arabian platform, which points to long-lasting platform exposure during the Rhaetian (Weidlich & Bernecker 2003). However, no evidence of karst phenomena (e.g. Bernecker et al. 1999; Haas 2004) is known from this isolated platform. On the other hand, drowning of carbonate platform may be often associated with debris flows (Zempolich 1993) and it is known from the southeast Bahamas that platform drowning may be caused by downfaulting and platform collapse (Mullins et al. 1991). At present, subaerial exposure as control mechanism is favored.

Baud, A., Béchennec, F., Cordey, F., Krystyn, L., Le Métour, J., Marcoux, J., Maury, R., Richoz, S., 2001. Permo-Triassic deposits: from the platform to the basin and seamounts. International Conference Geology of Oman, Excursion A01, 56.

Bernecker, M., 1996. Upper Triassic reefs of the Oman Mountains: Data from the South Tethyan Margin. Facies, 34: 41-76.

Bernecker, M., Weidlich, O., Flügel, E., 1999. Response of Triassic reef coral communities to sea-level fluctuations, storms and sedimentation: Evidence from a spectacular outcrop (Adnet, Austria). Facies, 40: 229-280.

Blendinger, W., Brack, P., Norborg, A. K., Wulff-Pedersen, E., 2004. Three-dimensional modelling of an isolated carbonate buildup (Triassic, Dolomites, Italy). Sedimentology, 51: 297-314.

Bosellini, A., 1984. Progradation geometries of carbonate platforms: examples from the Triassic of the Dolomites, northern Italy. Sedimentology, 31: 1-24.

Fischer, A. G., 1964. The Lofer cyclothems of the Alpine Triassic. *in* D. F. Merrian (ed.) Symposium on cyclic sedimentation, Lawrence, Kansas Geol. Surv. Bull., 169: 107-149.

Glennie, K. W., Boeuf, M. G. A., Hughes, Clarke, M. W., Moody-Stuart, M., Pilaar, W. H. F., Reinhardt, B. M., 1974. Geology of the Oman Mountains. Verh. Kon. Nederlands geol. mijnb. Genootschap, 31: 423 .

Goldhammer, R. K., Dunn, P. A., Hardie, L. A., 1990. Depositional cycles, composite sea-level changes, cycle stacking patterns, and the hierarchy of stratigraphic forcing: Examples from AlpineTriassic platform carbonates. Geological Society of America Buletin, 102: 535-562.

Haas, J., 2004. Characteristics of peritidal facies and evidences for subaerial exposures in Dachstein - type cyclic platform carbonates in the Transdanubian Range, Hungary. Facies, 50: 263-286.

Lehrmann, D. J., Wan, Y., Wei, J., Yu, Y., Xiao, J., 2001. Lower Triassic Peritidal Cyclic Limestone: An Example of Anachronistic Facies from the Great Bank of Guizhou, Nanpanjiang Basin, Guizhou province, South China. Palaeogeography, Palaeoclimatology, Palaeoecology, 173: 103-123.

Lehrmann, D. J., Wei, J., Enos, P., 1998. Controls on facies architecture of a large Triassic carbonate platform: the Great Bank of Guizhou, Nanpanjiang Basin, South China. Journal of Sedimentary Research, 68: 311-326.

Loosveld, R. J. H., Bell, A., Terken, J. J. M., 1996. The tectonic evolution of interior Oman. GeoArabia, 1: 28-50.

Mullins, H. T., Dolan, J., Breen, N., Andersen, B., Gaylord, M., Petruccione, J. L., Wellner, R. W., Melillo, A. J., Jurgens, A. D., 1991. Retreat of carbonate platforms: Response to tectonic processes. Geology, 19: 1089-1092.

Pillevuit, A., 1993. Les Blocs Exotiques du Sultanat d'Oman, Evolution paléogéographique d'une marge passive flexurale. Mémoires de Géologie (Lausanne), 17: 249.

Pillevuit, A., Marcoux, J., Stampfli, G., Baud, A., 1997. The Oman Exotics: a key to the understanding of the Neotethyan geodynamic evolution. Geodinamica Acta, 10: 209-238.

Robertson, A. H. F., Searle, M. P., 1990. The northern Oman Tethyan continental margin: stratigraphy, structure, concepts and controversies. *in* Robertson A. H. F., Searle, M. P., Ries, A.C. (eds.) The Geology and Tectonics of the Oman Region, London, The Geological Society, 49: 3-27.

Samankassou, E., Bernecker, M., Flügel, E., 2001. The Late Triassic Kawr platform, Sultanate of Oman: An analogue to the Dachstein platform, Northern Calcareous Alps, Austria? International Conference Geology of Oman, Abstract volume, 77-78.

Weidlich, O., Bernecker, M., 2003. Supersequence and composite sequence carbonate platform growth: Permian and Triassic outcrop data of the Arabian platform and Neo-Tethys. Sedimentary Geology, 158: 87-116.

Zempolich, W.G., 1993. The drowning succession in Jurassic carbonates of the Venetian Alps, Italy: A record of supercontinent breakup, gradual eustatic rise, and eutrophication of shallow-water environments. *in* Loucks, R.G., Sarg, J. F. (eds.) Carbonate sequence stratigraphy - recent developments and applications. AAPG Memoir, 47: 63-105.

Bioturbation and Early Triassic Environmental Crises

David J. Bottjer

Department of Earth Sciences, University of Southern California, Los Angeles, CA 90089-0740 USA; dbottjer@usc.edu

As data continues to be collected on aspects of the marine ichnologic record through the Early Triassic, all indicators point to a pattern of greatly reduced depth as well as reduced amount of bioturbation through this time (5-6 million years) (e.g., Schubert and Bottjer, 1995; Twitchett and Wignall, 1996; Ausich and Bottjer, 2002; Zonneveld

et al., 2002; Twitchett and Barras, 2004; Pruss and Bottjer, 2004a; Pruss et al., 2004). Bioturbation features are paleoecological indicators, and these patterns demonstrate that benthic marine communities were ecologically diminished for this relatively long time interval. The most likely cause(s) for this period of reduced bioturbation would have followed one of two temporal patterns. (1) The major stress of the end-Permian mass extinction, which caused this reduction in bioturbation, was maintained through the Early Triassic. (2) The major stress of the end-Permian mass extinction caused the initial reduction in bioturbation, and repeated pulses of similar stress, interspersed with times of more "normal" environmental conditions, kept bioturbation reduced through the Early Triassic. The strongest candidates for marine environmental stress include anoxia, increased carbon dioxide concentrations, and hydrogen sulfide poisoning (e.g., Wignall and Twitchett, 1996; Knoll et al., 1996; Kump et al., 2003).

Sedimentological and carbon isotope data indicate that geographically variable pulses of stressful environmental conditions characterized the Early Triassic (e.g., Woods et al, 1999; Payne et al., 2004; Pruss and Bottjer, 2004b). That ecological structure, including bioturbation, did not significantly recover during "normal" times between intervals of stress may be because such times were of too short duration to allow substantial recovery. Recent work on modern environments (Solan et al., 2004) demonstrates that reductions in biodiversity generally reduce bioturbation, particularly the depth of bioturbation, in otherwise "normal" shallow marine environments. Taken together these factors confirm that (2) is the more likely process to have produced the Early Triassic record, and that this series of pulses of environmental stress only ended at the dawn of the Middle Triassic.

Ausich, W. I., Bottjer, D. J., 2002. Sessile invertebrates. *in* Briggs, D. E. G., Crowther, P. R. (eds.) Palaeobiology II. Blackwell, Oxford, 384-386.

Knoll, A. H., Bambach, R. K., Canfield, D. E., Grotzinger, J. P., 1996. Comparative Earth history and the Late Permian mass extinction. Science, 273: 452-457.

Kump, L. R., Pavlov, A., Arthur, M., Kato, Y., Riccardi, A., 2003. Death by hydrogen sulfide: A kill mechanism for the end-Permian mass extinction. Geological Society of America Abstracts with Programs, 35: 203-204.

Payne, J. L., Lehrman, D. J., Wei, J., Orchard, M. J., Schrag, D. P., Knoll, A. H., 2004. Large perturbations of the carbon cycle during recovery from the end-Permian mass extinction. Science, 305: 506-509.

Pruss, S. B., Bottjer, D.J., 2004a. Early Triassic trace fossils of the western United States and their implications for prolonged environmental stress from the end-Permian mass extinction. Palaios, 19: 551-564.

Pruss, S. B., Bottjer, D. J., 2004b. Late Early Triassic microbial reefs of the western United States: A description and model for their deposition in the aftermath of the end-Permian mass extinction. Palaeogeography, Palaeoclimatology, Palaeoecology, 211: 127-137.

Pruss, S. B., Fraiser, M. L., Bottjer, D. J., 2004. Proliferation of Early Triassic wrinkle structures: Implications for environmental stress following the end-Permian mass extinction. Geology, 32: 461-464.

Schubert, J. K., Bottjer, D. J., 1995. Aftermath of the Permian-Triassic mass extinction event: Paleoecology of Lower Triassic carbonates in the western USA. Palaeogeography, Palaeoclimatology, Palaeoecology, 116: 1-39.

Solan, M., Cardinale, B. J., Downing, A. L., Engelhardt, K. A. M., Ruesink, J. L., Srivastava, D. S., 2004. Extinction and ecosystem function in the marine benthos. Science, 306: 1177-1180.

Twitchett, R. J., Wignall, P. B., 1996. Trace fossils and the aftermath of the Permo-Triassic mass extinction: Evidence from northern Italy. Palaeogeography, Palaeoclimatology, Palaeoecology, 124: 137-151.

Twitchett, R. J., Barras, C. G., 2004. Trace fossils in the aftermath of mass extinction events. *in* McIlroy, D. (ed.) Application of Ichnology to Palaeoenvironmental and Stratigraphic Analysis. Geological Society of London Special Publication 228: 395-415.

Wignall, P. B., Twitchett, R. J., 1996. Oceanic anoxia and the end Permian mass extinction. Science, 272: 1155-1158.

Woods, A. D., Bottjer, D. J., Mutti, M., Morison, J., 1999. Lower Triassic large sea-floor carbonate cements: Their origin and a mechanism for the prolonged biotic recovery from the end-Permian mass extinction. Geology, 27: 645-648.

Zonneveld, J.-P., Pemberton, S. G., MacNaughton, R. B., 2002. Ichnology and sedimentology of the Lower Montney Formation (Lower Triassic), Kahntah River and Ring Border fields, Alberta and British Columbia. Canadian Society of Petroleum Geologists Abstracts with Programs, p. 355.

Extinction-Survival-Recovery of Brachiopod Faunas During the Permian-Triassic Transition

Chen Zhongqiang

School of Earth and Geographical Sciences, The University of Western Australia, 35 Stirling Highway, Crawley, WA 6009, Australia;
zqchen@cyllene.uwa.edua.au

The end-Permian mass extinction not only caused the largest crash in global biodiversity since the Cambrian explosion (Sepkoski, 1981), but also redirected dramatically the course of biotic evolutions and is largely responsible for much of the structure of marine ecosystems today (Bowring et al., 1999). Brachiopoda is the outstanding example of a clade that suffered severely the event. The fossil record of this group in the pre-Mesozoic is very

Table 1. A proportional survival rate equates to the number of survival taxa divided by the number of total taxa

Phases	Number of taxa			Proportional survival rate (%)			Proportional extinction rate (%)			Origination rate (%)		
	Spe.	Gen.	Fam.	Spe.	Gen.	Fam.	Spe.	Gen.	Fam.	Spe.	Gen.	Fam.
MF 3	15	8	7	19.5	36.8	54.5	80.5	63.2	55.5	40	0	0
MF 2	41	19	11	42.3	47.5	44	57.7	52.5	56	19.5	0	0
MF 1	78	40	25	8.8	28.2	50	91.2	72.8	50	52.5	0	0
Pre-ext.	420	143	50									

A proportional extinction rate equates the number of extinct taxa divided by the number of total taxa. An origination rate equates to the number of new taxa divided by the number of total taxa.

abundant (Rudwick, 1970; Sepkoski, 1981), and, for the first time since their origin in the Early Cambrian, brachiopod's diversity declined rapidly in the Early Triassic oceans around the world as a consequence of the end-Permian mass extinction (Erwin, 1993). Consequently, Brachiopoda also lost their dominance in Mesozoic and later marine benthic communities and became subordinate organisms inhabiting largely in the deep oceans or marginal seas today (Rudwick, 1970).

As far as the end-Permian event is concerned, many questions remain about the magnitude and causes of this dramatic extinction. Similarly, interpretation of the delayed faunal recovery following this extinction remains highly disputed. The final recovery of marine faunas following this event is generally believed to occur in the early Middle Triassic (Anisian), about 5 million years after the extinction (Erwin, 1998). Recent several studies of this recovery based on data of other fossil groups suggest that simple, cosmopolitan, opportunistic generalists, and low-diversity paleocommunities were characteristic of the Early Triassic oceans. However, there are not yet any studies on the post-extinction recovery of the global brachiopod faunas. In particular, published data and current materials tend to indicate that the recovery pattern derived from brachiopod data will differ from that of other fossil groups (e.g., bivalves, gastropods and echinoids) because brachiopods show some clear differences to these other groups.

(1) Brachiopods are the most diverse fauna in the Permian oceans and are the second largest victims among the main marine fossil groups in the end-Permian mass extinction (Carlson, 1991). The brachiopod extinction-survival-recovery pattern should therefore have its own unique feature.

(2) Brachiopods are the most abundant representatives that survived the end-Permian event (Sheng et al., 1984). The relationships among the pre-extinction brachiopods, survivors and post-extinction recovery and radiating faunas are crucial to understand the process and mechanisms of brachiopod recovery after the event. As such, the brachiopod faunas are able to more precisely indicate biotic factors at extinction, survival and recovery intervals summarized by Kauffman and Erwin (1995).

(3) There are rare Lazarus genera (Jablonski, 1986) in marked contrast to a few Lazarus genera in other groups (e.g. gastropods), which commonly reappear near the close of the recovery interval (Erwin, 1998). Consequently, the recovery model of brachiopods is much less influenced by Lazarus effect at generic level, although the Lazarus effect affected this fossil group at familial level to some extent.

(4) Early Triassic brachiopods mainly comprise endemic elements and appear to record strong provinciality in sharp contrast to the current hypothesis based on the observation of other fossil groups.

In addition, significant taxonomic emendation and re-classification of the Brachiopoda, as appearing in the revised Brachiopod Treatises published since 1997, and much improved stratigraphic information obviously re-figure brachiopod extinction, survival and recovery patterns during the end-Permian event. Calibration of both the Permian-Triassic (P/T) boundary and end-Permian mass extinction horizon at the Meishan section as well as global correlations of high-resolution biozones and other geochemical anomaly signals also provide the possibility to elucidate the brachiopod extinction, survival and recovery during the P/T transition.

1. Extinction of brachiopod faunas.

According to the previously published data and our unpublished data, a total of 420 species belonging to 143 brachiopod genera within 50 families have been reported from the pre-extinction Changhsingian Stage worldwide. The new assessment of the "mixed faunas" reveals that 102 species (including 40 indeterminate species) belonging to 43 genera within 27 families are recorded in strata above the end-Permian extinction horizon or their counterparts in P/T boundary sections globally. These taxa include all elements present in the "Mixed Fauna Beds (MFBs) 1-3" above the extinction horizon, so the proportional extinction/survival rates based on these data may mask the true patterns of brachiopod extinction and survival. To understand the true survival rates of brachiopods in the three survival phases (MF 1-3 phases, corresponding to the conodonts *C. meishanensis*, *H. parvus* and *I. isarcica* zones, respectively), the proportional extinction/survival rates of brachiopods in these three phases are calculated at specific, generic and familial levels, respectively (Table 1).

The variations in diversity and proportional extinction/or survival rate reveal that a sharp drop in diversity of brachiopod faunas coincides with the widely accepted end-Permian mass extinction horizon, which is calibrated to the base of Bed 25 at Meishan (Jin et al., 2000). The generic and familial proportional extinction rates over the event are, apparently, much smaller than current estimates (e.g., Carlson, 1991). Therefore, a greater number of brachiopod genera and families survived the end-Permian mass extinction with proportional survival rates of 28.2% and 50%, respectively. The extremely low proportional survival rate of brachiopod species across the boundary between MFs 2 and 3 (19.5%) is conspicuous. This number is reduced by combining the brachiopods in both MF 1 and 2 [proportional surviving rates of brachiopods in MF 3 are 8.8% (species), 16.7% (genera), and 22% (family)]. This indicates a dramatic turnover of brachiopods across MFs 2 and 3 and corresponds to the boundary between the *H. parvus* and *I. isarcica* conodont zones. A low proportional survival rate coupled with a high origination rate of new taxa characterizes the brachiopod faunas at the aftermath of the end-Permian extinction. These two phases of low survival rates of the survival brachiopods correspond to two extinction events. This fact indicates that the post-extinction brachiopods were also affected by a subsequent crisis corresponding to the boundary between MFB 2 and MFB 3 so that most survivors were extinct approximately less than one myr after the event. This pattern partly supports the hypothesis of 3-phase of biotic extinction within the P/T boundary beds (Yang et al., 1993).

Biogeographically, brachiopods were widely distributed at the Austrazean, the Himalayan, Cathaysian, Western Tethyan, and Sino-Mongolian provinces, respectively (Shen et al., 2000; this study) during the pre-extinction Changhsingian. Of these, brachiopods habiting the Austrazean and Sino-Mongolian provinces became completely extinct. The former province belonged to the Gondawana realm, and the latter was close to the Boreal realm. The brachiopods surviving the event mainly were in regions near paleo-equatorial areas. Accordingly, the end-Permian extinction resulted in the movement of biogeographic provinces towards the palaeo-equator.

2. Survival strategies of brachiopod faunas.

Global reviews reveal that a great number of brachiopods survived the end-Permian mass extinction in South China, the Himalayan regions (southern Tibet, Nepal, Salt Range and Kashmir), southern Alps (Italy), Arctic Canada, western USA and Western Australia. Of these, the surviving brachiopods are most abundant and widespread in South China where they occur in 32 of the 42 P/T boundary sections around the world. These surviving brachiopods occur in three stratal intervals corresponding to the "MFBs" 1-3 of the P/T boundary beds. The surviving brachiopods were mainly Productida, followed by Spiriferida. In particular, small chonetids, chonetid-like productellids and smooth, thin-shelled ambocollid spiriferids are most abundant. Disaster taxon *Lingula* is extraordinarily abundant and widespread in the aftermath of the greatest extinction when many regions became devoid of articulate brachiopods. Widespread, broadly adapted and small-sized taxa preferentially survived. Frequent intrageneric speciation of widespread, widely adapted generalist genera enabled survival brachiopods to occupy rapidly and efficiently vacant ecospace in the aftermath of the end-Permian extinction. The ecologic habitats of the post-extinction brachiopods are subdivided into nearshore, epeiric sea, restricted carbonate platform, open carbonate platform, ramp and outer shelf environments. Of these, the survival brachiopods are most diverse in the open platform environments. The nearshore zone provided ideal habitats for the nonarticulated brachiopods to occupy; whereas the survivors in the outer shelf are predominantly chonetids and chonetid-like productids. The most successful survivors, the productid brachiopods, are widely distributed in six types of ecological habitats and thus have no apparent preference for specific environments. Biogeographically, brachiopods survived mostly in the palaeo-equatorial provinces and along the southern margins of the Palaeo-Tethys Ocean. Moreover, in both the Himalayan and South China regions where the survivors of the end-Permian extinction are highly diverse, but none of them participated in both post-extinction recovery so that these survivors fall into a pattern that was termed "Dead Clade Walking" (DCW) by Jablonski (2002).

3. Global recovery process and patterns of brachiopod faunas

Apart from the relict Permian elements, the true Mesozoic-type brachiopods (32 species from 20 genera and 12 families) have been reported from the Lower Triassic of the Spitzbergen, Primorye of Russia, Mangyslak of Kazakhstan, Alpine Europe, the Himalaya, South China, western USA and probably New Zealand. Their origination represents the recovery of Early Triassic brachiopods. The Early Triassic recovery of brachiopod faunas is characterized by widespread brachiopod dispersal, multiprovincialism and the presence of rare Lazarus genera at that time. Taxonomic selectivity of the recovery brachiopod faunas favors the rhynchonellides. The repopulation of post-extinction brachiopods varies geographically: there is a preference for regions either previously barren of latest Permian taxa and or where rare latest Permian and surviving brachiopods. This unique biogeographic selectivity is probably partly responsible for the depauperate nature of brachiopod faunas in the Triassic (even Mesozoic) oceans. Five intervals of extinction, survival, survival–recovery, recovery–dispersal and radiation, are recognized based on variations in brachiopod faunas of the latest Permian to Early Triassic. A dramatic reduction in brachiopod diversity at the end-Permian mass extinction is followed by several stepwise declines in diversity in the survival interval, the time during which the surviving brachiopods are dominated by geographically widespread generalist faunas that adapted to a wide variety of environments. The survival interval was followed by a slow re-population of new lineages dominated by progenitor taxa.

Bowring, S. A., Erwin, D. H., Isozaki, Y., 1999. The tempo of mass extinction and recovery: The end-Permian example. Proceedings of the National Academy of Sciences of the United States of America, 96: 8827-8828.

Carlson, S. J., 1991. A phylogenetic perspective on articulate brachiopod diversity and the Permo-Triassic extinction. *in* Dudley, E. (ed.) The unity of evolutionary biology, Proceedings of the 4th International Congress of Systematic and Evolutionary Biology. Dioscorides Press, Portland, Oregon, 119-142.

Erwin, D. H., 1993. The great Paleozoic crisis. Columbia University Press, New York, 327 pp.

Erwin, D. H., 1998. The end and the beginning: recoveries from mass extinctions. Trends in Ecology and Evolution, 13: 344-349.

Jablonski, D., 1986. Causes and consequences of mass extinction: a comparative approach. *in* Elliott, D. K. (ed.) Dynamics of Extinction. Wiley, New York, 183-229.

Jablonski, D., 2002. Survival without recovery after mass extinctions. Proceedings of the Natural Academy of Sciences of the United States of America, 99: 8139–8144.

Jin, Y. G., Wang, Y., Wang, W., Shang, Q. H., Cao, C. Q., Erwin, D. H., 2000. Pattern of marine mass extinction near the Permian-Triassic boundary in South China. Science, 289: 432-436.

Kauffman, E. G., Erwin, D. H., 1995. Surviving mass extinctions. Geotimes, 1995: 14-17.

Rudwick, M. J. S., 1970. Living and fossil brachiopods. Hutchinson University Library, London, 199 pp.

Sepkoski, J. Jr., 1981. A factor analytic description of the Phanerozoic marine fossil record. Paleobiology, 7: 36-53.

Sheng, J. Z., Chen, C. Z., Wang, Y. G., Rui, L., Liao, Z. T., Bando, Y., Ishii, K., Nakazawa, K., Nakamura, K., 1984. Permian-Triassic boundary in Middle and Eastern Tethys. Journal of Faculty of Science, Hokkaido University, Series 4, 21(1): 133-181.

Shen, S. Z., Archbold, N. W., Shi, G. R., 2000. Changhsingian (Late Permian) brachiopod palaeobiogeography. Historical Biology, 15: 121-134.

Yang, Z. Y., Wu, S. B., Yin, H. F., Xu, G. R., Zhang, K. X., Bi, X. M., 1993. Permo-Triassic events of South China. Geological Publishing House, Beijing, 153 pp.

Yin, H. F., Zhang, K. X., Tong, J. N., Yang, Z. Y., Wu, S. B., 2001. The Global Stratotype Section and Point (GSSP) of the Permian-Triassic Boundary. Episodes, 24(2): 102-114.

First Occurrence of Mesozoic Brachiopods Coinciding with Paleo-Oceanic Environmental Amelioration After the End-Permian Mass Extinction

Chen Zhongqiang[1], K. Kaiho[2], Tong Jinnan[3] and A. D. George[1]

[1] School of Earth and Geographical Sciences, University of Western Australia, 35 Stirling Highway, Crawley, WA 6009, Australia; zqchen@cyllene.uwa.edua.au

[2] Institute of Geology and Paleontology, Tohoku University, Sendai 980-8578, Japan

[3] Faculty of Earth Sciences, China University of Geosciences, Wuhan 430074, China

As the most devastating crisis in the history of life, the end-Permian mass extinction redirected significantly the evolutionary course of the Brachiopoda. After this event, brachiopods have undergone a prolonged and delayed recovery and their full recovery did not occur until early Middle Triassic (Erwin, 1998). As a result, the Early Triassic was a bad time for brachiopods, which are rare and sparsely distributed worldwide (Chen, in this volume). Since then, brachiopods have been forced to the marginal seas or deep-water environments in the Mesozoic and even Modern oceans (Ager and Sun, 1988). However, prior to their full recovery in Middle Triassic, some opportunistic generalists (*Meishanorhynchia*, for example) rebounded in the Early Triassic oceans, and they together with some Permian relicts characterize the Early Triassic brachiopod faunas (Dagys, 1993). These opportunists consist mainly of the rhynchonellids and spiriferinids, and they are morphologically close to the Mesozoic and even extant genera in many aspects (Chen et al., 2002). The late Griesbachian *Meishanorhynchia* from the Meishan section, South China is likely the oldest genus that originated in the Mesozoic, and thus, may signals the most initial rebound of brachiopod faunas after the end-Permian extinction (Chen et al., 2002). This study thus has the potential to discuss environmental effects to the delayed recovery of brachiopod faunas and paleo-oceanic environmental changes after the event.

To determine subtle vertical lithologic and lithofacies variations we measured the Yinkeng and Helongshan Formations of Griesbachian age in centimeter-scale and recognized six lithologic types of rocks based on constitutional proportions of terrigenous sediments, marls and calcite. In the field we attempted to observe lithology, sedimentary structures, and taphonomy of shell concentrations. Twenty-five samples were sectioned or polished to observe under the microscope, and additional specimens, primarily of Triassic brachiopod *Meishanorhynchia*, were also collected in order to facilitate identification and quantitative analysis of the newly originated Triassic brachiopods. Averagely 3 kg weight samples containing *Meishanorhynchia* were collected from each layer of the five fossil horizons. These tiny brachiopod specimens were extracted from each sample by physically splitting and

abrading the samples. In addition, we also collected 10 and 5 samples to measure calcite contents and Phosphorus (P) isotope values, respectively. The published carbon isotope data (Li, 1999; Cao et al., 2002) are also cited to indicate the geochemical signals of environmental change in the post-extinction oceans in Meishan.

The first occurrence of the Mesozoic brachiopods is associated with an increase of biodiversity of marine community (bivalves, ammonoids, conodonts and fishes) at the lower Helongshan Formation at the Meishan section, South China. On the exposure the most obvious lithologic change in the Griesbachian is that the beds of light gray marl and argillaceous limestone are thickening upwards, while the greenish calcareous mudstone and black shale thinning upwards. Marls and argillaceous limestone are very few and very thin, usually not more than 1 cm thick in the lower part of the section (Beds 29-33); upward to Beds 34-35, the numbers of marl beds gradually increase and the single bed gradually thickens, up to 1-5 cm thick. In Beds 36-37, the numbers of marl beds significantly increase and each single bed thickens up to 7-15 cm. These lithologic variations directly reflect increase of calcite contents throughout the Griesbachian. Although we do not know the relationship between oceanic calcite content and growth of shelly community, *Meishanorhynchia*-dominated shelly community is associated with in- to medium-bedded argillaceous limestone in Meishan, suggesting that calcareous substratum is conducive to population of shelly organisms. The lithologic sequences of the Yinkeng Formation of early Griesbachian age is characterized overall by the mudstone-dominated centimeter-scale cycles in the lower part and the marl- or argillaceous limestone-dominated centimeter-scale cycles in the upper part, indicating a long-term up-shallowing cycle in Griesbachian. In particular, a remarkable hummocky cross-stratification (HCS) bed occurring at the lower Helongshan Formation (upper Griesbachian) is sharp contrast to the mudstone-dominated succession with planar stratifications at the lower Yinkeng Formation. The former was usually generated in the high energy, below wave base environments (Ito et al., 2001), while the latter have been interpreted to be deposited at a deep-water basin environment as result of the maximum flood event at the beginning of the Triassic and the global anoxic event, which may be responsible for the end-Permian mass extinction (Wignall and Twitchett, 1996). The late Griesbachian occurrence of HCS indicates that the depositional environment was up-shallowing and the previously anoxic oceanic floor became oxygenic as frequent storms, when they produced the HCS, brought oxygen to the oceanic floor. Thus, the HCS beds bearing *Meishanorhynchia* represent a relatively shallow, oxygenic environment, which is in sharp contrast to the anoxic, deep-water basin oceanic conditions immediately after the end-Permian extinction (Wignall and Twitchett, 1996). The amelioration of paleo-oceanic environments is also strengthened by a positive shifting of carbon cycle at the late Griesbachian in Meishan (Li, 1999; Cao et al., 2002). The contemporaneous positive shifting cycle of carbon isotope excursion curves has been also recognized from other P/T sections in South China (Tong et al., 2003; Payne et al., 2004). Phosphorus isotope excursion curves demonstrate a comparable pattern: a dramatic negative shifting corresponding to the end-Permian extinction is followed by positive shifting cycle throughout the Griesbachian. The positive shifting of P isotope values probably indicates amelioration of marine productivity (Kaiho et al., 2001). Although the relationship between anomaly of the carbon isotope values and biotic extinction has long been a subject of conjecture (Payne et al., 2004), the positive shifting cycles of carbon and P isotope excursion curves are associated with environmental amelioration revealed by both sedimentary and biotic features in Meishan. This fact indicates that the first episode of environmental amelioration after the end-Permian crisis took place in late Griesbachian in Meishan.

Environmental amelioration in turn likely provided favorable oceanic conditions conducive to the growth of sessile brachiopods. The occurrence of the Mesozoic brachiopods coupled with an increase of biodiversity suggests that an initial recovery of marine organisms, particularly brachiopod faunas, probably occurred in late Griesbachian in South China. Twitchett et al. (2004) suggested that rapid recovery of marine community may have taken place in late Griesbachian in the region where the marine anoxia was absent. Alternatively, the paleo-oceanic environments have been obviously ameliorated in late Griesbachian, as evidenced above, although the earliest Triassic oceans in South China were obviously oxygen-restricted (Wignall and Twitchett, 1996). If the Payne et al. (2004) assumption that “the carbon isotope variations represent repeated environmental disturbances that directly inhibited biotic recovery” is correct, then more extensive paleo-oceanic environmental amelioration, signaled by the positive shifting cycle of carbon isotope excursion curves, is recognizable in South China. Consequently, we believe that the first episode of the global paleo-oceanic environmental amelioration after the end-Permian mass extinction took place in late Griesbachian when marine organisms may have initially rebounded, although the recovery of many fossil groups may be unsuccessful. For instance, although *Meishanorhynchia* is extremely abundant in late Griesbachian in Meishan, this Mesozoic brachiopod did not spread and radiate in the Early Triassic oceans in South China. This is probably because the oceans became stressed soon after, indicated by rapid negative shifting of carbon cycles by the end-Griesbachian (Tong et al., 2003; Payne et al., 2004). As such, once their favorable oceanic conditions (calcareous substratum, oxygenic sea floor, shallow water, and recovery of marine productivity) occurred, brachiopods might rebound locally. However, the stressed oceanic conditions indicated by large perturbation of the carbon cycles throughout the Early Triassic (Payne et al., 2004) obviously prevented the spread of the rebounding brachiopods. Brachiopoda therefore underwent overall unsuccessful recoveries, although some progenitor taxa rebound sparsely during the Early Triassic around the world.

Ager, D. V., Sun, D. L., 1988. Distribution of Mesozoic brachiopods on the northern and southern shores of Tethys. Palaeontologia Cathayana, 4: 23–51.

Cao, C. Q., Wang, W., Jin, Y. G., 2002. Carbon isotope excursions across the Permian-Triassic boundary in the Meishan section, Zhejiang Province, China. Chinese Science Bulletin, 47(13): 1125-1129.

Chen, Z. Q., Shi, G. R., Kaiho, K., 2002. A new genus of rhynchonellid brachiopod from the Lower Triassic of South China and implications for timing the recovery of Brachiopoda after the end-Permian mass extinction. Palaeontology, 45: 149–164.

Dagys, A. S., 1993. Geographic differentiation of Triassic brachiopods. Palaeogeography, Palaeoclimatology, Palaeoecology, 100: 79–87.

Erwin, D. H., 1998. The end and the beginning: recoveries from mass extinctions. Trends in Ecology and Evolution, 13: 344–349.

Ito, M., Ishigaki, A., Nishikawa, T., Saito, T., 2001. Temporal variation in the wavelength of hummocky cross-stratification: Implications for storm intensity through Mesozoic and Cenozoic. Geology, 29: 87-89.

Kaiho, K., Kajiwara, Y., Nakano, T., Miura, Y., Chen, Z. Q., Shi, G. R., 2001. End-Permian catastrophe by a bolide impact: evidence of a gigantic release of sulfur from the mantle. Geology, 29: 815-818.

Li, Y. C., 1999. Carbon isotope cyclostratigraphy of the Permo-Triassic transitional limestones in South China. Journal of Nanjing University (Natural Sciences), 35(3) : 277-285.

Payne, J. L., Lehrmann, D. J., Wei, J. Y., Orchard, M. J., Schrag, D. P., Knoll, A. H., 2004. Large perturbations of the carbon cycle during recovery from the end-Permian extinction. Science 205(5683): 505-509.

Tong, J. N., Zakharov, Y. D., Orchard, M. J., Yin, H. F., Hansen, H. J., 2003. A candidate of the Induan-Olenekian boundary stratotype in the Tethyan region. Science in China, Series D, 46(11): 1182-1200.

Twitchett, R. J., Krystyn, L., Baud, A., Wheeley, J. R., Richoz, S., 2004. Rapid marine recovery after the end-Permian mass-extinction event in the absence of marine anoxia. Geology, 32: 805–808.

Wignall, P. B., Twitchett, R. J., 1996. Oceanic anoxia and the end Permian mass extinction. Science, 272: 1155–1158.

Progress on the Cisuralian (Lower Permian) Time-Scale, Southern Urals, Russia

Vladimir I. Davydov[1] and Bruce Wardlaw[2]

[1] Dept. Geosciences, Boise State University, 1910 University Dr., Boise, ID, USA; vdavydov@boisestate.edu

[2] US Geological Survey, Reston, Virginia, USA; bwardlaw@usgs.gov

The Cisuralian Series (Lower Permian) has been formally established for the Lower Permian (Jin et al., 1994). The southern Ural Mountain region is the type area for the Cisuralian, comprising the Asselian, Sakmarian, Artinskian and Kungurian stages. These stages initially were defined and widely recognized on ammonoid phylogenies (Karpinsky 1889; Ruzhencev 1937, 1950, 1951, 1956). However, stage boundaries and subdivisions were established on the basis of fusulinaceans, the most abundant and best studied upper Paleozoic fossil group of the southern Urals. Body stratotypes for all stages were located in the southern Urals and it is expected that the boundary stratotypes (GSSP) for all Cisuralian stages will be formally established in this region. The Working Group to establish Cisuralian stages has achieved a significant progress in developing time scale (Chuvashov et al., 2003). Although GSSP of the base of the lowermost Cisuralian Asselian stage is already established at the Aidaralash section, NW Kazakhstan (Davydov et al., 1998), we are proposing to establish auxiliary stratotype section for the Global Stratotype section and Point for the Carboniferous-Permian boundary at Usolka section to adjust some of the features that are not present in Aidaralsh section. Particularly, conodont succession at Carboniferous-Permian boundary beds in Usolka section seems to represent much more details (Chernykh, 2005). Most important is the presence of numerous volcanic ash beds recently recovered in the section what make radiometric control of the most of the Cisuralian boundaries possible (Davydov et al., 2002).

The **Asselian** stage was established by Ruzhenzev (1954), but the stage in the Asselian body stratotype (Assel section, located on the ridge between the Assel and Uskalyk rivers in southern Bashkortostan) is incomplete. Ruzhenzev distinguished the Asselian by a particular ammonoid assemblage which in the Urals corresponds with the entire range of the fusulinid *Sphaeroschwagerina.* The Global Stratotype Section and Point (GSSP) for the base of the Permian and basal Cisuralian Asselian Stage was proposed at Aidaralash Creek, Aktöbe (formerly Aktyubinsk) region, northern Kazakhstan. Asselian in the southern Urals divides into six foraminiferal zones and an equal number of conodont zones (Shamov 1940; Rauser-Chernousova 1949; Davydov 1986, 1996; Davydov et al. 1997; Chuvashov et al. 1990; Chernykh and Chuvashov 1991). The strata of Late Paleozoic age at Aidaralash Creek were deposited on a narrow, shallow marine shelf that formed the western boundary of the orogenic zone to the east. The fluvial - deltaic conglomerate

- sandstone successions grade upwards into transgressive, marginal marine sequences of (beach and upper shore face) that, in turn, grade upwards into massive mudstone-siltstone and fine sandstone beds with ammonoids, conodonts and radiolarians interpreted as maximum flooding units. The maximum flooding zone is overlain by a regressive sequence (progressively, offshore to shoreface to delta front), which in turn is capped by an unconformity with a overlying conglomerate. The critical GSSP interval is completely within a maximum flooding unit; free of disconformities.

The position of the GSSP is at the first occurrence of the conodont *Streptognathodus isolatus*, which developed from an advanced morphotype in the *S. wabaunsensis* chronocline. This is located 27 m above the base of Bed 19, Airdaralash Creek (Davydov et al., 1998).

The first occurrences of *Streptognathodus invaginatus* and *S. nodulinearis*, also morphotypes of the '*wabaunsensis'* morphocline, nearly coincide with the first occurrence of *S. isolatus* in many sections, and can be used as accessory indicators for the boundary.

The GSSP is 6.3 m below the traditional fusulinid boundary, i.e. the base of the *Sphaeroschwagerina vulgaris aktjubensis-S. fusiformis* Zone (Davydov et al., 1998). The latter can be widely correlated from Spitsbergen, the Russian Platform, Urals, Central Asia, China and Japan, and is of practical value to identify the boundary between the Orenburgian and overlying Asselian stages. The traditional ammonoid boundary, 26.8 m above the GSSP, includes the termination of the *Prouddenites-Uddenites* lineage at the top of Bed 19, and the introduction of the Permian taxa *Svetlanoceras primore* and *Prostacheoceras principale* in Bed 20 (Davydov op. cit., figure 2). The evolution from *Artinskia irinae* to *A. kazakhstanica* maybe a chronocline that crosses the C/P boundary. A problem with the ammonoid taxa is that they are relatively rare, and many taxa may be endemic to the Urals.

Utilization of magnetostratigraphy to assist with recognition and correlation of the C/P boundary is difficult because it is in the Kiaman Long Reversed Polarity Chron. However, Davidov & Khramov (1993) cite reports that show that most of the *Ultradaixina bosbytauensi-Schwagerina robusta* fusulinid zone, just below the C/P boundary in Aidalarash is characterized by normal polarity. That same stratigraphic polarity relationship is also known elsewhere from the southern Urals, and the northern Caucasus and Donetz Basin, and possible correlates to the normally polarized magnetic zone in the Manebach Formation of the Thuringian Forest (Menning, 1987).

The conodont succession observed at Airdaralash is displayed in several sections in the southern Urals, especially the basinal reference section at Usolka. It is also displayed in the Red Eagle cyclothem of the MidContinent of the US (Boardman et al., 1998), the West Texas regional stratotype in the Wolfcamp Hills (Wardlaw and Davydov, 2000), and China (Wang, 2000) as well as many other intervening localities and, therefore, serves as an excellent boundary definition.

Base of Sakmarian Stage

Sakmarian (s. s.) in its present context was proposed by Ruzhenzev, 1955 with its stratotype at the Kondurovka section, (Karamuruntau Ridge, southern Orenburg Province) and based on ammonoid and fusulinid assemblages. No ammonoids are known in the lower portion of Sakmarian, and thus the base of this stage traditionally has been defined by first appearance species of *Schwagerina moelleri* ("*Pseudofusulina*" *moelleri* in Russian nomeclature). Because fusulinid species are provincial, this definition is effective only in the Boreal and in the western Tethyan realms. A Sweetognathid (conodont) chronomorphocline exhibiting the evolutionary change from *Sweetognathus expansus* (Perlmutter) to *Sweetognathus merrilli* Kozur at 115 meters above base (mab) (uppermost Bed 11 of Chuvashov et al., 1993 The boundary originally proposed by Ruzhencev (1950) was at the base of Bed 11(91 mab) at an unconformable formation break and based on the change in fusulinaceans faunas with *Schwagerina (Pseudofusulina) moelleri* occurring above the break. The actual introduction of the fusulinacean *Schwagerina (Pseudofusulina) moelleri* group occurs in beds 6-12 (Davydov et al., 1999), with traditional *Sch. moelleri* occurring in Bed 12, just a few meters above the first occurrence of *Sw. merrilli*. *Sweetognathus merrilli* is widespread and its FAD is well constrained throughout Kansas in the upper part of the Eiss Limestone of the Bader Limestone.

Base of Artinskian Stage

The Artinskian Stage as originally proposed by Karpinsky (1874) included all the Upper Paleozoic clastic deposits of the Preuralian Foredeep (Artinskian Sandstone by Murchison, 1845) overlying Carboniferous carbonates. Artinskian Stage in current context as established by Ruzhenzev (1954) was characterized by ammonoids and fusulinids. The body Artinskian stratotype is in a series of sandstone quarries on Kashkabash Mount near the Arti village on right bank of Ufa river, which actually corresponds only with the upper portion of Artinskian. The taxonomically diverse ammonoid assemblage from the Arty area was distinctly more advanced than the Sakmarian one in terms of cephalopod evolution and this stimulated Karpinsky (1874) to define two belts with ammonoids; the lower at the Sakmara River and the upper at the Ufa River. Most of the characteristics concerning the Artinskian are derived from investigation of clastic-rich sections and ammonoids phylogenies from the Preuralian Foredeep in the southern Urals best represented in Aktasty and Zhiltau sections (Ruzhenzev, 1954) and from carbonate sections and fusulinid phylogenies from the eastern margin of the Russian Platform (Rauser-Chernousova, 1949). Fusulinids and ammonoids species from the Urals are provincial and can not be used for GSSP definition. Conodonts are more appropriate.

The Sakmarian-Artinskian boundary deposits are well

represented in the Dal"ny Tulkus section, a counterpart of the Usolka section. The upper part of the Sakmarian Stage (Beds 28-31) at the Usolka River and Bed 18 at the Dal"ny Tulkus Section are composed of dark-colored marl, argillite, and carbonate mudstone, or less commonly, detrital limestone with fusulinids, radiolarians, rare ammonoids, and bivalves. The upper part of the Sakmarian includes fusulinids characteristic of the Sterlitamakian Horizon including *Pseudofusulina longa*, *P. fortissima*, *P. plicatissima*, *P. urdalensis* and *P. urdalensis abnormis*.

The best section appears to be the Dal"ny Tulkas section in Russia, a point that potentially defines base of Artinskain located within few meters where the chronomorphocline from *S. binodosus* to the FAD of *Sweetognathus whitei* is recovered. A sample from the Dal'ny Tulkas section (5045-8a) includes *S. binodos*us and *S. whitei* (including specimens with well defined pustulose fields and others with poorly developed and irregular fields). In a lower sample (5045-4a), *Sweetognathus obliquidentatus* and *S. sulcatus* co-occur; these taxa represent a near homeomorph of *Neostreptognathodus* by developing a shallow and partial sulcus separating the nodes. *Sweetognathus sulcatus* was previously reported from the Cerro Alto Formation in the Franklin Mountains of West Texas in an interval associated with *Diplognathodus stevensi* and *S. binodosus* (reported as *S. inornatus*, Ritter, 1986). It is possible that these neostreptognathodid-like elements represent evolutionary experimentation during the speciation event leading to *S. whitei* in which the bilobed nodes of *S. binodosus* separate in a very irregular fashion. This is reminiscent of the irregular nodes of *S. merrilli* in the lower part of its range and of *Sweetognathus clarki* (which includes *S. transitus*, *S. ruzhencevi*, *S. tschuvaschovi* in synonymy) during the evolution of *Neostreptognathodus pequopensis*. The above-mentioned conodonts occur in the limestone member (Bed 19) at the base of the Tyul'kas Formation (Chuvashov et al., 1990). That unit is also characterized by the fusulinids *Psuedofusulina callosa*, *P. urdalensis*, *P. karagasensis*, *P. concavatus*, *P*. ex. gr. *jurasanensis*, and *P. uralensis*. Ammonoids from the same unit include *Popanoceras annae*, *P. tchernowi*, and *Kargalites* sp.; the unit, 3.5 m higher than Bed 19, includes the ammonoids: *Neopronorites skvorzovi*, *Popanoceras annae*, and *P. congregale*.

The limestone member (Bed 19) and several levels in the Tyul'kas Formation yielded the conodonts *Mesogondolella bisselli* (Clark and Behnken) and *Sweetognathus whitei* (Rhodes). Several levels within the Tyul'kas Formation at the Usolka section have yielded radiolarians of the *Enactinosphaera crassicalthrata-Quinqueremis arundinea* Zone.

The defining chronomorphocline of *Sweetognathus binodosus* to *S. whitei* also can be recognized in the lower Great Bear Cape Formation on southwestern Ellesmere Island, Sverdrup Basin, Canadian Arctic (Henderson, 1988; Beauchamp and Henderson, 1994, Mei et al., 2002) and in the Schroyer to Florence Limestones of the Chase Group in Kansas, USA (Wardlaw et al., 2003).

Base of Kungurian Stage

The stratotype of the Kungurian Stage was not defined when the stage itself was established (Stuckenberg, 1890). Later on, the carbonate-sulphate section exposed along the Sylva River upstream of the town of Kungur was arbitrarily accepted for the stratotype. In line with a new position of the Kungurian lower boundary at the base of the Sarana Horizon (Chuvashov et al., 1999), a stratotype section in this area consists of: (1) the Sarana Horizon including the Sylva Formation of reefal limestones and its lateral equivalent Shurtan Formation composed of marls and clayey limestone, (2) the Filippovskian Horizon, (3) the Iren' Horizon. A disadvantage of the section is the poor paleontologic characteristics of the limy Kamai Formation underlying the Sarana Horizon; it contains only small foraminifers, bryozoans, and brachiopods inappropriate for age determination. Nevertheless, many features indicate that the formation corresponds to the Sarga Horizon.

The Shurtan Formation and lateral facies of Sylva bioclastic limestone yield conodonts of the *Neostreptognathodus pnevi* Zone. However, another section of the Artinskian-Kungurian boundary deposits located near the Mechetlino settlement at the Yuryuzan' River has good faunas both below and above the boundary interval and has been selected for a probable stratotype of the Kungurian lower boundary.

The probable stratotype section (Chuvashov et al., 1990, Chuvashov et al. 2002) is exposed along the right bank of the Yuryuzan' River downstream of the Mechetlino settlement. Beds 1-18 are Sarga Horizon, Gabdrashitovo Formation. Bed 13 comprises dark grey argillite with irregularly alternating thin layers of fine-grained sandstone and includes ammonoids and conodonts including *Neopronorites permicus*, *Medlicottia orbignyana*, *Uraloceras fedorowi*, *Sweetognathus* aff. *whitei*, and *Stepanovites* sp., all characteristic of the Sarga Horizon. Bed 15 is an olistostrome with a matrix comprising fusulinids, solitary rugose corals, brachiopods, bryozoa, crinoids, and calcareous algae. The fusulinid assemblage includes abundant *Pseudofusulina kutkanensis*, *P.* aff. *kusjanovi*, *P. franklinensis*, *P. postsolida*, *P. makarovi*, and *Parafusulina solidissima*. Bed 17 is composed of highly calcareous, dark grey argillite with grey, calcareous, fine-grained sandstone. This bed has yielded the conodonts *Neostreptognathodus kamajensis*, *N. pequopensis*, *N*. aff. *ruzhencevi*, and *Sweetognathus* ex. gr. *whitei* represented by aberrant specimens with reduced carinae. Bed 18 is a highly calcareous, yellowish-grey sandstone with thin

interbeds of greenish-grey argillite and abundant plant detritus, but lacks conodonts and fusulinids. Beds 19-20 are Kungurian Stage, Sarana Horizon, Mysovsk Formation, Transitional Member. Bed 19 comprises steel-grey carbonate mudstone with an admixture of extremely fine-grained clastics and rare argillite interbeds. The basal part includes *Neostreptognathodus clinei*, *N. pnevi*, *N. kamajensis*, *N. pequopensis*, and *Stepanovites* sp. Bed 20 is a yellowish-grey, thin-bedded, fine-grained, calcareous sandstone with thin argillite interbeds and abundant plant debris. Beds 21-22 are Filippovskoe Horizon, Mysovoi Formation, Ismagilovo Member. Bed 21 is composed of steel-grey carbonate mudstone and rare interbeds of microclastic limestone that yield the ostracod *Paraparchites burkemis* characteristic of the *Paraparchites humerosus* Zone and the conodonts *Neostreptognathodus pequopensis*, *N. pnevi*, *N.* aff. *ruzhencevi*, and *N. tschuvashovi*.

The best section appears to be the Metchetlino section or a nearby section in Russia, but a point cannot be defined precisely except that the definition will be the FAD of *Neostreptognathodus pnevi* within a chronomorphocline from advanced *Neostreptognathodus pequopensis*. Bed 17 yields *N. kamajensis* and *N. pequopensis* and bed 19 includes *N. kamajensis*, *N. pequopensis*, *N. clinei*, and *N. pnevi*. Bed 18 is a sandy lithofacies that has not yielded conodonts. A laterally equivalent section includes limestone facies within Bed 18; additional samples are required from bed 18 and 19 in this section near the Metchetlino section before a precise point can be defined.

The defining chronomorphocline can also be recognized in the upper Great Bear Cape Formation and upper Trappers Cove Formation on southwestern Ellesmere Island, Sverdrup Basin, Canadian Arctic (Henderson, 1988; Beauchamp and Henderson, 1994, Mei et al., 2002).

A Stratigraphic, Biostratigraphic, Paleobiologic Digital Information System: PaleoStrat and the CHRONOS System

V. I. Davydov[1], B. R. Wardlaw[2], T. Taylor[3], M. D. Schmitz[4], J. R. Groves[5], T. A. Schiappa[6] and W. S. Snyder[7]

[1] Dept. Geosciences, Boise State University, 1910 University Dr., Boise, ID, USA; vdavydov@boisestate.edu

[2] US Geological Survey, Reston, Virginia, USA; bwardlaw@usgs.gov

[3] Dept. Geosciences, Boise State University, Boise, ID, USA; ttylor@boisestate.edu

[4] Dept. Geosciences, Boise State University, Boise, ID, USA; ttylor@boisestate.edu

[5] Department of Earth Science, University of Northern Iowa, 121 Latham, Cedar Falls, IA 60614-0335,USA; john.groves@uni.edu

[6] Dept. of Geography, Geology and the Environment, VSH 225C, Slippery Rock University of Pennsylvania, Slippery Rock, PA 16057, USA; tamra.schiappa@sru.edu

[7] Dept. Geosciences, Boise State University, 1910 University Dr., Boise, ID, USA; wsnyder@boisestate.edu

Key words: Database, IT technologies, WEB interaction, global chronostratigraphy

PaleoStrat (www.paleostrat.org) is a digital information system for sedimentary, paleontologic and stratigraphic data that is hosted at Boise State University (Boise, Idaho, USA) and is part of the *CHRONOS System* (www.chronos.org). PaleoStrat provides a sample- and stratigraphically oriented database and visual and analytical tools that deliver detailed information in the context of stratigraphic successions. The PaleoStrat and *CHRONOS System* data include lithostratigraphic, biostratigraphic, taxonomic, sequence stratigraphic, cyclostratigraphic, geochronologic, major, trace, and isotope geochemical, and other data and metadata relevant to sedimentary geology and paleobiology research. These data and tools support a broad array of integrative research projects that need to combine data in a framework of geologic age and stratigraphic succession. Research topics supported by PaleoStrat include the paleobiologic evolution, extinction, radiation and migration, diversity of life, climate change, geochemical cycles, sequence and cyclostratigraphy, paleoceanography, crustal dynamics of orogenic systems, and many other aspects of the Earth system. We enable the deep-time geologic record to be understood within a framework of the chemical, physical, climatic, astronomical, eustatic, and tectonic processes that collectively govern the operation of the Earth system.

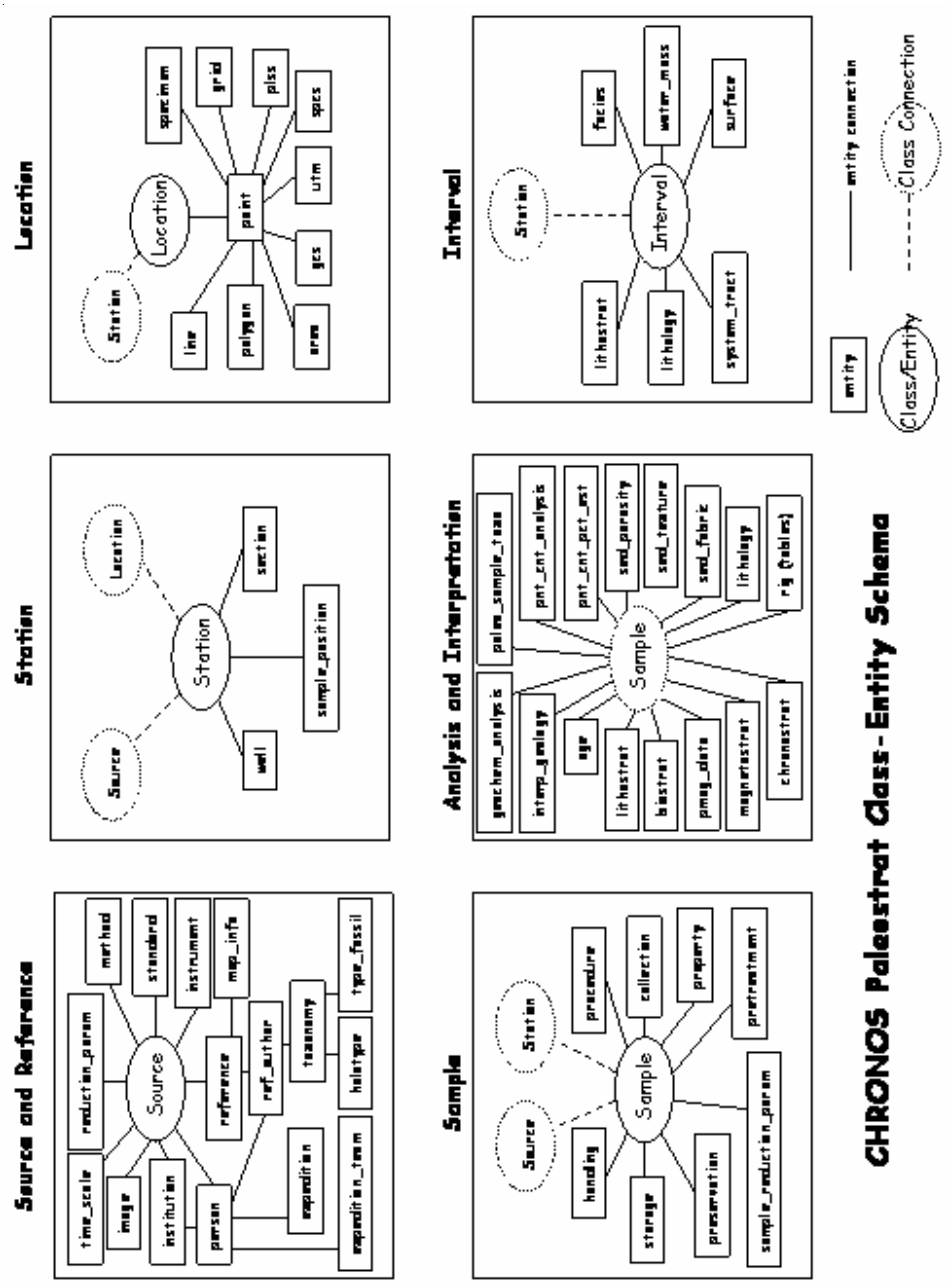

Figure 1. Simplified database concept for PaleoStrat

Personal Data, Published Data, and Long-term Data Preservation. PaleoStrat and the *CHRONOS System* provide a long-term interactive archive of critical data and will work with other geoinformatics projects, NSF, and other federal agencies to ensure the preservation of these data. PaleoStrat's "My Data" site allows individual users or working groups to store personal data prior to publication or public release while integrating these data with the larger, public data sets in their user space. These data will be accessible to the broader geoinformatics community once the user has indicated they can be made public ("published"), and will always be fully attributed to the person/group that developed the data ("branded"). Because it is part of a public database, the preservation of and access to these data are assured, providing also a mechanism to meet existing and upcoming reporting requirements for data by the US-NSF and other funding agencies.

Data Input. PaleoStrat will allow users to add data in a variety of ways. Data can be input in web forms or uploaded from spreadsheet templates designed on the PaleoStrat data model. As the geochemical and geochronological communities agree on standards, PaleoStrat could potentially capture data output from mass spectrometers and other instruments in preliminary databases, then allow the analysts to decide, as they now do manually, which data to pass through to the PaleoStrat database. Users who have large amounts of data that are not in digital format or that require reformatting can either send them to PaleoStrat where supervised and trained students, in consultation with the data provider, will digitize the data and metadata information needed for the database, or re-

quest support from a funding agency to do it themselves. To make accessible legacy data that do not easily fit into PaleoStrat, "flat" files (e.g., spreadsheets) and related metadata can also be networked (indexed) and made searchable. Some larger legacy data sets may require a small external grant to the individual researchers for local data input in collaboration with the PaleoStrat and *CHRONOS System* team, for which PaleoStrat will provide a letter of support.

Data Searching and Output. Data output can be very simple if: 1) the database remains relatively uncomplicated, and 2) the science question being asked is similarly reasonably straightforward. However, once the database (e.g., PaleoStrat) becomes more complex in terms of schemas (database structure) or their connectivity with other databases (e.g., of the *CHRONOS System*), the issue of searching and data output becomes a significant challenge. Hence, PaleoStrat will continue to evolve its approach to searching and data output. In general, we have considered several approaches to data output, including: 1) form-based, user-defined searches, and 2) GIS-based and TIS-based (Geographic and Timescale Information Systems, respectively) query interfaces, and 3) web service calls. In addition, users can write their own SQL (Structured Query Language) searches into any of the databases in the *CHRONOS System* including PaleoStrat. Because data in PaleoStrat are geospatially and temporally defined, data can be searched based on location and geologic age using GIS- and the temporal equivalent of GIS – TIS-type interfaces – and eventually paleogeographic maps. PaleoStrat provides the ability for stratigraphic sections to be searched for all data within the stratigraphic context of the section (e.g., lithology, geochemistry, biostratigraphy). A Graphical User Interface (GUI) based on location, geologic age, and stratigraphic succession is being developed that will allow the user to perform standard queries and will eventually allow the development of individual complex queries unbound by canned SQL searches. The PaleoStrat web site will allow users to save their searches to make future work easier. Finally, we plan to continue to work with the international community to develop better approaches to searching.

Tools. One of the distinctive aspects of the *CHRONOS System*, as encouraged by the community, is to provide the user with tools to analyze and visualize the data. The user community views the need for data and tools as a single activity, done in parallel, not in sequence or separately. Although this adds to the complexity of development for PaleoStrat the *CHRONOS System*, we have designed the system to provide this critical service. We also are working to accommodate the need to format data so the user can utilize proprietary, commercial tools on their own workstations or desktop computers (e.g., software available from RockWare.com).

Fundamental among the tools that PaleoStrat will offer via the *CHRONOS System* are algorithms that estimate the sequence, timing, and correlation of ancient events from the sum total of large amounts of local and potentially contradictory data. These tools enable the user to present the electronic stratigraphic record as a unified composite time line. Time scale data are provided through the partnership with the International Commission on Stratigraphy (ICS, www.stratigraphy.org), the definitive source for up-to-date information on the global time scale. *Chronos* also provides access to a suite of time scales (both local and global), translations among the various time scales, and user-generated age models. The community has identified graphic correlation, paleogeographic mapping, and statistical tools as key components of the toolkit. In the proof-of-concept phase, we focused on the "low hanging fruit," i.e., tools that can be easily modified and adapted for broader accessibility, but the suite of tools will continue to expand. These initial tools include the graphic-correlation tool ADP (age/depth plotting) and the stratigraphic sequencing tool CONOP9.

CONOP9 (P. Sadler, University of California, Riverside) sequencing tool provided as an integral web service from the *CHRONOS System* and hence to PaleoStrat. It is an extremely flexible solver for the stratigraphic sequencing problem and serves as an exploratory case study for tool implementation in general. Other components of the tool kit will include publication quality graphical and statistical tools (including the packages *PAST* by Øyvind Hammer [University of Oslo, http://folk.uio.no/ohammer/past/] and *Stratistics* by Roy Plotnick [University of Illinois Chicago]), paleogeographic maps, time scale conversion tools (of which two are already available), time series analysis tools (including interpolation, correlation, tuning, spectral analysis, digital filtering, demodulation, and orbital-insolation modeling), stratigraphic section construction tool, in addition to the existing web service that allows visualization of the full or partial 2004 Global Time Scale with the level of detail chosen by the user.

The Latest Permian-Early Triassic Biocalcification Crisis

Margaret L. Fraiser and David J. Bottjer

Department of Earth Sciences, University of Southern California, Los Angeles, CA 90090-0740; fraiser@usc.edu

The long interval of terrestrial and marine biotic degradation encompassing the latest Permian and Early Triassic has been attributed to a cascade of effects and feedback mechanisms ultimately initiated by continental flood basalt volcanism of the Siberian Traps (Wignall, 2001; Retallack et al., 2003) (Fig. 1). In the marine realm, CO_2 injected into the atmosphere by successive eruptions of flood basalt from the Siberian Traps was a major factor in the end-Permian mass extinction and the prolonged Early Triassic biotic crisis by facilitating hypercapnia (Knoll et al., 1996), global warming, marine anoxia, and the re-

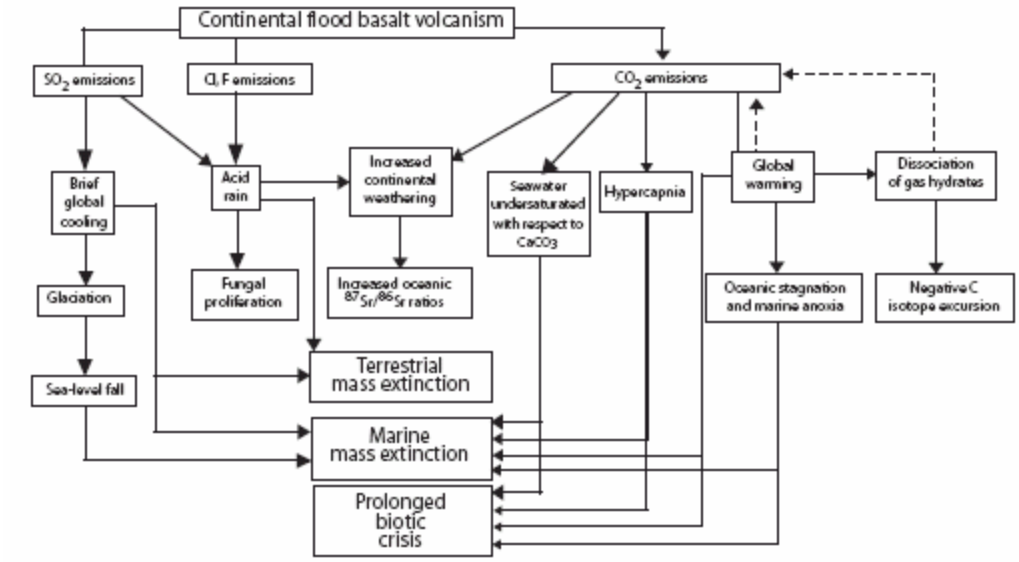

Figure 1. Comprehensive model for continental flood basalt-related mechanisms for the end-Permian mass extinction and the prolonged Early Triassic biotic crisis (modified from Knoll et al., 1996; Wignall, 2001)

lease of methane in methane hydrates (e.g., Wignall, 2001) (Fig. 1). Sedimentologic, isotopic, and paleontologic evidence support these mechanisms for ecological degradation linked to Siberian Trap volcanism. However, this model in its current state does not fully explain all latest Permian extinction patterns or all aspects of the Early Triassic marine biota. For example, paleontologic evidence for prolonged biotic crisis occurs in regions where there is no sedimentologic or isotopic evidence for anoxic seawater (e.g., Fraiser and Bottjer, 2004).

Extensive recent deliberation on the potential impacts of increasing atmosphere/ocean CO_2 concentrations due to anthropogenic input (Feely et al., 2004; Sabine et al., 2004) alludes that one mechanism is conspicuously missing from models of end-Permian/Early Triassic marine ecologic degradation: a biocalcification crisis. Passive diffusion of atmospheric CO_2 into the ocean causes [CO_3^{-2}] concentration and the $CaCO_3$ saturation state of seawater to decrease, causing a biocalcification crisis for many organisms (Feely et al., 2004; Sabine et al., 2004). The degree and rate of calcification among corals and coral reef communities (e.g., Kleypas et al., 1999), coccolithophores (e.g., Riebesell et al., 2000), and foraminiferans (e.g., Barker and Elderfield, 2002) decreases as the $CaCO_3$ saturation state of seawater decreases. Organisms with aragonitic and high-magnesium calcite skeletons may experience greater dissolution than calcite producers under increased atmospheric CO_2 conditions (Feeley et al., 2004). Furthermore, increased CO_2 may result in narrowing of inhabitable water for some biogenic carbonate producers and, as the ocean becomes increasingly undersaturated over time, the aragonite and calcite saturation depths will likely shoal and dissolution of $CaCO_3$ particles will increase (Feely et al., 2004; Sabine et al., 2004).

Based on modern observations, latest Paleozoic/earliest Mesozoic increases in atmospheric CO_2 due to Siberian Trap volcanism should have led to increased ocean CO_2 levels and decreased $CaCO_3$ saturation of seawater, causing a long-term biocalcification crisis in skeletonized invertebrate benthic marine organisms. Indeed, such a biocalcification crisis readily explains extinction patterns of major groups of reef organisms at the end of the Permian (Kiessling, 2002), and the protracted absence of colonial metazoan reefs and reef organisms (Kiessling, 2002), opportunistic behavior of many groups of organisms (Fraiser and Bottjer, 2004), and the decrease in size of many benthic marine organisms during the Early Triassic (Fraiser and Bottjer, 2004). Metazoan reef-builders (Kiessling, 2002) and larger shells (Fraiser and Bottjer, 2004) reappear when atmospheric CO_2 levels decrease. This particular effect of increased ocean CO_2 concentration, in addition to the associated effects of global warming, hypercapnia and marine anoxia, was a major contributor to this protracted interval of biotic crisis (Fig. 1).

The complex interplay of perturbations to the global atmosphere and ocean triggered by Siberian Trap volcanism was manifested in different ways in various parts of the globe, as demonstrated by a spatially and temporally varied biotic crisis. For example, while numerous lines of evidence outlined here indicate that surface waters in much of the world's oceans were undersaturated with respect to $CaCO_3$ during the latest Permian-Early Triassic, other lines of evidence, including submarine carbonate fans (Woods et al., 1999) and microbial reefs (Pruss and Bottjer, 2004), indicate that due to deep-water stagnation and anoxia, parts of the world's oceans experienced $CaCO_3$ supersaturation during this time. These varied regional and temporal patterns likely resulted from new upwelling patterns and sea level fluctuations related to impingement of superplumes and continental flood basalt province volcanism (Hallam and Wignall, 1999), for which the precise relationships still must be deciphered.

Evidence indicates that undersaturation of seawater with respect to $CaCO_3$ was also a contributing factor to the end-Triassic (Hautmann, 2004) and early Toarcian mass extinctions. These ancient biocalcification crises are an analogue for the fate of Earth's marine biota if anthropogenic input of atmosphere/ocean CO_2 continues to rise.

Barker, S., Elderfield, H., 2002. Foraminiferal calcification response to glacial-interglacial changes in atmospheric CO_2: Science, 297: 833-836.

Feely, R. A., Sabine, C. L., Lee, K., Berelson, W., Kleypas, J., Fabry, V. J., Millero, F. J., 2004. Impact of anthropogenic CO_2 on the $CaCO_3$ System in the oceans. Science, 305: 362-366.

Fraiser, M. L., Bottjer, D. J., 2004. The Non-Actualistic Early Triassic Gastropod Fauna: A case study of the Lower Triassic Sinbad Limestone Member. Palaios, 19: 259-275.

Hallam, A., Wignall, P. B., 1999. Mass extinctions and sea-level changes: Earth-Science Reviews, v. 48, p. 217-250.

Hautmann, M., 2004. Effect of end-Triassic CO_2 maximum on carbonate sedimentation and marine mass extinction. Facies, 50: 257-261.

Kiessling, W., 2002. Secular variations in the Phanerozoic reef ecosystem. *in* Phanerozoic Reef Patterns, SEPM Special Publication No. 72, 625-690.

Kleypas, J. A., Buddemeier, R. W., Archer, D., Gattuso, J.-P., Langdon, C., Opdyke, B. N., 1999. Geochemical consequences of increased atmospheric carbon dioxide on coral reefs. Science, 284: 118-120.

Knoll, A. H., Bambach, R. K., Canfield, D. E., Grotzinger, J. P., 1996. Comparative earth history and Late Permian mass extinction. Science, 273: 452-457.

Pruss, S. B., Bottjer, D. J., 2004. Late Early Triassic microbial reefs of the western United States: a description and model for their deposition in the aftermath of the end-Permian mass extinction. Palaeogeography, Palaeoclimatology, Palaeoecology, 11: 127-137.

Retallack, G. J., Smith, R. M. H., Ward, P. D., 2003. Vertebrate extinction across Permian–Triassic boundary in Karoo Basin, South Africa. Geological Society of America Bulletin, 115: 1133–1152.

Riebesell, U., Zondervan, I., Rost, B., Tortell, P. D., Zeebe, R. E., Morel, F. M. M., 2000. Reduced calcification of marine plankton in response to increased atmospheric CO_2. Science, 407: 364-367.

Sabine, C. L. *et al*., 2004. The ocean sink for anthropogenic CO_2. Science, 305: 367-371.

Wignall, P. B., 2001. Large igneous provinces and mass extinctions. Earth-Science Reviews, 53: 1-33.

Woods, A. D., Bottjer, D. J., Mutti, M., Morrison, J., 1999. Lower Triassic large seafloor carbonate cements: their origin and a mechanism for the prolonged biotic recovery from the end-Permian mass extinction. Geology, 27: 645-648.

Lower Triassic Magnetostratigraphy in Chaohu, Anhui Province, South China.

Hans J. Hansen[1] and Tong Jinnan[2]

[1] Geological Institute, University of Copenhagen, DK-1350 Copenhagen, Denmark; dinos@geol.ku.dk

[2] State Key Laboratory of Geo-Processes and Mineral Resources, China University of Geosciences, Wuhan 430074, China

288 m of marine sediments, that span the Permo-Triassic boundary, the complete Induan, and a major part of the Olenekian, were covered by 213 plugs. The complete sequence is composed of 5 normal intervals separated by reversed intervals (Fig. 1). The uppermost reversed interval remains open like the lowermost normal interval. The Permo-Triassic boundary rests in a normal period. The biostratigraphic Induan-Olenekian boundary is situated close to the top of the second normal interval. The section is the first Lower Triassic sequence from the Lower Yangtze region with definite biostratigraphic control (Fig 2).

The lower 10 m of Induan sediments from the ACP (North Pingdingshan) profile was sampled for magnetic susceptibility with a resolution of 2 cm (Fig. 3-4). The variation pattern corresponds to the bedding sequence. Assuming, that the pattern represents the Milankovitch periodicity, where the shortest pulses represent the precessional signal, we arrive at an average accumulation rate of around 60 cm/100 Kyr for the lower 10 m out of a total of 20 m, which constitutes the Induan part of the section. This suggests that the duration of the Induan period was 6-7 Myr assuming, that the upper 10 m did not change accumulation rate drastically.

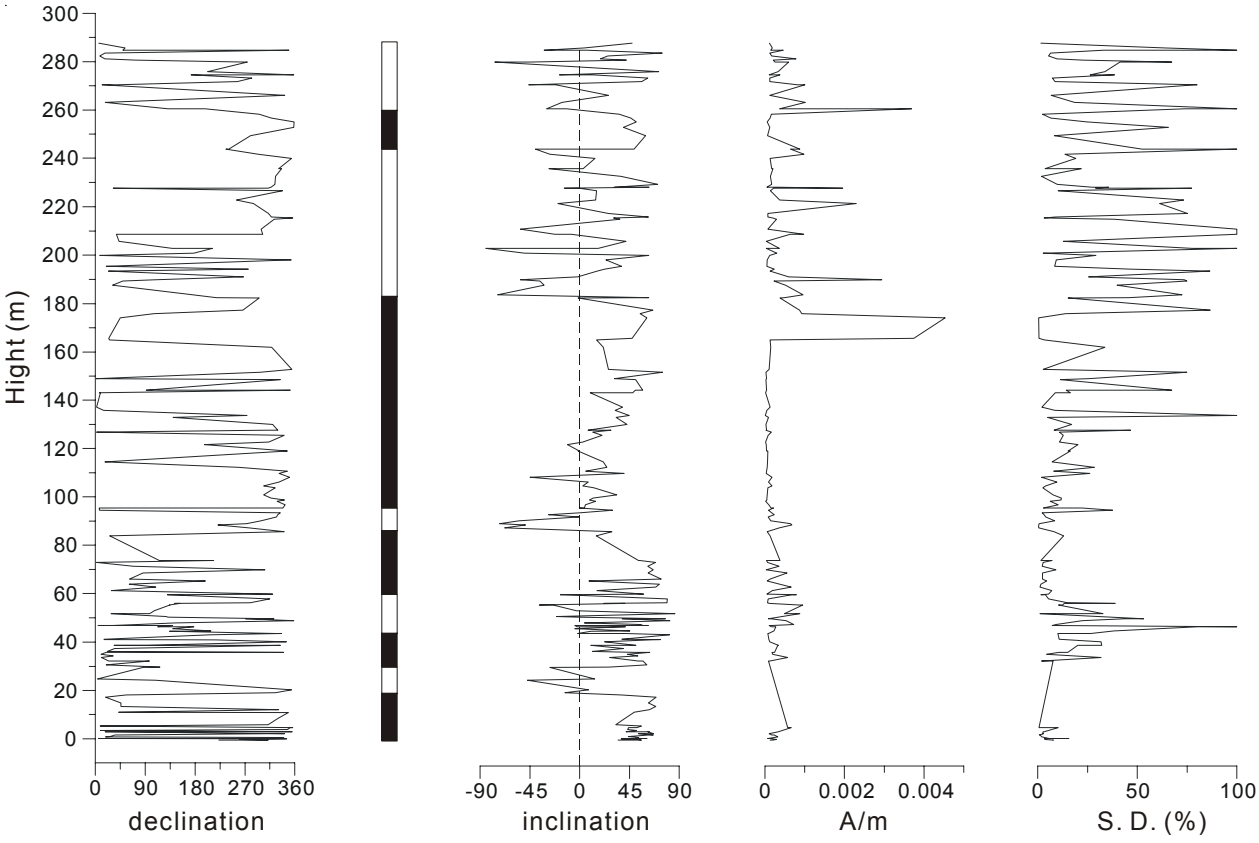

Figure1. Plot of magnetic declination, inclination, vector strength and standard deviation of the measurements.

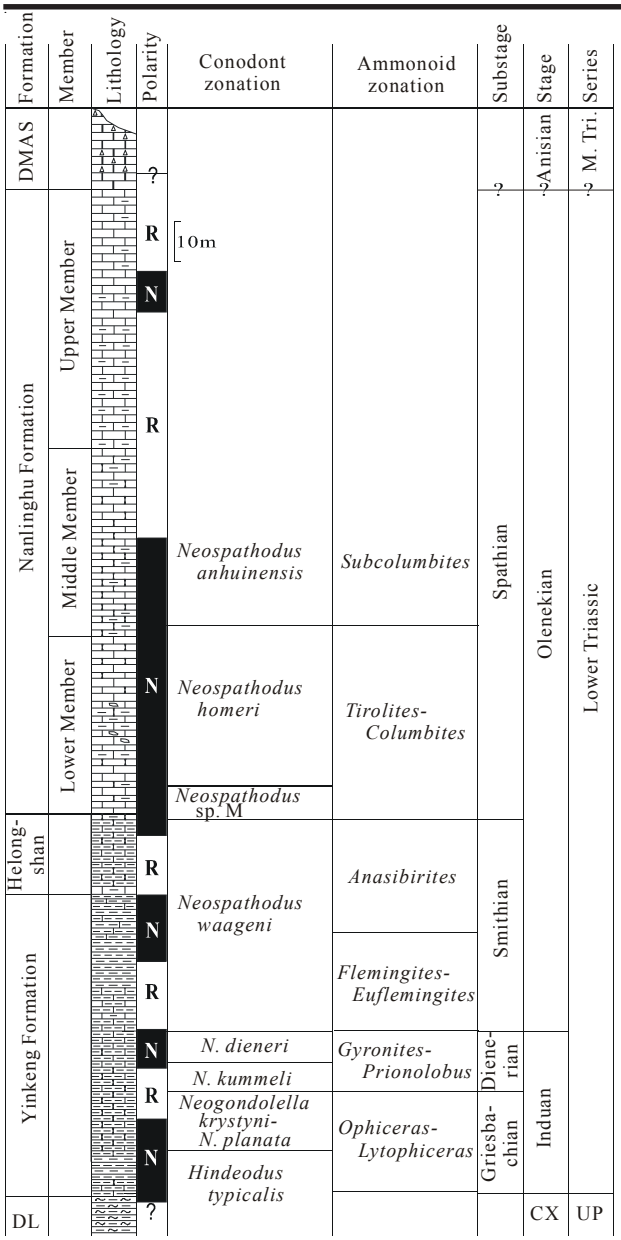

Figure 2. Plot of lithology, magnetic polarization and biostratigraphy

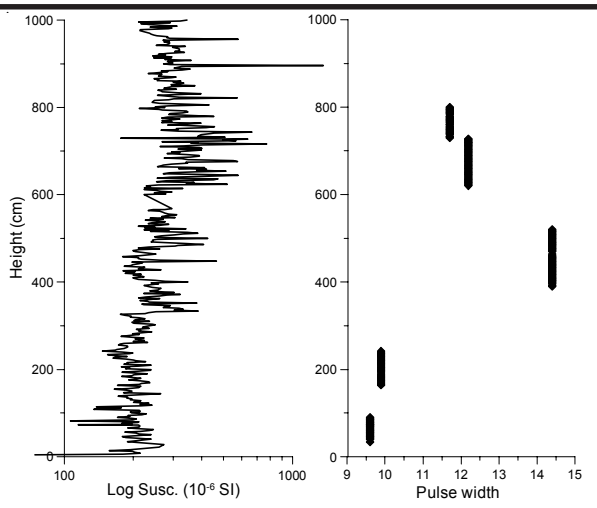

Figure 3. Variation of magnetic susceptibility and pulse-width of the lower 10 m of the Induan sediments from the ACP profile in Chaohu. A pulse is supposed to represent one precessional cycle in the Milankowitch band. The plot of pulse-width represents variation in accumulation rate.

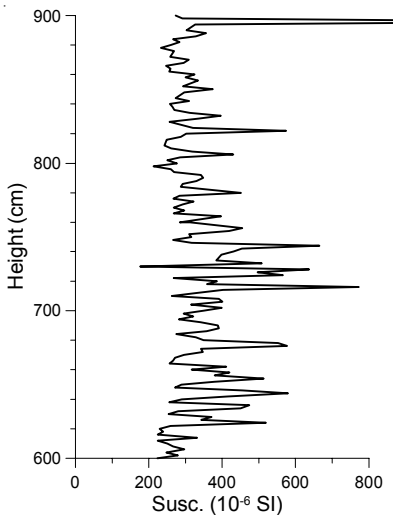

Figure 4. Detail of fig. 3 showing the structure of the suggested precessional cycles.

Brachiopod Miniaturization in the Permian-Triassic Life Crisis in South China

He Weihong

Faculty of Earth Sciences, China University of Geosciences, Wuhan 430074, P. R. China; whzhang@cug.edu.cn

In the Permian-Triassic life crisis in South China, a brachiopod fauna dominated by larger individuals in size, was replaced by the other brachiopod fauna dominated by smaller individuals. It is called brachiopod miniaturization here.

In South China, Changhsingian strata are mainly deposited in platform facies, basin facies, and shore facies (Yang et al., 1991). Meishan and Zhongliangshan sections are deposited in carbonate platform facies, Laibing, Guiding, Dongpan and Longtan sections are deposited in limestone-mudstone-siliceous rock-siliceous limestone basin facies, Qibaoshan section is deposited in shore clastic rock facies.

At Meishan and Zhongliangshan sections, the Changhsingian brachiopod fauna who is from the limestone intervals relatively far below the Permian-Triassic boundary, mainly consists *Spinomarginifera alpha*, *Cathaysia chonetoides*, *Haydenella kiangsiensis*, *Fusiproductus baoqingensis*, *Neowellerella pseudoutah*, *Leptodus* sp., *Meekella* sp., *Perigeyerella* sp., *Martinia* sp., *Araxathysis araxensis*, *Paracrurithyris pigmaea*, *Paryphella obicularia*, and *Waggenites* sp. (Zhao et al., 1981; Shen and He, 1991). The elements larger than 1 cm in size account for more than 50%. The brachiopod fauna

from the claystone and limestone intervals nearby the Permian-Triassic boundary mainly includes *Crurithyris* sp., *Cathaysia* sp., *Fusichonetes* sp., *Paracrurithyris pigmaea*, *Paryphella* sp., *Waagenites* sp., *Neochonetes* sp., *Spinomarginifera kueichowensis*, *S. chenyaoyenensis*, *Lissorhynchia pseudoutah*, *Acosarina* sp., *Araxathyris araxensis*, and *Neowellerella pseudoutah* (Zhao et al., 1981; Shen and He, 1991). The elements smaller than 1 cm in size accounts for 50% to 90%, so brachiopod miniaturization occurred nearby the Permian-Triassic boundary. Besides, at the Meishan section, brachiopod miniaturization is companied by the extinctions of some foraminifera, conodont and ammonoid species. At the Laibing and Guiding sections, the Changhsingian brachiopod fauna who is from the limestone, mudstone and siliceous limestone intervals relatively far below the Permian-Triassic boundary, is dominated by individuals larger than 2 cm in size (Zhao et al., 1981; Liao, 1987; Shen and He, 1994). The brachiopod fauna from the limestone and mudstone intervals near the Permian-Triassic boundary is dominated by individuals smaller than 1 cm (Zhao et al., 1981; Liao, 1987; Shen and He, 1994). At the Dongpan section, southern Guangxi, the brachiopod fauna from the siliceous mudstone intervals relatively far below the Permian-Triassic boundary, is mainly composed of *Anidanthus* sp. and *Costatumulus* sp., 2 to 3 cm in size. The brachiopod fauna from the siliceous mudstone intervals close to the Permian-Triassic boundary is mainly composed of *Paracrurithyris pigmaea* and *Spinomarginifera* sp., smaller than 6 mm in size. Besides, at the Dongpan section, brachiopod miniaturization seems more evident more close to the Permian-Triassic boundary and is companied by the extinctions of some radiolarian and foraminifera species. At the Longtan section, the brachiopod fauna from the mudstone intervals nearby the Permian-Triassic boundary, is characterized by lower diversity and smaller species than the brachiopod fauna from the siliceous rock intervals far below the Permian-Triassic boundary (Liao, 1979). At the Qibaoshan section, Jiangxi Province, the brachiopod fauna from the top part of Changhsingian mudstone and silty mudstone, consists *Orthotetina rubber*, *O. regularis*, *Haydenella subextensa*, *H. kiangsiensis*, *Oldhanina lianyangensis*, *Leptodus* sp., *Waagenenites* sp., *Neochonetes* sp., *Rugosomarginifera chenyaoyenensis*, *Spinomarginifera chengyaoyenendis*, *S. kueichowensis*, *Crurithyris* sp., *Martinia* sp. (Yang et al., 1991), and the individuals larger than 1 cm account for more than 60%. The brachiopod fauna from the basal part of the Triassic mudstone and silty mudstone intervals only consists *Crurithyris pusilla* (Yang et al., 1991), smaller than 5 mm. Besides, in Guangyuan, Sichuan Province, Yongding, Fujian Province, and Zhangyi, Hunan Province, the brachiopod faunas nearby the Permian-Triassic boundary are characterized by small species (Liao, 1979; Zhao et al., 1981; Shen et al., 1994).

In sum, brachiopod miniaturization happened in either platform facies, basin facies or clastic rock facies during the Permian-Triassic interval, and related to the mass extinction in South China. Besides, whether the rock facies near the Permian-Triassic boundary changes with time going or not, the brachiopod miniaturization occurred. So brachiopod miniaturization is different from community replacement controlled by rock facies, and is related with the Permian-Triassic events.

The Permian-Triassic brachiopod miniaturization is resulted from paleoenvironmental stress, such as sea-level rising, anoxic event, or lack of nutrition in marine water (Liao, 1979; Shen et al., 1994; Shen and Shi, 1996; Shen and Archbold, 2002). Brachiopod miniaturization is a special appearance in the Permian-Triassic life crisis. Knowing whether brachiopod miniaturization happened in sudden or step by step and knowing why brachiopod miniaturization happened are very important for understanding the pattern and causes of the Permian-Triassic massive extinction.

Liao Zhuting, 1979. Brachiopod Assemblage Zone of Changhsing Stage and brachiopods from Permo-Triassic Boundary Beds in China. Acta Stratigraphica Sinica, 3(3): 200-208. (In Chinese)

Liao Zhuting, 1987. Paleoecological characters and stratigraphic significance of silified brachiopods of the Upper Permian from Heshan, Laibin, Guangxi. *In* Nanjing Institute of Geology and Paleontology (ed.) Stratigraphy and Palaeontology of Systemic Boundares in China Perman and Triassic Boundary (1). Nanjing University Press, Nanjing. 81-125 (In Chinese with English abstract)

Shen Shuzhong, He Xilin, 1991. Changxingian brachiopod assemblage sequence in Zhongliang Hill, Chongqing. Journal of Stratigraphy, 5(3): 189-196. (in Chinese)

Shen Shuzhong, He Xilin, 1994. Changhsingian brachiopoda fauna from Guiding, Guizhou. Acta Palaeontologica Sinica, 33(4): 440-454. (In Chinese with English abstract)

Shen Shuzhong, Fan Bingheng, Zhang Xiaoping, 1994. Brachiopod communites from Changxingian to Triassic basement in Sichuan-Guizhou and their controlling factors. Oil and Gas Geology, 15(4): 267-274. (In Chinese with English abstract)

Shen Shuzhong, Shi, G. R., 1996. Diversity and extinction patterns of Permian brachiopoda of South China. Historical Biology, 12: 93-110.

Shen Shuzhong, Archbold, N. W., 2002. Chonetoidea (Brachiopoda) from the Lopingian (Late Permian) of South China. Alcheringa, 25: 327-349.

Yang Zunyi, Wu Shunbao, Yin Hongfu, Xu Guirong, Zhang Kexin, 1991. Permo-Triassic Events of South China. Geological Publishing House (Beijing), 183 p. (In Chinese with English abstract)

Zhao Jinke, Sheng Jinzhang, Yao Zhaoqi, Liang Xiluo, Chen Chuzhen, Rui Lin, Liao Zhuoting, 1981. The Changhsingian and the Permian—Triassic Boundary in South China. Nanjing Institute of Geology and Palaeontology, Bulletin, 2: 1-57. (In Chinese with English abstract)

Correlation of the Proposed Base-Olenekian GSSP from Chaohu, China to Western Canada

Charles M. Henderson

Applied Stratigraphy Research Group, Department of Geology and Geophysics, University of Calgary, Calgary, Alberta, Canada T2N 1N4; charles.henderson@ucalgary.ca

The proposed GSSP for the Induan-Olenekian boundary is located in the low-latitude Tethyan Realm within the West Pingdingshan Section at Chaohu, Anhui Province, China (Tong *et al*., 2004). The proposed GSSP level coincides with the FAD (first appearance datum) of the conodont *Neospathodus waageni*; a secondary marker includes the FAD, 26 cm higher, of the ammonoids *Flemingites* and *Euflemingites*. Zhao *et al*. (2004) defined three new subspecies of *N. waageni*, including *N. waageni waageni*, *N. waageni* n.subsp. *A*, and *N. waageni* n. subsp. *B*. They indicate that the first subspecies to appear is *N. waageni* n.subsp. *A* and place the base of the Olenekian at this FAD. Other correlation tools like magnetozones and carbon-isotopic shifts are not discussed in the subsequent comparison with western Canada because these techniques have not been performed on the western Canadian succession.

In western Canada the Induan-Olenekian boundary has been investigated at Opal Creek in Kananaskis Country, Alberta (50°40'32"N; 115°04'50"W) and in several subsurface wells in the Peace River Basin of west-central Alberta. These sections were located on what was the NW margin of Pangea and could be referred to the Boreal Realm although provincialism is not really significant during this time period.

The Lower Triassic at Opal Creek consists dominantly of fine-grained siliciclastics and is on the order of 310 metres thick. The basal Phroso Siltstone Member of the Sulphur Mountain Formation comprises 39 metres of planar laminated silty black shale and rare ripple-laminated siltstone beds; the black colour and general lack of bioturbation are particularly characteristic of the unit. The base of this member represents a major transgressive surface that began in the Latest Permian (Henderson, 1997) according to the presence of *Clarkina* sp.cf. *changxingensis*; *Hindeodus parvus*, the index for the basal Triassic, appears at a single level 1.5 metres above the base and a maximum flooding surface occurs at 21 metres. The overlying Vega Member of the Sulphur Mountain Formation includes resistant beds of brown-weathering coarse siltstone and very fine-grained sandstone and the contact with the underlying member is transitional. Simple horizontal burrows and rare tool marks are visible on the soles of many of the sandstone beds. Higher up, trace fossils exhibiting more complex behaviours, such as *Diplocraterion*, *Thalassinoides*, and *Lockiea* become more common. Ripple cross-laminated beds and occasional hummocky cross-stratified beds are present throughout the Vega Member. The base of the mid-Induan (Dienerian) is recognized by the appearance of *Neospathodus kummeli* at 83 metres. A 3rd or 4th order sequence boundary is interpreted at 97 metres. Loading features become very common in the Upper Dienerian indicating high rates of sedimentation. A second 3rd order sequence boundary is recognized by a very sharp change in lithofacies at 166 metres and marks the Induan-Olenekian (Dienerian-Smithian) boundary. Relatively abundant specimens of *Neospathodus waageni* were recovered from samples immediately overlying this sequence boundary in dark grey silty shale that exhibit high gamma ray values. Most of the specimens have the roughly equidimensional shape and straight basal margin profile characteristic of *N. waageni* subsp. *A*. At least one specimen has a more elongate rectangular shape reminiscent of *N. waageni* subsp. *B*. Further supports for the correlation with the Lower Olenekian are two occurrences of *Euflemingites romunderi* at 170 and 183 metres. Overlying strata represent a progradational succession of very fine to fine-grained sandstone that were deposited in a relatively shallow marine setting and have yielded very few fossils. A second section in Kananaskis Country at Hood Creek includes debris-flow breccias at the Induan-Olenekian sequence boundary, deposition of which may have been triggered by tectonic activity. More evidence of this tectonic activity is interpreted from observations in the subsurface of the Peace River Basin to the north.

In the Peace River Basin, Lower Triassic strata are referred to the Montney Formation. Detailed examination of core and extensive wire-line log correlation has resulted in the recognition of numerous parasequence sets and a major mid-Montney sequence boundary. These units are correlated with the Lower Induan (Griesbachian; parasequence sets G1-G3), Upper Induan (Dienerian; parasequence sets D1-D8), Lower Olenekian (Smithian; parasequence sets S0-S5) and Upper Olenekian (Spathian; parasequence sets Sp1-Sp2). Griesbachian parasequences record latest Permian and Early Triassic transgression over subaerially exposed Permian Belloy Formation. Dienerian strata form a series of highstand, prograding parasequences that downlap basinward onto a maximum flooding surface. Sedimentation during the Induan was influenced by tectonic activity on two major normal faults (Dunvegan and Rycroft faults) as indicated by gentle warping of the Induan-Olenekian sequence boundary and underlying strata. The Induan-Olenekian lowstand in the Peace River Basin is interpreted to have been primarily influenced by tectonics rather than eustasy. Tectonic shortening created a series of downwarped or incised valleys along the Montney coastline and resulted in the basinward, coevally emplaced Sexsmith-Valhalla turbidite fan complex (Kendall, 1999). Overlying Smithian and Spathian transgressive and highstand parasequences in the Upper Montney Formation do not exhibit the same degree of tectonic control as Lower Montney strata and therefore show a simple prograding clinoform geometry. Petroleum production occurs from shoreface, dolomitized coquina/sandstone plays as well as the turbidite succession to the west, both of which are associated with the Induan-Olenekian sequence boundary. Cores from the various

parasequence sets have been sampled extensively and have yielded numerous conodonts; this is the only means of dating these units in the subsurface (Kendall, 1999; Panek, 2000). The range of key taxa in the subsurface are as follows: *Neospathodus dieneri* (parasequence sets D3-S0), *Neospathodus waageni* (parasequence sets S0 to S5; only *N. waageni* subsp. *A* in S0 and *N. waageni* subsp. *B* common in S4), *N*. sp. cf. *pakistanensis* (parasequence set S0), and *Meekella meeki* (parasequence sets S3-S5).

One of the requirements for GSSP establishment is that the point should be as widely correlatable as possible. The fact that *Neospathodus waageni sensu lato* occurs immediately above a significant sequence boundary in Western Canada and is followed shortly thereafter by the ammonoid *Euflemingites romunderi* means that a local natural mid-Lower Triassic boundary is directly correlatable with the proposed GSSP in Chaohu on the other side of the Panthalassa Ocean. Furthermore, the earliest *Neospathodus waageni sensu lato* in western Canada are assignable to *N. waageni* subsp. *A* just as they are at Chaohu. The fact that this boundary as defined by various biotic markers can be recognized in these widely separated regions in both surface and subsurface localities lends considerable support to the formal adoption of the proposed GSSP at Choahu by the Subcommission for Triassic Stratigraphy.

Henderson, C. M., 1997. Uppermost Permian conodonts and the Permian-Triassic Boundary in the Western Canada Sedimentary Basin. Bulletin of Canadian Petroleum Geology, 45(4): 693-707.

Tong Jinnan, Zakharov, Y. D., Orchard, M. J., Yin Hongfu, Hansen, H. J., 2004. Proposal of Chaohu Section as the GSSP Candidate of the Induan-Olenekian Boundary. Albertiana, 29: 13-28.

Kendall, D. M., 1999. Sedimentology and stratigraphy of the Lower Triassic Montney Formation, Peace River Basin, subsurface of northwestern Alberta. Unpublished Master's thesis, University of Calgary, Calgary, Alberta, 368 pp.

Panek, R., 2000. The sedimentology and stratigraphy of the Lower Triassic Montney Formation in the subsurface of the Peace River area, northwestern Alberta. Unpublished Master's thesis, University of Calgary, Calgary, Alberta, 275 pp.

Zhao Laishi, Orchard, M. J., Tong Jinnan, 2004. Lower Triassic conodont biostratigraphy and speciation of *Neospathodus waageni* around the Induan-Olenekian boundary of Chaohu, Anhui Province, China. Albertiana, 29:41-43.

$\delta^{13}C$ curve of Lower Triassic marine sediments in Iran

Micha Horacek*, Sylvain Richoz[+], Rainer Brandner[#], Leopold Krystyn[§], Christoph Spötl[#]

** Institut für Erdwissenschaften, Karl-Franzens-Universität Graz, Austria*

[+] Geological Museum, UNIL-BFSH2, 1015 Lausanne, Switzerland

[#] Institut für Geologie und Paläontologie, Universität Innsbruck, Austria

[§] Institut für Paläontologie, Universität Wien, Austria

Stable carbon isotope curves derived from Lower Triassic carbonate rocks from three Iranian sections are established to investigate changes in the carbon cycle during the Early Triassic in this area. The sections are located in southern central, in northern and north-western Iran. All the curves show similar patterns with only slight variations and clearly define a Lower Triassic $\delta^{13}C$ trend. It features high Permian isotope values and the decrease to more depleted $\delta^{13}C$ values across the Permian-Triassic boundary (PTB). In the upper Griesbachian an increase to more positive values is observed. In the Dienerian the carbon isotope values remain approximately at this level, with small variations and increasing values upwards. It is followed by a steep, short and pronounced positive excursion with maximum values of almost +8‰ V-PDB is followed by a negative shift to values below 0‰. At the Smithian-Spathian boundary a positive excursion to values above +3‰ is recorded. It is followed by a decrease into the Spathian and an increase to another positive step at the Spathian-Anisian boundary.

This study confirms an existing $\delta^{13}C$ curve from the Dolomites (N-Italy). The Iranian isotope curves validate the curve derived in N-Italy to represent an at least Tethys-wide signal. Also a study from southern China gives a similar isotope pattern, stratigraphical uncertainties between our sections and the locality in China still have to be solved, however.

The high amplitude oscillations of the carbon isotope curve possess a high frequency in the upper Lower Triassic and give decisive evidence for quick and profound changes in the carbon cycle during the Early Triassic. Stratification of the ocean interrupted by episodic overturns which transport deep ocean water to the ocean surface is a probable mechanism to produce the recorded isotope variations within geologically very short time. Isotopically light organic carbon is removed from the ocean surface water into the deep ocean water during stratification, leading to enriched carbon isotope signals in the surface ocean. During overturns in deep ocean water accumulated organic carbon is reintroduced to the surface water, thus causing depleted $\delta^{13}C$ values.

Investigation of Lower Triassic Chaohu limestone with Mössbauer spectroscopy: Clues to explain Lower Triassic marine carbon isotope fluctuations

Micha Horacek[1], Werner Lottermoser[2], Xiang-Dong Wang[3]

[1] Institute of Earth Sciences, Department of Mineralogy and Petrology, Karl-Franzens-University Graz, Universitaetsplatz 2, 8010 Graz, Austria

[2] Div. of Mineralogy and Material Sciences, Paris-Lodron-University Salzburg,

[3] NIGPAS National Institute of Geological and Palaeontological Sciences, Nanjing, People´s Republic of China

The Permian/Triassic boundary was the severest mass extinction in Earth history. The exact mechanisms that culminated to this devastating result are still not entirely unravelled, also the causes that led to a strongly extended survival interval after the extinction are still dubious. Investigations of the $\delta^{13}C$ isotope values of Lower Triassic marine carbonates gave a curve with profound and short timed oscillations. One hypothesis to explain the observed features in the Lower Triassic is the strong variation in oxygen availability in sea water caused by periods of well circulated ocean water masses followed by periods of intense stratification.

We applied ^{57}Fe Mössbauer spectroscopy, which enables us to identify Fe^{2+} und Fe^{3+} phases, giving evidence for reducing and oxidizing sedimentation environments, respectively. As a result we only discriminated 4 phases in combinations of maximally three: | pyrite, a Fe^{2+}-phase, paramagnetic Fe^{2+} and paramagnetic Fe^{3+}. Six samples have been analyzed from the Chaohu section in south China. Due to the low iron content of the samples, they had to be measured for several weeks. This explains the small number of samples.

The sample from the uppermost Permian contains exclusively pyrite as Fe bearing phase. In the Lower Triassic a sample directly from the $\delta^{13}C$ maximum at the Induan/Olenekian boundary contains mainly pyrite, less paramagnetic Fe^{2+} and a minor amount of a Fe^{2+}- phase. Two samples from the Smithian, that gives very light carbon isotope values have a Fe^{3+}- (probably paramagnetic Fe^{3+}) and the Fe^{2+}-phase as their major Fe phases and minor amounts of paramagnetic Fe^{2+}. At the base of the Spathian pyrite is the major Fe phase together with smaller, almost equal amounts of Fe^{2+} and the Fe^{2+}-phase.

We interpret these results by a sedimentation environment at Chaohu that remained for the most time of the investigated interval under reducing conditions. Only in the Smithian there existed a period of increased availability of free oxygen. This can be explained with a "stratified ocean" situation, only interrupted by a short period of circulation, bringing oxygen rich water to the seafloor.

Deep-Sea Chert and Shallow-Sea Carbonate from the End-Permian Mid-Panthalassa

Yukio Isozaki

Department of Earth Science and Astronomy, The University of Tokyo, 3-8-1 Komaba, Meguro, Tokyo 153-8902, Japan; isozaki@chianti.c.u-tokyo.ac.jp)

The Jurassic accretionary complex in Japan contains numerous large allochthonous blocks/lenses of Middle-Upper Permian and Lower Triassic mid-oceanic rocks, i.e., deep-sea chert and shallow-sea atoll carbonates, that were derived from the lost superocean Panthalassa (Isozaki et al., 1990). Spanning across the Permo-Triassic (P-T) boundary, these accreted oceanic rocks recorded vital pieces of information on the end-Permian global environmental change relevant to the greatest mass extinction in the Phanerozoic. The Permo-Triassic deep-sea cherts in Japan record a unique oceanic episode called the superanoxia, i.e., ca. 20 million year long deep-sea anoxia that continued from the Lopingian to Anisian across the P-T boundary (Isozaki, 1997). It is noteworthy that the onset of superanoxia coincides with another mass extinction at the Guadalupinan-Lopingian (G-L) boundary and that the anoxia culminated at the P-T boundary. Also recognized is remarkable biotic reorganization of radiolarians at the two boundaries. These deep-sea features indicate a two-stepped change in oceanography of the superocean in the Late Permian.

The shallow-sea carbonates primarily deposited on ancient mid-oceanic seamount complexes, on the other hand, record biotic turnover and extinction of fusulinids at the G-L and P-T boundaries (Ota et al., 2000; Ota & Isozaki, submitted). Both changes are coupled with negative shift in $\delta^{13}C_{carb}$ (Musashi et al., 2001). Thus Panthalassa-derived oceanic rocks, of both deep-sea and shallow-sea facies, demonstrate a significant environmental change in the entire superocean during the Late Permian, particularly in two steps at the G-L and P-T boundaries.

Owing to the difference in lithofacies and fossil content, biostratigraphical correlation between the deep-sea cherts and shallow-sea carbonates has a little difficulty, however, another point to be noted is the occurrence of a unique acidic tuff bed at the G-L boundary in shallow-sea paleo-atoll carbonates (Isozaki & Ota, 2001). This G-L boundary acidic tuff may potentially work as a key bed for regional correlation and strongly suggests that an extensive area, at least western Panthalassa, was influenced by a severe acidic volcanism at the G-L boundary. The rhyo-dacitic geochemistry of the volcanism indicates that the responsible eruption(s) may have been highly violent and thus explosive enough to cover the top of mid-oceanic seamount but also to trigger the global-scale environmental turmoil including superanoxia and relevant mass extinction at the G-L boundary. The P-T boundary in South China is marked by acidic tuff beds (Yin et al., 1998; Bowring et al., 1998), therefore, both the two Late Permian extinction-related (P-T and G-L) boundary events may have been caused by large-scale acidic volcanism of

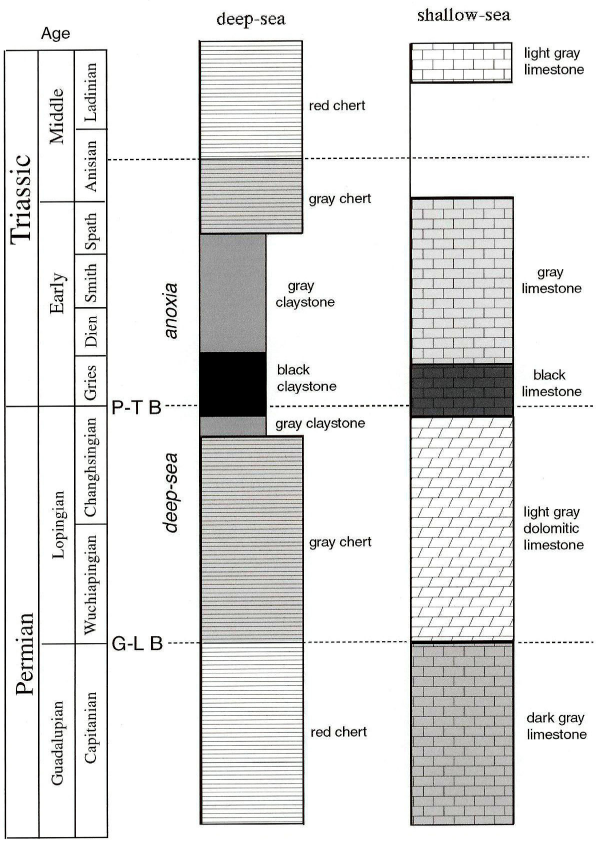

Figure 1. Correlation of the Permo-Triassic mid-oceanic deep-sea cherts and shallow-sea carbonates from mid-Panthalassa.

similar origin.

Bowring, S. A., Erwin, D. H., Jin, Y. G., Martin, M. W., Davidek, K. and Wang, W., 1998, Science 280, 1039-1045.

Isozaki, Y., 1997: Science 276, 235-238.

Isozaki, Y., Maruyama, S. and Furuoka, F., 1990: Tectonophysics 181, 179-205.

Isozaki, Y. and Ota, A., 2001: Proc. Japan Academy 77B, 104-109.

Musashi, M., Isozaki, Y., Koike, T., and Kreulen, R., 2001: Earth Planet. Sci. Lett. 191, 9-20.

Ota, A., Kanmera, K. and Isozaki, Y., 2000: Jour. Geol. Soc. Japan 106 853-864.

Yin, H. F., Zhang, K. X., Tong, J. N., Ynag, Z. Y. and Wu, S. B., 1998: Episodes 24, 102-114.

Conodont Biostratigraphy Across the Permian-Triassic Boundary at Chaotian Section, Northern Sichuan, China

Ji Zhansheng[1], Yao Jianxin[1], Yukio Isuzaki[2], Tetsuo Matsuda[3] and Wu Guichun[1]

[1] Institude of Geology, Chinese Academy of Geological Sciences, Beijing, 100037, China; jizhansheng@vip.sina.cn

[2] Department of Earth Science and Astronomy, Graduate School of Arts and Sciences, University of Tokyo, Japan

[3] Kyoei Consultant Corporation

This paper mainly reports the conodont sequences across the Permian-Triassic Boundary (PTB) at the Chaotian section, Guangyuan, Sichuan, province, South China. The section consists of the Maokou Formation (Guadalupian), Wujiaping Formation (Wuchiapingian), Dalong Formation (Wuchiapingian to Changsingian), and Feixianguan Formation (Griesbachian) in ascending order. The strata across PTB in Chaotian section are lithologically divided into 7 units, i.e. Unit A to G in ascending order. Unit A to D belongs to Dalong Formation. Unit E to G belongs to Feixianguan Formation.

Three conodont zones, i. e., *Clarkina postwangi* zone, *C. meishanensis* zone and *Hindeodus parvus* zone were identified in ascending order. And three ammonite zones, i.e. *Pseudostephanites-Tapashanites* Zone, *Pseudotirolites-Pleuronodoceras* Zone, *Hypophiceras* Zone were recognized. According to the correlation of the conodonts and Ammonites with other sections, the Chaotian section is continuous across the Permian-Triassic boundary biostratigraphically.

Based on the study of conodont, the exact mass extinction horizon of the Permian conodonts is at the topmost of the Dalong Formation below the *Hypophiceras* bed, coinciding to the lithological transition from the Dalong limestone to the Feixianguan marl.

However, the first appearance of *Hindeodus parvus* is in the sample numbered as F1 at the base of the Unit F, which is 1.4 m higher than the mass extinction bed. The interval between the mass extinction bed and the FAD of the *H. parvus* at the Chaotian section is thicker than that of the Meishan section, in that this interval is only 0.15 m. The same phenomenon could also be seen in the Shangsi, Huaying sections too according to our study. The Unit E of the Chaotian section suggests an extremely deteriorated environment for conodont before its renascence in the Early Triassic.

Based on the analysis of the quantitative change of the conodont individuals in the uppermost Permian, the conodont fauna had declined gradually before the last definitive shock near PTB. The repeatedly-occurred tuff layers near the PTB displayed ingenerated relationship with the gradual decline and mass extinction of the Permian conodont.

Explosive Radiation of Shell-Eating Marine Reptiles During the Post-Permian Recovery

Jiang Da-yong[1], Ryosuke Motani[2], Lars Schmitz[2], Hao Wei-cheng[1] and Sun Yuan-lin[1]

[1] *Department of Geology and Geological Museum, Peking University, Beijing 100871, China; djiang@pku.edu.cn*

[2] *Department of Geology, University of California, Davis, CA 95616, USA*

The Grenzbitumenzone of Besano/Monte San Giorgio area of Italy/Switzerland border, which contains the Anisian/Ladinian boundary, yields articulated fossils of marine reptiles. Elsewhere in the world, marine reptile fossils from the Anisian are usually incompletely preserved, and therefore the specimens from Grenzbitumenzone have played an important role in interpreting the evolution of marine reptiles during the Middle Triassic. However, it is known that the depositional environment of this basin was not representative of the global average—it was not fully connected to the oceans, and had anoxic bottom water (Furrer, 1995). Ichthyosaurian species from the basin, for example, are so far endemic to the area, and dominated by forms that have tiny teeth luminescent of Early Triassic ichthyosaurs.

A locality in the Xinmin District, Panxian County, Guizhou Province, P. R. China has been yielding articulated skeletons of Anisian marine reptiles in the past half a decade, providing a fresh perspective of the evolution of marine reptiles in the Middle Triassic outside the Grenzbitumenzone (Li et al., 2004). The fossils are mostly from the Pelsonian of the middle Anisian, thus representing slightly earlier time period than the Italy/Switzerland locality. In marked contrast to the Grenzbitumenzone fauna, the Xinmin fauna is characterized by a high proportion of durophagous (shell-eating) species. An estimate by the District indicates more than 700 of the 800 specimens collected belong to two species of mixosaurid ichthyosaurs with crushing dentition that are being named elsewhere. There are two more genera of marine reptiles with crushing teeth, which, again, will be named elsewhere. In total, four of the six genera that can be recognized in the fauna are durophagous.

A literature survey reveals that the dominance of durophagous forms in the Xinmin fauna is probably a closer reflection of the global trend during the Middle Triassic than the scarcity of durophagous species seen in the Grenzbitumenzone fauna. For example, the Middle Triassic Sulphur Mountain Formation is dominated by the ichthyosaur *Phalarodon*, which has crushing teeth. The Ladinian of Spitsbergen (Upper Saurian Level) is also dominated by *Phalarodon*. The taxonomic composition is biased toward durophagous forms in the Anisian of Nevada—in addition, there is an undescribed fragment that most likely represents a placodont. Given that many groups of durophagous marine reptiles have their first definitive fossil record in the Anisian, an hypothesis emerges that there was an explosive radiation of shell-eating marine reptiles in the Anisian.

We tested this hypothesis based on generic diversity of durophagous marine reptiles, including ichthyosaurs, placodonts, thalattosaurs, and the controversial *Omphalosaurus*. Only those genera with massive crushing teeth were considered as durophagous in the analysis. The generic count is highest in the Anisian, where 13 genera are currently recognized, and then almost continuously decreased from thereon. No durophagous marine reptile is known from the Jurassic. The database of marine reptile fossils from the Triassic is very incomplete, preventing statistical tests of this observed trend.

The generic diversity pattern indicates that there was a rapid (in geological sense) diversification of durophagous marine reptiles in the Anisian (or possibly the latest Olenekian). The timing of the diversification roughly corresponds to the stabilization of carbon isotope ratio fluctuation, which indicates the overall environmental instability after the Permian came to an end (Payne et al., 2004). It is possible that these marine reptiles quickly took advantage of shelled invertebrates, which in turn were recovering from the end-Permian extinction, in the environment that was being stabilized.

Furrer, H., 1995. The Kalkschieferzone (Upper Meride Limestone; Ladinian) near Meride (Canton Ticino, Southern Switzerland) and the evolution of the Middle Triassic intraplatform basin. Eclogae geol. Helv., 88: 827-852.

Li, C., Rieppel, O., LaBarbera, M. C., 2004. A Triassic aquatic protorosaur with an extremely long neck. Science, 305: 1931.

Payne, J. L. et al., 2004. Large perturbations of the carbon cycle during recovery from the end-Permian extinction. Science, 305: 506-509.

Lower Triassic Radiolarian Biostratigraphy from Arrow Rocks in the Waipapa Terrane, North Island, New Zealand

Yoshihito Kamata[1], Akihiro Matsuo[1], Atsushi Takemura[2], Satoshi Yamakita[3], Yoshiaki Aita[4], Toyosaburo Sakai[4], Noritoshi Suzuki[5], Rie, S. Hori[6], Masayuki Sakakibara[6], Shizuo Takemura[2], Kazuto Kodama[7], Hamish J.Campbell[8] and Bernhard Spörli [9]

[1] Department of Earth Science, Faculty of Sciences, Yamaguchi Universituy, Yamaguchi, 753-8512, Japan; kamakama@po.cc.yamaguchi-u.ac.jp

[2] Geoscience Institute, Hyogo University of Teacher Education, Yashiro-cho, Kato-gun, Hyogo 673-1494, Japan

[3] Department of Geology, Faculty of Education & Culture, Miyazaki University, Miyazaki 889-2192, Japan

[4] Department of Geology, Faculty of Agriculture, Utsunomiya University, Utsunomiya 321-8505, Japan

[5] Institute of Geology and Paleontology, Graduate School of Science, Tohoku University, Sendai 980-8578, Japan

[6] Department of Earth Science, Faculty of Science, Ehime University, Matsuyama 790-8577, Japan

[7] Marine Core Research Center, Kochi University, Kochi 780-8520, Japan

[8] Institute of Geological & Nuclear Sciences Ltd. PO Box 31-312, Lowe Hutt, New Zealand

[9] Department of Geology, The University of Auckland, Private Bag 90219, Auckland, New Zealand

Across the Permian-Triassic (P-T) boundary event, which was the greatest crisis during the Phanerozoic Era, various kind of taxa were completely extinct and even survived organisms were sustained a serious loss in their lineages (e.g., Sepkoski, 1989; Erwin, 1993). Formerly, examination of the P-T boundary has been done in mainly shallow marine carbonate sequences on continental shelves around Pangea, and many hypotheses for a cause have been proposed such as oceanic anoxia (Wignall and Hallam, 1992; Hallam and Wignall, 1997; Wignall and Twitchett, 1996), vast volcanism (Reichow et al., 2002), methane expulsion (Krull and Retllack, 2000) and extraterrestrial impact (Berker et al., 2001).

Isozaki (1994, 1997) described lithological and biostratigraphical transition of close P-T boundary sequences from Japanese accretionary complexes. The sequence consists mainly of bedded chert of deep-sea pelagic origin accumulated in Panthalassa. As mentioned by Isozaki (1994), deep-sea sediments have better chances to record oceanic environments than that of shallow continental shelves, because deep-sea sediments should be escaped from a cessation of geological record due to regional sea level fluctuations. In addition to the invaluableness, documentation of environmental change in deep-sea facis and comparison with that of shallow marine facies lead to better understanding of the anoxia. Then, he documented extension and time duration of 'superanoxia' in Panthalassa and Tethys. Wignall and Twitchet (2002) revised the process of the onset of anoxia including deep-sea envirnment during the P-T boundary interval.

As pointed by Twitchett et al. (2004), however, the faunal diversity and recovery process considering the onset of anoxia during the P-T boundary interval have not been fully understood. Krystyn et al., (2003) and Twitchett et al. (2004) reported an abundant and rapidly recovered marine fauna during Griesbachian from Oman, and reinterpreted the Griesbachian assemglage of the Kathwai Member of Salt Ranges, Pakistan, where was located in the Neo-tethys and was well-oxygenated during Griesbachian, as not a holdover fauna, but a rapid-recover fauna. In order to ascertain that the widespread anoxic and dysaerobic conditions delayed biotic recovery during the Early Triassic, further environmental analyses and biostratigraphy are required, especially Lower Triassic pelagic sequences.

Radiolaria, a marine zooplankton consisting a silica-test drastically changed its fauna across the P-T boundary as well as other organisms. Faunal and biostratigraphical data of Early Triassic radiolarian are still scarce, although many paleontologist have attempted to clarify them in the context of understanding the Permian-Triassic (P-T) boundary event and recovery process of radiolarians after the event. Despite all this effort, useful faunas of only late Olenekian (Spathian) age have been recovered.

Recently, Late Permian and Early Triassic bedded chert sequences have been reported in accretionary complexes at Arrow Rocks, North Island, New Zealand (Takemura et al., 1998, 2002). We have examined radiolarian and conodont biostratigraphies ranging from Middle Permian to Middle Triassic age in the section. In this presentation, We would like to show mainly radiolarian biostratigraphy in the Lower Triassic bedded chert sequence.

These strata are restricted in exposure to a small islet (Arrow Rocks) and are constituents of the Waipapa Terrane, an accretionary complex. The Arrow Rocks sequence consists mainly of basalt, limestone, tuff, mudstone, siliceous mudstone and chert. This sequence is almost continuous and is divided into eight lithological units, from Units 1 to 8 in ascending order (Takemura et al., 1998 ; 2002). Early Triassic (late early Induan to Olenekian = late Griesbachian to Spathian) conodont faunas belonging to the *Neogondolella carinata*, *Neospathodus kummeli*, *Neospathodus dieneri*, *Neospathodus cristagalli*, *Neospathodus pakistanensis*, *Neospathodus waageni*, and *Chiosella timorensis* Zones have been obtained from Unit 2B to Unit 5 (Yamakita et al., 2003).

Four sections have been measured on Arrow Rocks (ARB, ARD, ARE and ARH) which correspond to the interval from the Unit 2B to Unit 5. The ARB, ARD and ARE

sections are located in the central part of Arrow Rocks, and ARH section is in the northern part. ARB section mainly consists of brick red color chert with intercalation of thin mudstone layers. ARD section consists of recrystallized grey chert with intercalations of black siliceous mudstone. ARE section is comprised of well-bedded grey and red chert. ARH is represented by grey and brownish red chert with intercalations of a distinctive vermilion red chert. Under the microscope, chert consists mainly of microcrystalline quartz, clay minerals, and radiolarian tests, subordinate sponge spicules and opaque mineral grains. Radiolarian test are usually filled with microcrystalline quartz. These micro-biogenic siliceous materials and clay minerals are main composition, and no terrigenous materials which are larger than silt size in diameter contained in these bedded chert. While the 'apparent' sedimentation rate (Matsuda Isozaki, 1991) of this chert sequence indicates very slow (c.a. 5.1m/m.y.) and comparable with that of Japanese Triassic chert (c.a. 1.0-4.0 m/m.y.) by Matsuda and Isozaki (1991). These line of evidence provably indicate that the ocean basin accumulated these bedded chert was similar tectonic setting to that of accreted Japanese bedded chert (Matsuda and Isozaki, 1991).

Detailed radiolarian biostratigraphy of Early Triassic (late Early Induan to Olenekian) chert sequences from Arrow Rocks has established that Early Triassic radiolarians have Permian and Triassic (i.e. Paleozoic and Mesozoic) affinities (Kamata et al., 2003, Takemura et al., 2003). External form of the 'Permian-type' radiolarians is similar to that of diagnostic Permian genera, whereas 'Triassic-type' radiolarians are characterised by forms close to those of the nassellarian of Mesozoic.

In late early to early late Induan (late Griesbachian to early Dienerian), fauna includes Permian affinity of *Hegleria* and *Uberinterna* belong to the entactiniids, and latentifistulids such as *Ishigaum* and *Kimagior*. Albaillellarians, which is a representative group of Permian, are absent (Takemura et al., 2003).

Late Induan (middle to late Dienerian) fauna is characterized by an abundance of spherical forms and Permian genera, but is accompanied with 'Mesozoic' nassellarians. A few specimens of spicular type that resemble the Palaeoscenidiidae, which is well reported from Middle Triassic sequences of Tethys and Panthalassa, were also obtained. Albaillellarians have never been obtained, although spherical 'Permian-type' radiolarians are dominant in this fauna.

In the latest Induan to Olenekian (late Dienerian to Spathian), radiolarian fauna are characterized by occurrence of Spathian to Anisian affinity. A few genera of nassellaria appeared and fauna diversity slightly increased during this interval. To sum up the radiolarian biostratigraphy in the Arrow Rocks as follows;

(1) Some of representative Permian groups may well have survived the boundary event and inhabited by late Induan (late Dienerian).

(2) 'Mesozoic' nessellarians, which have been believed that it appeared in the late Olenekian (Spathian), must have appeared by the late Induan (Dienerian).

(3) During the late Induan (middle to late Dienerian), faunal change from Permian dominant to Triassic fauna occurred. 'Permian-type' types disappeared, whereas the 'Mesozoic' nassellarians appeared during this time.

These are much differing from general hitherto understanding of radiolarian biostratigraphy across the P-T boundary.

In addition to the peculiar biostratigraphy, the lithological nature of Arrow Rocks has to be notable for comparison with lithological change of deep-sea chert reconstructed from Japanese and Canadian accreted complexes (Isozaki, 1994, 1997). The latter is marked by interruption of chert sedimentation, and the rock unit is replaced by claystone or black carbonaceous claystone across the boundary. Almost all pelagic sequence of the Arrow Rocks is composed of bedded chert from the Induan to Olenekian (Griesbachian to Spathian), and there is no thick claystone rock unit. Moreover, almost bedded chert has reddish color, except for interval of Unit 3 (late late Induan= late Dienerian). Although we have not done environmental analyses such as isotopic and geochemical data at present, biostratigraphical and lithogical nature of Arrow Rocks indicate that depositional environment of the sequence was remarkably differ from that of Japanese and Canadian sequences. Oceanic rocks of the Waipapa Terrane are presumed to be formed on the Phenix Plate, and the ocean basin was being transported from low to high latitudes toward the convergent zone at the eastern Gondwana margin during the Permian and Triassic (Sporli et al., 1989). There is a large possibility that difference of paleolatitudal location between the New Zealand and Japanese-Canadian complexes in the Panthalassa might have influenced oceanic environment, and was cause of particular biostratigraphical and lithological nature in both basins.

Berker, L., Poreda, R. J., Hunt, A. G., Bunch, T. E. B., Rampino, M. R., 2001. Impact event at the Permian-Triassic boundary: Evidence from extraterrestrial noble gasses in fullerences. Science, 209: 1530-1533.

Erwin, D. H., 1993. The great Paleozoic crisis: Life and death in the Permian. New York, Columbia University Press, 327p.

Hallam, A., Wignall, P. B., 1997. Mass extinction and their aftermath. Oxford, Oxford University Press, 320p.

Isozaki, Y., 1994. Superanoxia across the Permo-Triassic boundary: Recorded in accreted deep-sea pelagic chert in Japan. Canadian Society of Petroleum Geologist Memoir, 17: 805-812.

Isozaki, Y., 1997. Permo-Triassic boundary superanoxia and stratified superocean: records from lost deep sea. Science, 276: 235-238.

Kamata, Y., Matsuo, A., Takemura, A., Yamakita S., Aita Y., Sakai T., Suzuki N., Hori, R. S., Sakakibara M,, Fujiki T., Ogane K., Takemura S., Sakamoto S.,

Kodama, K., Nakamura Y., Campbell, H. J., Spörli, K. B., 2003. Late Induan (Dienerian) radiolarians from Arrow Rocks in the Waipapa Terrane, North Island, New Zealand. Tenth Meeting of the International Associationof Radiolarian Paleontologist, 2003, September, Switzerland. 70-71.

Krull, E. S., Retllack, G. J., 2000. $\delta^{13}C$ depth profiles from paleosols across the Permian-Triassic boundary: Evidence for methane release. Geological Society of America Bulletin, 112: 1459-1472.

Krystyn, L., baud, A., Richoz, S., and Twitchett, R.J., 2003, A unique Permian-Triassic boundary section from Oman. Palaeogeography, Palaeoclimatology, Palaeoecology, 191: 329-344.

Reichow, M. K., Saunders, A. D., White, R.V., Pringle, M. S., Al´Mukhamedov, A. I., Medvedev, A., Kirda, N. P., 2002. $^{40}Ar/^{39}Ar$ dates from the West Siberian Basin: Siberian flood basalt province doubled. Science, 296: 1846-1849.

Sepkoski, J. J., Jr., 1989. Periodicty in extinction and the problem of catastrophism in the history of life. Journal of Geological Society, London, 146: 7-19.

Sporli, K. B., Aita, Y., Gibson, G. W.,1989. juxtaposition of Tethyan and non-Tethyan Mesozoic radiolarian faunas in mélanges, Waipapa terrane, north Island, New Zealand. Geology, 17: 753-756.

Takemura, A., Aita, Y., Hori, R. S., Higuchi, Y., Sporrli, B. K., Campbell, H., Kodama, K., Sakai, T., 1998. Preliminary report on the lithstratigraphy of the Arrow Rocks, and geologic age of the northern part of the Waipapa Terrane, New Zealand. News of Osaka Micropaleontologists, Special Volume, 11: 47-57.

Takemura, A., Aita, Y., Hori, R. S., Higuchi, Y., Sporli, K. B., Campbell, H. J., Kodama, K., Sakai, T., 2002. Triassic radiolarians from the ocean-floor sequence of the Waipapa Terrane at Arrow Rocks, Northland, New Zealand. New Zealand Journal of Geology and Geophysics, 45: 289-296.

Takemura, A., Sakai, M., Yamakita, S., Kamata, Y., Aita, Y., Sakai, T., Suzuki, N., Hori, S. R., Sakakibara, M., Kodama, K., Takemura, S., Sakamoto, S., Ogane, K., Koyano, T., Satake, A., Nakamura, Y., Campbell, H. J., Spörli, K. B., 2003. Early Triassic radiolarians from Arrow Rocks in the Waipapa Terrane, North Island, New Zealand. Tenth Meeting of the International Associationof Radiolarian Paleontologist, 2003, September, Switzerland.

Wignall, P. B., Hallam, A., 1992. Anoxia as a cause of the Permian/Triassic extinction: facies evidence from northern Italy and western United States. Palaeogeography, Palaeocli,atology, Palaeoecology, 93: 21-46.

Wignall, P. B., Twitchett, R. J., 1996. Oceanic anoxia and the end Permian mass extinction. Science, 272: 1155-1158.

Wignall, P. B., Twitchett, R. J., 2002. Extinct, duration, and nature of the Permian-Triassic superanoxic event. *in* Koebarl, C., MacLeod, K.G. (eds.) Catastrophic events and mass extinctions: Impacts and beyond. Geological Society of America Special Paper, 356: 395-413.

Yamakita, S., Takemura, A., Aita, Y., Sakai, T., Kamata, Y., Suzuki, N., Hori, R. S., Sakakibara, M., Fujiki, T., Ogane, K., Takemura, S., Sakamoto, S., Kodama,K., Nakamura, Y., Campbell, H., Spörli, K. B., 2003. Conodont age control for the radiolarian-bearing Early Triassic chert sequence at Arrow Rocks, New Zealand. Tenth Meeting of the International Associationof Radiolarian Paleontologist, 2003, September, Switzerland.

Isarcicella Population in the Lowermost Triassic of Slovenia

Tea Kolar-Jurkovsek and Bogdan Jurkovsek

Geological Survey of Slovenia, Dimiceva 14, SLO – 1000 Ljubljana, Slovenia; tea.kolar@geo-zs.si, bogdan.jurkovsek@geo-zs.si

In Slovenia, large geotectonic units of the Eastern Alps and the Dinarides come in contact along the Periadriatic lineament. During Upper Permian, the extended Slovenian carbonate platform was established south of the Periadriatic lineament (Buser 1996) with typical limestone deposition that became later mainly dolomitized. The Upper Permian fossiliferous limestones west of the Ljubljana city (Idrija-Ziri area) are known under the term Zazar Formation that is equivalent to the Bellerophon Formation of the Carnian Alps and Dolomites. In the Idrija-Ziri area, there is no break in sedimentation at the Permian-Triassic boundary interval, but in many sections this transition is in dolomitic facies that is difficult to determine paleontologically.

The Lower Triassic beds of the Slovenian carbonate platform are characterized with much terrigeneous influx. The oldest beds of the Lower Triassic succession are represented by gray laminated limestone and cellular dolomite that have not been paleontologically dated. Two lower Triassic limestone sequences belonging to the oldest Triassic member, the so-called Laminated Limestone (Mlakar 2002) of the Ziri area have been investigated by means of conodonts. They demonstrated presence of the *Isarcicella* population. The Ziri 28 section is characterized by exclusive occurrence of the genus *Isarcicella*, whereas in the Ziri/Vrsnik 61 section it is accompanied by rare *Neospathodus* representatives.

Further study will be focused to the area west of these two sections, where in certain sequences also the carbon isotopic anomalies across the Permian-Triassic boundary have been observed (Dolenec et al. 2004).

Buser, S., 1996. Geology of Western Slovenia and its paleogeographic evolution. *in* Drobne, K. et al. (eds) The role of impact processes in the geological and biological evolution of planet Earth. International Workshop, September 27 – October 2, 1996, Postojna/Slovenia,

111-123, Ljubljana.

Dolenec, T., Ogorelec, B., Dolenec, M., Lojen, S., 2004. Carbon isotope variability and sedimentology of the Upper Permian carbonate rocks and changes across the Permian-Triassic boundary at the Masore section (Western Slovenia). Facies, 50: 287-299.

Mlakar, I., 2002. On the origin of the hydrographic net and on some karst phenomena in the Idrija region. Acta Carsologica, 31(2): 9-60.

Biostratigraphy and Event Stratigraphy Around the Permian-Triassic Boundary (PTB) in Iran and Implications for the Causes of the PTB Biotic Crisis

Heinz W. Kozur

Rézsü u. 83, H-1029 Budapest, Hungary; kozurh@helka.iif.hu

In several sections of four areas with pelagic open sea deposits in Iran (Abadeh and Shahreza in Central Iran, Jolfa and Zal in NW Iran) the conodont succession and events around the PTB were investigated in detail. A very detailed conodont zonation was elaborated from the *Clarkina nodosa* up to the *Isarcicella isarcica* Zone. All events could be very well dated and by cross correlation with continental lake deposits with well recognisable Milankovitch cyclicity not only the numerical age of the events could be well recognised but also the duration of most of the conodont zones could be calculated. The following 9 conodont zones were discriminated: *C. nodosa*, *C. changxingensis*-*C. deflecta*, *C. zhangi* (~ 70 000 years), C. *iranica* (~ 60 000 years), *C. hauschkei* (~ 15 000 years), *C. meishanensis*-*Hindeodus praeparvus*, *Merrillina ultima*-*Stepanovites*? *mostleri* (the two zones together ~ 120 000 years), *H. parvus* (~ 100 000 years) and *I. isarcica* (~ 0,5 Ma) Zones. No detailed cross correlation is possible for the *C. nodosa* and *C. changxingensis*-*C. deflecta* Zones but comparing the thickness of the two overlying zones in unreduced sections, under assumption of probably constant sedimentation rate, the *C. nodosa* Zone is about as long as the *C. iranica* Zone or a little shorter (~ 50 000 to 60 000 years) and the *C. changxingensis*-*C. deflecta* Zone is about as long as the *C. zhangi* and *C. iranica* Zones together (~ 130 000 years). The unusual short duration of all conodont zones in the interval from the *C. nodosa* up to the *H. parvus* Zone indicates high ecologic stress. The extremely short *C. hauschkei* Zone Is the uppermost zone with warm water conodonts and it is cut by the extinction even for warm water conodont faunas at the top of that zone. In Abadeh section, situated about at the tropic of capricorn only a poor cool water conodont fauna is present in the *C. hauschkei* Zone. In the more northern sections, closer to the equator in that time, the poor cool water fauna begin only at the base of the *C. meishanensis*-*H. praeparvus* Zone.

The *C. zhangi* Zone, *C. meishanensis*-*H. praeparvus* Zone and *H. parvus* Zone can be directly correlated with the same conodont zones in South China. The *C. changxingensis*-*C. deflecta* Zone can be roughly correlated, but the underlying *C. nodosa* Zone is not present in South China. The *C. hauschkei* Zone may be present in South China but not in Meishan, where both the *C. iranica* and *C. hauschkei* Zones are missing. The *M. ultima*-*S.*? *mostleri* Zone can be well correlated with the *C. zhejiangensis* Zone at Meishan. The *C. hauschkei* Zone can be correlated until Greenland, where *C. hauschkei borealis*, which is also present in Iran, occurs in the lowermost *Otoceras boreale* Zone. The *C. meishanensis*-*H. praeparvus* and *H. parvus* Zones can be also directly correlated with the same zones in the Boreal realm.

In three horizons, the Dorashamian warm water conodont fauna is replaced by a cool water fauna with *H. typicalis* and few *Merrillina* sp. Especially well recognisable is the uppermost horizon in the lower *C. zhangi* Zone. This level can be well correlated with continental beds by a short reversed interval which comprises the upper *C. changxingensis*-*C. deflecta* Zone and most of the *C. zhangi* Zone. In the Germanic Basin it occurs in the uppermost Zechstein lower Fulda Formation and lowermost upper Fulda Fm. On the Russian Platform it corresponds to the Nedubrovo Formation, in which a fallout of mafic tuffs from the Siberian Trap is present several 1000 km away from the eruption centres. In the Germanic Basin and in Iran this horizon contains volcanic microsphaerules. Thus, a direct connection of the immigration of cool water fauna into the tropical realm with an especially strong explosive activity of the Siberian Trap volcanism can be recognised. As these faunal changes are the same as at the base of the Boundary Clay also for this horizon a short cooling event due to strong volcanism can be assumed. Additional influence by an impact cannot be excluded.

The following events can be observed close to the PTB in the Iranian sections (1) A continuous drop of $\delta^{13}C_{carb}$ can be observed which starts with values around 3 ‰ in the *C. nodosa* Zone and goes to values slightly below 0 ‰ at the base of the *H. parvus* Zone. After a short recovery in the upper *H. parvus* Zone, mostly a second negative excursion can be observed in the lower *I. isarcica* Zone. Within the continuous drop from the *C. nodosa* Zone up to the base of the Triassic only a short recovery to values maximally around 2 ‰ was in the uppermost *C. meishanensis*-*H. praeparvus* Zone. The strong and abrupt negative excursion in the Boundary Clay of Meishan is a secondary signal, which we found also in Iran, when weathered Boundary Clay with very low carbonate content (as in Meishan) was investigated as in Abadeh and Jolfa. However, if unweathered Boundary Clay was investigated, like in Shareza, Zal and Gerennavár of Bükk Mountains, Hungary, this negative excursion is not present. It is very interesting that the interval with strong ecologic stress indicated by the very short conodont zones coincides with the continuos drop in $\delta^{13}C_{carb}$. (2) Short reversed horizon (duration according to cross correlation with continental beds ~ 110 000 years) in the upper *C. changxingensis*-*C. deflecta* Zone and in the largest part

of the *C. zhangi* Zone. (3) Sudden facies change at the base of the Boundary Clay which is accompanied by a strong extinction event of the warm water fauna (and therefore related to a strong climatic change) which did not much affect the eurytherm benthos (small foraminifers, ostracods),. Whereas the base of the Boundary Clay is a synchronous event which indicates rapid drop in biogenic carbonate production (most probably because of blocking of sunlight), the extinction of the warm water faunas is diachronous, and lies at the tropic of capricorn (Abadeh section) at the base of the *C. hauschkei* Zone, 1000 km closer to the palaeoequator and at the palaeoequator themselves at the base of the *C. meishanensis-H. praeparvus* Zone. (4) Strong climatic change at the base of the Boundary clay (see 3). (5) High energy event at the base of the Boundary Clay which can be also observed in the several 1000 km away Bükk Mountains. It is probably related to huge tsunamies. (6) Rapid, but stepwise extinction of the eurytherm benthos in the interval from the base of the *M. ultima-S.*? *mostleri* Zone up to the very base of the *H. parvus* Zone, which occurs in the southern sections earlier than in the northern sections closer to the palaeoequator. (7) Maximum of microbialites, in shallower sections also large stromatolite or thrombolite bodies in the *H. aprvus* Zone which begins already in the *M.ultima-S.*? *mostleri* Zone. (8) Presence of an about 300 000 years long interval with more frequent than average microsphaerules with a first maximum in the cool water horizon of the lower *C. zhangi* Zone (mostly volcanic microsphaerules) and a second strongest maximum in the lower but not lowermost Boundary Clay (cosmic and volcanic sphaerules). Except event 6 all events can be traced also in other marine and continental sections.

Especially important is the fact that the PTB in the investigated Iranian sections lies in red sediments or, if it lies in light grey sediments as in Abadeh, the ostracod fauna indicates high oxygen content in the bottom water. Therefore, the anoxia cannot be the reason for the extinction event but they only locally or regionally overprint the extinction event, where they are present.

Correlation of the Continental Uppermost Permian and Lower Triassic of the Germanic Basin with the Marine Scale in the light of New Data from China and Iran

Heinz W. Kozur

Rézsü u. 83, H-1029 Budapest, Hungary;
kozurh@helka.iif.hu

The correlation of pelagic sediments with high-resolution biostratigraphic control with continental beds belongs to the most difficult stratigraphic questions. For detailed correlation not only interfingering of marine and continental beds must be used but also abiotic events. Yin Hongfu and co-workers made very important and excellent studies on the eventostratigraphy around the Permian-Triassic boundary (PTB) in Meishan and other South Chinese pelagic sections, and correlated all events very precisely with the high-resolution biostratigraphy of these sections (e.g. Yin Hongfu & Zhang Kexin, 1996, Yin Hongfu et al., 1996a, b, 2001). All events around the PTB can be found also in Iran, where they were correlated very detailed with the conodont biostratigraphy (Kozur, 2004 and in press, Korte et al., 2004 a, b, c). The detailed conodont zonation is shown in Fig. 1. All these events are also present around the PTB in continental beds of the Germanic Basin, and allow a very precise correlation of the PTB and eventostratigraphic markers below and above this boundary (Fig. 2). Detailed bio- and eventostratigraphic data were also published around the Olenekian base from the proposed GSSP of the Olenekian base at Chaohu (Tong et al., 2004, 2005). Further important data about the Gangetian to Smithian ammonoid and conodont chronology were reported by Bhargava et al. (2004) and Krystyn et al. (2004) from extremely ammonoid- and conodont- rich sediments of Spiti (India).

The PTB in continental beds of the Germanic Basin lies at the top of the *Falsisca postera* Zone. It is confirmed by a minimum in $^{13}C_{carb}$ and $^{13}C_{org}$ in the same bed and the same event succession as in Meishan and the Iranian sections. The boundary between the *F. postera* and the *F. verchojanica* Zone can be also found in Dalongkou close to the LOD of *Dicynodon*. The co-occurrence of *Dicynodon* with *Lystrosaurus* is therefore uppermost Permian and not lowermost Triassic. Most of the Lystrosaurus fauna (without Dicynodon) is, however, Triassic in age and coincides with the Gangetian Substage. The Gangetian-Gandarian boundary in continental beds is characterised by the disappearance (LOD) of *Falsisca* and the roughly contemporaneous LOD of *Lystrosarus* and the first occurrence (FAD) of spined conchostracans (*Molinestheria*, *Vertexia*, *Cornia*). It lies in the uppermost Calvörde Formation in the middle of magnetozone 1r (both in marine and continental beds). The base of the Olenekian in continental beds of the Germanic Basin was mostly placed at the base of the Hardegsen Fm. (Menning, 1995) or at the base of the Volpriehausen Fm. (Menning, 2000), but this was not supported by biostratigraphic or magnetostratigraphic evidences. Szurlies (in press) and Szurlies et al. (2003) used the magnetostratigraphic data of Scholger et al. (2000) from the Southern Alps and put the base of the Olenekian inside the Volpriehausen Fm., but such magnetostratigraphic correlations made only a sense, if not only reliable magnetostratigraphic data are used but also the correlation of the magnetozones within the marine Triassic must be checked in the sections, where they were measured. The palaeomagnetic data of Scholger et al. (2000) are reliable, but these authors did not regard the well known biostratigraphic data summarised in Farabegoli & Perri (1998) from the same Pufels (Bulla) section, where the magnetostratigraphic investigations were made. The top of the normal zone 2n is close to the base of the Olenekian (Tong et al., 2005) and not in the middle Gandarian (Dienerian) as shown by Scholger et al. (2000). The top of magnetozone 2n in Pufels (Bulla) is close to the top of the upper Gandarian *Claraia aurita* Zone and about 3 m below sample Bu 45 of Farabegoli &

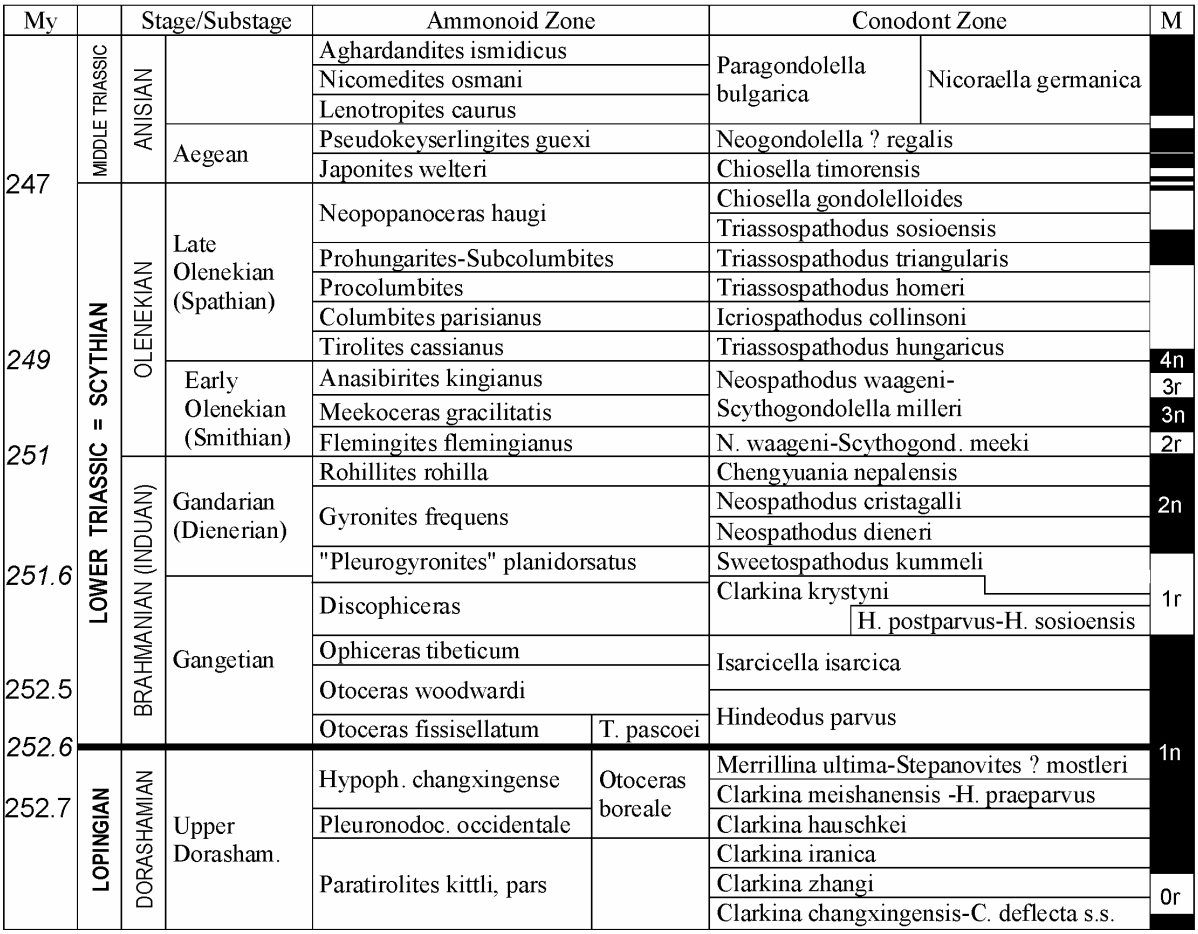

Figure 1. Ammonoid and conodont zonation of the pelagic marine Lower Triassic
Numerical scale calculated from radiometric data (normal numbers) and astronomic calibration (in italics). Palaeomagnetic data from Zakharov & Sokarev (1991), Muttoni et al. (1996), Scholger et al. (2000), Szurlies & Kozur (2004), Tong et al. (2005). Dating of the magnetozones partly strongly changed (Scholger et al., 2000) or slightly changed (Muttoni et al., 1996). Grey interval: No reliable palaeomagnetic data or no detailed correlation.

Perri (1998) with the lower Olenekian *Pachycladina obliqua* conodont fauna, which begins in a limestone bed immediately below the top of 2n. Thus, in contrast to the correlation by Scholger et al. (2000), also in the Pufels (Bulla) section the top of the magnetozone 2n is close to the base of the Olenekian confirming the data by Tong et al. (2005). On the base of conchostracans, which are well correlated with the marine scale, Kozur (e.g., 1993, 1999) placed the base of the Olenekian inside the Lower Buntsandstein upper Bernburg Fm. The position of the magnetostratigraphic zone 2n in the Chaohu GSSP candidate and after biostratigraphic correlation also in the Pufels (Bulla) section confirms this position of the Olenekian base.

Bhargava, O. N., Krystyn, L., Balini, M. Lein, R., Nicora A., 2004. Revised litho- and sequence stratigraphy of the Spiti Triassic. Albertiana, 30: 21-39.

Farabegoli, E., Perri, M. C., 1998. Stop 4.3 - Permian-Triassic boundary and Early Triassic of the Bulla section (Southern Alps, Italy. Lithostratigraphy, facies and conodont biostratigraphy. Giorn. Geol., ser 3ª, 60, Spec. Issue, ECOS VII Southern Alps Field Trip Guidebook, 292-311.

Geluk, M. C., Röhling, H. G., 1999. High-resolution sequence stratigraphy of the Lower Triassic Buntsandstein: A new tool for basin analysis. Zbl. Geol. Paläont. Teil I, 1998(7-8): 727-745.

Korte, C., Kozur H. W., in press. Carbon isotope stratigraphy across the Permian-Triassic boundary at Jolfa (NW-Iran), Peitlerkofel (Sas de Pütia, Sass de Putia), Pufels (Bula, Bulla), Tesero (all three southern Alps, Italy) and Gerennavár (Bükk Mts., Hungary). Journ. Alpine Geol.

Korte, C., Kozur, H. W. Joachimski, M. M., Strauss, H., Veizer, J., Schwark, L., 2004a. Carbon, sulfur, oxygen and strontium isotope records, organic geochemistry and biostratigraphy across the Permian/Triassic boundary in Abadeh, Iran. Int. J. Earth Sci. (Geol. Rdsch.), 93: 565-581.

Korte, C., Kozur, H. W., Mohtat-Aghai, P., 2004b. Dzhulfian to lowermost Triassic $d^{13}C$ record at the Permian/Triassic boundary section at Shahreza, Central Iran. Hallesches Jahrb. Geowiss., Reihe B, Beiheft 18: 73-78.

Korte, C., Kozur, H. W., Partoazar, H., 2004c. Negative

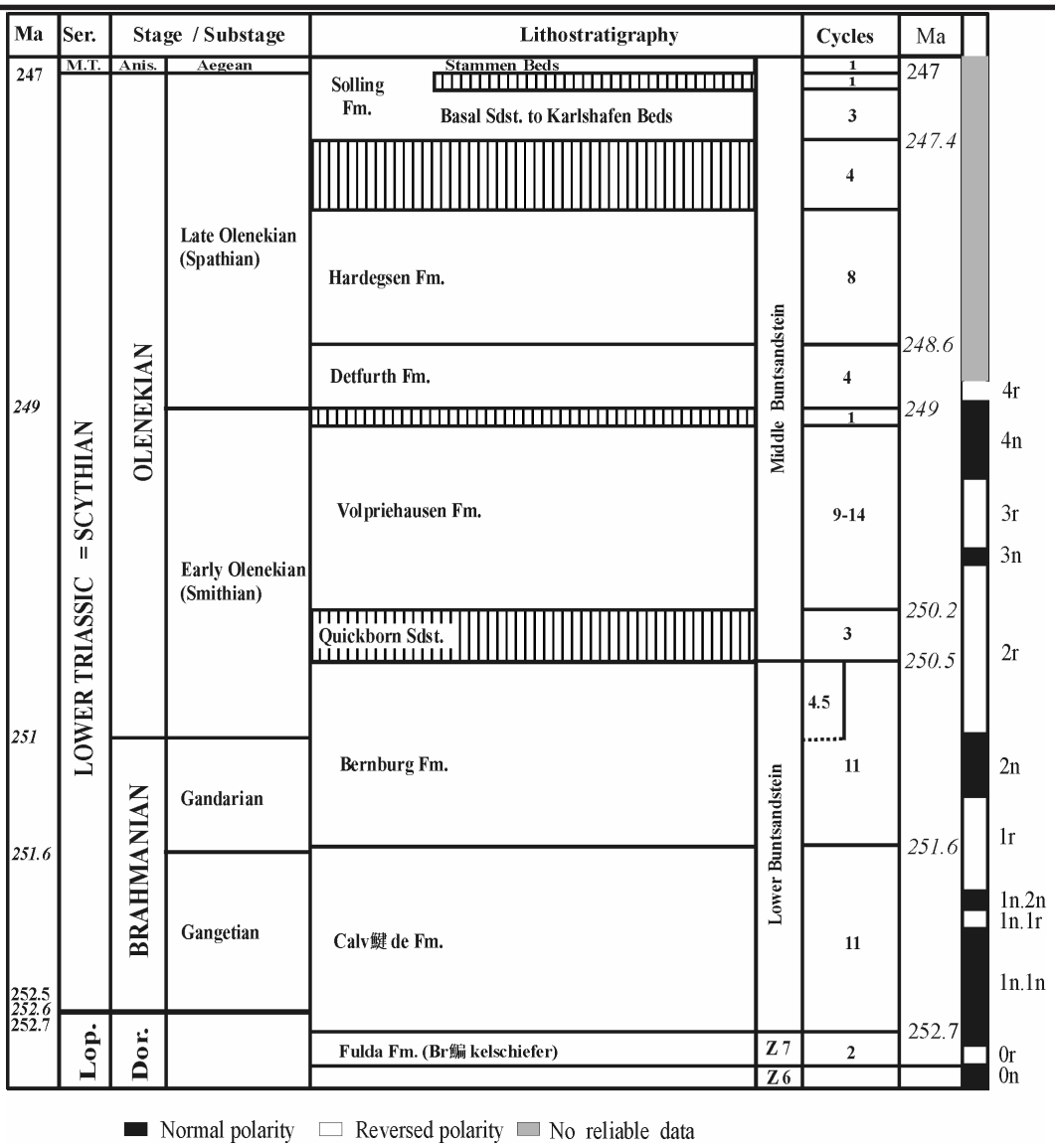

Figure 2. Correlation of the uppermost Permian and Lower Triassic (uppermost Zechstein to Middle Buntsandstein) of the Germanic Basin with the international scale. Slightly modified cycles and palaeomagnetic data after Geluk & Röhling (1999), Röhling (1991), Szurlies (1998, 2004). Numerical ages calculated from radiometric data and astronomic calibration after Kozur (2003a,b).

carbon isotope excursion at the Permian/Triassic boundary section at Zal, NW-Iran. Hallesches Jahrb. Geowiss., Reihe B, Beiheft 18: 69-71.

Kozur, H., 1993. Range charts of conchostracans in the Germanic Buntsandstein. *in* Lucas, S. G., Morales, M. (eds.) The nonmarine Triassic. New Mexico Mus. Nat. Hist. & Sci., Bull., 3: 249-253.

Kozur, H. W., 1999. The correlation of the Germanic Buntsandstein and Muschelkalk with the Tethyan scale. Zbl. Geol. Paläont. Teil I, 1998 (7-8): 701-725.

Kozur, H. W., 2003a. Integrated ammonoid, conodont and radiolarian zonation of the Triassic and some remarks to stage/substage subdivision and the numeric age of the Triassic stages. Albertiana, 28: 57-83.

Kozur, H. W., 2003b. Integrated ammonoid, conodont and radiolarian zonation of the Triassic. Hallesch Jahrb. Geowiss., B 25: 49-79.

Kozur, H. W., 2004. Pelagic uppermost Permian and the Permian- Triassic boundary conodonts of Iran. Part 1: Taxonomy. Halle. Jahrb. Geowiss., Reihe B, Beih. 18: 39 - 68.

Kozur, H. W., in press. Pelagic uppermost Permian and the Permian-Triassic boundary conodonts of Iran. Part II: Investigated sections and evaluation of the conodont faunas. Halle. Jahrb. Geowiss., Reihe B, Beih., 19.

Krystyn, L., Balini, M., Nicora, A., 2004. Lower and Middle Triassic stage and substage boundaries in Spiti. Albertiana, 30: 40-53.

Menning, M., 1995. A numerical time scale for the Permian and Triassic Periods: An integrated time analysis. *in* Scholle, P. A., Peryt, T. M., Ulmer-Scholle, D. S. (eds.) The Permian of Northern Pangea, 1: 77-97.

Menning, M., 2000. Stratigraphische Nomenklatur für die Germanische Trias (von Alberti 1834) und die Dyas (Marcou 1859, Geinitz 1861). Z. geol. Wiss., 28(1/2),

281-290.Muttoni, G., Kent, D.V., Meco, S., Nicora, A., Gaetani, M. and Balini, M., Germani, D., and Rettori, R., 1996. Magneto-biostratigraphy of the Spathian to Anisian (Lower to Middle Triassic) Kcira section, Albania. Geophys. J. Int., 127: 503-514.

Röhling, H.–G., 1991. A lithostratigraphic subdivision of the Lower Triassic in the northwest German Lowland and the German Sector of the North Sea, based on Gamma–Ray and Sonic Logs.– Geol Jb., A 119, 3–24.

Scholger, R., Mauritsch, H. J., Brandner, R., 2000. Permian-Triassic boundary magnetostratigraphy from the Southern Alps (Italy). Earth Planet. Sci. Lett., 176: 495-508.

Szurlies, M., in press. Magnetostratigraphy: the key to a global correlation of the classic Germanic Trias - case study Volpriehausen Formation (Middle Buntsandstein), central Germany. Earth and Planetary Sci. Lett.

Szurlies, M., Bachmann, G. H., Menning, M., Novaczyk, N. R., Käding, K. C., 2003. Magnetostratigraphy and high-resolution lithostratigraphy of the Permian-Triassic boundary interval in Central Germany. Earth Planet. Sci. Letters, 212(2003): 263-278.

Tong Jinnan, Zakharov, Yu. D., Orchard, M. J., Yin Hongfu, Hansen, H. J., 2004. Proposal of Chaohu section as the GSSP candidate of the Induan-Olenekian boundary. Albertiana, 29: 13-27.

Tong Jin-nan, Zhao Lai-shi, Zuo Jing-xun, Hansen, H. J., Zakharov, Y. D., 2005. An integrated Lower Triassic sequence in Chaohu, Anhui Province. Earth Sci. Journ. China Univ. Geosci., 30(1), 40-46.

Yin hongfu, Zhang Kexin, 1996a. Eventostratigraphy of the Permian-Triassic boundary at Meishan section, South China. *in* Yin Hongfu (ed.) The Palaeozoic-Mesozoic boundary—Candidates of global stratotype section and point of the Permian-Triassic boundary, 84-96, Wuhan (China University of Geosciences Press).

Yin, H., Sweet, W. C., Glenister, B. F., Kotlyar, G., Kozur, H., Newell, N. D., Sheng, J., Yang, Z., Zakharov, Y. D., 1996b. Recommendation of the Meishan section as Global Stratotype Section and Point for basal boundary of Triassic System. Newsl. Stratigr., 34(2): 81-108.

Yin Hongfu, Zhang Kexin, Tong Jinnan, Yang Zunyi, Wu Shunbao, 2001. The Global Stratotype Section and Point (GSSP) of the Permian-Triassic boundary. Episodes, 24(2): 102-114.

Muth (Spiti, Indian Himalaya) – A Candidate Global Stratigraphic Section and Point (GSSP) for the Base of the Olenekian Stage.

Leopold Krystyn[1], Om N. Bhargava[2] and Devendra K. Bhatt[3]

[1] Department of Palaeontology, Vienna University, A-1090 Vienna, Althanstrasse 14, Austria; leopold.krystyn@univie.ac.at

[2] 103, Sector 7, Panchkula 134 109, Haryana, India

[3] 57 Clay Square, Lucknow 226 024, Uttar Pradesh, India

Southern Tibet and the High Himalayan Range are now located in the Tibetan Zone known as the highest tectonic element of the Himalayan orogen. During the Lower Triassic time this zone was part of the tropical Indian Gondwana margin and formed a large deeper-neritic basin close to or below storm wave base with long-term stable environmental conditions. In this basin, pelagic fossils such as ammonoids, specific bivalves and conodonts were widespread deposited in fine-grained carbonates (distal tempestites or bioclastic wackestones). These are now found in prolifically in many places of northern India, Nepal and Tibet. The original low palaeolatitude, a high preservation potential and good fossil extractability are the fundamentals of an extraordinary pelagic faunal diversity record (Diener, 1897, Krafft & Diener, 1909, Waterhouse, 1996, Bhatt et al., 1999) and underline the past and present importance of the region for the chronostratigraphic subdivision of the Lower Triassic and for high-resolution fossil zonations. Waterhouse has recently proposed a new detailed ammonoid subdivision of the entire Lower Triassic for Nepal, and Spiti data with special reference to the Induan-Olenekian boundary are presented herein. A more recent geological monograph of Spiti has been published by Bhargava and Bassi, 1998.

The Muth section is situated in Lahul & Spiti district, northern Himachal Pradesh State of India in the Western Himalayas and is formerly proposed as candidate GSSP for the Induan-Olenekian boundary (Lower Triassic). It is reachable from Shimla (or Manali) through the main road along the Sutlej and Spiti valleys till Lingti and, from there up the Pin valley road up to the village of Muth (3800 m). Due to high altitude, access to the outcrop may be hindered by snowfall during the winter months but is principally unrestricted all year long. The travel to Spiti and Muth is open to persons of all nationalities.

Sediments representing the Lower Triassic in Spiti are found in the Mikin Formation (formerly Tamba Kurkur Fm.), subdivided recently into three members (Bhargava et al., 2004). Varying lithologies within the middle member allow discrimination of three intervals named for their diagnostic ammonoids from base to top as: 1) two to three meters thick *Gyronites* beds (the former *Meekoceras* beds of Krafft), 2) two meters thick *Flemingites* beds and 3) up to 10 m thick *Parahedenstroemia* beds. As for the

underlying lower member (*Otoceras* beds), the intervals can be traced along the Pin and Lingti rivers over tens of kilometres across strike and seem to constitute identical time-equivalent rock units. Faunistic studies of the I-O boundary interval so far have been concentrated in Muth section where board and lodging is available. The village itself rests on the Mikin Formation that extends from Muth towards northwest along a tributary valley for several kilometers to the crest between the Pin and Parahio valleys. Extensive continuous exposures on the northern valley slope provide excellent conditions for measuring and sampling of the sequence at many places between 3900 m and 5000 m altitude (see fig. 1 in Krystyn et al., 2004). For logistic reasons, work was concentrated at two sites, one 100 m above the village called as M 03 and another, newly sampled in 2004, named as M 04. The latter is more difficult to reach as it is located at 4200m in altitude, though extensive outcrop weathering provides better conditions for megafossil collection. Both places show identical rock sequences and can be correlated bed-by-bed. This allows a comprehensive data set presentation within one composite section (fig. 1) where the conodont file is equally known from both places whereas the ammonoid data are mostly derived from M 04.

The *Flemingites* beds constitute a monofacial succession of: (1) in the lower part approximately 1dm- and (2) in the upper third c. 5 cm-bedded, dark grey limestones. Fifteen layers, numbered as 12A to 12C, 13A to C, 14A to C, 15A to C and 16A to C record a sequence of four ammonoid as well as conodont zones, some of them with corresponding boundaries. From the base to the top the following ammonoid zones with their conodont counterparts are discriminated: 1) a "*Gyronites*" sp. Zone containing ammonoids of typical Induan affinity time-equivalent to the *nepalensis* Zone, 2) the *Rohillites rohilla* Zone equivalent to the *eowaageni* respectively *N. waageni* n. subsp. A Zone sensu Zhao Laishi et al., 2004, 3) the *Flemingites griesbachi* Zone coeval to the *elongata* = *N. waageni* n. subsp. B Zone and 4) the *Euflemingites* Zone corresponding to the top of the *elongata* and the (lower) *N. w.* w*aageni* Zone.

The new ammonoid sequence is presently recorded only from Muth, but counterparts of at least the *griesbachi* Zone may be found widespread in the eastern Tethys (Salt Range, Nepal, Tibet, Timor, China). The Muth zonal scheme gives way to three I-O boundary options: 1) the FO (or FA) of R*ohillites rohilla* in bed 13C: it marks the entry of flemingitids or typical Olenekian (Smithian) ammonoids (= O 1). The contemporaneous appearance of kashmiritids and of *Pseudohedenstroemia himalayica* strengthens the event; the latter may indicate apparent synchronicity with the appearance of *Hedenstroemia* in the Boreal; 2) the FO/FA of *Flemingites griesbachi* (and of *Flemingites* s. str.) in bed 14B (= O 2) and 3) the FO of

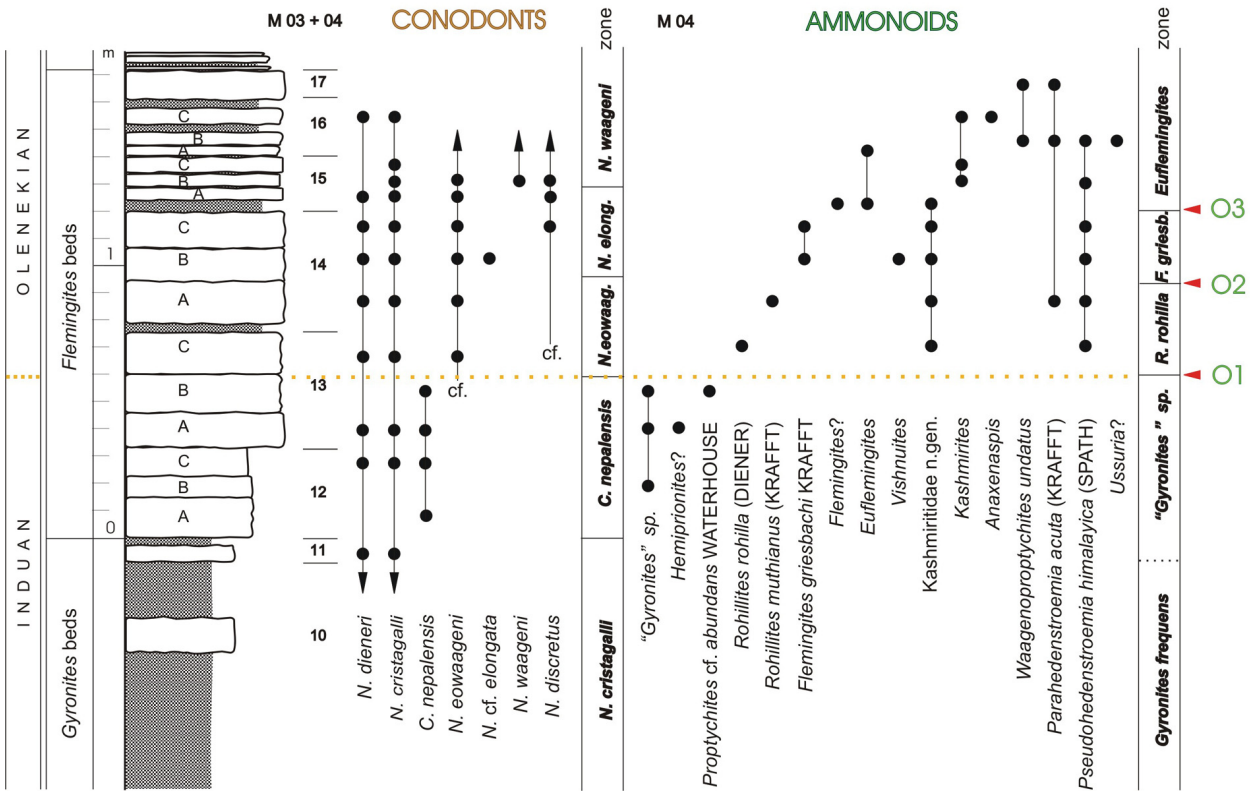

Figure 1. Ammonoid and conodont biochronology of the proposed Induan-Olenekian boundary candidate GSSP at Muth, Spiti.

Euflemingites in bed 15A (= O 3). Option 1 represents the most distinct ammonoid boundary, which seems to correlate with the onset of the *N. waageni* group also in Chaohu, China (Tong et al., 2003), a datum preferred by the Subcommission on Triassic Stratigraphy. It may be recognizable by conodonts in the Boreal realm through disappearance of *C. nepalensis*. Options 2 and 3 are less distinctive ammonoid boundaries despite the fact that the pandemic genus *Euflemingites* may represent the only direct stratigraphic link between low and high palaeolatitudes faunas within the whole time interval.

From a biochronological viewpoint, Muth is an obviously superior site compared to Chaohu, the other presently proposed candidate (Tong et al., 2003). The Chaohu sections have a) fewer macrofaunal elements, confined to an interval above the proposed boundary, and b) miss *C. nepalensis* as a complementary boundary proxy. Muth on contrary shows a reduced sediment accumulation rate reaching only half of the boundary beds thickness of Chaohu. Demonstration of sedimentary completeness and stratigraphic continuity is thus fundamental in Muth and is provided by the described successive appearance data of phylogeneticly related ammonoid and conodont taxa. A severe handicap of Muth section is a regional thermal overprint (CAI 3,5) that precludes a reliable magnetostratigraphy. A meaningful chemostratigraphy, however, is still possible (Atudorei, pers. comm.) and scheduled for 2005.

Bhargava, O. N., Bassi, U. K., 1998. Geology of Spiti-Kinnaur Himachal Himalaya. Geol. Surv. India Mem., 124: 1-210.

Bhargava, O. N., Krystyn, L., Balini, M., Lein, R., Nicora, A., 2004. Revised litho- and sequence stratigraphy of the Spiti Triassic. Albertiana, 30: 21-39.

Bhatt, D. K., Joshi, V. K., Arora, R. K., 2004. Conodont biostratigraphy of the Lower Triassic in Spiti Himalayas, India. Journal Geological Society of India, 54: 153-167.

Diener, K., 1897. Himalayan fossils. The Cephalopoda of the Lower Triassic. Palaeontologia Indica, (ser. 15) 2(1): 1-191.

Krafft, A., Diener, C., 1909. Himalayan fossils. Lower Triassic Cephalopoda from Spiti, Malla johar, and Byans. Palaeontologia Indica, (ser. 15) 6(1): 1-186.

Krystyn, L., Balini, M., Nicora, A., 2004. Lower and Middle Triassic stage boundaries in Spiti. Albertiana, 30: 39-53.

Tong Jinnan, Zakharov, Y. D., Orchard, M. J., Yin Hongfu, Hansen, H. J. 2003. A candidate of the Induan-Olenekian boundary stratotype in the Tethyan region. Science in China, 46: 1182-1200.

Waterhouse, J. B., 1996. The Early and Middle Triassic ammonoid succession of the Himalayas in western and central Nepal, Part 3: Late Middle Scythian ammonoids. Palaeontographica, 241: 101-167.

Zhao Laishi, Orchard, M. J., Tong Jinnan, 2004. Lower Triassic biostratigraphy and speciation of *Neospathodus waageni* around the Induan-Olenekian boundary of Chaohu, Anhui Province, China. Albertiana, 29: 41-43.

A revised Lower Triassic intercalibrated ammonoid-conodont time scale of the eastern Tethys Realm based on Himalayan data.

Leopold Krystyn

Department of Palaeontology, Vienna University, Althanstrasse 14 – 1090 Vienna, Austria

The Himalayas are known since long as host of large and diverse Lower Triassic faunas, most of which unfortunately lack precise stratigraphic distribution data in the rock record. Useless from viewpoint of modern biochronological standards they otherwise are of great importance for their substantial historic contribution to the chronostratigraphic subdivision of the Lower Triassic stages and substages. Bearing that in mind a thorough reinvestigation of sections in Spiti from where a major part of the fauna was derived, has been started within recent years (Krystyn et al., 2004).

Results of the study lead to a considerable improvement of the (eastern) Tethyan ammonoid zonal scheme with the introduction of new zones around the Gangetian (=Griesbachian) – Brahmanian (=Dienerian) and the Dienerian – Smithian boundary (fig. 1). Correlated on a regional scale with other schemes established in the eastern Tethys (Salt Range, Tibet, southern China) as well as on a long distance scale with those from western Panthalassa (Primoriye) and from the Arctic (Canada, Siberia) the actual superiority of the Himalayan faunal sequence will be demonstrated and discussed. In the light of the presented data a reinstallation of parts of the classical stage and/or substage terminology of Mojsisovics et al., 1895 against younger and less adequate subdivisions (i.e. Induan, Griesbachian, Dienerian) is highly recommended and should be considered

References

Krystyn, L., Balini, M. and Nicora, A., 2004: Lower and Middle Triassic stage and substage boundaries in Spiti. Albertiana,30 Suppl.: 39-52.

Mojsisovics, E. v., Waahen, W. and Diener, C., 1895: Entwurf einer Gliederung der pelagischen Sedimente des Trias-Systems. Sitzungsber. Akad. Wiss Wien, math.-naturwiss. Kl., 104: 1279-1302.

<table>
<tr><th>St.</th><th>Subst.</th><th></th><th>Ammonoids</th><th>Conodonts</th><th></th><th>Bivalves</th></tr>
<tr><td rowspan="8">OLENEKIAN</td><td rowspan="3">Spathian</td><td rowspan="3"></td><td>undifferentiated</td><td>N. gondolelloides</td><td></td><td rowspan="3"></td></tr>
<tr><td>Tirolites</td><td>undifferentiated</td><td></td></tr>
<tr><td>Nordophiceras</td><td>I. collinsoni</td><td></td></tr>
<tr><td rowspan="5">Smithian</td><td rowspan="5"></td><td>Anawasatchites / Anasibirites</td><td rowspan="3">G. milleri</td><td></td><td>“P.” himaica</td></tr>
<tr><td>Juvenites / Meekoceras</td><td rowspan="3">N. waageni</td><td></td><td rowspan="5"></td></tr>
<tr><td>Euflemingites</td><td></td></tr>
<tr><td>Flemingites griesbachi</td><td rowspan="2">N. eowaageni</td><td></td></tr>
<tr><td>Rohillites rohilla</td><td></td></tr>
<tr><td rowspan="4">INDUAN (=BRAHMANIAN)</td><td rowspan="2">Diener.</td><td rowspan="2">Gandar.</td><td>Prionolobus sp. A</td><td colspan="2">C. nepalensis</td></tr>
<tr><td>Gyronites frequens</td><td colspan="2">N. cristagalli
N. dieneri</td></tr>
<tr><td rowspan="5">Griesbachian</td><td rowspan="5">Gangetian</td><td>“Pleurogyronites“ planidorsatus</td><td colspan="2">N. kummeli
Ng. discreta</td><td rowspan="2">Claraia griesbachi</td></tr>
<tr><td>Discophiceras</td><td rowspan="3">I. isarcica</td><td rowspan="2">Ng. krystyni</td></tr>
<tr><td>Ophiceras tibeticum</td><td rowspan="3"></td></tr>
<tr><td>Otoceras woodwardi</td><td rowspan="2">Ng. meishanensis</td></tr>
<tr><td>Otoceras clivei</td><td>H. parvus</td></tr>
</table>

Fig. 1:Ammonoid and conodont zones in the Lower Triassic of Spiti.

End-Permian Extinction and Biotic Recovery: A Complete Record from an Isolated Carbonate Platform, the Great Bank of Guizhou, South China

Daniel J. Lehrmann[1], Jonathan L. Payne[2], Paul Enos[3], Jiayong Wei[4], Youyi Yu[4], Samuel A. Bowring[5], Jahandar Ramezani[5], Michael J. Orchard[6], Paul Montgomery[7], Daniel P. Schrag[2] and Andrew H. Knoll[2]

[1] University of Wisconsin, Oshkosh, WI, U.S.A. lehrmann@uwosh.edu

[2] Harvard University, Cambridge, MA, U.S.A.

[3] University of Kansas, Lawrence, KS, U.S.A.

[4] Guizhou Bureau of Geology, Guiyang, Guizhou, P.R.C.

[5] Massachusetts Institute of Technology, Cambridge, MA, U.S.A.

[6] Geological Survey of Canada, Vancouver, B.C., Canada

[7] ChevronTexaco, Bellaire, TX, U.S.A.

The end-Permian extinction and subsequent Early Triassic biotic recovery are exceptionally well recorded in marine strata of the Nanpanjiang Basin, south China. The Nanpanjiang Basin is a deep-marine embayment in the southern margin of the Yangtze Plate, which was located in the Eastern Tethys near the equator during the Permian and migrated northward to approximately 12°N by the beginning of the Middle Triassic (Enkin et al., 1992; Enos, 1995).

Several isolated carbonate platforms within the basin contain conformable Permian-Triassic boundary (PTB) sections and expanded well exposed Lower and Middle Triassic sections. The Great Bank of Guizhou (GBG) is the northernmost platform and it contains the longest uninterrupted Permian and Triassic sections in the basin, spanning the interval from the Upper Permian through the Late Triassic (Lower Carnian). Stratigraphic sections through the PTB and Lower-Middle Triassic recovery interval are exposed in the platform interior, platform margin, and basin margin. A detailed chronostratigraphy for the basin margin sections on the GBG is constrained by conodont biostratigraphy, magnetostratigraphy, carbon isotope stratigraphy, and U-Pb age dates. Exposure of a two-dimensional cross-section enables physical correlation between platform and basin strata.

The GBG nucleated on antecedent topography near the Permian margin of the Yangtze Platform during transgression in the Late Permian. The GBG evolved from a low-relief bank rimmed with oolite shoals and gentle basin-margin slopes during the Early Triassic to a *Tubiphytes* reef-rimmed platform with more than 400 m of relief and

steep basin-margin slopes in the Middle Triassic (Anisian - Early Ladinian). Finally, the platform developed a high-relief erosional escarpment before it was drowned and buried by siliciclastic turbidites at the beginning of the Late Triassic, Carnian (Lehrmann et al., 1998).

Conformable PTB sections in the platform interior exhibit an upward change from Upper Permian cherty skeletal packstone with diverse open-marine fossils to an interval of microbialite crust (calcimicrobial framestone) 15 m thick with interbeds of grainstone in the basal Griesbachian, followed by microgastropod packstone and lime mudstone. The microbial crust is composed of globular thrombolitic structures resembling *Renalcis* that from a framework with constructional cavities. Lenses of lime grainstone interbedded with the microbial crust contain abundant thin-shelled bivalves. Associated echinoderms and articulate brachiopods indicate open marine conditions during deposition of the microbialite crust (Lehrmann et al., 2003). Regional control on genesis of the crust is demonstrated by its presence on all isolated platforms in the basin. Global control is indicated by occurrence of the crust in distant localities in the western Tethys and Panthalassa (cf. Baud et al., 1997; Sano and Nakashima, 1997).

The Upper Permian skeletal packstone contains *Palaeofusulina*, *Colaniela*, *and Clarkina changxingensis* indicating a Changxingian age. The lowermost sample for conodonts from the microbialite crust was collected 65 cm above the base of the unit and contains *Hindeodus parvus*. Thus, the conformable biostratigraphic PTB is interpreted to occur within the basal 65 cm of the crust. The PTB-event horizon, marking the greatest loss of Permian fossils, is interpreted to occur at the contact between the Upper Permian skeletal packstone and the microbialite crust lacking discernable Permian fossils. *Isarcicella isarcica* first appears immediately above the crust, at the level of the microgastropod packstone. The consecutive first occurrence of *H. parvus* followed by *I. isarcica* thus places the microbialite crust in the basal Griesbachian *H. parvus* zone.

Lower Triassic strata in the platform interior are approximately 400 m thick including: 50 m of thinly bedded lime mudstone and 100 m of dolo-oolite overlying the Griesbachian microbialite crust, followed by 180 m of Dienerian and Smithian peritidal cyclic limestone containing about 30 intervals of calcimicrobial mounds. Fossils are rare. All facies have a low diversity biota dominated by mollusks. Fabrics in the calcimicrobial mounds are identical to those found immediately above the PTB. The Olenekian-Anisian boundary occurs within massively dolomitized peritidal strata in the platform interior. Relative age assignments were made by physical tracing and carbon isotope correlation to basin margin facies at the Guandao section (Payne et al., 2004).

The basin margin succession is continuously exposed from the PTB through the Carnian at the Guandao section on the northern margin of the GBG. The Lower Triassic succession consists of 250 m of laminated black pelagic carbonate, subordinate shale, and interbeds of carbonate turbidites and debris flow breccias with oolite clasts. Beginning early in the Anisian strata contain a more diverse skeletal biota including *Tubiphytes* fragments, crinoids, mollusks, and fossiliferous clasts transported from platform margin reefs.

The Guandao section has a well developed chronostratigraphy constrained by abundant conodonts, magnetostratigraphy, and radiometric ages from several volcanic ash horizons. The Olenekian-Anisian boundary is especially well constrained providing a high-resolution record of a critical interval of biotic recovery. Fourteen conodont zones were defined for the Lower Triassic and basal Anisian. The Olenekian-Anisian boundary is characterized by the first occurrence of *Chiosella timorensis.* Additional constraints on placement of the boundary include: the last occurrences of *Ns. abruptus* and *Ns. triangularis* (Orchard, 1995) well below the boundary, the occurrence of *Ns. symmetricus* and *Ns. homeri* below and extending slightly above the boundary, and the first occurrence of *Gd. tethydis*, *Ni. germanicus*, and *Ni. kockeli* above the boundary.

Several volcanic ash horizons straddle the boundary. Preliminary U-Pb age dates indicate an age of 248 ma for the O-A boundary. Given that age dates for the end-Permian extinction horizon from independent labs appear to be converging near 252 Ma (see Bowring et al., 1998; Mundil et al., 2004), the duration of the Early Triassic Epoch and the interval of delayed recovery was approximately 4 million years.

The pattern of biotic recovery was examined in PTB through Ladinian sections in the platform interior and basin margin through analysis of the diversity and abundance of fossil grains. Preliminary results from taxonomic analysis of 608 thin sections, including point counts of 349 thin sections (300 points per slide) represent platform interior and basin margin settings from the Late Permian through the Middle Triassic. Data were compiled at the stage level to obtain broad estimates of the abundance and composition of fossil grains within platform and basin margin strata. The abundance of skeletal grains as a fraction of total rock volume decreased by more than an order of magnitude across the PTB in both platform (31% to 1%) and basin settings (7.4% to 0.005%). Abundance did not increase until the Spathian. The diversity of skeletal grains likewise decreased dramatically across the PTB. The magnitude of the decrease in abundance of fossil metazoan reefs either coincide with or slightly post-date stabilization of the carbon cycle in the Anisian (Payne et al., 2004). Notably large negative carbon excursions coincide with the onset of the two episodes of microbialite crust and mound genesis in the platform interior. These observations suggest that repeated environmental disturbances responsible for perturbations of the carbon cycle also directly inhibited biotic recovery. The occurrence of peculiar microbialite crusts and mounds during the period of low biodiversity and carbon cycle instability indicates that the environmental disturbances that retarded

biotic recovery may have also stimulated precipitation of the crusts. Therefore, we favor a scenario in which the removal of environmental disturbances allowed biotic recovery to proceed in the Middle Triassic. Characterizing the precise nature and geographic distribution of the environmental controls on biotic recovery may shed light on the nature of interactions between the physical environment and organic evolution that shaped the biotic recovery, and may also constrain interpretations of the mechanism underlying the end-Permian extinction.

Atudorei, V., Baud, A., 1997. Carbon isotope events during the Triassic. Albertiana, 20: 45-49.

Baud, A., Atudorei, V., Sharp, Z., 1996. Late Permian and early Triassic evolution of the Northern Indian margin: Carbon isotope and sequence stratigraphy. Geodinamica Acta, 9: 57-77.

Baud, A., Cirilli, S., Marcoux, J., 1997. Biotic response to mass extinction: the lowermost Triassic microbialites. Facies, 36: 238-242.

Bowring, S. A., Erwin, D. H., Jin, Y. G., Martin, M. W., Davidek, K., Wang, W., 1998. U/Pb zircon geochronology and tempo of the end-Permian mass extinction. Science, 280: 1039-1045.

Enkin, R. J., Yang Z., Chen Y., Courtillot, V., 1992. Paleomagnetic constraints on the geodynamic history of the major blocks of China from the Permian to the present. Journal of Geophysical Research, 97(B10): 13953-13989.

Enos, P., 1995. Permian of China. in, Scholle, P. A., Peryt, T. M., Ulmer-Scholle, D. S. (eds.) The Permian of Northern Pangea. Springer-Verlag, Berlin, 2: 225-256.

Krull, E. S., Lehrmann, D. J., Druke, D., Kessel, B., Yu, Y. Y., Li, R., 2004. Stable carbon isotope stratigraphy across the Permian-Triassic boundary in shallow marine carbonate platforms, Nanpanjiang Basin, South China. Palaeogeography, Palaeoclimatology, Palaeoecology, 204(3-4): 297-315.

Lehrmann, D. J., Payne, J. L., Felix, S. V., Dillett, P. M., Wang H., Yu Y., Wei J., 2003, Permian-Triassic boundary sections from shallow-marine carbonate platforms of the Nanpanjiang Basin, south China: Implications for oceanic conditions associated with the end-Permian extinction and its aftermath. Palaios, 18: 138-152.

Lehrmann, D. J., Wei, J., Enos, P., 1998. Controls on facies architecture of a large Triassic carbonate platform: The Great Bank of Guizhou, Nanpanjiang Basin, South China. Journal of Sedimentary Research, 68: 311-326.

Mundil, R., Ludwig, K. R., Metcalfe, I., Renne, P. R., 2004. Age and timing of the end Permian mass extinction: U/Pb geochronology on closed system zircons. Science, 305: 1760-1763.

Orchard, M. J., 1995. Taxonomy and correlation of Lower Triassic (Spathian) segminate conodonts from Oman and revision of some species of *Neospathodus*. Journal of Paleontology, 69: 110-122.

Payne, J. L., Lehrmann, D. J., Wei, Jiayong, Orchard, M. P., Schrag, D. P., Knoll, A. H., 2004. Large Perturbations of the Carbon Cycle During Recovery from the End-Permian Extinction. Science, 23: 506-509.

Sano H., Nakashima K., 1997. Lowermost Triassic (Griesbachian) microbial bindstone-cementstone facies southwest Japan. Facies, 36: 1-24.

Tong Jinnan, Zakharov, Y. D., Orchard, M. J., Yin Hongfu, Hansen, H. J., 2004. Proposal of Chaohu section as the GSSP candidate of the Induan-Olenekian boundary. Albertiana, 29: 13-28.

Study on the Lower Triassic Sedimentology in Chaohu, Anhui Province, China

Li Shuangying[1], Tong Jinnan[2], Liu Kongyan[1], Wang Fanjian[1] and Huo Yangyang[1]

[1] College of Resources and Environment, Hefei University of Technology, Hefei 230009, China; lsy@mail.hf.ah.cn

[2] Faculty of Earth Sciences, China University of Geosciences, Wuhan 430074, China

The Lower Triassic is lithostratigraphically composed of the Yinkeng, Helongshan and Nanlinghu formations in Chaohu, Anhui Province, and continues in conformity with the underlying Upper Permian Dalong Formation and overlying Middle Triassic Dongmaanshan Formation. The lithology is mainly carbonate rocks such as micrite, wackestone and nodular limestone, as well as mudstone and shale. The Lower Triassic of Chaohu is one of the classic sequences in South China and it has received considerable studies including paleontology, biostratigraphy, ecostratigraphy, sequence stratigraphy, sedimentology, and so on. This paper intends to provide a brief summary on the recent advance in the study of the Lower Triassic sedimentology in Chaohu.

1. **Cyclic deposition**. Deposits of the Lower Triassic in Chaohu comprise the lithological cycles of micritic carbonates and fine siliceous clastic sediments. No coarse clastic sediments occurred except for some gravity-flow deposits. The cyclic deposits would be a good indicator of the sea-level fluctuation and related to the eustatic changes. The depositional rate in the Early Triassic is calculated at 6.7cm/ka on an average, and each cycle lasted 97.5 years, forming a depositional sequence of 0.654 cm thick. The nodular limestone and mudstone in the Helongshan Formation constitute 10 cycles and each cycle is 238.7 cm thick and ranges 35.57 ka. A cycle is 260.7 cm thick and lasts 38.84 ka in the lower part of the Nanlinghu Formation, taking account of the sediments comprising 23 cycles in the strata. These cycles seem corresponding with the 41 ka oblique cycle in the Milankovitch periodicity. The Yinkeng, Helongshan and Nanlinghu Formations consist of three type-II cycles and

each cycle last 1.33 ma, it resembles 1.23 ma Milankovitch eccentricity cycle and also corresponds with the third-order sequence in sequence stratigraphy (1~2 Ma). The Lower Triassic thus mainly expresses the cycles such as 97.5 years, 41 ka oblique cycle, and 1.23 Ma eccentricity cycle, among which the cycle of hundred years was resulted from the sea-level fluctuation while the 41ka cycle and 1.23 Ma cycle are from the Milankovitch periodicity.

2. **Origin of nodular limestone.** Nodular limestone is well developed in the Yinkeng and Helongshan Formations as well as the middle and lower parts of the Nanlinghu Formation. It is in a gray, dark gray, yellowish or occasionally reddish color, and usually thin- to medium-bedded with a micritic texture and nodular structure. The nodules are distributed in a disperse pattern or in apparently separated but actually connected or continuous catenulate lines, paralleled to the bedding surfaces. A single nodule is commonly lenticular in shape and 3-6 mm x 10-15 mm in size. Fossils such as thin-shelled bivalves and ammonoids are found in the nodular bodies. Mudrock is embedded among the nodules in bands of about 0.327cm thick. It scarcely contains fossils except for some ostracods. The clay minerals in the mudrock are mostly illite, and secondly kaolinite, occasionally chlorite and montmorillonite.

The nodular limestones are formed by alternate deposits of carbonate and terrigenous muddy component. As a result of carbonate being easier cemented and fractured than mud component, thin limestone beds are fractured into chains and embedded into mudstones due to latter compression. The alternate deposits are controlled by CCD fluctuation, and the change of CCD is straightly reflected by eustatic movement. So, deposit of nodular limestones shows eustatic cycle, not deposits of gravity flow and symbolizes not deposit of slope facies.

3. **Anoxic deposition.** The V/Ni ratio is a useful environmental index of anoxic deposition. A high V/(V+Ni) (e”0.7-0.8) may indicate a strongly stratified anoxic water column, and a medium V/(V+Ni) (0.4-0.60) indicates a dysoxic water according to the study on shale, limestone and siliceous sediments (Hatch and Leventhal, 1992; Li et al., 1995). In the Lower Triassic of Chaohu, the highest content of V is 160.6×10^{-6} (the average 57.54×10^{-6}), and V/(V+Ni) ratios are between 0.82-0.39 (the average 0.64), so it reflects an anoxic-dysoxic environment. The V/(V+Ni) ratio shows a tendency in the Lower Triassic of Chaohu. The V and V/(V+Ni) values are relatively high in the Yinkeng Formation (the average 66.2×10^{-6} and 0.67, respectively); medium in the Helongshan Formation (the average 37.9×10^{-6} and 0.61); and mostly low in the Nanlinghu Formation (the average 12.1×10^{-6} and 0.52). As a result, it indicates that the Yinkeng and Helongshan Formations were formed in an anoxic condition and the Nanlinghu Formation in a dysoxic environment.

4. **Volcanic turbidite deposit.** Developed in the upper part of the Nanlinghu Formation at the Majiashan Section of Chaohu is a series of pyroturbidite deposits composed largely of dacite breccia, crystal and glass shard dacite tuff breccia and tuff, 1.8 m thick with distinct boundaries. Study indicates that the pyroturbidite deposits were formed from some underwater eruptions and transportations. The turbidite is composed of two cycles of the Bouma sequences, Members A-C and A-E, and might be resulted from the collision between the North China and Yangtze Blocks during the early Indosinian Epoch.

5. **Paleogeography**. The Lower Yangtze region was a carbonate ramp during the Early Triassic inclining northward, on which Chaohu was in a deeper part. Seasonal storms might touch the base of the ramp in the upper part, where is above the oxidation interface in an opening shallow sea. There is, however, short of storm deposits in Chaohu and it is below the oxidation interface in a deep facies based on the Wilson’s model (Wilson, 1975).

Sulfur Isotopic Anomalies Across the Permo-Triassic Boundary and Through the Early Triassic

Pedro J. Marenco[1], Frank A. Corsetti[1], David J. Bottjer[1], Aymon Baud[2] and Alan Jay Kaufman[3]

[1] *Department of Earth Sciences, University of Southern California, Los Angeles, CA 90089-0740, USA; marenco@usc.edu*

[2] *Geological Museum, UNIL-BFSH2, Lausanne, CH-1015, Switzerland*

[3] *Geology Department, University of Maryland, College Park, MD 20742-4211, USA*

The biotic recovery from the end-Permian mass extinction was unique among mass extinction recoveries in that it was delayed for ~6 million years (Martin et al., 2001; Mundil et al., 2004; for comparison, the K-T rebound took less than 1 m.y. for most taxa, e.g., Hallam and Wignall 1997). The causes of the mass extinction are still debated. Hypothesized extinction mechanisms can be grouped into ‘geologically instantaneous’ events and ‘long-lived’ events. Instantaneous extinction mechanisms in general do not account for the unusually long duration of the extinction aftermath.

A growing body of geochemical evidence would suggest that the extinction and the delayed recovery were linked by anomalous ocean/atmospheric chemistry (although it is possible that the causes of the mass extinction and the delayed recovery may be decoupled). Recent sulfur isotopic analyses of carbonate associated sulfate (CAS) across a Permo-Triassic boundary section in Italy show a positive isotopic excursion interpreted to have resulted from prolonged oceanic anoxia (Newton et al., 2004). Our high resolution CAS analysis of Permo-Triassic boundary sections in Turkey provides greater detail than previously available. In Turkey, as in Italy, Upper Permian strata exhibit extreme sulfur isotopic fluctuations over a short stratigraphic interval (~10‰ per meter). High sulfur isotopic values are found at the boundary and continue to

rise through a series of nearly periodic 5‰ per 2 meter fluctuations into the Lower Triassic. Application of the Kah et al. (2004) model to the sulfur isotopic fluctuations at the Permo-Triassic boundary suggests that the oceanic sulfur reservoir size must have been significantly decreased before the boundary and through the earliest Early Triassic.

The cause(s) of the observed sulfur isotopic variations may or may not be related to the cause(s) of the mass extinction. With a large sulfur reservoir size, only an extremely large input of sulfur with anomalous isotopic compositions can explain the observed $\delta^{34}S$ variations observed at the boundary. However, with an extremely small sulfur reservoir, the amount of anomalous sulfur needed to perturb the $\delta^{34}S$ composition of the ocean is much smaller. For example, the amount of $\delta^{34}S$ depleted sulfur emitted as SO_2 by the Siberian Traps has been estimated to be on the order of $5x10^{18}$g (Kamo et al., 2003); with a small sulfur reservoir, this amount may have been enough to produce extreme sulfur isotopic fluctuations at the Permo-Triassic boundary.

Previously reported CAS and gypsum sulfur isotopic analyses from the western United States and elsewhere (e.g., Holser, 1984; Marenco et al., 2003) suggest that anomalous oceanic conditions were still present at the end of the Early Triassic (Spathian). Our recent analyses of CAS from the western U.S. (Nevada, Utah, Idaho, and Montana) suggests that the Early Triassic sulfur isotopic system was more complex than previously interpreted from evaporite data. The CAS data reported here supports a long-lived extinction mechanism the nature of which is yet to be resolved.

Hallam, A., Wignall, P. B., 1997. Mass extinctions and their aftermath. Oxford University Press, 320p.

Holser, W. T., 1984. Gradual and abrupt shifts in ocean chemistry during Phanerozoic time. *in* Holland, H. D., Trendall, A. F. (eds) Patterns of Change in Earth Evolution, Springer-Verlag, 432p.

Kah, L. C., Lyons, T. W., Frank, T. D., 2004. Low marine sulphate and protracted oxygenation of the Proterozoic biosphere. Nature, 431: 834-837.

Kamo, S. L., Czamanske, G. K., Amelin, Y., Fedorenko, V. A., Davis, D. W., Trofimov, V. R., 2003. Rapid eruption of Siberian flood-volcanic rocks and evidence for coincidence with the Permian-Triassic boundary and mass extinction at 251 Ma. Earth and Planetary Science Letters, 214: 75-91.

Marenco, P. J., Corsetti, F. A., Bottjer, D. J., Kaufman, A. J., 2003. Killer oceans of the Early Triassic. Geological Society of America, Abstracts with Programs, 35(6): 386.

Martin, M. W., Lehrmann, D. J., Bowring, S. A., Enos, P., Ramezani, J., Wei Jiayong, Zhang Jiyan, 2001. Timing of Lower Triassic carbonate bank buildup and biotic recovery following the end-Permian extinction across the Nanpanjiang Basin, South China. Geological Society of America, 2001 Abstracts with Programs, 33(6): 201.

Mundil, R., Ludwig, K. R., Metcalfe, I., Renne, P. R., 2004. Age and timing of the Permian mass extinctions: U/Pb dating of closed-system zircons. Science, 305: 1760-1763.

Newton, R., Pevitt, P., Wignall, P. B., Bottrell, S., 2004. Large shifts in the isotopic composition of seawater sulphate across the Permo-Triassic boundary in northern Italy. Earth and Planetary Science Letters, 218: 331-345.

The Triassic of the Southwestern United States and North-Western Mexico: Age Constraints on Sequence Boundaries of Correlative Non-Marine and Marine Sequences

John E. Marzolf

Department of Geology, Southern Illinois University, Carbondale, Illinois, 62901, USA; marzolf@geo.siu.edu

In the southwestern United States, the predominantly non-marine Triassic stratigraphy of the southern Colorado Plateau is divided by widespread regional unconformities into four tectonosequences: the Moen-kopi, Holbrook, Chinle, and Dinosaur Canyon (Marzolf, 1994, 2000) (Fig. 1). The Moenkopi tectono-sequence is further divided into three higher order sequences, the Timpoweap, Virgin, and Shnabkaib; the Chinle into two, the Shinarump – Blue Mesa and Moss Back – Owl Rock (Fig. 1). Lucas (1999) divided the land vertebrate assemblages within Triassic strata of the Colorado Plateau into six land vertebrate faunachrons: the Nonesian, Perovkan, Otischalkian, Adamanian , Reveultian, and Apachean. The Nonesian is restricted to the Shnabkaib sequence in the upper Moenkopi tectonosequence; the Perovkan, to the Holbrook tectonosequence. Vertebrate tetrapods that characterize the Otischalkian, Adamanian, and Reveultian, are restricted to the Chinle tectonosequence; the Otischalkian and Adamanian to the Shinarump - Blue Mesa sequence and the Reveultian to the Moss Back - Owl Rock sequence. The Apachean is restricted to the lower Dinosaur Canyon tectonosequence below the Triassic – Jurassic boundary.

To the west and southwest of the Colorado Plateau, correlative sequences identified in predominantly marine strata of northwestern Nevada (Oldow and others, 1993; Marzolf and Anderson, in press) and northwestern Sonora, Mexico (Gonzalez-León, 1997) place ammonite-based age constraints on correlative boundaries in the non-marine sequences and their included fauna and flora (Fig. 1). Ammonites have been identified from five

tectonosequences, both in northwestern Nevada (Nichols and Silberling, 1977; Silberling, 1984; Oldow and others, 1993) and in northwestern Sonora (Gonzalez-Leon, 1997; Estep and others, 1997). Ammonite ages for four of these tectonosequences establish correlation with the Moenkopi, Holbrook, Chinle, and Dinosaur Canyon tectonosequences on the Colorado Plateau (Marzolf and Anderson, in press). Ammonites and other invertebrate macrofossils collected from the fifth tectonosequence, here named the Panther Canyon tectonosequence, indicate a late Ladinian(?) to early Carnian age. The Panther Canyon tectonosequence's stratigraphic position between tectonosequences correlative with the Holbrook and Chinle tectnosequences of the Colorado Plateau is consistent with this age assignment.

Although lithostratigraphic units in the upper Holbrook and throughout the Panther Canyon tectonosequence are sparsely fossiliferous, the ages of all five tectonosequences are tied to the marine ammonite standard. Furthermore, close proximity of identified ammonites to sequence boundaries place constraints on the age range of bounded sequences. Sequences can be no younger than the oldest ammonite zone overlying a sequence boundary and no older than the youngest ammonite zone underlying a sequence boundary. Thus, the boundary between the Moenkopi and Holbrook tectonosequences, U-2, lies near the Spathian - Anisian boundary between the *Subcolumnbites* and *Caurus* zones. The boundary between the Holbrook and Panther Canyon tectonosequences, U-3, is not well constrained above. It is younger than the *Occidentalis* zone and older than the *Desatoyense* zone. As nearly 500 meters of strata lie between U-3 and the *Desatoyense* zone, U-3 may be near the Anisian – Ladinian boundary. The boundary between the Panther Canyon and Chinle tectonosequences, U-4, lies near the middle Carnian between the *Desatoyense* and *Dilleri* zones. The higher-order sequence boundary, u-c, lies near the Carnian – Norian boundary between the *Macrolobatus* and *Kerri* zones. The boundary between the Chinle and Dinosaur Canyon tectonosequences, U-5, lies near the Norian-Rhaetian boundary between the *Cordilleranus* and *Amoenum* zones. Finally, U-7, at the top of the Dinosaur Canyon tectonosequence lies within the upper Hettangian, near the base of the *Angulata* (*Sunrisense*) zone. The Dinosaur Canyon tectonnosequence contains the Triassic – Jurassic boundary.

The apparent global or trans-Pangean extent of these sequence boundaries (Embry,1997; Marzolf, 2000) offers the possibility of further refinement of age constraints for use in global correlation of marine and non-marine Triassic strata.

Embry, A. F., 1997. Global sequence boundaries of the Triassic and their identification in the Western Canada Sedimentary Basin. Bulletin of Canadian Petroleum Geology, 45: 415-433.

Estep, J. W., Lucas, S.G., Gonzalez-León, C. M, 1997, Middle Triassic ammonites from Sonora, Mexico. Revista Mexicana de Ciencias Geologicas, 14(2): 155-159.

Gonzalez-León, C. M., 1997. Sequence stratigraphy and paleogeographic setting of the Antimonio Formation (Late Permian-Early Jurassic, Sonora, Mexico. Revista Mexicana de Ciencias Geologicas, 14(2): 136-148.

Lucas, S. G., 1999. Tetrapod correlation of the non-marine Triassic. Zentralblatt für Geologie und Paläontologie, 3: 498-521.

Marzolf, J. E., 1994. Reconstruction of the early Meso-

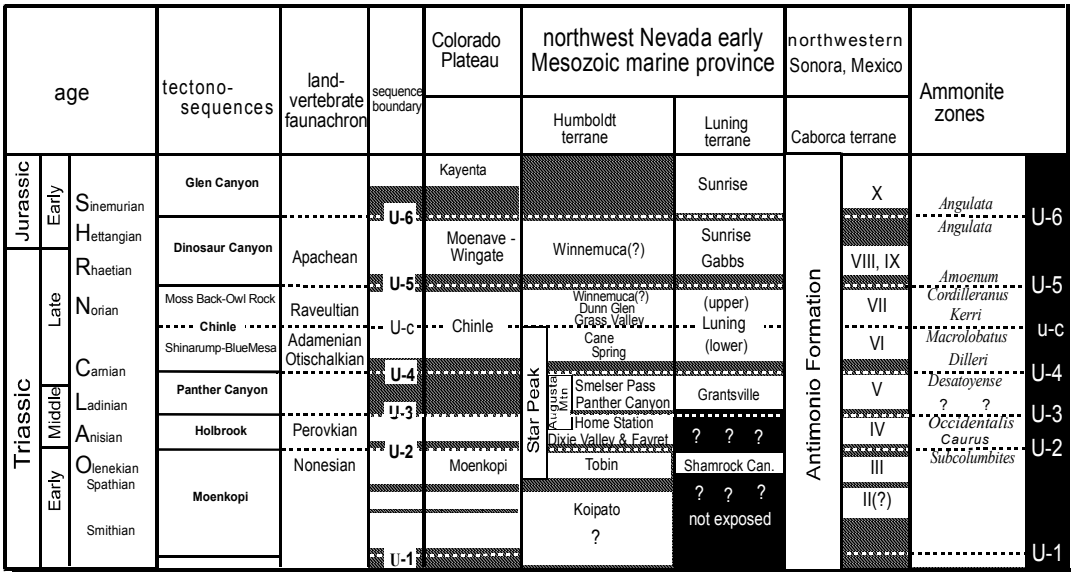

Figure 1. Correlation of non-marine and marine Triassic tectonosequences of the southwestern United States and northwestern Mexico. Data for age designations for northwestern Nevada from Nichols and Silberling (1977); Silberling (1984); Oldow and others (1993); data for northwest Sonora from Gonzalez-León (1997); Estep and others (1997).

zoic Cordilleran cratonal margin adjacent to the Colorado Plateau. *in* Caputo, M., Peterson, J. E., Franczyk, K. J. (eds.) Mesozoic systems of the Rocky Mountain Region, USA, Rocky Mountain section of the Society of Sedimentary Geology, Denver, CO, 181-216.

Marzolf, J. E., 2000. Triassic paleogeography of the Panthalassan margin of Southwestern North America: A sequence stratigraphy-based regional synthesis. Zentralblatt für Geologie und Paläontologie, 3: 1497-1538

Marzolf, J. E., Anderson, T. H., in press. Lower Mesozoic facies and crosscutting sequence boundaries: Constraints on displacement of the Caborca terrane, Geological Society of America.

Nichols, K. M., Silberling, N. J., 1977. Stratigraphy and depositional history of the Star Peak Group (Triassic), northwestern Nevada. Geological Society of America Special Paper 178, 73 p.

Oldow, J. S., Satterfield, J. I., Silberling, N. J., 1993. Jurassic to Cretaceous transpressional deformation in the Mesozoic marine province of the northwestern Great Basin. *in* Lahren, M. M., Trexler, J. H., Jr., Spinosa, C. (eds.) Crustal evolution of the Great Basin and the Sierra Nevada: Cordilleran/Rocky Mountain Section, Geological Society of America Guidebook, Department of Geological Sciences, University of Nevada, Reno, 129-147.

Silberling, N. J., 1984. Map showing localities and correlations of age-diagnostic lower Mesozoic megafossils, Walker lake 1º x 2º quadrangle.

Extinction and Survival of Permian to Early Triassic Marine Myalinidae (Bivalvia: Pterioida)

Christopher A. McRoberts

Department of Geology, State University of New York at Cortland, Cortland, New York USA 13045; mcroberts@cortland.edu

In terms of taxonomic richness and morphologic innovation, the marine Myalinidae represent one of the most successful bivalve families of the Late Paleozoic and Early Mesozoic (Fig. 1). Although myalinids are known from the early Carboniferous (or perhaps even the Devonian), they did not reach their peak until the Middle Permian, where richness exceeded eight genera and 25 species. Myalinid diversity declined between the Middle and Late Permian becoming exceedingly rare in the Changhisingian where they likely persisted in marine refugia. Following the end-Permian mass extinction, the marine Myalinidae were greatly diminished in taxonomic and ecological diversity only to become extinct by the end of the Early Triassic. Globally, about six species belonging to two genera (*Promyalina* and *Myalinella*.) are represented in Early Triassic strata. Induan and Olenekian myalinids, mostly *Promyalina*, are a significant component in low-diversity but locally abundant paleocommunities, often associated with *Unionites, Eumorphotis, Permophorus* and rarely *Claraia*. Similar myalinid associations are recognized globally and are best explained as disaster paleocommunties in a protracted survival phase following the end-Permian extinctions. Myalinidae are largely unknown form the Middle Triassic as taxa originally assigned to this family (e.g., species of *Aviculamyalina*) are better placed in other pteriomorphian clades.

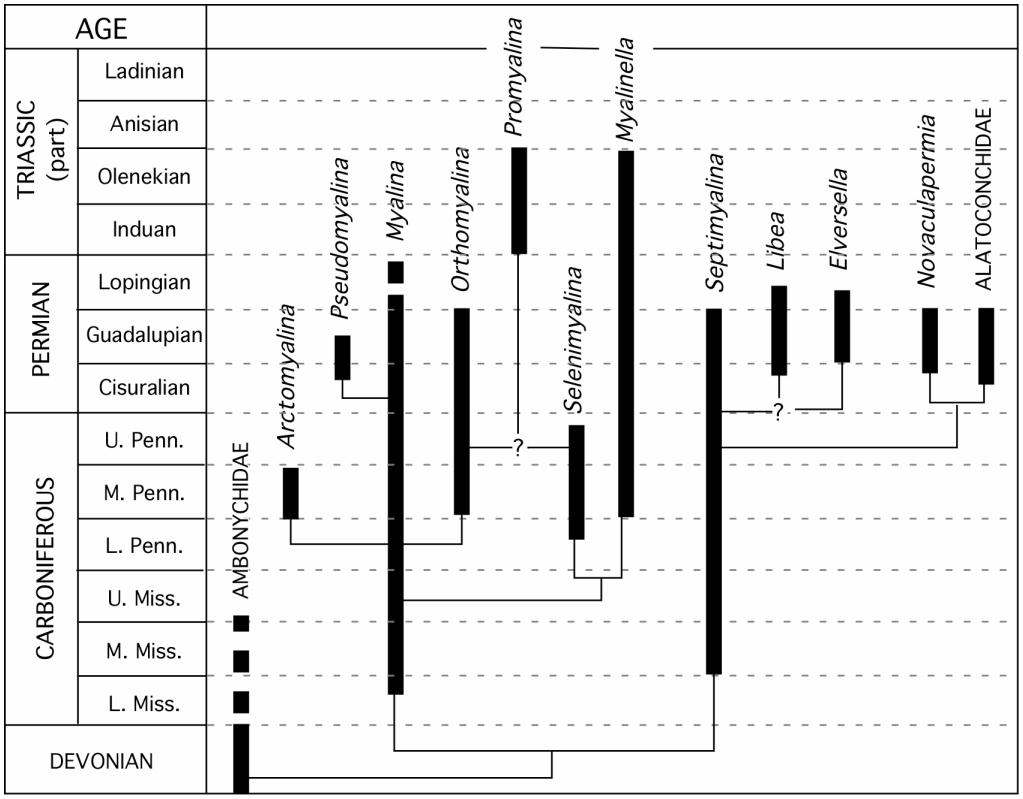

Figure 1. Generic ranges and possible phylogeny of marine Myalinidae

Orbital Tuning of the Indusian and Olenekian Stages Using Sedimentary Cycles of the Germanic Trias

M. Menning and M. Szurlies

GeoForschungsZentrum Potsdam, Telegrafenberg C, D-14473 Potsdam, Germany; menne@gfz-potsdam.de, szur@gfz-potsdam.de

Amongst geological time scales the duration of the Indusian* and Olenekian stages varies from 1.3 m.y. to 6 m.y. and from 3.1 m.y. to 5 m.y. respectively. The overestimated duration of 6 m.y. (Menning 1995) has been derived from the time span Calvörde Folge (s1) to Detfurth Folge (s4) of Central Europe which corresponds to the Indusian according to Kozur (1975). Meanwhile the stratigraphic range of the Indusian has been reduced (Kozur 2003) and, equivalently, the Olenekian has been enlarged in relation to the classic Germanic Trias of Central Europe.

Since the U-Pb SHRIMP age of 251.2±3.4 Ma of Claoué-Long et al. (1991) for bed 25 in the Global Stratotype Section and Point (GSSP) in Meishan, just below the Permian-Triassic boundary (PTB), additional isotopic dating has yielded ages from 249.9 Ma (Ar-Ar, Renne et al. 1995) up to c. 253 Ma (U-Pb IDTIMS, Mundil et al. 2001) for the PTB. Most time scales use an age of 251 Ma. An U-Pb IDTIMS age of c. 247 Ma has been suggested for the Olenekian-Anisian boundary (Lehrmann et al. 2003), however the significance of this age is vague because is has not yet been published in detail. The numerical age for the Anisian-Ladinian boundary (*Eoprotrachyceras curionii*) has been estimated to 240.7 Ma (Mundil et al. 1996, U-Pb IDTIMS), <240 Ma (Pálfy et al. 2003, U-Pb IDTIMS), and c. 241.0 Ma (Menning et al. in press, orbital tuning).

Our time estimates are based on:

1. an age of 252.5 Ma for the Changhsingian-Indusian (Permian-Triassic) boundary (PTB) which is derived from the U-Pb IDTIMS ages of 252.6 ± 0.2 Ma for bed 25 in Meishan (Mundil et al. 2004) and of 240.7 Ma for the Anisian-Ladinian boundary (Mundil et al. 1996),

2. the correlation of the PTB (Yin et al. 2001) with the lower part of the cycle 1.2 (Calvörde Folge) of Central Europe (Kozur 1999, Szurlies et al. 2003).

3. The Indusian-Olenekian boundary is within cycle 2.6 of the Bernburg Folge (Menning et al. in press) using magnetostratigraphic evidence of Szurlies et al. (2003) and preliminary magnetostratigraphic evidence of Tong et al. (2004).

4. The Olenekian-Anisian boundary has been dicussed as being in between the base of the Solling Folge (s6) and the top of the Röt Folge (s7). According to magnetostratigraphic evidence it is probably in the late Solling Folge (s6) of Central Europe (Szurlies in prep.). However, provisionally we assign the base of the Anisian as the boundary between the Solling Folge (s6) and the Röt Folge (s7)

5. The Anisian-Ladinian boundary (*Eoprotrachyceras curionii*) is in Folge m9 (late Late Muschelkalk; Hagdorn et al. in Menning et al. in press).

6. The climatically induced sedimentary cycles of the Buntsandstein and Muschelkalk of Germany are small excentricity cycles of a duration of c. 100 k.y. They are used to tune orbitally (Milankovitch 1941) the duration of the Folgen which are (quasi isochronous) time slices.

Using the above model the Indusian stage, which can be defined in South China between the FAD of the conodonts *Hindeodus parvus* in Meishan (GSSP, Yin et al. 2001) and *Neospathodus waageni* in the West Pingdingshan section of Chaohu (proposed GSSP, Tong et al. 2004), covers a time span of 1.4 m.y. to 1.5 m.y. (cycles ~s1.2 to ~s2.5) and the Olenekian stage has a duration of c. 3.7 m.y. (cycles ~s2.6 to ~s6.4).

* The name of the first Triassic stage has been derived from the river Indus (Himalaya). But, Kiparisova & Popov (1956) named this stage by mistake =4A:89 (Induan) instead of =4CA:89 (Indusian). As we want the stage name to refer to its source area, we have used the term Indusian.

Claoué-Long, J. C., Zhang, Z., Ma, G., Du, S., 1991. The age of the Permian-Triassic boundary. Earth Planet. Sci. Lett., 105: 182-190.

Kiparisova, L. D., Popov, Ju. N., 1956. Subdivision of the Lower Series of the Triassic System into stages. Dokl. Akad. Nauk SSSR, 109(4): 842-845. (in Russian)

Kozur, H., 1975. Probleme der Triasgliederung und Parallelisierung der germanischen und tethyalen Trias. Teil II: Anschluß der germanischen Trias an die internationale Triasgliederung. Freiberger Forsch.-H., C 304: 51-77.

Kozur, H. W., 1999. The correlation of the Germanic Buntsandstein and Muschelkalk with the Tethyan scale. Zbl. Geol. Paläont., Teil I, 1998, 7/8: 701-725.

Kozur, H. W., 2003. Integrated ammonoid, conodont and radiolarian zonation of the Triassic and some remarks to stage/substage subdivision and the numeric age of the Triassic stages. Albertiana, 28: 57-74.

Lehrmann, D., Enos, P., Montgomery, P., Payne, J., Orchard, M., Bowring, S., Ramezani, J., Martin, M., Wei, J., Wang, H., Yu, Y., Xiao, J., Li, R., 2002. Integrated biostratigraphy, magnetostratigraphy, and geochronology of the Olenekian-Anisian boundary in marine strata of Guandao section, Nanpanjiang Basin, south China: implications for timing of biotic recovery from the end-Permian extinction. IUGS Subcommission on Triassic Stratigraphy, STS/IGCP 467 Field Meeting, Veszprém 2002: 7-8, Budapest (Geological Institute of Hungary, Hungarian Geological Society).

Menning, M., 1995. A numerical time scale for the Permian and Triassic periods: an integrated time analysis. *in* Scholle, P. A., Peryt, T. M., Ulmer-Scholle, D.S. (eds.) The Permian of Northern Pangea. 1: 77-97, Berlin (Springer).

Menning, M., Gast, R., Hagdorn, H., Käding, K.-Ch., Simon, Th., Szurlies, M., Nitsch, E., in press. Zeitskala für Perm und Trias in der Stratigraphischen Tabelle von Deutschland 2002, zyklostratigraphische Kalibrierung der höheren Dyas und Germanischen Trias und das Alter der Stufen Roadium bis Rhaetium 2005. Newsl. Stratigr.

Milankovitch, M., 1941. Kanon der Erdbestrahlung und seine Anwendung auf das Eiszeitproblem. Königlich Serbische Akademie, 33: 633 pp., Beograd.

Mundil, R., Brack, P., Meier, M., Rieber, H., Oberli, F., 1996. High resolution U-Pb dating of Middle Triassic volcanoclastics: Time-scale calibration and verification of tuning parameters for carbonate sedimentation. Earth Planet. Sci. Lett., 141: 137-151.

Mundil, R., Ludwig, K. R., Metcalfe, I., Renne, P. R., 2004. Age and timing of the Permian mass extinction: U/Pb dating of closed-system zircons. Science, 305: 1760-1763.

Mundil, R., Metcalfe, I., Ludwig, K. R., Renne, P. R., Oberli, F., Nicoll, R. S., 2001. Timing of the Permian-Triassic biotic crisis: implications from new zircon U/Pb age data (and their limitations). Earth Planet. Sci. Lett., 187(1/2): 131-145.

Pálfy, J., Parrish, R. R., David, K., Vörös, A., 2003. Mid-Triassic integrated U-Pb geochronology and ammonoid biochronology from the Balaton Highland (Hungary). J. Geol. Soc., 160: 271-284.

Renne, P. R., Zhang, Z.-C., Richards, M. A., Black, M. T., Basu, A. R., 1995. Synchrony and causal relations between Permian-Triassic boundary crisis and Siberian flood volcanism. Science, 269: 1413-1415.

Szurlies, M., in prep. Towards a geomagnetic polarity scale for the Lower Triassic: implications from the Central European Basin, Germany. Earth Planet Sci. Lett.

Szurlies, M., Bachmann, G. H., Menning, M., Nowaczyk, N. R., Käding, K.-C., 2003. Magnetostratigraphy and high-resolution lithostratigraphy of the Permian-Triassic boundary interval in Central Germany. Earth Planet. Sci. Lett., 212: 263-278.

Tong, J., Zakharov, Y. D., Orchard, M. J., Yin, H.-F., Hansen, H. J., 2004. Proposal of Chaohu section as the GSSP candidate of the Induan-Olenekian boundary. Albertiana, 29: 13-28.

Yin, H.-F., Zhang, K.-X., Tong, J.-N., Yang, Z.-Y., Wu, S.-B., 2001. The Global Stratotype Section and Point (GSSP) of the Permian-Triassic boundary. Episodes, 24(2): 102-114.

Age Constraints on the *Neospathodus triangularis* Zone, Upper Spathian (Triassic), in the Dalishan Section, Jiangsu Province, China.

I. Metcalfe[1], R. S. Nicoll[2] and X. F. Wang[3]

[1] Asia Centre, University of New England, Armidale, NSW, Australia; imetcal2@une.edu.au

[2] Department of Earth and Marine Sciences, Australian National University, Canberra, ACT, Australia

[3] Centre for Stratigraphy and Paleontology, Yichang Institute of Geology and Mineral Resources, Yichang, Hubei, PRC

The Dalishan Section, near Dantu, Jiangsu Province, China, extends from the Permian-Triassic boundary to near the top of the Lower Triassic. The section is poorly exposed except in the lower part at the P-T boundary and in a small quarry near the top. The P-T boundary interval is exposed in a stream bed and is either very condensed or includes an unconformity. Limestone (DL2) 2 m above the P-T boundary contains an Upper Dienerian fauna that includes *Neospathodus cristigalli*. This is directly overlain by limestones of middle to upper Smithian age (*waggeni – milleri* Zones) that contain *Platyvillosus costatus*.

The upper quarry section contains medium to thick limestone beds that are of Upper Spathian age (*Neospathodus triangularis* Zone) containing a fauna that includes *N. triangularis*, *N. abruptus* and *N. homeri*. Within the limestone exposure is an ash bed that is up to 20 cm thick. Conodonts from samples both below and above the ash bed contain *N. triangularis* Zone conodonts.

Analysis of zircons from the ash bed is now in progress. This tightly biostratigraphically controlled ash bed provides a key chronologic tie point for the age of the upper Olenekian (Spathian).

Chronostratigraphic and Biostratigraphic Control on the Permian- Triassic Boundary in the Zhongzhai Section, Guizhou Province, Southwest China.

R. S. Nicoll[1] and I. Metcalfe[2]

[1] Department of Earth and Marine Sciences, Australian National University, Canberra, ACT, Australia; bnicoll@goldweb.com.au

[2] Asia Centre, University of New England, Armidale, NSW, Australia

The recovery of conodonts associated with ash beds in the key Zhongzhai Section, near Langdai, Liuzhi, Guizhou Province, provides precise and definitive control on both the stratigraphic level and age control on the Permian-Triassic boundary in the transition from marine to non-marine facies of western Guizhou and eastern Yunnan Provinces of southwestern China. In the Zhongzhai section the Triassic Yelang Formation is presumed to rest conformably on either the Longtan or Dalong Formation, depending on the interpretation of the section.

In the Zhongzhai Section the boundary interval consists of a lower limestone, 20 cm thick, that contains fragments of *Hindeodus* sp. and *Clarkina* sp. This is overlain by a 50 cm thick black shale bed containing an abundant brachiopod fauna, but no conodonts. This bed is in turn overlain by a 25 cm thick limestone that contains *Clarkina* sp., *Hindeodus changxingensis*, *H. praeparvus* and *H.* aff. *H. eurypyge*. Directly over this limestone is a 5 cm thick ash bed followed by a 10 cm thick black shale, which is overlain by a second, upper, ash bed that is 3 cm thick. Both ash beds were sampled for zircons study. On top of the upper ash bed is a 15 cm thick silty limestone containing an abundant dwarf conodont fauna, dominated by *Hindeodus*, and containing *H. parvus*. We tenatively place the Permian – Triassic boundary at the level of the black shale located between the two ash beds.

TIMS dates on zircons from ash beds adjacent to the Permian–Triassic boundary in the Zhongzhai Section provide a valuable control section in tracing the distribution of the ash clouds associated with volcanism on the South China Block in the Late Permian and earliest Triassic.

Conodont Biostratigraphy and Palaeogeography of the Triassic on the Western, Northwestern and Northern Margins of the Australian Plate

Robert S. Nicoll

Department of Earth and Marine Sciences, Australian National University, Canberra, ACT, Australia; bnicoll@goldweb.com.au

In the Triassic the northern margin of Gondwanan Pangea opened onto the Meso-Tethys Ocean. The then continental margin was formed by the Lhasa and West Burma Blocks and the New Guinea portion of the Australian Plate. Along what would become the margin of the Australian Plate were a series of cratonic basins, from the Perth Basin in the south, through the Bonaparte Basin to poorly defined Triassic basinal structures on islands of the Banda Arc. Only along the northern margin of present-day New Guinea and some of the islands of the Northern Banda Arc did continental margin shelf areas open directly onto the Meso-Tethys Ocean. Within this setting Triassic sediments were deposited in tectonically controlled basins. Conodonts and other fossils are beginning to allow high-resolution correlation of sedimentary sequences and events within and between these basins.

Early Triassic Conodonts of the Genus *Isarcicella*

Robert S. Nicoll[1] and Ian Metcalfe[2]

[1] Department of Earth and Marine Sciences, Australian National University, Canberra, ACT, Australia; bnicoll@goldweb.com.au

[2] Asia Centre, University of New England, Armidale, NSW, Australia

The conodont genus *Isarcicella* is an important, but rare, component of the earliest Triassic (Induan). *Isarcicella* appears to have evolved from *Hindeodus*, probably *H. parvus* in the earliest Triassic with the rounding the cross-section of the carina denticles, an increase in the width of the scaphate Pa element, a marked increase in the width of the posterior part of the cusp, and later, the development of lateral denticulation on one or both sides of the cusp. The ramiform elements of the *Isarcicella* apparatus have not been isolated, but the genus is presumed to conform to the standard, *Hindeodus*-like, septimembrate apparatus structure.

Based on gross morphology two evolutionary lineages of *Isarcicella* can be recognised. The *staeschei* lineage is characterised by that develop a pronounced lateral bulge on only one side of the element. The *expansa* lineage develops a bulge on both sides of the element. In early forms, these bulges lack denticulation, but in later forms denticles develop on one or both sides of the carina.

Because the total stratigraphic range of *Isarcicella* ap-

pears to be restricted to the *Hindeodus parvus* and *Isarcicella* Zones, found only in lower part of the Griesbachian Substage of the Induan Stage of the Early Triassic, and because this interval is rarely more than a few meters thick, the morphologic evolution of the genus is rarely apparent. In most sections most morphologies appear together. In the rare section, such as that at Shangsi in northern Sichuan Province, where *Isarcicella* is found through over 30 meters of section, the complexity of morphology is observed to increase upwards in the section.

On the Explosive Radiation of Lower Triassic Conodonts: A New Multielement Perspective

Michael J. Orchard.

Geological Survey of Canada, 101-605 Robson St., Vancouver, B.C. V6B 5J3, Canada; morchard@nrcan.gc.ca

After late Paleozoic decline, few conodont genera remained by the Late Permian and yet most, if not all, survived the P-T boundary extinction. Rapid evolution followed, as is well documented in the *Hindeodus-Isarcicella* stock, which provides a definitive biozonation for the boundary interval. A second major stock, represented by the gondolelloids, provides biozone indices throughout the Middle-Late Permian as well as an alternate scheme for the early Induan (Orchard & Krystyn, 1998). The latter represents the alleged upper range of the principal (sole?) Permian representative of the gondolelloid stock, '*Clarkina*'. However, an incomplete record suggests that conservative gondolelloids - *Neogondolella* of this work - continued through the Lower Triassic and beyond. A third group, represented by Permian *Merrillina* and '*Stepanovites*', survived the boundary events and evolved into some species assigned to Triassic '*Neospathodus*' and *Ellisonia.*

With the disappearance of the *Hindeodus* stock in the late Griesbachian, the major Triassic radiation began. In the Canadian Arctic, the latest Griesbachian zone of the ammonoid *Bukkenites strigatus* includes 'conservative' *Neogondolella carinata* group and representatives of several new gondolelloid lineages variously characterized by: 1) strong blade/carina growth and platform reduction (i.e. *krystyni - discreta - kummeli)*; 2) long discrete anterior denticles and posterior platform enlargement (i.e. *labiatus - nepalensis - buurensis)*; 3) thickened platforms and large basal loops (leading to *Scythogondolella*?); and 4) unnamed 'conservative' neogondolellids (e.g. precursors of *N. composita*). In addition, 5) early 'neospathodids' (i.e. *cristagalli* and *dieneri)* and 6) *Merrillina*-like elements broadly corresponding to '*Neospathodus*' *peculiaris* appeared, some of them probably allied to 7) extant ellisonids. This increase in diversity may have arisen as a result of opportunistic exploitation of post-extinction, vacated eco-space but subsequent development of many of these taxa remains obscure, although we do know it was considerable. Described late Induan (Dienerian) conodont faunas are generally low in diversity, commonly consisting of only one or two species of *Neospathodus*. Exceptions to this are known from remnants of Panthalassa Ocean atolls where rare collections consist of abundant *Neogondolella* as well as *Neospathodus*. Nevertheless, these are but a glimpse of the major modification of conodont elements that occurred during this interval because by the Olenekian numerous new conodont taxa appeared about whose origins and development we know little. Early Olenekian (Smithian) faunas contain four-times as many conodont genera as those known from the late Induan (Dienerian) and mark an explosive radiation unrivalled since the Devonian.

The key to understanding the evolution of Lower Triassic (indeed all) conodonts lies in multielement taxonomy. The most remarkable aspect of the newly emerged Olenekian conodonts was morphological diversity of both the P_1 elements - on which basis all former phyletic lineages have been postulated - and their multielement apparatuses. In the absence of natural assemblages, reconstruction of these multielement species is in its infancy but preliminary reconstructions identify at least eleven apparatuses within Lower Triassic Gondolelloidea alone, compared with perhaps one in the Late Permian. In addition, many more apparatuses await reconstruction amongst the ellisonids. As far as we know, most of these apparatuses evolved during the Induan. Examples of the new multielement reconstructions of thirteen Olenekian genera assigned to the superfamily Gondolelloidea are presented, eight of which are new (*Conservatella*, *Columbitella*, *Discretella*, *Meekella*, *Novispathodus*, *Spathicuspus*, *Wapitiodus*), and five of which are reinterpreted (*Cornudina*, *Cratognathus*, *Guangxidella*, *Neospathodus*, *Triassospathodus*). Multielement *Neogondolella* (=*Clarkina*) is shown as the starting point for these other genera, most of which have formerly been interpreted as single element taxa. Species originally described as *'Neospathodus'* are now assigned to no less than nine different multielement genera! All complete apparatuses are regarded as consisting of 15 elements. A pair of enantiognathiform S_1 elements is the diagnostic character for the superfamily. Assembly of genera into subfamilies is based on similarity in the morphology of homologous ramiform elements, with emphasis on the position of the antero-lateral processes relative to the cusp in the alate S_0 elements; the development of a second anterolateral process in the digyrate S_2 elements; and the occurrence and position of an accessory antero-lateral process in the bipennate S_3 elements (Orchard, 2005).

Orchard, M. J., Krystyn, L., 1998. Conodonts of the lowermost Triassic of Spiti, and new zonation based on *Neogondolella* successions. Revista Italiana di Paleontologia Stratigraphia, 104(3): 341-368.

Orchard, M. J., 2005. Multielement Conodont Apparatuses of Triassic Gondolelloidea. Special Papers in Palaeontology, 73: 1-29.

Life Strategies for Lingulids to Survive and Thrive Following the End-Permian Mass Extinctions

Peng Yuanqiao[1, 2], Guang R. Shi[1], Gao Yongqun[3] and Yang Fengqing[2]

[1] School of Ecology and Environment, Deakin University, Melbourne Campus, 221 Burwood Highway, Burwood, VIC 3125, Australia; ype@deakin.edu.au

[2] Faculty of Earth Sciences, China University of Geosciences, Wuhan 430074, Hubei Province, P.R. China

[3] China University of Geosciences Press, Wuhan 430074, Hubei Province, P.R. China

The end-Permian mass extinctions devastated most of the organisms in the sea and on land. As the greatest of all mass extinctions in deep time, the Permian-Triassic boundary (PTB) mass extinction witnessed about 90% loss of all species in the marine realm, and about 70% die-off of continental species in the non-marine realm (Erwin, 1993, 1994; Yang et al., 1993; Hallam and Wignall, 1997). Under this big mass extinction background, no reef and no coal beds/seams, have ever been found in the Early Triassic stratigraphic records, forming respectively reef gap (Flugel, 1994) and coal gap (Retallack et al., 1996) in the geological history over the whole world.

A few survivors from the Late Permian were struggling in the Early Triassic catastrophe, among them, the Early Triassic lingulids were one successive group of those conquerors during that time. Lingulids, usually defined as '*Lingula*' but maybe not according to Emig (2003), are globally distributed in the Lower Triassic. They have been reported in the Lower Triassic in eastern Russia, Japan, South China, western Australia, western Pakistan, Iran, Hungary, Italy, eastern Greenland and northwestern USA (see reviews of Xu and Grant, 1994). It is noteworthy that lingulids were found in the Lower Triassic associated with typical Early Triassic bivalves *Pteria*, *Claraia* and ammonoids *Ophiceras* from many sections in South China (Fig. 1).

Not only just survived the mass extinction event, lingulids also thrived in the Early Triassic marine realm, forming a lingulid cosmopolitan assemblage under the situation of the end-Permian devastation and the Early Triassic still stressful environments (e.g. Payne et al., 2004). Compared to hundreds of species found in the Late Permian deposits, only a few species of brachiopods occur in the earliest Triassic strata. Among these high-density but low-diversity survivors, lingulids briefly proliferated in the earliest Triassic marine realm (Xu and Grant, 1994 and references therein), forming a lingulid cosmopolitan assemblage as bivalve *Claraia* and ammonoid *Ophiceras* did in the aftermath of the end-Permian mass extinction (Hallam and Wignall, 1997).

Advantages for lingulids to survive and thrive during the Permian-Triassic boundary (PTB) catastrophe are discussed herein. The shell compositions of organophosphates of lingulids protected them from solution in the probably highly acid sea (e.g. Knoll et al., 1996), which was vital for organisms of calcareous shells. The small-

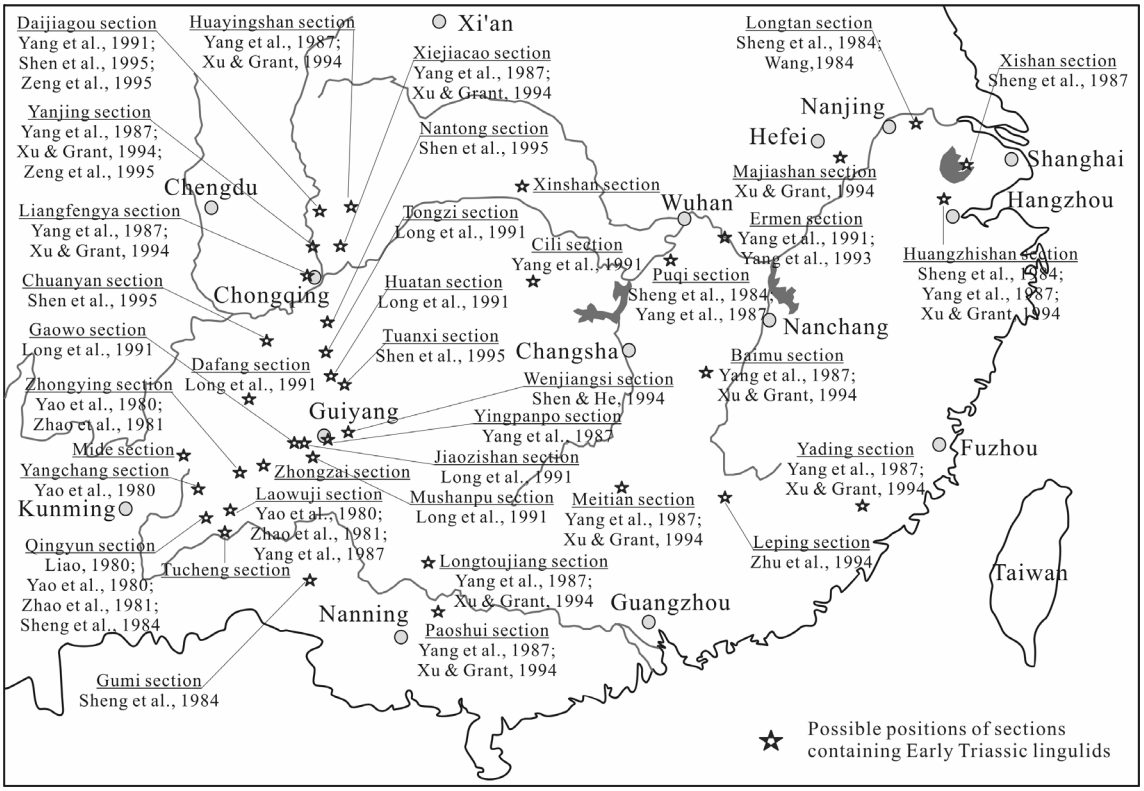

Figure 1. Wide distribution of Early Triassic lingulid fauna in South China

sized shell and cave dwelling living styles made them more tolerate to the anoxic environments (e.g. Hallam and Wignall, 1997) and the shortage of food supply (e.g. Twichett, 2001) , and they became even smaller for better adaptation in the still stressful environments of the Early Triassic aftermath, which might be one of the key responses for them to thrive. The wide ecological adaptations for lingulids from high-latitude to low-latitude and from the shoreface to the relatively deep sea (Pickerill et al., 1984, and references cited therein) are also vital for them to survive the catastrophic situations and then thrive during the end-Permian and Early Triassic disaster period.

Emig, C. C., 2003. Proof that *Lingula* (Brachiopoda) is not a living-fossil, and emended diagnoses of the family Lingulidae. Notebooks on Geology-Letter 2003/01 (CG2003_L01_CCE).

Erwin, D. H., 1993. The great Paleozoic crisis: life and death in the Permian. Columbia University Press, New York, 327 pp.

Erwin, D. H., 1994. The Permo-Triassic extinction. Nature, 367: 231-236.

Flugel, E., 1994. Pangean shelf carbonates: controls and paleoclimate significance of the Permian and Triassic reefs. *in* Klein, G. V. (ed.) Pangea: paleoclimate, tectonics and sedimentation during accretion, zenith and breakup of a supercontinent. Geological Society of America Special Paper, 288: 247-266.

Hallam, A., Wignall, P. B., 1997. Mass extinctions and their aftermath. Oxford University Press, Oxford, 320 pp.

Knoll, A. H., Bambach, R. K., Canfield, D. E., Grotzinger, J. P., 1996. Comparative earth history and Late Permian mass extinction. Science, 273: 452-457.

Payne, J. L., Lehrmann, D. J., Wei, J. Y., Orchard, M. J., Schrag, D. P., Knoll, A. H., 2004. Large perturbations of the carbon cycle during recovery from the end-Permian extinction. Science, 305: 506-509.

Pickerill, R. K., Harland, T. L., Fillion, D., 1984. In situ lingulids from deep-water carbonates of the Middle Ordovician Table Head Group of Newfoundland and the Trenton Group of Quebec. Canadian Journal of Earth Sciences, 21: 194-199.

Retallack, G. J., Veevers, J. J., Morante, R., 1996. Global coal gap between Permian-Triassic extinctions and middle Triassic recovery of peat forming plants. Geological Society of America Bulletin, 108: 195-207.

Twitchett, R. J., 2001. Incompleteness of the Permian-Triassic fossil record: a consequence of productivity decline? Geological Journal, 36: 341-353.

Xu, G. R., Grant, R. E., 1994. Brachiopods near the Permian-Triassic boundary in South China. Smithsonian Institution Press, Washington D.C.

Yang, Z. Y., Wu, S. B., Yin, H. F., Xu, G. R., Zhang, K. X., Bi, X. M., 1993. Permo-Triassic events of South China. Geological Publishing House, Beijing, 153 pp.

Aligning Marine and Non-Marine Permian-Triassic Boundary Sections Using Biostratigraphy and High-Resolution Eventostratigraphy: An Example from Western Guizhou and Eastern Yunnan, Southwestern China

Peng Yuanqiao[1, 2], Yin Hongfu[1], Gao Yongqun[3], Yang Fengqing[1] and Yu Jianxin[1]

[1] Faculty of Earth Sciences, China University of Geosciences, Wuhan 430074, Hubei Province, P.R. China

[2] School of Ecology and Environment, Deakin University, Melbourne Campus, 221 Burwood Highway, Burwood, VIC 3125, Australia; ype@deakin.edu.au

[3] China University of Geosciences Press, Wuhan 430074, Hubei Province, P.R. China

Both vertically and laterally continuous Permian-Triassic boundary (PTB) sequences from marine via on-shore (marine and terrestrial alternate) to terrestrial facies are well-outcropped in western Guizhou and eastern Yunnan, southwestern China, making this area a potential hotspot for the study of high-resolution subdivision and correlation of the PTB from marine facies to land (Peng et al., 2002, 2005). Six PTB sections from marine via on-shore to terrestrial facies in this area are well-studied (Fig. 1). Among them, two (the Chahe and Zhejue sections) are terrestrial PTB sections, two (the Mide and Tucheng sections) are on-shore (marine and terrestrial alternate) ones and the other two (the Zhongzai and Gaowo sections) are shallow marine ones (see Fig. 1 for positions of these sections).

The PTB of these sections from marine to terrestrial facies in western Guizhou and eastern Yunnan can be subdivided and correlated with high-resolution through biostratigraphy as well as eventostratigraphy. Biostratigraphically, plant fossils of the Cathaysian *Gigantopteris* flora are found dominating in the Upper Permian of both the terrestrial and the on-shore PTB sections (Nanjing Inst., 1980; Wang and Yin, 2001; Peng et al., 2005), making the Upper Permian of these two facies correlative. Marine fossils found in the on-shore and the shallow marine PTB sections shape another way for the direct biostratigraphic correlation of these sections. As bridge sections, the on-shore PTB ones provide both marine and terrestrial fossil evidences to indirectly correlate the terrestrial PTB sections with their marine counterparts in western Guizhou and eastern Yunnan. Under this biostratigraphic framework control and applying the concept of the Permian-Triassic boundary stratigraphic set (PTBST) composed of PTB clayrocks of volcanic origin in all these PTB sections from marine via on-shore to terrestrial facies (Peng et al., 2001, 2005), the PTB in western Guizhou and eastern Yunnan can be subdivided and correlated with high-resolution among these different facies.

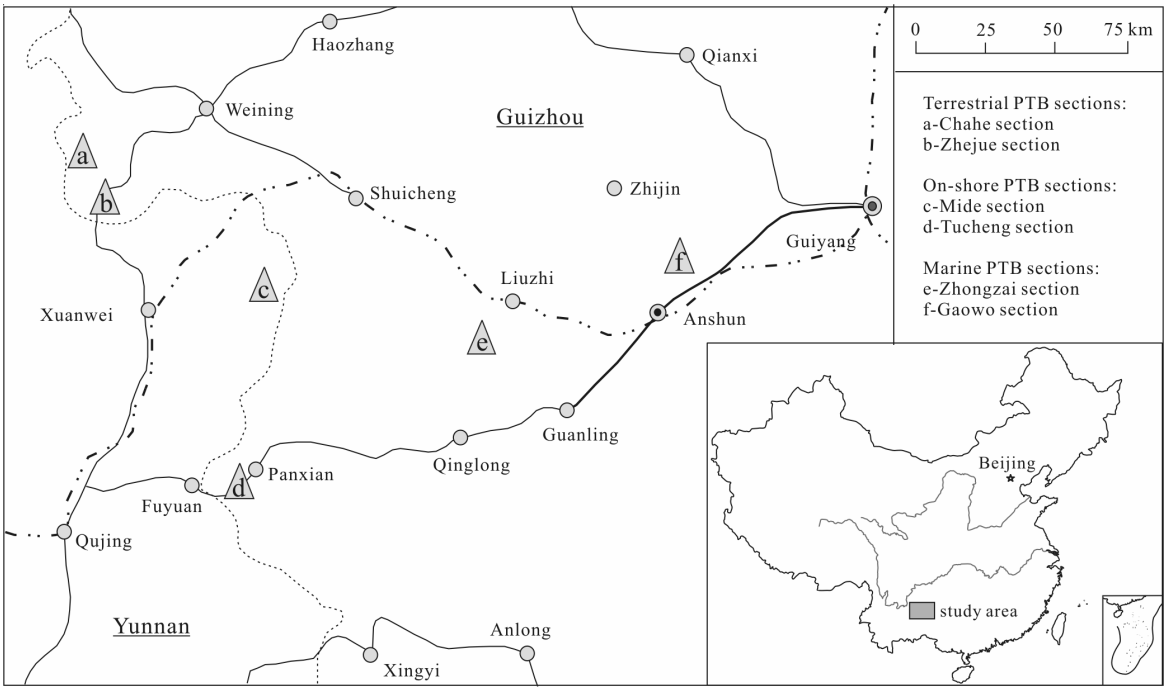

Figure 1. The geographic position and transportation roots in western Guizhou and eastern Yunnan, southwestern China

The most important evidence for the high-resolution correlation of the PTBST in South China is the finding of the Early Triassic index fossil *Hindeodus parvus* (Kozur and Pjatakova) in the PTBST other than the Meishan Global Stratotype Section and Point (GSSP) section. This time, not just supported by the similar vertical PTBST sequence in western Guizhou and eastern Yunnan, *Hindeodus parvus* was also found in the PTBST of the Zhongzai section (one of the shallow marine PTB sections in western Guizhou and eastern Yunnan, section e of Fig. 1) (I. Metcalfe, 2004, pers. comm. in Florence, Italy). This finding provides strong support not only for the high-resolution subdivision of the PTB in western Guizhou and eastern Yunnan and also for the high-resolution correlation of the PTBST from this area to the other parts of South China, and especially to the Meishan GSSP section.

In the meantime, the carbon isotopic excursions across the PTBST in both marine and terrestrial PTB sections are also correlative in South China, and even worldwide with the reference to the Meishan GSSP section in South China. Three distinct stages of $\delta^{13}C_{org}$ excursion can be identified from the PTB strata of the Chahe section in western Guizhou and eastern Yunnan, i.e. of higher values in the Upper Permian, dropping and forming a main excursion from higher to lower values in the PTBST, and then remaining at lower values and slowly recovering upwards in the Lower Triassic (Peng et al., 2005). This serves well for the definition and correlation of the PTB from marine to terrestrial facies in western Guzhou and eastern Yunnan, southwestern China with other biostratigraphic and eventostratigraphic markers (Peng et al., 2005). It can also be well correlated with the changing trends in the PTBST at some other well known marine PTB sections (such as the Meishan GSSP section and the Shangsi section) in South China (Yan et al., 1989; Xu and Yan, 1993; Cao et al., 2002) and worldwide in both marine and terrestrial realms (Baud et al., 1989; Wang et al., 1994; Macleod et al., 2000; Ward et al., 2005; and many others). The worldwide drop event in $\delta^{13}C$ is thus usually suggested as one of the auxiliary markers for the demarcation of the PTB when fossil evidences are absent, especially in the terrestrial realm (Peng et al., 2005; Ward et al., 2005), though actually the sharp negative excursion in $\delta^{13}C$ is slightly older than the formal stratigraphic PTB defined by the first appearance of conodont *Hindeodus parvus* at the Meishan GSSP section (Jin et al., 2000; Cao et al., 2002).

Baud, A., Magaritz, M., Holser, W. T., 1989. Permian-Triassic of the Tethys: carbon isotopic studies. Geologische Rundschau, 78: 649-677.

Cao, C. Q., Wang, W., Jin, Y.G., 2002. Carbon isotopic excursions across the Permian-Triassic boundary in the Meishan section, Zhejiang Province, China. Chinese Science Bulletin, 47: 1125-1129.

Jin, Y. G., Wang, Y., Wang, W., Shang, Q. H., Cao, C. Q., Erwin, D. H., 2000. Pattern of marine mass extinction near the Permian-Triassic boundary in South China. Science, 289: 432-436.

MacLeod, K., Smith, R., Koch, C., Ward, P., 2000. Timing of mammal-like reptile extinctions across the Permian-Triassic boundary in South Africa. Geology, 28: 227-230.

Nanjing Institute of Geology and Palaeontology, Academica Sinica, 1980. Late Permian coal-bearing strata and palaeontological fauna in western Guizhou and eastern Yunnan. Beijing: Science Press, 277pp.

Peng, Y. Q., Tong, J. N., Shi, G. R., Hansen, H. J., 2001. The Permian-Triassic Boundary Stratigraphic Set: char-

acteristics and correlation. Newsletters on Stratigraphy, 39: 55-71.

Peng, Y. Q., Wang, S. Y., Wang, Y. F., Yang, F. Q., 2002. A proposed area for study of Accessory Section and Point of terrestrial Permian-Triassic boundary. Journal of China University of Geosciences, 13: 157-162

Peng, Y. Q., Zhang, S. X., Yu, J. X., Yang, F. Q., Gao, Y. Q., Shi, G. R., 2005. High-resolution terrestrial Permian-Triassic eventostratigraphic boundary in western Guizhou and eastern Yunnan, southwestern China. Palaeogeography, Palaeoclimatology, Palaeoecology, 215: 285-295.

Wang, K., Geldsetzer, H. H. J., Krouse, H. R., 1994. Permian-Triassic extinction: organic ~^{13}C evidence from British Columbia, Canada. Geology, 22: 580-584.

Wang, S. Y., Yin, H. F., 2001. Study on terrestrial Permian-Triassic boundary in eastern Yunnan and western Guizhou. China University of Geosciences Press, Wuhan.

Ward, P. D., Botha, J., Buick, R., De Kock, M.O., Erwin, D. H., Garrison, G. H., Kirschvink, J. L., Smith, R., 2005. Abrupt and gradual extinction among Late Permian land vertebrates in the Karoo basin, South Africa. Science, 307: 709-714.

Xu, D. Y., Yan, Z., 1993. Carbon isotopic and iridium event markers near the Permian/Triassic boundary in the Meishan section, Zhejiang Province, China. Palaeogeography, Palaeoclimatology, Palaeoecology, 104: 171-176.

Yan, Z., Ye, L. F., Jin, R. G., Xu, D. Y., 1989. Features of stable isotope near the Permian-Triassic boundary of the Shangsi section, Guangyuan, Sichuan. *in* Li, Z. S., Zhan, L. P., Dai, J. Y., Jin, R. G., Zhu, X. F., Zhang, J. H., Huang, H. Q., Xu, D. Y., Yan, Z., Li, H. M. (eds.) Study on the Permian-Triassic biostratigraphy and event stratigraphy of northern Sichuan and southern Shaanxi. Geological Publishing House, Beijing, 166-171.

Early Radiation and Geographic Dispersal of Ichthyopterygians (Reptilia, Diapsida)

Lars Schmitz[1*], Jiang Da-yong[2], Ryosuke Motani[1], Hao Wei-cheng[2] and Sun Yuan-lin[2]

*[1] Department of Geology,University of California, Davis, CA 95616,USA;*schmitz@geology.ucdavis.edu*

[2] Department of Geology and Geological Museum, Peking University, Beijing 100871, P. R. China

Ichthyopterygians are a diverse group of marine reptiles that existed from the Early Triassic (Olenekian) to the Mid-Cretaceous (Cenomanian). According to our current fossil record the early radiation of ichthyopterygians was very rapid. There are no definitive records for ichthyopterygians in the Induan or Smithian. The Spathian, however, documents a sudden appearance of six species. The timing of this radiation is earlier than the abrupt end of carbon cycle fluctuation in the early Anisian, which supposedly marks the stabilization of marine ecosystems after the P/T mass extinction (Payne et al., 2004). However, it coincides with the early phase of global diversity recovery (Erwin, 1994). The Anisian marks a second radiation phase of ichthyopterygians. Probably only two taxa survived the Olenekian/Aegean boundary; however, the overall diversity increased to 12 species, dominated by the Mixosauridae (six species). The Ladinian documents eight species.

Most of our current knowledge of early ichthyosaurs is based on data from a few localities only. Hence, the picture of ichthyosaurian biogeography is necessarily diffuse. Nevertheless, we are able to recognize two large-scale patterns. Olenekian ichthyopterygians tend to have a very limited geographic range, whereas later forms inhabited much larger areas. Furthermore, Olenekian ichthyopterygian faunas mainly consist of a single taxon, whereas all later faunas are more diverse taxonomically.

The Olenekian *Chaohusaurus geishanensis* has only been discovered in the Qinglong Formation (Anhui, China), and *Grippia longirostris* is also restricted to a single locality, Spitsbergen (arctic Norway). The up to 2.5 m long *Utatsusaurus hataii* is solely known from the Japanese Osawa Formation, with the possible exemption of one fragmentary specimen from the Vega Phroso Member (Sulphur Mountain Formation) in British Columbia, Canada (Nicholls and Brinkman, 1993).

The fossil record indicates that Spitsbergen might be unique among Olenekian localities in having more than a single ichthyopterygian taxon. The Upper Sticky Keep Formation of Spitsbergen contains three vertebrate-bearing horizons: the *Grippia*-Level (Olenekian), and the Lower (Olenekian) and Upper (Ladinian) Saurian Levels. Besides the name-giving genus, the *Grippia*-Level yields fragmentary remains of much larger ichthyopterygians. The taxonomy of these is controversial; however, there is no doubt that they are distinct from *Grippia longirostris*. The Lower Saurian Level also contains two different forms, which are tentatively referred to *Isfjordosaurus minor* and ?*Besanosaurus* (McGowan and Motani, 2003).

In the Middle Triassic we see a distinct change in the dispersal of ichthyopterygians. The patchy biogeographic pattern changes towards much wider geographic ranges, which is probably due to enhanced swimming capabilities achieved by the modifications of the body plan. All forms are well adapted to an aquatic lifestyle, but there are distinct differences in their body plan (McGowan and Motani, 2003). The earliest ichthyopterygians have slender bodies with already fin-shaped limbs. The caudal fin has a small dorsal lobe, which can be deduced from osteological features of the neural spines. The skull is proportionally small compared to later forms. The predominant group of the Middle Triassic, the Mixosauridae, is morphologically intermediate between basal ichthyopterygians and derived fish-shaped forms of the

Jurassic. They retain the dorsal lobe of the caudal fin, but the trunk is not as slender as in basal forms. Distinguishing features are a high crest along the midline of the skull and very high but short vertebral centra in the caudal region.

The large-sized *Cymbospondylus* has been documented in the east Pacific realm, possibly Spitsbergen, and in the Monte San Giorgio basin in the southern Alps, but is not known from China so far. The Mixosauridae, containing the genera *Mixosaurus* and *Phalarodon*, have an even wider geographic distribution. *Mixosaurus* occurs widely in the Tethys realm (Monte San Giorgio, Guizhou), and *Phalarodon* is spread over the northern hemisphere (Germanic Basin, possibly Monte San Giorgio, Guizhou, Nevada, British Columbia, Spitsbergen).

A finer-scale analysis of the stratigraphic range and geographic occurrence of the Mixosauridae demonstrates the current limits, despite the recent discovery of a Pelsonian locality in the Xinmin district, Panxian County, Guizhou Province, China, which fills a long-standing geographical gap. Overall, the family ranges from the middle Anisian (Pelsonian, possibly Bithynian) into the Ladinian. The earliest mixosaurids appear in the Pelsonian, possibly in the Bithynian. *Phalarodon atavus* occurs in the lower part of the Muschelkalk of the German Basin, an epicontinental extension of the western Tethys; the new locality in China yields a new taxon that will be named elsewhere, and *Phalarodon* cf. *P. fraasi* (Jiang et al., 2004). This might indicate a tethyan origin of the Mixosauridae. However, the timing of the appearance of *Phalarodon* outside the Tethys cannot be exactly determined, because an important locality, the Sulphur Mountain Formation is biostratigaphically not dated precisely (Nicholls et al., 1999). The first unequivocal occurrence of *Phalarodon* is in the late Anisian of Nevada, with *P. fraasi* and *P. callawayi* (Schmitz et al., 2004).

The diversity pattern indicates that the radiation of ichthyopterygians occurred very fast and in two phases (Spathian and early Anisian). While early ichthyopterygians had limited geographic distributions, later forms (Cymbospondylidae and Mixosauridae in particular) were almost cosmopolitan.

Erwin, D. H., 1994. The Permo-Triassic extinction. Nature, 367: 231-236.

Jiang, D.-Y., Schmitz, L., Hao, W.-C., 2004. Two species of Mixosauridae (Ichthyosauria) from the Middle Triassic of south-western China). Journal of Vertebrate Paleontology, 24 (3, supplement): 76A

McGowan, C., Motani, R., 2003. Ichthyopterygia. Handbook of Paleoherpetology, Part 8. Verlag Dr. Friedrich Pfeil, München, 175 pp.

Nicholls, E. L., Brinkman, D. B., 1993. A new specimen of Utatsusaurus (Reptilia: Ichthyosauria) from the Lower Triassic Sulphur Mountain Formation of British Columbia. Canadian Journal of Earth Sciences, 30: 486-490.

Nicholls, E. L., Brinkmann, D. B., Callaway, J. M., 1999. New material of Phalarodon (Reptilia: Ichthyosauria) from the Middle Triassic of British Columbia and its bearing on the interrelationships of mixosaurs. Palaeontographica, Abteilung A, 252: 1-22.

Payne, J. L., Lehrmann, D. J., Wei, J., Orchard, M. J., Schrag, D. P., Knoll, A. H., 2004. Large perturbations of the carbon cycle during recovery from the end-Permian extinction. Science, 305: 506-509.

Schmitz, L., Sander, M, Rieppel, O., Storrs, G., 2004. The mixosaurs (Ichthyosauria, Mixosauridae) from the Middle Triassic of the Augusta Mountains (Nevada, USA) with the description of a new species. Palaeontographica, Abteilung A, 270: 133-162.

End-Permian Mass Extinction Pattern in the Northern Peri-Gondwanan Region

Shen Shuzhong[1*], Cao Changqun[1], Charles M. Henderson[2], Wang Xiangdong[1], G. R. Shi[3], Wang Wei[1] and Wang Yue[1]

[1] Nanjing Institute of Geology and Palaeontology, Chinese Academy of Sciences, 39 East Beijing Road, Nanjing 210008, P.R. China; [*]szshen@nigpas.ac.cn

[2] Department of Geology and Geophysics, University of Calgary, Calgary, AB, Canada T2N 1N4

[3] School of Ecology and Environment, Deakin University, Melbourne Campus, 221 Burwood Highway, Burwood, Victoria 3125, Australia

The Permian-Triassic extinction pattern in the peri-Gondwanan region is documented biostratigraphically, geochemically and sedimentologically based on three marine sequences deposited in southern Tibet and comparisons with the sections in the Salt Range, Pakistan and Kashmir. Results of biostratigraphic ranges for the marine faunas reveal an end-Permian event comparable in timing with that known at the Meishan section in low palaeolatitude and Spitsbergen and East Greenland in northern Boreal settings although patterns earlier in the Permian vary. The previously documented delayed (late Griesbachian) extinction at the Selong Xishan section is not supported based on our analysis. The event is exhibited by an abrupt marine faunal shift slightly beneath the Permian-Triassic boundary (PTB) from benthic taxa- to nektic taxa-dominated communities. The climate in the continental margin of Meso-Tethys before the extinction event was yet cold. However, a rapid climatic warming event was associated with the extinction event as indicated by the southward invasion of abundant warm-water conodonts, warm-water brachiopods, and gastropods. Stable isotopic values of $d^{13}C_{carb}$, $d^{13}C_{org}$ and $d^{18}O$ show a sharp negative drop slightly before the extinction interval. Sedimentologic and microstratigraphic analysis reveals a regression event, as marked by a Caliche Bed at the Selong Xishan section and the micaceous siltstone in the topmost part of the Qubuerga Formation at the Qubu

and Tulong sections. The regression event was immediately followed by a rapid transgression beneath the PTB. Alternatively, the "Caliche Bed" may be interpreted as a secondary carbonate deposit precipitated around a solution-collapse breccia, in which case relative sea-level fluctuations are equivocal. The basal Triassic rocks fine upward, and are dominated by dolomitic packstone/wackestone containing pyritic cubes, bioturbation and numerous tiny foraminifers, suggesting that the studied sections were deposited in the initial stage of the transgression and hence may not have been deeply affected by the anoxic event that is widely believed to characterise the zenith of the transgression.

The Patterns of Recovery of Tetrapod Communities in the Early Triassic of Europe and Southern Gondwana: A Comparison and Implications

Michael A. Shishkin

Palaeontological Institute, Russian Academy of Sciences, Moscow, Russia; shishkin@paleo. ru

The Early Triassic (Scythian) history of terrestrial tetrapods is primarily documented by faunal successions of East Europe and South Africa. The European succession includes the *Benthosuchus-Wetlugasaurus* (*B-W*) Fauna and succeeding *Parotosuchus* Fauna. These correspond to the regional Vetlugian and Yarenskian Superhorizons and cover the whole range of the Scythian. In South Africa, the coeval faunal units are known from the Karoo basin and termed the *Lystrosaurus* Zone and Lower *Cynognathus* Subzone (Shishkin et al., 1995). These two successions show striking difference in their taxonomic composition, in the patterns of evolutionary change within their earlier members, and, lastly, in the ways of faunal replacement that occurred in the transition from the earlier member to younger one.

Specifically, this implies the following. (1) Both of the East European faunas are dominated by temnospondyl amphibians, while those of South Africa by therapsid reptiles. (2) The European *B-W* Fauna demonstrates 3 to 4 low-rank transformations through its range, while in its presumed South African equivalent, the *Lystrosaurus* Zone assemblage, the biotic changes are much less manifest (see below). (3) In contrast to the pattern demonstrated by South African succession, in East Europe the evolution from the *B-W* Fauna to *Parotosuchus* Fauna was underlain mainly by phylogenetic changes or by replacements within closely related groups.

The latter pattern of change is detectable in many ways. Of temnospondyl genera dominating the European *B-W* Fauna, the capitosaurid *Wetlugasaurus* is very close to the ancestry of succeeding *Parotosuchus*, while the benthosuchid trematosauroids form a morphocline (*Benthosuchus – Thoosuchus – Angusaurus*) toward the condition in true trematosaurids, known from the *Parotosuchus* Fauna. The early Vetlugian aberrant brachyopoid *Tupilakosaurus* is replaced by closely related Yarenskian brachyopid *Batrachosuchoides* (with some barren interval between them). Amongst parareptiles, the Vetlugian procolophonids *Tichvinskia* and *Orenburgia* persist into the early Yarenskian and give rise to more advanced taxa. Similarly, of rauisuchid archosaurs, *Tsylmosuchus* ranges across the Vetlugian-Yarenskian boundary and is later replaced by *Vychegdosuchus*. Similar ranging is also suggested for succeeding genera of proterosuchid and erythrosuchid archosaurs. Lastly, the same sort of replacement pattern is demonstrated by accompanying fish dominants. The lepidosirenid dipnoan *Gnathorhiza*, typical to the Vetlugian. is known to survive into the early Yarenskian time, in which it initially coexists with the ceratodontid *Ceratodus*, an index genus of the late Olenekian. In summation, the late Scythian (Yarenskian) European vertebrate fauna was basically autochtonous in origin.

By contrast, the Gondwanan *Lystrosaurus* Zone assemblage is not directly ancestral to the *Cynognathus* Zone community, which is markedly distinct in composition. The guide temnospondyl amphibians of these faunal members (lydekkerinids and capitosaurids respectively) are only distantly related. Likewise, the reptilian families of the *Lystrosaurus* Zone do not persist into the succeeding zone, except for the Procolophonidae and possibly some cynodont lineages.

Since late 80ies of XX century the attempts were made to account for this discontinuity by suggesting a wide chronological gap between the South African biozones, such that the *Lystrosaurus* Zone was placed in the early Induan and *Cynognathus* Zone in the late Olenekian (Anderson and Cruikshank, 1978, Battail, 1988). As the candidates to fill the gap between them there were suggested the fauna of the Arcadia Formation of Australia and/or that of the Middle Sakamena Group of Madagascar. But in fact, none of the Scythian assemblages known 'can be shown to be of intermediate position through possession of a transitional taxonomic composition' between the South African biozones (Cosgriff, 1984).

The alternative concept suggests that South African succession is not disjunct, with the *Lystrosaurus* Zone ranging from the Induan to early Olenekian (Ochev, Shishkin, 1984, 1989; Shishkin et al., 1995,1996). This conclusion is primarily based on the fact that in East Europe the appearance of *Procolophon*-like procolophonids with differeniated teeth falls on the early Olenekian (late Vetlugian). It should be stressed that in South Africa *Procolophon* is most abundant in the upper part of the *Lystrosaurus* Zone, which is barren of the index genus *Lystrosaurus* (Neveling et al., 1999). On the other hand, the basal beds of the zone contain the primitive procolophonid *Owenetta* which is comparable by evolutionary level with *Phaanthosaurus* from the Induan (Vokhmian Horizon) of East Europe. All this supports the attribution of the upper part of the *Lystrosaurus* Zone to the Early Olenekian.

The next following member of South African succession, the Lower *Cynognathus* Subzone, is unquestionably late Olenekian in age (Shishkin et al., 1995), hence a time gap between it and the *Lystrosaurus* Zone seems highly unlikely. Combined with a sharp difference in their taxonomic composition, this fact leads to conclusion that biotic events underlying the rise of the *Cynognathus* assemblage were caused mostly by biogeographic changes rather than strictly phylogenetic ones (Shishkin et al., 1996). The amphibian component of the assemblage was suggested to have been derived mainly from the Australo-Tasmanian, and partially Euramerican, ancestors.

Recently, based on new amphibian finds from the *Lystrosaurus* Zone, some authors (Damiani et al., 2000, 2001) concluded that the zone actually extends to the late Olenekian, and that some genera are shared by both the *Lystrosaurus* and *Cynognathus* zones, thus pointing to their closer phylogenetic links than it was presumed earlier.

These conclusions are clearly ill-evidenced. Of the finds presumed to substantiate them, the first one is a benthosuchid-designed lower jaw, originally assigned to trematosaurid *Trematosuchus* (Neveling et al., 1999) and later re-identified as Trematosauridae gen.ind. Its dating by Damiani et al. (2000) is based on the belief that all the trematosaurids are late Olenekian in age. In reality, the bulk of them belong to the Smithian (*Arctoceras blomstrandi* Zone of Spitsbergen and *Flemingies flemingianus* Zone of Madagascar). In addition, the pattern of the postglenoid area (PGA) of the mandible in question is by far more primitive than in trematosaurids, showing neither the presence of dorsal concavity nor a clear-cut demarcation between the dorsal and lingual PGA sides. By the latter character and limited backward extent of the prearticular, the mandible is even more primitive than in the late Vetlugian European trematosauroids (Thoosuchinae). All this shows unequivocally that the South African find is not younger in age than the early Olenekian.

Another alleged evidence of immediate faunal links between two South African biozones is said to be provided by a fragment of the capitosaurid mandible from the *Lystrosaurus* Zone (Damiani et al., 2001). It was attributed to so-called *Watsonisuchus*, a genus based on the holotype of *'Wetlugasaurus' magnus* Watson from basal part of the *Cynognathus* Zone. This attribution was also extended by the cited authors to Australian 'parotosuchians', which have been distinguished by Schoch and Milner (2000) as a genus *Rewanobatrachus.* Both the South African find and *Rewanobatrachus* (pers.obs.) are the *Wetlugasaurus*-grade capitosaurids showing a primitive design of the PGA (type I by MaryaD´ska et Shishkin, 1996). The latter displays (a) posteriorly tapered dorsal surface; (b) parallel dorsal ridges (crista surangularis and c. medialis), separated only by a groove, and (c) weakly developed or absent lingual ridges.

On the other hand, the South African find is clearly distinct from *'Watsonisuchus' magnus*, which is actually an advanced, *Parotosuchus*-grade form. Although in the holotype of *'W.' magnus* the PGA is incompletely preserved, it shows all principal characters of the *Parotosuchus* PGA pattern (type III), including the broad dorsal surface with widely diverging c.surangularis and c. medialis, well developed lingual ridges and high postglenoid wall. In all these respects, the *'Watsonisuchus'* type is undistiguishable from *Kestrosaurus* Haughton**,** the commonest *Parotosuchus*-grade amphibian of the Lower *Cynognathus* Subzone, and most likely is a junior synonym of *Kestrosaurus* (Shishkin et al., 2004).

Hence, no amphibian genera are actually known to be shared by the *Lystrosaurus* and *Cynognathus* zones of South Africa. But the fact of occurrence of the capitosaurid in the *Lystrosaurus* Zone deserves attention and should be assessed in the context of the overall early Scythian capitosaurid record in Gondwana.

In South Africa, the discussed capitosaurid find supplements the lydekkerind-dominated amphibian assemblage which also includes a dissorophoid and a very poor record of rhinesuchids, rhytidosteids and tupilakosaurids. In the *Lystrosaurus* Zone of Antarctica the capitosaurids are equally known from just a single scrap, associated with a lydekkerinid and tupilakosaurid; published data on the presence there of brachyopids and rhytidosteids (cf. Cosgriff, 1984) are based on indeterminate fragments (pers.obs.). In the Panchet Beds of India, apparently of Induan age, the amphibians are also dominated by lydekkerinids, but show some increase in the role of capitosaurids. The latter include *Pachygonia* and some of specimens attributed to lydekkerinids (*Indobenthosuchus*) and *Indolyrocephalus*. Other local amphibians comprise a lonchorhynchine, a tupilakosaurid and primitive rhytidosteoid.

The only purely terrestrial assemblage from the early Scythian of Gondwana that shows the abundance of capitosaurids is that of the Arcadia Formation in Australia. These forms are associated there primarily with rhytidosteoids, a brachyopid, and early chigutisaurid. In other areas of Australo-Tasmania, the primitive capitosaurids are known from the assemblages of the Knocklofty Formation and Blina Shale, dominated by rhytidosteids and brachyopids. Outside the region, especially notable is the assemblage from the nearshore marine sediments of the Middle Sakamena Group of Madagascar. Here the capitosaurids are common and include *Edingerella* and *Deltacephalus* (often erroneously attributed to lydekkerinids), occurring together with the trematosaurids and rhytidosteids.

In all, these data warrant the conclusion that during the early Scythian the center of the capitosaurid radiation in southern Gondwana fell on the Australo-Tasmanian region. The rest of the territory, except (to some extent) for India and some coastal biotopes, obviously belonged to remote marginal zones of the capitosaurid dispersal. This primarily refers to the Afro-Antarctic realm.

To assess the run of further faunal events in southern Gondwana, of primary importance is the fact that only in Australo-Tasmania the early Scythian capitosaurids are accompanied by brachyopids. It is just the set of temnospondyl families that forms the main amphibian component of the succeeding Lower *Cynognathus* Subzone assemblage of South Africa. Moreover, the commonest members of the Australo-Tasmanian Brachyopidae (*Blinasaurus*) and Capitosauridae (*Rewanobatrachus*) are fairly close to their equivalents in the *Cynognathus* Zone, i.e. to *Batrachosuchus* and *Kestrosaurus* ('*Parotosuchus*') respectively, and sometimes even synonymized with them. By contrast, in the *Lystrosaurus* Zone of Afro-Antarctica these groups are either lacking or (as with capitosaurids) exceedingly scarce. Hence, it is seems very likely that they came to South Africa from Australo-Tasmania or its vicinity as a result of the overall re-pattering of tetrapod distribution in Gondwana during the Olenekian.

Turning to reptilian constituent of the faunas discussed, the above conclusion may be also indirectly supported by the pattern of the Triassic dicynodont record in Gondwana. In South Africa this record shows a gap that separates the ranges of the genus *Lystrosaurus* and typical kannemeyerids; i.e., it spans the upper part of the *Lystrosaurus* Zone (Neveling et al., 1999) and the Lower *Cynognathus* Subzone (Shishkin et al., 1995). Thus, it seems likely that the gap covers the entire Olenekian. On the other hand, the poorly known dicynodont from the early Olenekian(?) Arcadia Formation of Australia may belong to kannemeyerids (Thulborn, 1984), in spite of some statements to the contrary. This form is somewhat larger than the typical *Lystrosaurus* individuals, and its fragments are not uncommon (pers.obs.). All this seems to warrant the suggestion that the re-appearance of dicynodonts in the Middle *Cynognathus* Subzone of South Africa might have been caused by their expansion from Australo-Tasmania. This conclusion, in turn, is not at variance with a well known fact of the overall discontinuity between the reptilian components of the *Lystrosaurus*- and *Cynognathus* Zones.

The paper is supported by the Russian Foundation for Basic Research, Grant No. 04-05-64741, and by the Programme of the Russian Academy of Science: "The Origin and Evolution of the Biosphere".

Anderson, J. M., Cruickshank, A. R. I., 1978. The biostratigraphy of the Permian and the Triassic. Part 5. Palaeontol. Africana, 21: 15-44.

Battail, B., 1988. Biostratigraphie des formations permo-triasiques continentales à Vertébrés tétrapodes et biogéographie du Gondwana. Ann. Soc. géol. Nord, 57: 37-44.

Cosgriff, J. W., 1984. The temnospondyl labyrinthodonts of the earliest Triassic. J. Vert. Paleont., 4(1): 32-46.

Damiani, R., Neveling, J., Hancox, P. J., Rubidge, B. S., 2000. First trematosaurid temnospondyl from the *Lystrosaurus* Assemblage Zone of South Africa and its biostratigraphic implications. Geological Magazine, 137(6): 659-665.

Damiani, R. J., Neveling, J., Hancox, P. J., 2001. First record of a mastodonsaurid (Temnospondyli, Stereospondyli) from the Early Triassic *Lystrosaurus* Assemblage Zone (Karoo Basin) of South Africa. N. Jb. Geol. Paläont. Abh., 221(2): 133-144.

MaryaD´ska, T., Shishkin, M. A., 1996. New cyclotosaurid (Amphibia: Temnospondyli) from the Middle Triassic of Poland and some problems of interrelationships of capitosauroids. Prace Muzeum Ziemi, 43: 53-83.

Neveling, J. Rubidge, B. S., Hancox, P. J., 1999. A lower *Cynognathus* Assemblage Zone fossil from the Katberg Formation. S. Afr. J. Sci., 95: 555-556.

Ochev, V. G., Shishkin, M. A., 1984. Principles of global correlation of the continental Triassic based on tetrapods. Abstr. 27th Internat. Geol. Congr., 1: 146.

Ochev, V. G., Shishkin, M. A., 1989. On the principles of global correlation of the continental Triassic on the tetrapods. Acta Palaeont.Polon., 34(2): 149-173.

Schoch, R. R., Milner, A. R., 2000. Handbuch der Paläoherpetologie. Theil 3B. Stereospondyli. Dr. Friedrich Pfeil Verlag. München, 1-203.

Shishkin, M. A., Rubidge, B., Hancox, J., 1995. Vertebrate biozonation of the Upper Beaufort Series of South Africa - a new look on correlation of the Triassic biotic events in Euramerica and southern Gondwana. Sixth Symp. on Mesozoic Terr. Ecosyst. and Biota, Beijing, China Ocean Press, 39-41.

Shishkin, M. A., Rubidge, B., Hancox, J., 1996. Comparison of tetrapod faunal evolution during Early Triassic in Eastern Europe and South Africa. Abstr. 9th Biennial Conference S. Afr. Pal. Soc., Stellenbosch: (unpaged).

Shishkin, M. A., Rubidge B., Hancox J., Welman, J., 2004. Re-evaluation of *Kestrosaurus* Haughton, a capitosaurid temnospondyl amphibian from the Upper Beaufort Group of South Africa. Russian Journal of Herpetology, 11(2): 121-138.

Thulborn, R. A., 1984. Early Triassic reptiles of Australia. *in* Reif, W.-E., Westphal, F. (eds.) Third Symposium on Mesozoic Terrestrial Ecosystems, Short Papers, Tubingen (Attempto Verlag), 243-248.

Conodont and Cephalopod Fauna near Ladinian-Carnian Boundary Interval at Luoping County, Yunnan Province, China

Sun Zuoyu, Hao Weicheng, Sun Yuanlin, Jiang Dayong

Department of Geology and Geological Museum, Peking University, Beijing 100871, P. R. China; sunzuoyu@pku.edu.cn

Ladinian-Carnian boundary bed is well developed at Banqiao in Luoping County, Yunnan Province, (Fig. 1), where is paleogeographically confined to the Eastern Tethys and located on the boundary between the Upper Yangtze Sedimentary Province (marine sedimentary basins) and Youjiang Sedimentary Province (continental deposits) (Tong, 2000; and see the process of changes in Fig. 2). Considering that the definition and correlation of the Middle-Late Triassic boundary is still a disputed problem (Yin et al., 2000), this continuous Banqiao L-C boundary sequence yielding abundant conodont associated with cephalopod and bivalve fossils promises to supply some basic data for this important boundary and a basic correlation from Western Tethys (Balini et al. 1998, 2000).

Eight genus and sixteen species of Cephalopod fossils can be identified, and three ammonoid zones can be recognized: (1) "*Anolcites*-bearing" bed, (2) *Protrachycerus-Trachycerus* assemblage zone, and (3) *Trachyceras multituberculatum* zone. "*Anolcites*-bearing" bed, which is in the massive, lightly red coloured limestone and is a marker horizon over much of SW China, comprises *Anolcites clicnoidis* Wang & He, *Anolcites* cf. *doleriticus*, *Anolcites* sp. and *Germanonautilus brooksi* Smith. This bed can be correlated with the Upper *regoledanus* zone of Lombardy (Southern Italy) and Spiti (Tethys Himalaya) (Balini et al. 1998, 2000) and indicates an early Late Ladinian age. *Protrachycerus- Trachycerus* assemblage zone comprises *Protrachyceras deprati*, *P. costulatum*, *P*.sp.A, *P*. sp. B., *Trachyceras douvillei*, *T. sinense* and *T.* sp., which was also found at Kaiyuan, Yunnan (Mansuy, 1912), Liuzhi, Guizhou (Wang, 1993) and Guanling. Guizhou (Hao et al., 2003). Considering the traditional marker of the base of Carnian stage, this assemblage zone cross the Ladinian-Carnian boundary unequivocally, moreover, covers a complete stratigraphic interval. A few meters above this interval, a great turning from marine sedimentary to continental deposits happens (Fig. 2).

Conodont sequence is associated with ammonite "*Anolcites*-bearing" bed and *Protrachycerus-Trachycerus* assemblage zone, comprising species of chronostratigraphic significance such as *Paragondolella polygnathiformis*, *P. auriformis*, *P. maantangensis*, *P. tadpole*, *P. navicula navicula*, *P. foliata foliata*, *P. foliata inclinata*, *P. jiangyouensi*. Similar conodont sequence has also been found from SW Guizhou (Yang, 1995; Yang et al., 1995, 2002; Sun et al., in press) and their evolutionary relationship has been discussed (Sun et al., in press). That these conodonts well co-concur with ammonites during "*Anolcites*-bearing" bed and *Protrachycerus-Trachycerus* assemblage zone maybe possess potential for further study on the L-C boundary.

It is worthy to be noted that there are vertebral fishes and marine reptiles found 40 m below the "*Anolcites*-bearing" bed and 20m below the famous *Keichousaurus* bed, including cf. *Askeptosaurus* (Sun et al. in press), *Lariosaurus* sp. (Sun et al. in press) and some as yet undescribed specimens of *Keichousaurus* sp. Regarding its unique surrounding matrix, as well as the Late Ladinian age, this occurrence promises to represent a new and interesting, diverse and important fossil marine reptile assemblage, possibly quite different from those recently reported from China.

Balini, M., Krystyn, L., Torti, V., 1998. The Ladinian-Carnian Boundary interval of Spiti (Tethys, Himalaya). Albertiana, 21: 26-32.

Balini, M., Germani, D., Nicora, A., Rizzi, E, 2000. Ladinian/Carnian ammonoids and conodonts from the classical Schilpario-Pizzo Camino area (Lombardy): revaluation of the biostratigraphy and paleogeography. Rivista Italiana di Paleontologia e Stratigrafia, 106(1): 19-58.

Hao Weicheng, Sun Yuanlin, Jiang Dayong et al., 2003. Cephalopods of the "Falang Formation" (Triassic) from Guanling and Zhenfeng Counties, Guizhou Province, China. Acta Geol. Sin., 77(4): 430-439.

Mansuy, H., 1912. Etute Geologique du Yunnan Oriental, pt.II, Mem. Serv. Geol. Indochine, I(II), 1-147, pls. 22-25.

Sun Zuoyu, Maisch, W. M., Hao Weicheng, Jiang Dayong, (in press). A Middle Triassic thalattosaur (Reptilia: Diapsida) from Yunnan (China). N. Jb. Geol. Paläont. Mh.

Sun Zuoyu, Hao Weicheng, Maisch, M. W., Pfretzschner, H. U., Jiang Dayong, (in press). A lariosaur (Reptilia: Sauropterygia) from the Middle Triassic (Ladinian) Gejiu Formation of Yunnan, China. N. Jb. Geol. Paläont.

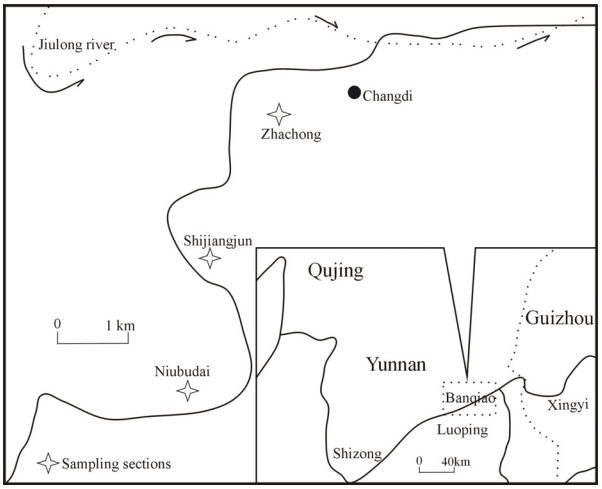

Figure 1. Map showing locality of the sampling sections

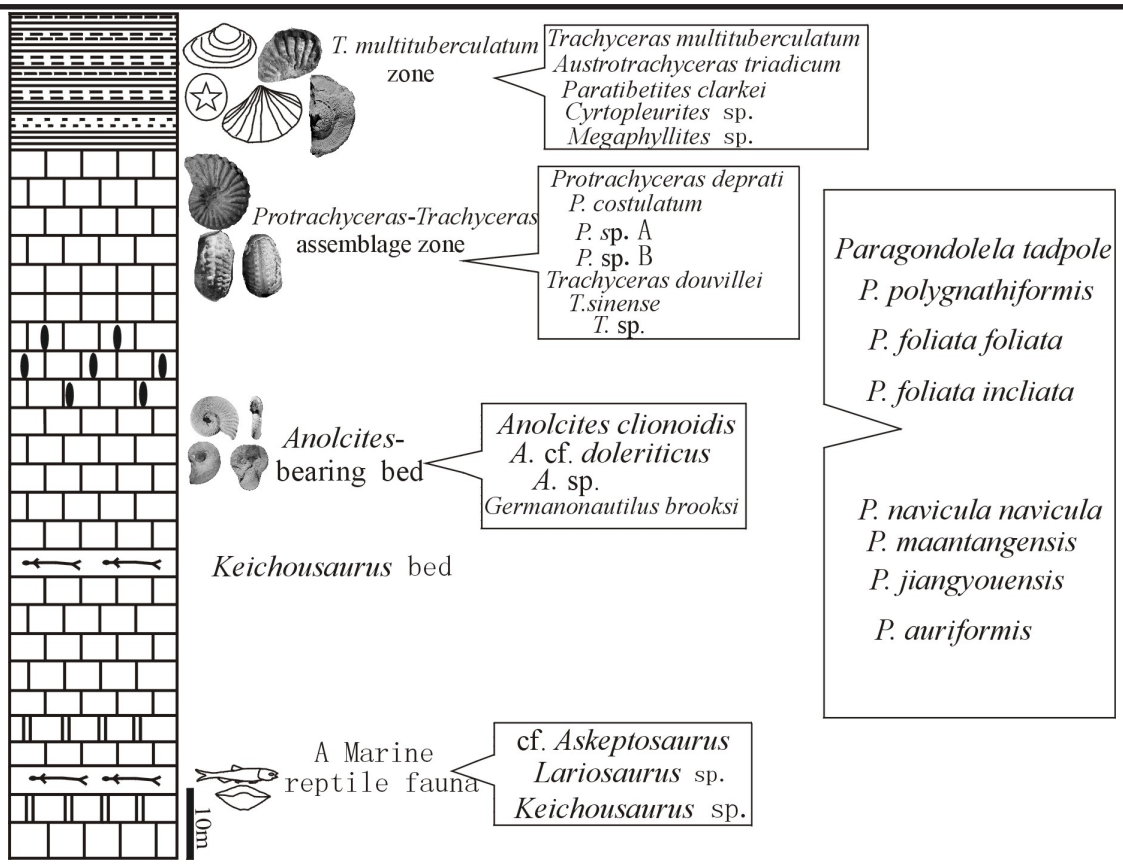

Figure 2. Conodont and Cephalopod faunae around the Ladinian- Carnian boundary at Luoping County, Yunnan Province, China

Mh.

Sun Zuoyu, Hao Weicheng, Jiang Dayong, (in press). Conodont biostratigrphy near Ladinian-Carnian boundary interval in Guanling County, Guizhou, China. Journal of Stratigraphy.

Tong Jinnan, Liu Zhili, 2000. The Middle Triassic stratigraphy and sedimentary paleogeography of South China. Albertiana, 24: 37-47.

Wang Yigang, 1993. Ammonoids from Falang Formation (Ladinian-E. Carnian) of southwestern Guizhou, China. Acta Palaeontologica Sinica, 22(2): 153-162.

Yang Shouren, Liu Jiang, Zhang Mingfa, 1995. Conodonts from the "Falang Formation" of Southwestern Guizhou and their age. Journal of Stratigraphy, 19(3): 161-170.

Yang Shouren, 1995. Ladinian-Carnian conodonts and their biostratigraphy in Asia. Proceeding of the IGCP Symposium on Geology of SE Asia and Adjacent Areas. Journal of Geology. Series B(5-6): 127-138

Yang Shouren, HaoWeicheng, Jiang Dayong, 2002. Conodonts of the "Falang Formation" from Langdai, Liuzhi County, Guizhou Province and their age significance. Geological Review, 48(6): 586-592.

Yin Hongfu, Yang Zunyi, Tong Jinnan, 2000. On status of the international Triassic Research. Journal of Stratigraphy, 24(2): 109-143.

Lower Triassic Carbon Isotope Stratigraphy in Chaohu, Anhui: Implication to Biotic and Ecological Recovery

Tong Jinnan[1], Douglas H. Erwin[2], Zuo Jinxun[1] and Zhao Laishi[1]

[1] State Key Laboratory of Geo-Processes and Mineral Resources, China University of Geosciences, Wuhan 430074, China; jntong@cug.edu.cn

[2] Department of Paleobiology, NMNH, Smithsonian Institution, Washington DC 20560, USA

The most profound biotic and ecological crisis in the Earth's history occurred at the end of the Permian. The Mesozoic biotic recovery and ecosystem reconstruction encompassed most of the Early Triassic. The study of the great Paleozoic-Mesozoic biotic and environmental transition should involve not only the Permian/Triassic boundary but also the Lower Triassic. The carbon isotope composition of the sediments has been taken as one of the key markers to throw light on the biotic evolution and environmental changes, i.e. paleo-atmosphere and paleo-ocean. The sharp excursion in $\delta^{13}C$ coincident with the mass extinction at the end of the Permian has been widely recognized and studied, but few studies have examined carbon isotopes of the Early Triassic biotic and ecological recovery. This paper presents a Lower Triassic carbonate $\delta^{13}C$ (and $\delta^{18}O$) sequence based on the Lower Triassic in Chaohu, Anhui Province, South China. The se-

quence is well-constrained with conodont and ammonoid biostratigraphy, and lay on a relatively deep part of the Lower Yangtze carbonate ramp.

The Lower Triassic carbon isotope record in Chaohu (Figure 1) shows two distinct cycles from strongly negative to positive values, representing two periods of recovery. According to the regional tectonic setting and the depositional sequence, the sequence from the Permian/Triassic boundary to the middle Spathian in Chaohu follows the global trend in the composition of oceanic carbon isotopes, while the upper Spathian was clearly influenced by local environmental conditions. The negative $\delta^{13}C$ anomaly at the Permian/Triassic boundary and in the lower Griesbachian is believed to be the direct result of the mass extinction at the end of the Paleozoic. The gradual increase of $\delta^{13}C$ from the middle Griesbachian to the upper Dienerian may be explained by the primitive recovery of the ecosystems dominated by opportunistic species. This poorly functioning ecosystem collapsed in the Smithian and enlarged the biotic and ecological crisis, resulting in the negative $\delta^{13}C$ of the middle Smithian.

Mesozoic ecosystems started to develop in the late Smithian and fully recovered by the beginning of the Spathian, causing a rapid shift from negative to positive values at the Smithian/Spathian boundary. The high $d^{13}C$ in the early Spathian returned to present-day normal levels in the middle and late Spathian, indicating that the Mesozoic ecosystems were recovered. The slightly negative $d^{13}C$ in the upper Spathian of Chaohu originated from the local tectonic development causing a restricted and dysoxic depositional basin.

A Novel Palaeoecological Method for Quantifying Biotic Recovery in the Aftermath of the End-Permian Mass Extinction Event

Richard J. Twitchett[1, 2]

[1] Department of Earth and Planetary Science, University of Tokyo, 7-3-1 Hongo, Tokyo 113-0033, Japan

[2] School of Earth, Ocean and Environmental Sciences, University of Plymouth, Drake Circus, Plymouth, PL4 8AA, UK; rtwitchett@plymouth.ac.uk

The Late Permian extinction event was critical to the evolutionary history of the marine biosphere, and understanding this event, and the recovery that followed, is crucial to understanding the subsequent evolution of the marine biosphere. However, much of the renewed interest in the Permian-Triassic interval has focussed, not surprisingly,

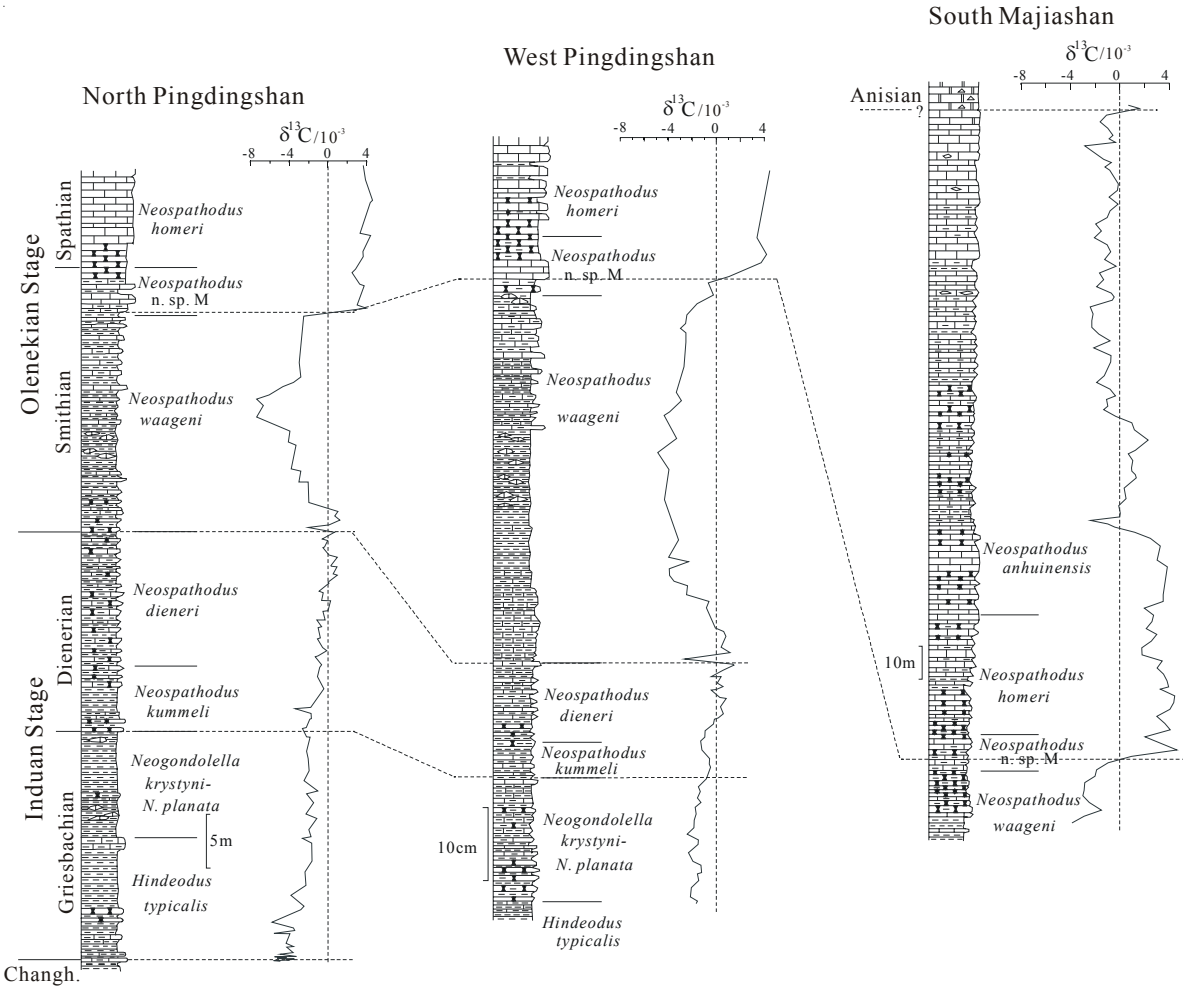

Figure 1. Lower Triassic carbon isotope stratigraphic sequences in Chaohu and their correlation

on the question of extinction cause. With one or two exceptions, little effort has been directed towards understanding the Triassic recovery. The present majority view can probably be summarised thus: the post-Permian recovery was very long, possibly the longest of the Phanerozoic (e.g. Erwin, 1993), and this lengthy recovery was caused by long-lived environmental stresses, probably oceanic anoxia (e.g. Hallam, 1991).

However, studies of the post-Permian biotic recovery are being severely hindered by the lack of rigorous, widely applicable method(s) of quantifying biotic recovery and, even more basic, a definition of "recovery" itself. Thus, many of the perceived conflicts on this issue (e.g. Chen et al., 2002) are merely caused by different authors having different concepts of the meaning of "recovery". In order to proceed in a meaningful (i.e. scientific) manner, concepts such as "recovery" need to be rigorously defined and methods of quantifying recovery need to be constructed, tested and revised where necessary. The debate needs to be opened.

A definition of post-extinction "recovery"?

After modern, small scale disturbances to the marine ecosystem (e.g. oil slicks, algal blooms, hypoxic events), the recovery interval can simply be defined as the interval of time between the event occurring, and the return to "normal", i.e. pre-event, conditions. This "return to normality" (return to pre-event conditions) may be defined on the basis of the return of all displaced species, the re-establishment of a pre-event climax community, the re-establishment of pre-event interspecific interactions etc. Although, it should be noted that due to the stochastic nature of biological systems, conditions never return to a precise pre-event state.

In the geological past, the major extinction events resulted in the permanent loss of some taxa and/or ecological restructuring on such a scale (e.g. Droser et al., 2000; McGhee et al., 2004) that a return to pre-event conditions was typically not possible. Also, measuring parameters such as ecological interactions is difficult from the fossil record. However, if we accept that there is a fundamental difference between "background" and "extinction" times then the return to background conditions (i.e. "return to normality") should be recognisable. The question is how? Other models of extinction-recovery events (e.g. Kauffman and Erwin, 1995) failed to define the end of the recovery interval.

Taxonomic diversity and recovery

The simplest method is a definition based on taxonomic diversity: i.e. defining the return to normality (i.e. the end of the recovery interval) as the return to pre-event levels of diversity. The question of scale and taxonomic level are important. If we apply this definition to the end-Permian event, then, on a global scale, family level diversity did not return to pre-event values until the mid-Jurassic. This definition means that post-Permian recovery took some 100 million years and that, *by definition*, the global biosphere had not returned to background conditions (i.e. "normality") prior to the Late Triassic extinction event.

However, there are obvious taxonomic and fossil record bias problems inherent to any method that involves a literal reading of the fossil record in terms of diversity. These problems are especially relevant to the P-Tr interval, where there is a very significant and long-lived Lazarus effect in most, if not all, marine groups (e.g. Erwin, 1996; Twitchett, 2001) likely due to problems of preservation and facies bias. Recently, Smith and Jeffery (1998) have shown that, even within a single clade, there are major taxonomic problems with present data sets and that extinction studies lacking a phylogenetic (cladistic) methodology are, at best, naïve. Finally, a simple measurement of taxonomic diversity cannot determine recovery at the local or regional scale: alpha diversity may peak in the immediate aftermath of the biotic crisis (temporarily exceeding pre-event levels) due to the influx of many, short-lived, opportunist taxa that clearly do not represent a recovered community. This has been shown to occur in studies of both fossil (e.g. Looy et al., 2001) and recent (e.g. Lu and Wu, 2000) ecosystems. Thus, a diversity-based definition of recovery would not allow one to compare the rates of recovery between, for example, high and low palaeolatitudes. Thus, definitions of recovery that are based entirely on measuring fossil diversity, such as measuring the rate of originations (e.g. Kirchner and Weil, 2000), should be largely avoided and are meaningless for regional comparisons. They may have limited use globally, and within specific groups, if exceptional care is taken.

Palaeoecological definitions of recovery

Given the problems associated with using taxonomic diversity as a measure of recovery, ecological methods are preferred. As the taxonomic and ecological effects of extinction events are to some extent decoupled (e.g. Droser et al., 2000; McGhee et al., 2004), these methods should be viewed as complimentary. In addition, such a methodology should enable comparisons of rates of recovery (1) at sub-global scale (i.e. between regions, individual localities and/or environmental settings), (2) between geological events of different scales, and (3) between ancient and modern events. A number of potential palaeoecological indicators of recovery are available. Parameters regarded as being of particular use include:

Ichnology: Trace fossils provide the only record of the response of the majority soft-bodied benthos to mass extinction intervals (Twitchett and Barras, 2004) and have many other advantages over shelly fossils. They result from the interaction of an organism with its environment, and so provide information on animal diversity as well as environmental conditions. The end-Permian extinction event resulted in a dramatic decrease in ichnodiversity and was followed by a stepwise re-appearance of ichnotaxa through the Early and Middle Triassic (e.g. Twitchett and Wignall, 1996; Twitchett, 1999). "Return to normality" could be defined as the point when all common ichnogenera present in the pre-event assemblages have reappeared. In the aftermath of the end-Permian event, in low palaeolatitudes, this occurs in the Middle Triassic with

the return of *Zoophycos*.

Tiering: This describes the vertical stratification of marine suspension feeding organisms above and below the sediment surface (Ausich and Bottjer, 1982). There have been secular changes of tiering levels through time, and the major mass extinction episodes appear to result in a dramatic, but temporary, reduction in both infaunal and epifaunal tiering (e.g. Twitchett and Barras, 2004). Tiering can be measured or inferred from fossil remains. Return of tiering to pre-event levels is another possible ecological definition for the end of the recovery interval. In the aftermath of the end-Permian event, preliminary data indicate that this occurs in the Middle Triassic.

Dominance and evenness: Ecological parameters such as dominance and evenness can be calculated for any fossil assemblage. Ecological theory predicts that these should vary during extinction-recovery intervals: pre-event communities should comprise K-selected organisms with high diversity and high evenness, whereas in the immediate aftermath of the event, low-diversity, high-dominance assemblages of r-selected organisms should be present. Data from the end-Permian event support these predictions (e.g. Twitchett et al., 2004). The return to pre-event levels of evenness should mark the end of recovery and the "return to normality". However, care is needed when using these criteria to measure recovery because the values measured from fossil shell beds will have been affected by taphonomic factors such as hydrodynamic sorting or dissolution.

Body size: Animals in the aftermath of extinction events are typically smaller than during pre-event times. Preliminary data indicate that this temporary size reduction, termed the "Lilliput Effect" by Urbanek (1993), affects the entire marine benthos during the P-Tr event, as well as most of the nekton and terrestrial animals too. The return to pre-event size may mark the return to normality and the end of recovery. It could be measured within specific lineages or groups, or be used to compare regional rates of recovery. However, the size of preserved fossil marine benthic animals may depend on taphonomic factors (e.g. sorting) as well as local environmental conditions such as food supply and temperature.

A novel palaeoecological recovery model

In addition to allowing one to define the end of the recovery interval and the return to normality of benthic marine ecosystems, the palaeoecological parameters outlined above can also be used to subdivide the recovery interval itself into a number of recovery stages (Twitchett et al., 2004). This enables a detailed comparison of the rates of recovery between localities, regions or individual extinction events that has not been previously possible. The extinction-recovery model of Kauffman and Erwin (1995), which can only be used at the global level, defines just one intra-recovery stage boundary (the end of the Survival Interval) and that has previously being used to compare the rates of recovery after the major extinction events (Erwin, 1998). The novel palaeoecological method discussed herein offers a higher resolution, complimentary method of comparing biotic recovery. Four recovery stages have been determined and are defined on a combination of ecological parameters, especially tiering levels and ichnology (Table 1). The data from trace fossils and body fossils can be used together or separately, which is advantageous if one or other record is not preserved.

Preliminary results have indicated that the shallow marine settings of Neotethys were sites of the most rapid recovery (Twitchett et al., 2004) and that outside Neotethys, higher palaeolatitudes recovered quicker than lower palaeolatitudes (Twitchett and Barras, 2004). Following the end-Permian event, final (Stage 4) recovery is reached in the Middle Triassic (ca. 10 Myr after the event), whereas in the Early Jurassic, marine ecosystems reach the final stage of recovery by the *angulata* Zone of the late Hettangian, ca. 3 Myr after the Late Triassic event (Barras and Twitchett, in review).

Table 1. Palaeoecological model of biotic recovery for shallow marine ecosystems: definitions of recovery stages (modified from Twitchett et al., 2004).

Recovery stage	Palaeoecological characteristics
1	Only the lowest epifaunal and shallowest infaunal tiers are occupied. Trace fossils are typically simple fodinichnia (e.g., *Planolites*) of small (<5 mm) diameter. Shelly fossil faunas typically comprise low-diversity and high-dominance assemblages of small sized animals.
2	Return of domichnia (e.g., *Diplocraterion*) and an increase in depth of infaunal tiering. No significant change in epifaunal tiering. Some increase in evenness of fossil assemblages. Some taxa show size increase.
3	Appearance of higher-tier epifaunal organisms (e.g., crinoids). Return of infaunal crustaceans (indicated by, e.g., *Rhizocorallium*, *Thalassinoides* burrows). Continued increase in evenness and body size. Burrow diameters typically less than 25mm.
4	Return of pre-event low-dominance (high evenness) assemblages and return to pre-extinction burrow and body sizes. Return of highest-tier and deepest-tier organisms. *Thalassinoides* burrows commonly exceed 25 mm in diameter.

Ausich, W. I., Bottjer, D. J., 1982. Science 216, 173-174.

Barras, Twitchett, R. J., in review. Palaeogeography, Palaeoclimatology, Palaeoecology.

Chen, Z. Q., Shi, G. R., Kaiho, K., 2002. Palaeontology 45, 149–164.

Droser, M. L., Bottjer, D. J., Sheehan, P. M., McGhee, G. R., 2000. Geology 28, 675–678.

Erwin, D. H., 1993. The Great Paleozoic Crisis, Columbia University Press, New York, 327pp.

Erwin D. H., 1996. In, D. Jablonski, D. H. Erwin, J. H. Lipps (Eds.), Evolutionary Paleobiology, University of Chicago Press, Chicago, pp. 398-418.

Hallam, A., 1991. Historical Biology 5, 257–262.

Kauffman, E. G., Erwin, D. H., 1995. Geotimes 14, 14-17.

Kirchner, J. W., Weil, A., 2000. Nature 404, 177-180.

Looy, C. V., Twitchett, R. J., Dilcher, D. L., Konijnenburg-Van Cittert, J. H. A., Visscher, H., 2001. Proceedings of the National Academy of Sciences, USA 98, 7879–7883.

Lu, L., Wu, R. S. S., 2000. Marine Biology 136, 291–302.

Smith, A. B., Jeffrey, C. H., 1998. Nature 392, 69-71.

Twitchett, R. J., 1999. Palaeogeography, Palaeoclimatology, Palaeoecology 154, 27–37.

Twitchett, R. J., 2001. Geological Journal 36, 341-353.

Twitchett, R. J., Barras, C. G., 2004. In: D. McIlroy (ed.), The Application of Ichnology to Palaeoenvironmental and Stratigraphic Analysis, Geological Society, London, Special Publications, 228, 397-418.

Twitchett, R. J., Wignall, P. B., 1996. Palaeogeography, Palaeoclimatology, Palaeoecology 124, 137–152.

Twitchett, R. J., Krystyn, L., Baud, A., Wheeley, J. R., Richoz, S., 2004. Geology 32, 805-808.

Urbanek, A., 1993. Historical Biology 7, 29-50.

The Lilliput Effect in the Aftermath of the End-Permian Extinction Event

Richard J. Twitchett[1, 2]

[1] Department of Earth and Planetary Science, University of Tokyo, 7-3-1 Hongo, Tokyo 113-0033, Japan

[2] School of Earth, Ocean and Environmental Sciences, University of Plymouth, Drake Circus, Plymouth, PL4 8AA, UK; rtwitchett@plymouth.ac.uk

One of the most widespread, and yet virtually unstudied, of evolutionary phenomena is the "Lilliput effect". This term, coined by Urbanek (1993), describes the pattern of size change through extinction events: in the aftermath of biotic crises fossil organisms are often much smaller than expected. Body size is a key element in animal evolution. It is a fundamental character of living organisms, with implications for many aspects of an animal's biology, behaviour and ecology (e.g. Cotgreave, 1993). Understanding the causes of the Lilliput effect should provide important insights into the nature of ecological, environmental and biological change during biotic crises (during the extinction itself and the subsequent recovery interval).

Urbanek's (1993) initial observations were on size decrease in Silurian graptolites. Since this study, size decrease in surviving animal taxa (i.e. the Lilliput effect) has been recognised in the aftermath of the major extinction episodes of the Phanerozoic and has been documented in a wide variety of animal groups (e.g. Girard and Renaud, 1996; Jeffery, 2001). There is anecdotal evidence that the phenomenon occurs after smaller scale biotic crises as well, such as in the Early Jurassic (Hallam, 1998), and it is associated with short, sharp warming episodes in the latest Cretaceous (Abramovich and Keller, 2003). It therefore appears to be a factor (the only one?) that is common to all known extinction events.

The Permian-Triassic Lilliput Effect: evidence

One of the most obvious, startling, frustrating and interesting characteristics of Early Triassic fossils is their incredibly small size. Qualitative observations indicate that small body size is a characteristic of all animal groups at this time: benthic, nektonic, invertebrate, vertebrate, marine and terrestrial. The only possible exception is the high latitude otoceratids. In over a decade of collecting from fossiliferous Lower Triassic strata world wide, the author has failed to find a single benthic mollusc or brachiopod with a linear dimension of 100mm or greater, and most specimens are much less than 50mm in size. In general, Olenekian specimens are larger than Induan ones.

Quantitative data support these qualitative observations. For example, Early Triassic gastropods (Fraiser and Bottjer, 2004) and ophiuroids (Twitchett et al., 2005) are significantly smaller than their modern counterparts. Many taxa are also statistically smaller than predecessors from the Carboniferous or Early Permian (unpublished data). Several invertebrate genera, e.g. *Bellerophon* and *Lingula* (Price-Lloyd and Twitchett 2002), show a statistically significant decrease in size through the end-Permian extinction event followed by a subsequent increase in the late Induan. This size reduction in individual taxa from pre-event to immediate post-extinction aftermath is the Lilliput Effect *sensu stricto* of Urbanek (1993). It is not confined to shelly taxa, but is also recorded in the soft-bodied, burrowing infauna as a significant decrease in trace fossil burrow diameters (Twitchett, 1999). Small size relative to much later (e.g. modern) or much earlier (e.g. Carboniferous) times was not considered in Urbanek's (1993) discussions or definition of the Lilliput effect, and herein is termed the Lilliput effect *sensu lato*.

The Permian-Triassic Lilliput effect: possible causes

There are several possible explanations for these observations that can be distinguished from fossil data if rigorous analyses are performed. Key possibilities include:

Selectivity of extinction: a simple explanation for the

Lilliput effect *sensu lato* is that the end-Permian extinction event was selective against large-sized taxa, leaving just the smaller ones behind. The analyses have yet to be performed to test the size selectivity of the end-Permian extinction, but, to date, no other mass extinction event has shown a size selectivity (e.g. Jablonski, 1996) so it would be unexpected. Also, simple size selection could not account for the observations of within lineage size reduction in the survivors (the Lilliput effect *sensu stricto*) demonstrated by Price-Lloyd and Twitchett (2002).

Selectivity of preservation: one other characteristic of the Early Triassic is the poor quality of the fossil record. In all benthic invertebrate groups analysed to date, the Lazarus effect increases dramatically through the Late Permian and into the Early Triassic (e.g. Erwin, 1996). At its peak in the earliest Triassic, the Lazarus effect may typically reach 90% in marine invertebrate groups (i.e. only 10% of the taxa that we know must have been present are recorded as fossils). If the Lazarus effect exhibits a size bias (if large taxa are, for some reason such as rarity, less likely to be fossilised than smaller ones) then this could explain the Lilliput effect *sensu lato*. Such a size bias is possible (c.f. Twitchett 2001) but has ever been tested. However, this explanation would not explain the Lilliput effect *sensu stricto*.

Other preservational aspects that may affect the size range of fossils in an assemblage include taphonomic aspects such as hydrodynamic sorting. However, these factors can easily be taken into account (for example, by comparing pre- and post-even taxa from similar depositional settings; or by collecting and measuring fragmentary specimens as well as complete ones; or by sampling from a number of different localities). Taphonomic factors are not a cause of the Permian-Triassic Lilliput effect.

Facies bias: another potential cause of the observed size changes is the pronounced facies change through the Permian-Triassic interval that is observed in most localities. The dramatic sea level rise at this time means that, in most places, there is a change to deeper water facies in the immediate post-extinction interval. Throughout the geological record, fossil animals preserved in deeper facies are typically smaller than conspecifics in shallower water facies. For autochthonous fauna the reasons may be environmental (e.g. reduction in food supply, temperature, oxygen etc. - see below), whereas for the allochthonous fauna the cause is taphonomic (i.e. hydrodynamic size sorting in more distal tempestites or turbidites). The question of facies bias has not been adequately addressed.

Environmental changes: If the observed Lilliput effect reflects a real ecological response, and is not due to any facies or preservational bias, then the mostly likely cause is some sort of environmental change. Food shortage is one example that has been proposed to explain specific examples of size decrease (e.g. Girard and Renaud, 1996; Urbanek 1993), but other possibilities exist (e.g. Hallam, 1965; Korn, 1995). Three key factors are considered the most likely potential causes of the Permian-Triassic Lilliput effect: (1) increased temperature, (2) decreased food supply, and (3) reduced oxygen levels. Unfortunately, these three environmental changes are all linked: global warming may lead to reduced ocean circulation that, in turn, promotes anoxia and curtails nutrient recycling leading to much lower levels of primary production. In addition, high-resolution temperature records have yet to be constructed for the Permian-Triassic interval and levels of primary productivity are also difficult to quantify.

However, Price-Lloyd and Twitchett's (2002) data concerning the Lilliput effect *sensu stricto* in the lower Werfen Formation of northern Italy show that a return to pre-event size begins prior to any apparent increase in oxygen levels. Also, regional variations in the size of *Claraia* from identical, oxygen-restricted facies may indicate that factors apart from oxygenation are also important. For example, the extremely large size of Griesbachian *Claraia* from the basal Kockatea Shale of western Australia has is probably due to locally enhanced productivity at that site. Higher latitude Griesbachian *Claraia* are generally larger than specimens from lower palaeolatitudes, which suggests that temperature may also have a role (unpublished data).

On the other hand, the Lilliput effect *sensu lato* (i.e. the fact that Early Triassic fossils are far smaller than during earlier or later geological periods) may well be explained by secular changes in oceanic oxygenation (Twitchett, ms in prep.). Globally, small size correlates well with the extent and duration of the Permian-Triassic Superanoxic Event. In addition, there is no known locality where conditions were continuously anoxic or euxinic through the Griesbachian: intervals of anoxia or euxinia alternated with intervals of elevated oxygen levels, which allowed a limited benthos to colonise. If the durations of these oxygenated intervals were shorter in the earliest Griesbachian, but longer in the later Induan, then this could also explain the Lilliput effect. Although short-term alternations on the order of a few years or tens of years are impossible to discern from current geological or geochemical data, data supporting this hypothesis are provided by growth line analysis of Induan *Lingula*. These results show that there is no change in the rate of growth between small, early Griesbachian specimens and larger, late Griesbachian specimens, but simply a difference in longevity (unpublished data). Thus, changes in the duration of the colonisation windows between anoxic intervals may be a cause of the Lilliput effects *sensu stricto*.

Abramovich, S., Keller, G., 2003. Marine Micropalaeontology 48, 225-249

Cotgreave, P., 1993. Trends in Ecology and Evolution 8, 244-248.

Erwin, D. H., 1996. In, D. Jablonski, D.H. Erwin, J.H. Lipps (Eds.), Evolutionary Paleobiology, University of Chicago Press, Chicago, pp. 398-418.

Fraiser, M. L., Bottjer, D. J., 2004. Palaios 19, 259-275.

Girard, C., Renaud, S., 1996. Comptes Rendus de l'Academie des Sciences, Serie IIa 323, 435-442.

Hallam, A., 1965. Palaeontology 8, 132-155.

Hallam, A., 1998. Geobios 30, 921-930.

Jablonski, D., 1996. In, D. Jablonski, D. H. Erwin, J. H. Lipps (Eds.), Evolutionary Paleobiology, University of Chicago Press, Chicago, pp. 256-289.

Jeffery, C.H., 2001. Paleobiology 27, 140-158.

Korn, D., 1995. Lethaia 28, 155-165.

Price-Lloyd, N., Twitchett, R. J., 2002. Geological Society of America Abstracts with Programs 34(6), 355.

Twitchett, R. J., 1999. Palaeogeography, Palaeoclimatology, Palaeoecology 154, 27–37.

Twitchett, R. J., 2001. Geological Journal 36, 341-353.

Twitchett, R. J., Feinberg, J. M., O'Connor, D. D., Alvarez, W., & McCollum, L., 2005. Palaios (in press).

Urbanek, A., 1993. Historical Biology 7, 29-50.

Olenekian Foraminifers of the Gorny Mangyshlak, Eastern Precaucasus and Western Caucasus: Correlation, Paleoecological and Paleobiogeographical Aspects

Valery Ja. Vuks

All Russian Geological Research Institute (VSEGEI), Sredny pr., 74, 199106 St. Petersburg, Russia; valery_vuks@vsegei.ru

The discovery of the Lower Triassic foraminiferal assemblage in the Gorny Mangyshlak allows us to open new region for the distribution of foraminifers in the world. Triassic foraminiferal association of the Gorny Mangyshlak is close to the foraminiferal assemblages of the Western Caucasus and Eastern Precaucasus, but the first one is poor. Triassic deposits of the Western Caucasus and Eastern Precaucasus (south part of Russia) include diverse assemblages of foraminifera therefore this fauna may be used as a standard reference succession for correlating coeval foraminiferal associations in the entire Caucasus region and other regions of the former USSR (for instance: Mangyshlak). Besides, the foraminiferal assemblages of the Western Caucasus and Eastern Precaucasus include more widely distributed species in coeval foraminiferal assemblages of Europe and Asia. Sometimes it allows their use in the interregional correlation. In 1991 the foraminiferal zonation for dividing the Triassic deposits of the Western Caucasus and Eastern Precaucasus was proposed.

The Triassic deposits of the Western Caucasus are presented in the area of North-Western subsidence of the Peredovoy range in the Laba and Belaya River basins. The Triassic occurs with deep erosion on different Paleozoic horizons, and is overlain by the Jurassic with erosion. The lower part of the Triassic deposits in the Western Caucasus is represented by the Tkhach Group. The Tkhach Group is assigned to the Lower-Middle Triassic and is composed of the Yatyrgvarta, Maly Tkhach and Acheshbok Formations. The Maly Tkhach Formation (Lower Anisian) conformably overlies the Yatyrgvarta Formation with local erosion. The Yatyrgvarta Formation correlates with the upper part of the Indian – Olenekian. This Formation is mainly represented by thin-bedded limestones and a basal horizon, which consists of thick-bedded limestones, sandstones and conglomerates. The thickness is about 200-300 m. Ammodiscus minutus local zone is in the upper part of the Yatyrgvarta Formation and indicate a correlation to the Lower Olenekian interval (Meekoceras gracilitatus zone). The bivalves and ammonoids support the Early Olenekian age assignment. The typical species of this local zone are *Ammodiscus minutus* Efim., *Nodosaria hoae skyphica* Efim., *N. orbicamerata* Efim., *N. shablensis* Trif., *Dentalina luperti* Efim., *D. splendida* Schleif. and others. The feature of the taxonomical composition of this assemblage is the domination of diverse representatives of the nodosariids. Foraminifers are very small and have the bad preservation. Besides, the number of radiolarians is more than foraminifers.

In the Eastern Precaucasus the Neftekumsk Formation (Lower Triassic, Lower Olenekian), which conformably overlies the Kumanskaya Formation (Induan? - Lower Olenekian), consists of grey and dark grey limestones with the grey organic-clastic limestone and argillite beds, but in the upper part of this formation there is grey massive bioherm limestones with tuff beds. The thickness is about 900 m. The Early Olenekian age is supported by conodonts: upper part of the Pachycladina-Furnishius beds and lower part of the Neospathodus conservativus beds, which correlate to Meekoceras gracilitatus zone of the Lower Olenekian. In the upper part of this Formation there is the foraminiferal assemblage, which corresponds to the above-mentioned association from the Ammodiscus minutus local zone of the Western Caucasus. The typical species of this foraminiferal assemblage are *Glomospira* aff. *regularis* Lipina, *G. sinensis* (Ho), *Glomospirella facilis* Ho, *Nodosaria hoae skyphica* Efim., *N. orbicamerata* Efim., *N.* cf. *ordinata* Trif., *N.* aff. *piricamerata* Efim., *N. shablensis* Trif., *Dentalina splendida* Schleif. and others. The feature of the taxonomical composition of this assemblage is the domination of the primitive attached agglutinated foraminifers and diverse representatives of the nodosariids.

The Kultayiskaya Formation (Lower Triassic, Lower Olenekian) of the Eastern Precaucasus conformably overlies the Neftekumsk Formation and consists of grey and brown clay limestones. The thickness is about 300 m. The Dem'yanovskaya Formation (Lower Triassic, Upper Olenekian) of the Eastern Precaucasus conformably overlies the Kultayiskaya Formation and represented by dark grey argillites with limestone and siltstone beds. The thickness is about 450 m. In the lower part of the Kultayiskaya Formation there is beds with *Owenites* sp., *Juvenites sinuosus* Kipar., *Paranannites* cf. *gracilis* Kipar., *Parussuria* sp., which correlates to Meekoceras

gracilitatus zone of the Lower Olenekian. Besides, in this Formation there is the conodont assemblage, which corresponds to the Neospathodus conservativus beds. The upper part of this beds correlate to Anasibirites pluriformis zone of the Lower Olenekian. In the upper part of the Dem'yanovskaya Formation there are two ammoniod beds: Columbites parisianus and Procolumbites karataucikus beds, Stacheites undatus beds. These ammoniod beds accordingly correlate to Columbites parisianus zone and Prohungarites crasseplicatus zone of the Upper Olenekian of the Tethyan scale. Moreover, in the lower part of this Formation there is the conodont assemblage, which corresponds to the Neogondolella jubata zone. This conodont zone correlates to the Tirolites cassianus zone of the Upper Olenekian. In the upper part of the Kultayiskaya Formation (?) and Dem'yanovskaya Formation there are the foraminiferal assemblage with characteristic species: *Glomospira sinensis* (Ho), *Verneuilinoides edwardi* Schroed., *Meandrospira pusilla* (Ho), *Dentalina luperti* Efim., *Nodosaria angulocamerata* Efim., *N. hoae skyphica* Efim., *N. ordinata* Trif., *N. piricamerata* Efim., *N. pseudoprimitiva* Efim. The typical feature of the taxonomical composition of this assemblage is the domination diverse representatives of the nodosariids. Nodosariids are very small and have the bad preservation. Moreover, there are of the primitive attached agglutinated foraminifers and representative of the *Meandrospira* genera. This association correlates to the foraminiferal assemblages from the Meandrospira pusilla zone (Western Carpathian, Bulgaria).

The Triassic of the Gorny Mangyshlak conformably overlies Permian and overlain by the Jurassic with erosion. The Tartaly Formation (Lower Triassic, Upper Olenekian) overlies the Dolnapa Formation (Lower Triassic, Induan? - Lower Olenekian) conformably and consists of grey argillites with limestone beds. The thickness is about 500 m. The Karadzhatyk Formation (Lower Triassic, Upper Olenekian) conformably overlies the Tartaly Formation. The Tartaly Formation contains microfossils and fossil fragments of macrofossils. In the Tartaly Formation there are four beds with ammonoids: Dorikranites beds, Kiparisovites beds, Tirolites beds, Columbites beds. The Late Olenekian age of this Formation is dated by ammonoids (Tirolites cassianus and Columbites parisianus zones). Besides ammonoids, the Columbites beds contain abundant recrystallized fossil fragments, microgastropods, ostracods and foraminiferal assemblage. This foraminiferal association is represented by *Tolypammina gregaria* Wendt, *Planiinvoluta* ex gr. *carinata* Leisch., *Nodosaria hoae* (Trif.), *N.* aff. *hoae* (Trif.), *N.* cf. *ordinata* (Trif.), *N. pseudoprimitiva* Efim., *N.* cf. *shablensis* Trif., *N.* sp., "*Frondicularia*" ex gr. *elegantula* K. M.-Maclay, *Lenticulina* sp., *Astacolus* sp. The feature of the taxonomical composition of this assemblage is the domination of the primitive attached foraminifers and diverse representatives of the nodosariids. Foraminifers are very small and have the bad preservation. This foraminiferal assemblage is similar to associations from the Lower Triassic (Olenekian) of the Western Caucasus and Eastern Precaucasus (for instance - foraminiferal association of the Meandrospira pusilla zone).

The foraminiferal zonation of the Western Caucasus and Eastern Precaucasus has several zones which are correlated to the coeval zones of the Carpathians and Balkans. One of them, Meandrospira pusilla zone is established in the Lower Triassic (Olenekian) of the Western Carpathians and Bulgaria, and it is in the Olenekian of the Eastern Precaucasus.

Recently the new samples from the boreholes of the Eastern Precaucasus have studied. Mainly it was samples from the Dem'yanovskaya formation of the Upper Olenekian. The taxonomical composition of the Olenekian foraminiferal assemblage from these samples is close to the coeval associations which were found from other boreholes of these deposits earlier. So, the preliminary results of the definition confirm the taxonomical composition of this Olenekian foraminiferal assemblage. The described assemblage of the Dem'yanovskaya formation and Olenekian foraminiferal associations from the Western Caucasus have several the same species. The genera composition of the defined assemblage of the Western Kazakhstan (Gorny Mangyshlak) is close to the Olenekian assemblages from the Eastern Precaucasus and Western Caucasus, Bulgaria and Western Carpathians. So, there is possibility to correlate the Upper Olenekian deposits of the Gorny Mangyshlak to the coeval deposits of the Eastern Precaucasus and after correspond to the Upper Olenekian of the Bulgaria and Western Carpathians according to foraminifers. The foraminifers from the Gorny Mangyshlak were found with several ammonoids which indicate the age of these deposits as the Upper Olenekian. The foraminiferal assemblages from the Western Caucasus and Eastern Precaucasus were found together ammonoids and conodonts which define the age of these deposits. It is very important point because it allows us precisely correlate the very specific and poor foraminiferal association to the global stratigraphic scale. Thus, the foraminiferal correlation of the Olenekian deposits of the studied regions is supported by macrofauna (ammonoids and conodonts). Consequently, in general it is possible to compare with confidence the Olenekian foraminiferal assemblages of the Gorny Mangyshlak with the Meandrospira pusilla associations of the world (Italy, China and others).

The primitive agglutinated foraminifers and diverse representatives of the nodosariids usually dominate in the Olenekian assemblages of the Gorny Mangyshlak, Western Caucasus, and Eastern Precaucasus. Besides, these associations are not rich and foraminifers are very small and with the bad preservation. Such foraminiferal association usually indicates to the adverse paleoenvironmental situation for development of this fauna. According to the information about the macrofauna in the Upper Olenekian of the Gorny Mangyshlak, it is known that the ammonoid assemblages are more diverse and richer than the bivalve associations. Both types of the biotic assemblages have a lot of the endemic forms. Bivalves and these foraminifers

are benthic fauna, and these biotic associations are poor. Consequently, in this paleobasin on the territory of the Gorny Mangyshlak, it was very specific and adverse conditions on the bottom for the benthic biota. In the Lower Olenekian of the Western Caucasus the planktonic biota (radiolarians) is more diverse than benthic fauna (foraminifers). In the Olenekian of the Eastern Precaucasus there is very similar situation, but the foraminiferal communities are more diverse. So, in the Olenekian time in the paleobasins on the territory from the Western Caucasus to the Gorny Mangyshlak it were the adverse paleoenvironmental situation for development of the benthic fauna, but in the paleobasin on the territory of the Eastern Precaucasus it was better (especially for the Late Olenekian time).

According to the information about the fauna in the Olenekian of the considered regions, it is known that the planktonic assemblages are more diverse and richer than the benthic associations. All types of the biotic assemblages have a lot of the endemic forms. Consequently, in these paleobasins it was very specific and adverse conditions on the bottom for the benthic biota. The Olenekian foraminiferal associations from the Western Caucasus and Eastern Precaucasus are more diverse and richer than the coeval foraminiferal assemblage of the Gorny Mangyshlak, but they are close. Consequently, we can mark that in Olenekian time there was good connection between paleobasins on the territories of the Gorny Mangyshlak, Eastern Precaucasus and Western Caucasus, but the western part of the considered territory has better condition for the fauna development and migration. It is supported by another fauna (ammonoids, conodonts and other). The study of the taxonomic composition of the Olenekian foraminiferal assemblages from the Gorny Mangyshlak, Western Caucasus and Eastern Precaucasus allows us to mark that these communities are close to the foraminiferal associations from the Carpathians and Balkans. Consequently, the paleobasins on these territories have good connections and foraminifers have possibility to migrate between these regions.

Thus, the Olenekian transgression makes the conditions for existence of the different groups of fauna and microfauna on the studied territories. The maximum of the transgression was in the Late Olenekian time and it allows the biota to move to the paleobasins on the territories of the Caucasus and Central Asia (Mangyshlak) and to create the close biotic assemblages on the territory from Caucasus and Gorny Mangyshlak to Europe.

This work was supported by the Peri-Tethys Program, the Cariplo Foundation for Scientific Research and Landau Network-Centro Volta, IGCP 467. The author warmly thanks these organizations and Prof. M. Gaetani, Prof. G. Cassinis, Dr. M. J. Orchard for their support.

Calcimicrobialite after End-Permian Mass Extinction in South China

Wang Yongbiao*, Tong Jinnan, Wang Jiasheng and Zhou Xiugao

Faculty of Earth Science, China University of Geosciences, Wuhan 430074, China;
**wangyb@cug.edu.cn*

Calcimircobialites have widespread distribution in South China. Since the discovery of calcimicrobial mounds and biostromes by Lehrmann (1999) in the area of Bianyang, Guizhou Province, similar sedimentary buildups have been reported from many places in South China, such as in east Sichuan (Stephen et al., 1999), Guangxi, Hubei and Jiangxi.

All the microbialites found in the above areas were produced on the boundary of end-Permian mass extinction, having sharp contact with the underlying foraminifera-calcareous algae wackstone of Late Permian. The foraminifera-calcareous wackstone is rich in Late Permian fossils *Palaeofusulina* sp. and *Collaniella* sp. Occurrence of the PTB index conodont *Hindeodus parvus* in the calcimicrobialites (Lehrmann et al., 2003; Steve et al., 2002) correlate it to the PTB bed, Bed 27 of the Global Stratotype Section at Meishan, Zhejiang Province.

Field work shows that microbialites are mainly located on the reef facies or non-reef facies of extremely shallow carbonate platforms, terminating quickly into deep water facies. This characteristic distribution implies that the microbialites should have very close ecological relations with the reefs or shallow carbonate platforms, which, we think, should have the same ecological effect as reefs.

Calcimicrobialites near the PTB in South China are a succession of carbonate buildup with a thickness of 3-15m generally. Compared with the overlying or underlying layers, calcimicrobialites are particular in structure or geochemical composition. It could be seen clearly in field that microbialites in different areas usually display different types of structures. However, most of the microbialites share very similar fabric. So far as we know, all the microbialites in south China are composed of two kinds of carbonate, micritic matrix and coarse crystal digitates or patches.

The sparry calcite in digitate or patch structures easily remind people of the sparry cement growing in rock cavities during carbonate diagenesis. However, our work shows that the sparry carbonate and micritic matrix have very similar geochemical composition as well as the value of isotope carbon ($d^{13}C$) and oxygen ($d^{18}O$). The isotopic feature of the sparry calcite and micritic matrix support a marine origin, not fresh water travertines.

The fossil assemblage in the microbialites was a microfossil-dominated community accompanied by microgastropods, bivalves and ostracodes. Microbes were the main part as well as the important basis of this com-

munity. So far, two types of microfossils can be identified, chambered and spherical (spheroids) body respectively. The chambered microfossils preliminarily identified as *Renalcis* or *Epiphyton*, a kind of fossil cyanobacteria, mainly occur in the Bianyang section of Guizhou Province. Coccoids are another kind of microfossils, which have been found in Bianyang of Guizhou, east Sichuan, Tiandong of Guangxi and southeast of Hubei. Because cyanobacteria have no rigid original skeletons and external sheaths are often the main part which can be calcified and preserved as fossils, identification of fossil cyanobacteria is mainly based on the morphology and different dimensions. In regard to morphology and dimensions, the coccoid microfossils in the microbialites have some similarities to the spherical individual-cell fossils (*Leptoteichos* sp.) discovered in the Proterozoic stromatolites from Tuanshan Formation, North China (Zhu, 1993), as well as the spherical microbe *Entophysalis* found in modern stromatolites (Horodyski et al., 1975).

Cyanobacteria have experienced a long span of geologic history from Precambrian to present, but its basic shapes remain almost unchanged (Pratt, 1984). So, it was regarded as evolutionary conservative (Mendelson et al., 1982). However, this type of algae often has important environmental implications.

Red tide in modern oceans or algae overgrowth in freshwater lakes resulting from ultrophication is considered as an indicator of environmental deterioration. Wide spread distribution of end-Permian microbialites in South China and even globally on the top of reefs or shallow carbonate platforms may tell some special information.

Acknowledgements The authors thank Cao Ruiji and Dai Yongding for their valuable advices in the identification of microfossils. Yu Youyi provided important support for field work. This work was supported by the National Natural Science Foundation of China (Grant Nos. 40232025, 40325004).

Lehrmann, D. J., 1999. Early Triassic calcimicrobial mounds and biostromes of the Nanpanjiang basin, south China. Geology, 27(4): 359-362.

Stephen, K., Zhang, T. S., Lan, G. Z., 1999. A ?microbialite carbonate crust at the Permian-Triassic boundary in south China, and its palaeoenvironmental significance. Palaeogeography, Palaeoclimatology, Palaeoecology, 146: 1-18.

Lehrmann D. J., Payne, J. L., Felix, S. V. et al., 2003. Permian-Triassic boundary sections from shallow-marine carbonate platforms of the Nanpanjiang Basin, South China: Implications for oceanic conditions associated with the end-Permian extinction and its aftermath. Palaios, 18(2): 138-152.

Steve, K., Guo, L., Swift, A. et al., 2002. ?Microbialites in the Permian-Triassic boundary interval in central China: structure, age and distribution. Facies, 47: 83-90.

Zhu, S. X., 1993. Stromatolites in China (in Chinese). Tianjin University Press, Tianjin. 191-196.

Horodyski, R. J., Vonder Haar, S. P., 1975. Recent calcareous stromatolites from Laguna Mormona (Baja California) Mexico. Journal of Sedimentary Petrology, 45(4): 894-906.

Pratt, B. R., 1984. *Epiphyton* and *Renalcis*-diagenetic microfossils from calcification of coccoid blue-green algae. Journal of Sedimentary Petrology, 54(3): 948-971.

Mendelson, C. V., Schope, J. W., 1982. Proterozoic microfossils from the Sukhaya Tunguska, Shorikha, and Yudoma Formations of the Siberian platform, USSR. Journal of Paleontology, 56(1): 42-83.

The Wuchiapingian-Changhsingian Boundary (Upper Permian) at Meishan of Changxing County, South China

Wang Yue[a], Shen Shuzhong[a], Cao Changqun[a], Wang Wei[a], Charles Henderson[b] and Jin Yugan[a]

[a] Nanjing Institute of Geology and Palaeontology, Chinese Academy of Sciences, 39 East Beijing Road, Nanjing, Jiangsu, China 210008; ywangc@jlonline.com

[b] Departments of Geology and Geophysics, University of Calgary, Calgary, Alberta, Canada T2N 1N4

The Changhsingian represents the second and last stage of the Upper Permian, which is also known as the Lopingian Series. It is officially referred to as an informal chronostratigraphic unit (Remane *et al*., 2000) since formal recognition of this stage boundary has not yet been presented to the International Union of Geological Sciences for ratification. Among the potential candidates for the GSSP of this boundary, Section D at Meishan appears very promising. It not only has historic priority, but is also represented by a fully developed marine sequence with highly diverse faunas and microflora.

Meishan is located between the cities of Nanjing and Shanghai in Changxing County, Zhejiang Province, SE China. Stratigraphic successions of Late Paleozoic and Early Triassic rocks are well exposed and have been extensively studied over the past 25 years. In 2000, the upper part of Section D was ratified by IUGS as the GSSP for the Permian-Triassic boundary (Yin et al., 2001). The lower part of Section D has also been well studied in terms of many fossil groups (Sheng *et al*., 1984), magnetostratigraphy (Li and Wang, 1989), chemostratigraphy (Li, 1998), radiometric dating (Bowring *et al*., 1998; Mundil *et al*., 2001) and sequence stratigraphy (Zhang et al., 1997). In 1981, Zhao et al. (1981) proposed to formally define the base of the Changhsingian Stage at the horizon between the *Clarkina orientalis* Zone and the *C. subcarinata* Zone that is located at the base of Bed 2. They indicated that the base of

this stage is also marked by the occurrence of *Palaeofusulina*, along with the tapashanitid and pseudotirolitid ammonoids. Since the well-defined faunal changes in major fossil groups such as conodonts, brachiopods, ammonoids, corals and fusulinaceans across the boundary (Jin et al., 1997) may be accentuated by the presence of a significant unconformity, effect have been made to look for a suitable boundary a little higher in the section. Wardlaw and Mei (2000) suggested the First Appearance Datum (FAD) of *Clarkina subcarinata* as a marker for the base of the Changhsingian. Later, Mei et al. (2001a, 2001b) found the *C. longicuspidata – C. wangi* lineage in Bed 4, and suggested the FAD of *C. wangi* in the lineage as the lower boundary of the Changhsingian, which is 88 cm above the base of the Changxing Limestone. However, this proposal was disputed by Wang et al. (2001), who believed that there is a depositional gap between the Longtan Formation and the Changxing Limestone as previously suggested by others (Zhu and Zhu, 1984).

Meishan Section C, about 300 m west of Section D, was recently excavated. Detailed studies on the lithology and palaeontology of the boundary strata provide strong evidence for a conformable succession from Wuchiapingian to Changhsingian. A complete evolutionary lineage from *Clarkina orientalis* - *C. longicuspidata – C. wangi* is confirmed at this section and the index fossils of the Changhsingian, *Sinoceltites*, *Tapashanites* and *Palaeofusulina sinensis* are found around the proposed boundary level.

Bowring, S. A., Erwin, D. H., Jin, Y. G., Martin, K. D., Wang, W., 1998. U/Pb zircon geochronology and tempo of the end-Permian mass extinction. Science, 280: 1039-1045.

Jin, Y. G., Wardlaw, B. R., Glenister, B. F., Kotlyar, G. V., 1997. Permian chronostratigraphic subdivisions. Episodes, 20(1): 10-15.

Li, H. M., Wang, J. D., 1989. Magnetostratigraphy of Permo-Triassic boundary section of Meishan of Changxing, Zhejiang. Scientia Sinica, Series B, 32(11): 1401-1408.

Li, Y. C., 1998. Carbon and oxygen isotope stratigraphy of the Upper Permian Changxingian limestone in Meishan Section D, Changxing, Zhejiang. Journal of Stratigraphy, 22(1): 26-34. (in Chinese with English abstract)

Mei, S. L., Henderson, C. M., Cao, C. Q., 2001a. Conodont definition for the base of the Changhsingian Stage, Lopingian Series, Permian. Proceedings of the International Conference on the Global Stratotype of the Permian-Triassic boundary and the Paleozoic-Mesozoic Events, Changxing, Zhejiang, China, 65-67.

Mei, S. L., Henderson, C. M., Wardlaw, B. R., 2001b. Progress on the definition for the base of the Changhsingian. Permophiles, 38: 36-37.

Mundil, R., Metcalfe, I., Ludwig, K. R., Renne, P. R., Oberli, F., Nicoll, R. S., 2001. Timing of the Permian-Triassic biotic crisis: implications from new zircon U/Pb age data (and their limitations). Earth and Planetary Science Letters, 187(1-2): 131-145.

Remane, J., Faure-Muret, A., Odin, G. S., 2000. The International Stratigraphic Chart: The Division of Earth Sciences. UNESCO, 5: 1-14.

Sheng, J. Z., Chen, C. Z., Wang, Y. G., Rui, L. Liao, Z. T., Bando, Y., Ishii, K., Nakazawa, K., Nakamura, K., 1984. Permian-Triassic boundary in middle and eastern Tethys. Journal of the Faculty of Science, Hokkaido University, Series IV, XXI(1): 133-181.

Wang, C. Y., Chen, L. D., Tian, S. G., 2001. A Recommendation: A desirable area and sections for the GSSP of the Changhsingian lower boundary. Permophiles, 39: 9-11.

Wardlaw B. R., Mei, S. L., 2000. Conodont definition for the basal boundary of the Changhsingian Stage. *in* Jin, Y. G. (ed.) Conodont definition on the basal boundary of Lopingian stages: A report from the International Working Group on the Lopingian Series. Permophiles, 36: 39-40.

Yin, H. F., Zhang, K. X., Tong, J. N., Yang, Z. Y., Wu, S. B., 2001. The Global Stratotype Section and Point (GSSP) of the Permian-Triassic Boundary. Episodes, 24(2): 102-114.

Zhang, K. X., Tong, J. N., Yin, H. F., Wu, S. B., 1997. Sequence Stratigraphy of the Permian-Triassic boundary section of Changxing, Zhejiang. Acta Geologica Sinica, 71(1): 90-103.

Zhao, J. K., Sheng, J. Z., Yao, Z. Q., Liang, X. L., Chen, C. Z., Rui, L., Liao, A. T., 1981. The Changhsingian and Permian-Triassic boundary of South China. Bulletin of the Nanjing Institute of Geology and Palaeontology, Academia Sinica, 2: 1-112. (in Chinese)

Zhu, D. S., Zhu, G. P., 1984. It is not the transitional belt of the Changxing Formation and Dalong Formation of the Daxiaowang County. Geology of the Coalfield in Zhejiang, 2: 42-44. (in Chinese)

The Permian-Triassic Time Slice Project of *CHRONOS*: A Progress Report

Bruce R. Wardlaw[1], Vladimir I. Davydov[2] and Peter Sadler[3]

[1] *US Geological Survey, Reston, VA 20192 USA; bwardlaw@usgs.gov*

[2] *Boise State University, Boise, ID 83725 USA; vdavydov@boisestate.edu*

[3] *University of California, Riverside, CA 92521 USA; peter.sadler@ucr.edu*

The Permian-Triassic Time Slice project's goal is to build a better, integrated chronostratigraphic framework to resolve the sequence of events to constrain the causes of the end-Permian catastrophic extinction and track the Triassic recovery. The project is developing data entry tools and techniques through PaleoStrat. PaleoStrat (http://www.PaleoStrat.org) is the sample based data entry and manipulation system for the *CHRONOS* integrated chronostratigraphic database network; part of the NSF funded initiative for Geoinformatics. Details of the projects formation and its international participants can be found on the PaleoStrat or *CHRONOS* website (http://www. Chronos.org).

The Permian-Triassic Time Slice Project covers the interval of the Capitanian (late Guadalupian, Middle Permian), Lopingian (Wuchiapingian and Changhsingian, Late Permian) and Induan (Griesbachian and Dienerian, Early Triassic) and extends from the base of the *Jinogonodolella postserrata* conodont zone to the base of the *Neospathodus waageni* conodont zone (lower Smithian). It covers the time span roughly from 265 Ma to 248 Ma or approximately 17 million years.

Key to developing a refined chronostratigraphy was the creation of a taxonomic dictionary and catalogue, specifically for conodonts, but adequate for all fossil groups. Following the lead of the Biologic Community and the taxonomic database working group of Global Biodiversity Information Facility (GBIF), a taxonomic dictionary is a compilation of holotype information and a catalogue is a comprehensive compendium. In our case the catalogue includes a complete reference citation, original taxonomic description, digital image library of all photographed and some research specimens, and a dynamic, interactive synonymy. Each holotype was entered into ITHUN (International Taxon/Holotype Unique Number), following the Global Unique Indentifier (GUID) concept. This streamlines computer manipulation of fossil data.

Data from 31 of some 50 targeted sections have been compiled for an initial test run of correlation tools. Data include multiple sets of conodont and ammonoid distributions, other fossil distributions, magnetostratigraphy, geochemical signatures, sequence stratigraphy and ages derived from radio-isotopic geochronology. Of primary interest was applying a modified version of Constrained Optimization (CONOP). CONOP9 utilizes first and last appearance and event data in an inversion technique: finding better and better solutions by comparing solutions to the data in an iterative simulated annealing process.

In an example of correlation techniques (fig. 1), we show the correlation of Meishan and Shangshi sections, first drawn by the paleontologist, then graphically correlated based on the same data, then a broader correlation based on existing and new data in an initial CONOP correlation. The disparity in sampling in the Shangshi section (only a few of the new samples have been completed) reduces the correlation to a few intervals in the section. Many more samples have been collected for both conodonts and radio-isotopic geochronology and that data should be available soon. We continue to input data and refine our taxonomy and welcome any new input. We have developed easy-to-use input spreadsheets that can be uploaded to PaleoStrat and the latest versions are available from the website.

PERMO-TRIAS TEST WEIGHTED LEVEL PENALTIES
best penalty- 63.00000 file lists penalties in best order, **descending**

	Events	Radiometric age
	Youngest event	
82	Hindeodus parvus LAD {in 2 sections}	
81	Hindeodus eurypyge LAD {in 2 sections}	
78	Hindeodus priscus LAD {in 2 sections}	
76	Hindeodus praeparvus LAD {in 2 sections}	
75	Volcanic Ash Meishan Bed 36 {in 1 sections}	250.2 Ma
74	Hindeodus typicalis LAD {in 2 sections}	
73	Volcanic Ash Meishan Bed 33 {in 1 sections}	250.4 Ma
72	Hindeodus changxingensis LAD {in 1 sections}	
71	Volcanic Ash Meishan Bed 28 {in 1 sections}	250.7 Ma (**Mundil 252.5 +/- 0.3**)
69	Hindeodus latidentatus LAD {in 2 sections}	
68	Hindeodus parvus FAD {in 2 sections}	**Base of Triassic**
67	Hindeodus praeparvus FAD {in 2 sections}	
66	Hindeodus eurypyge FAD {in 2 sections}	
65	Clarkina meishanensis LAD {in 1 sections}	
64	Hindeodus priscus FAD {in 2 sections}	
63	Clarkina zhejiangensis LAD {in 1 sections}	
62	Clarkina meishanensis FAD {in 1 sections}	
61	Hindeodus changxingensis FAD {in 1 sections}	
60	Clarkina zhejiangensis FAD {in 1 sections}	
59	Volcanic Ash Meishan Bed 25 {in 1 sections}	251.4 Ma (**Mundil > 254.0**)
56	Clarkina yini LAD {in 2 sections}	
55	Clarkina changxingensis LAD {in 2 sections}	
53	Volcanic Ash Shangsi tuff 09 {in 1 sections}	252.5 Ma
52	Volcanic Ash Shangsi tuff 27 {in 1 sections}	253.2 Ma
51	Clarkina parasubcarinata LAD {in 2 sections}	
49	Extinction event {in 2 sections}	
46	Clarkina yini FAD {in 2 sections}	
45	Clarkina obtusus LAD {in 1 sections}	
44	Clarkina zhangi FAD {in 1 sections}	
43	Clarkina deflecta FAD {in 1 sections}	
42	Volcanic Ash Meishan Bed 22 {in 1 sections}	252.3 Ma
39	Hindeodus typicalis FAD {in 2 sections}	
38	C-13 Peak One {in 1 sections}	
37	C-13 Peak Two {in 1 sections}	
36	Clarkina postwangi LAD {in 1 sections}	
35	Clarkina subcarinata LAD {in 1 sections}	
34	Clarkina predeflecta LAD {in 1 sections}	
33	Clarkina obtusus FAD {in 1 sections}	
32	Hindeodus latidentatus FAD {in 2 sections}	
31	Clarkina changxingensis FAD {in 2 sections}	
28	Clarkina postwangi FAD {in 1 sections}	
27	Shangsi tuff 16 {in 1 sections}	253.7 Ma
26	Clarkina prechangxinensis LAD {in 1 sections}	
25	Clarkina prechangxinensis FAD {in 1 sections}	
24	Clarkina wangi LAD {in 2 sections}	
23	Clarkina predeflecta FAD {in 1 sections}	
22	Clarkina subcarinata FAD {in 1 sections}	
19	Meishan Bed 7 {in 1 sections}	253.4 Ma (**254.7+/- 0.2**)
17	Clarkina orientalis LAD {in 2 sections}	
14	Clarkina wangi FAD {in 2 sections}	
12	Clarkina orientalis FAD {in 2 sections}	
11	Meishan Bed 3 {in 1 sections}	**(257.2 +/- 0.7 Ma)**
10	Clarkina guangyuanensis LAD {in 1 sections}	
9	Shangsi tuff 08 {in 1 sections}	257.3 Ma
6	Clarkina guangyuanensis FAD {in 1 sections}	
5	Shangsi tuff 03 {in 1 sections}	259.1 Ma
4	Shangsi tuff 01 {in 1 sections}	260. 8 Ma
3	Clarkina parasubcarinata FAD {in 2 sections}	
	Oldest event	

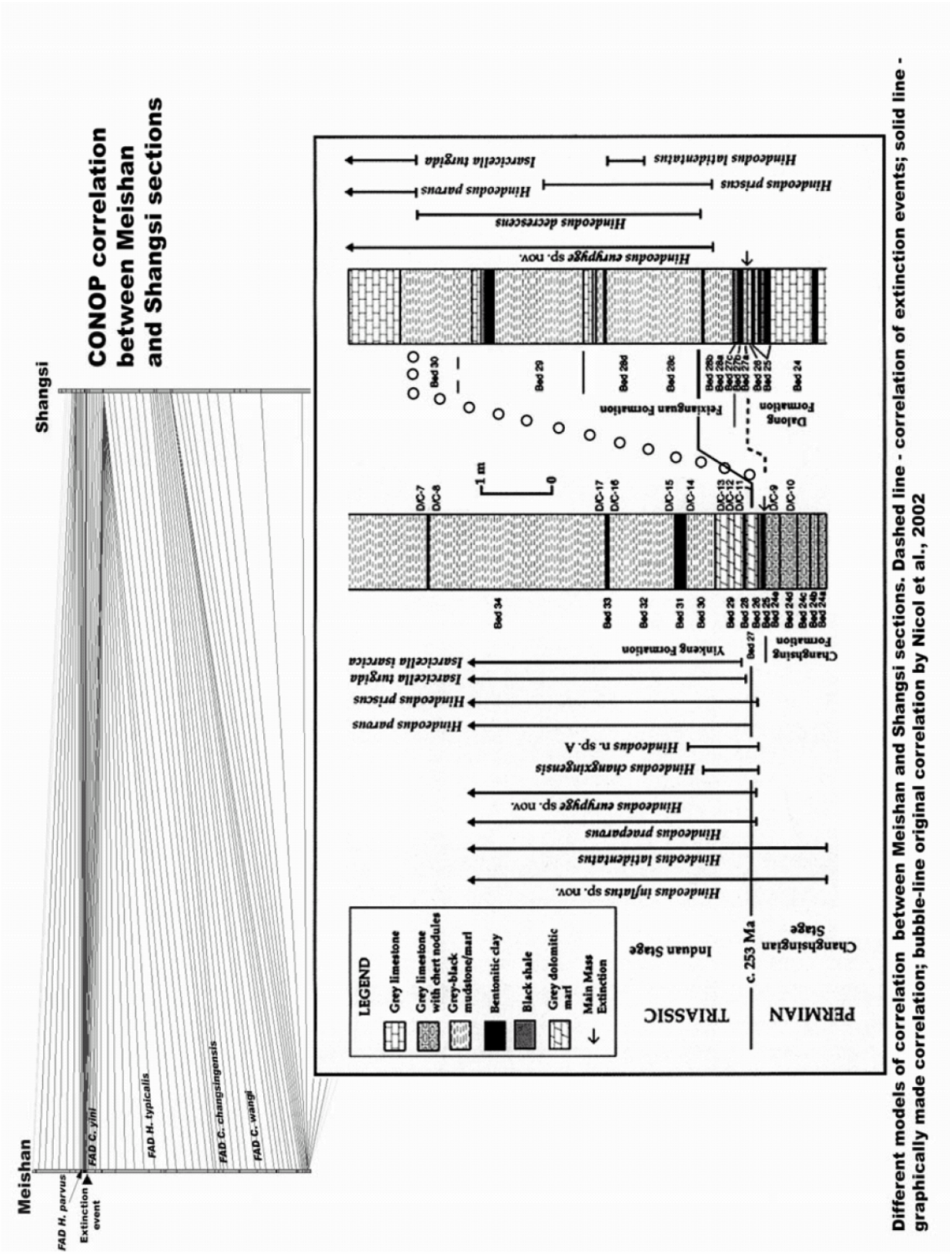

Different models of correlation between Meishan and Shangsi sections. Dashed line - correlation of extinction events; solid line - graphically made correlation; bubble-line original correlation by Nicol et al., 2002

PTB Mass Extinction and Earliest Triassic Recovery Overlooked? A Reinterpretation of Earliest Triassic Microbial Carbonates of the Central European Basin (Germany)

Oliver Weidlich

Royal Holloway, University of London; Egham, Surrey, TW20 0EX, United Kingdom; o.weidlich@gl.rhuk.ac.uk

Introduction – The Central European Permo-Triassic basin represents a land-locked basin with occasional connections to the North Pangea shelf and the Tethys. Earliest Triassic deposits are predominantly siliciclastic; carbonates are restricted to the Bernburg and Calvoerde Formations (Lower Bunter) during Griesbachian and Dinerian. Oolites and microbial carbonates with a variety of textures are the dominant limestone facies. The latter were firstly described by Kalkowsky (1908) and gave rise to the frequently used term "stromatolite". In the field appearance of microbial carbonates is variable, comprising all transitions between domal and encrusting morphotypes. Following the reinvestigations of Paul & Peryt (2000) two different types of microstructures occur, namely spongy-fenestrate or fan-like fabrics.

Oolites exhibit a variety of sediment structures, including horizontal bedding, planar cross bedding, erosion and symmetric oscillation ripples. Sediment texture is variable, ranging from packstone to floatstone, locally with strong bimodality in grain size. Oolite groundmass is heterogeneous with varying percentages of detrital quartz and micas. Ooid types comprise normal ooids, regenerated ooid fragments, superficially incrusted ooid clasts and cerebroid ooids. The latter are regarded to be the result of microbial origin. The cortex of ooids consists of concentric and radial-fibrous microfabrics. Microfabric changes – e.g. from radial-fibrous to concentric - may occur within one single ooid.. The proposed textural and compositional heterogeneities within single ooids as well as within oolites suggest rapid changes of water energy and chemistry over short periods of time. Most likely phases of increased precipitation repeatedly occurred and were subsequently punctuated by non-deposition and erosion.

Invertebrate fossils have not been described yet and no descriptions of skeletal grains from thin sections exist for the carbonates of the Harz area. However, current reinvestigation of microfacies revealed the presence of ostracods and of strongly recrystallized thin shells of likely bivalve origin.

PTB mass extinction overlooked? – After a long-lasting controversy of the depositional environment most scientist agreed that carbonate sedimentation took place in a playa lake environment with variable salinities (see Paul & Peryt (2000) for discussion). A marine genesis was rejected, because of the lack of calcified metazoans. It is noteworthy, however, that published models dealing with

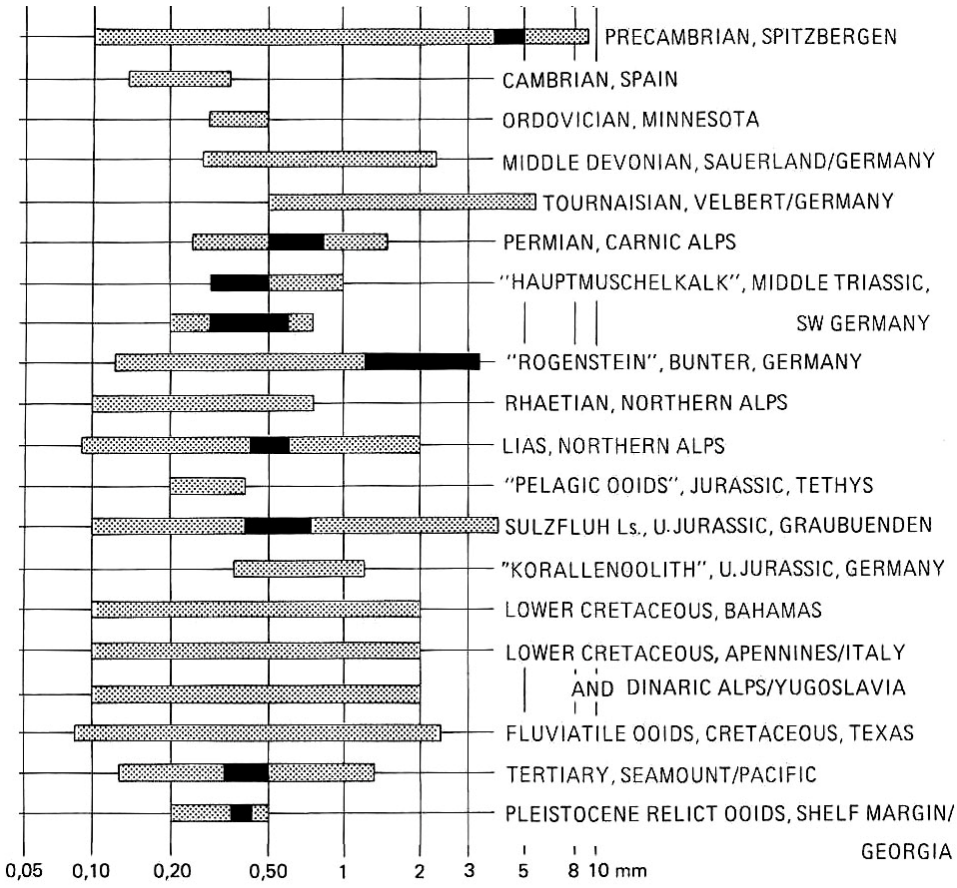

Figure 1. Grain size patterns of Neoproterozoic and Phanerozoic ooids (Flügel, 1982). Note the similarity in the size of Neoproterozoic and earliest Triassic (Lower Bunter) ooids.

the effect of the PTB and the earliest Triassic recovery on calcified metazoans have never been considered for the interpretation of the depositional environment of the enigmatic Lower Bunter.

Reinterpretation of depositional environment – This abstract tries to consider the consequences of the PTB mass extinction for Early Triassic benthic marine carbonate production in the appropriate way and to re-interpret the depositional environment. The following observations from earliest Triassic marine carbonates also apply for the microbial precipitates of the Bunter:

- Microbial carbonates prevailed on global scale in tropical seas while skeletal reefbuilders were absent for up to 7 million years (see Flügel (2002), Weidlich (2002) and Weidlich et al. (2003) for summary).

- Lehrmann et al. (2001) and other authors used the term "anachronistic" carbonate factory for earliest Triassic carbonates from South China because of their striking similarities to Neoproterozoic carbonates. Interestingly, the peak in the size of ooids of the Lower Bunter resembles Precambrian ooids from Spitsbergen (Flügel, 1982: Fig. 19) and differs from Phanerozoic marine and lacustrine ooids, see Fig. 1

- Earliest Triassic bivalve and brachiopod shell beds with low diversity have been repeatedly described from the Tethys and other marine basins (e.g. Boyer et al., 2004). Evidence for recrystallized thin shells trapped in stromatolites or forming nuclei of Lower Bunter ooids has not been used for environmental interpretation.

- Stable carbon and oxygen isotopes of Lower Bunter ooids and stromatolites exhibit trends very similar to the composition of Triassic sea water.

Considering these data a marine environment devoid of calcified benthic invertebrates during the aftermath of a mass extinction is more likely than a playa lake. Measured PTB-sections from East Greenland (Wignall & Twitchett, 2002), the most important seaway connecting the Central Permo-Triassic basin and the North Pangean shelf, document a long-term transgression during the PTB and the earliest Triassic. Most likely relatively cool seawater from polar regions entered the equatorial basin. Increase in water temperature in combination with high water energies and scarcity of calcified metazoans most likely give the rise to rapid and discontinuous carbonate precipitation largely controlled by microbes.

Boyer, D. L., Bottjer, D. J., Droser, M. L., 2004. Ecological Signature of Lower Triassic Shell Beds of the Western United States. Palaios, 19: 372–380.

Flügel, E., 1982. Microfacies analysis of Limestones.. Springer-Verlag, Berlin, 1-633 pp.

Flügel, E., 2002. Triassic reef patterns. *in* Kiessling, W., Flügel, E., Golonka, J. (eds.) Phanerozoic reef patterns. SEPM Spec. Publ., 72: 391-463. SEPM, Tulsa.

Kalkowsky, E., 1908. Oolith und Stromatolith im norddeutschen Buntsandstein. Zeitschrift der deutschen geologischen Gesellschaft, 60: 68-125.

Lehrmann, D. J., Wang, Y., Wei, J., Yu, Y. Y., Xiao, J., 2001. Lower Triassic peritidal cyclic limestone: an example of anachronistic carbonate facies from the Great Bank of Guizhou, Nanpanjiang Basin, Guizhou province, South China. Palaeogeography, Palaeoclimatology, Palaeoecology, 173: 103-123.

Paul, J., Peryt, T. M., 2000. Kalkowsky's stromatolites revisited (Lower Triassic Buntsandstein, Harz Mountains, Germany). Palaeogeography, Palaeoclimatology, Palaeoecology, 161: 435-458.

Weidlich, O., 2002. Middle and Late Permian reefs - distributional patterns and reservoir potential. *in* Kiessling, W., Flügel, E., Golonka, J. (eds.) Phanerozoic reef patterns. SEPM Special Publication, 72: 339-390. SEPM, Tulsa.

Weidlich, O., Kiessling, W., Flügel, E., 2003. The Permian-Triassic boundary interval as a model for forcing marine ecosystem collapse by long-term atmospheric oxygen drop. Geology, 31: 961-964.

Wignall, P. B., Twitchett, R. J., 2002. Permian–Triassic sedimentology of Jameson Land, East Greenland: incised submarine channels in an anoxic basin. Journal of the Geological Society, London, 159: 691-703.

Lower Triassic Seafloor Precipitates from East-central California: Sedimentology and Paleobiological Significance

Adam D. Woods[1], David J. Bottjer[2] and Frank A. Corsetti[2]

[1] Department of Geological Sciences, California State University, Fullerton, 800 N. State College Blvd., Fullerton, CA 92834-6850, USA; awoods@fullerton.edu

[2] Department of Earth Sciences, University of Southern California, Los Angeles, CA 90089-0740, USA

The late Early Triassic (Smithian-Spathian) Union Wash Formation of east-central California, USA, comprised of micritic limestones and calcareous shales and siltstones deposited along the western margin of North America, contains a variety of inorganic calcium carbonate precipitates that appear to have grown directly on the seafloor (Woods et al., 1999). Seafloor precipitates have been documented from the Union Wash Formation at 2 localities that represent distinct depositional environments: 1) Darwin Hills, CA (outer shelf to slope environment); and 2) Union Wash, CA (basinal environment) (Stone et al., 1991; Woods and Bottjer, 2000; Woods et al, 1999). The precipitates are comprised of acicular to bladed, 0.25-0.5mm-thick calcium carbonate crystals that have been replaced by a mosaic of equant low-Mg calcite crystals, suggest-

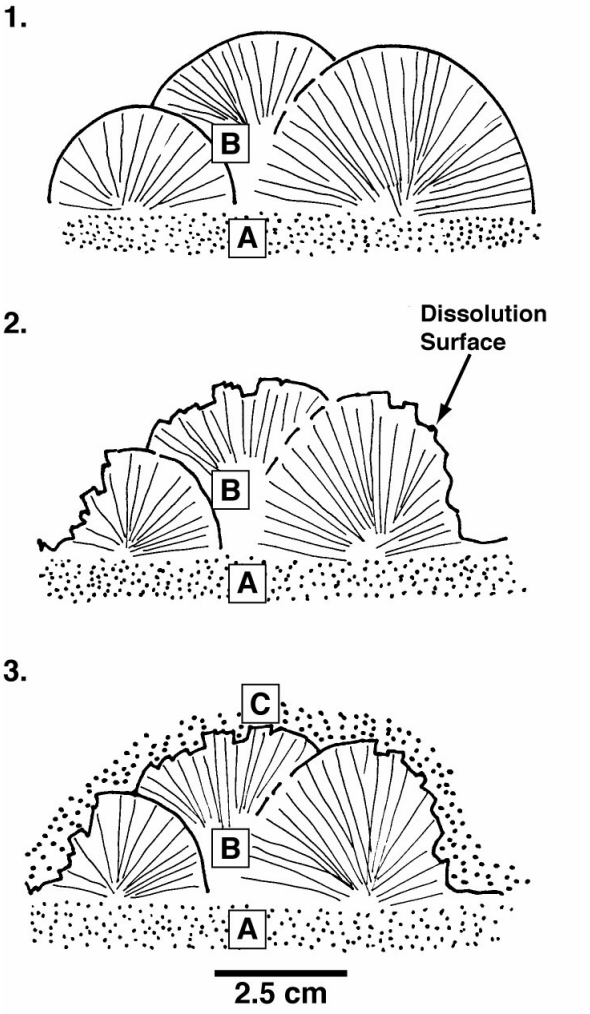

Figure 1. Idealized depositional sequence for precipitates and associated sediments. 1: Growth of precipitates (B) upwards from the seafloor (A). 2: Dissolution of precipitates due to fluctuating bottom water conditions. 3: Deposition of tan siltstone and cessation of precipitate growth. From Woods et al. (1999)

ing either an original aragonite or high-Mg calcite mineralogy (Woods et al., 1999). Precipitate morphology varies from large fans and hemispheres, up to 30 cm across, at the Darwin Hills locality, to laterally extensive crusts (typically < 2 cm thick) at the Union Wash locality. Synsedimentary growth of precipitates on the seafloor is suggested by: 1) lack of evidence of cross-cutting of original sedimentary features; 2) precipitate growth that was nearly parallel to bedding; and 3) calcareous siltstone lenses that appear to have halted precipitation of some crystals while neighboring crystals continued to grow (Woods, et al., 1999).

The 853 m-thick sequence of the Union Wash Formation at Darwin Hills is interpreted to have been deposited in an outer shelf to slope environment based on widespread soft sediment folding, slumping, and synsedimentary brecciation (Stone et al. 1991). Seafloor precipitates occur in the upper member of the Union Wash Formation, and are found within 2 stratigraphic intervals: 1) a lower, 130 m-thick, black micritic limestone interval; and 2) an upper, 30 m-thick gray micritic limestone unit. The two precipitate-bearing units are separated by a 23 m-thick sequence of interfingering tan shale and fossiliferous siltstone. The lower, micritic unit is bedded at a 5 cm-thick scale for the lowermost 50 m, and becomes massive higher in the section (Stone et al., 1991). Precipitates found within the lower, bedded portion of the unit make up approximately 10-20% of the rock, and occur as black, discontinuous bodies, typically 2-3 cm in thickness and 10-20 cm across. The boundary between precipitate masses and surrounding rock is sharp, and the precipitates do not persist into the overlying bed. The precipitate bodies are present as 2 end-members. The first end-member consists of masses of laminated black calcite separated by thin (< 1mm-thick), tan siltstone partings that appear to be laterally continuous into the dark gray micritic limestone that surrounds the masses. Where the calcite laminae are thin (< 5 mm), they are comprised of small (< 0.1mm) crystals with random orientations. Where laminae thickness exceeds about 5 mm, crystal growth appears to become more ordered, with larger (0.25-0.5mm-thick) crystals oriented perpendicular to the seafloor, forming fan shaped, undulating crusts (typically < 1cm thick). The second end-member is comprised of clumps of well-developed hemispheres that commonly form an interlocking mosaic (Figure 1), with lateral and upside-down growth of precipitates into cavities created between adjacent hemispheres. Hemispheres commonly exhibit evidence of dissolution as well as multiple phases of growth. The remaining space between hemispheres is infilled with tan siltstone that is likely turbiditic in origin. Many hemispheres appear to have been overturned, probably by turbidity currents sweeping across the seafloor: the presence of quartz silt and crystal debris between crystals suggests that the precipitates had an open, delicate structure, allowing them to be easily disturbed. The precipitate-bearing unit becomes massive around 50 meters above the base, and precipitate growth is more ubiquitous (comprising up to 75% of the rock). Large (up to 30 cm in radius), well developed precipitate hemispheres are more common in the upper part of the unit. An increase in hemisphere size may imply faster growth rates or may be the result of less frequent smothering of precipitate growth by silt. Solitary hemispheres are rare in this interval; instead, hemispheres typically occur in large clusters that may extend several meters laterally and up to 50 cm vertically. The precipitate clusters exhibit multiple phases of growth, suggesting that new growth preferentially occurred on older precipitate substrates as opposed to nucleating on the seafloor. Interstices between hemispheres within precipitate clusters are typically filled with silty gray micrite or tan siltstone. Precipitates are common throughout the upper portion of the unit, but completely disappear in the overlying shales and siltstones. Precipitates return briefly within the lower 5 m of the upper micritic limestone, occurring as hemispheres, 5-10 cm in height, but disappear above this interval.

Precipitates have also been documented from the Union Wash locality, located 65 km north of Darwin Hills (Woods et al., 1999; Woods and Bottjer, 2000). Deposition of the 773.5 m-thick sequence of calcareous shales and micritic limestone is believed to have occurred in a basinal setting

based on the fine-grained nature of the rock and a general lack of benthic fauna (Stone et al. 1991). Precipitates are found within 4 separate stratigraphic intervals within the middle member of the Union Wash Formation at this locality (Woods and Bottjer, 2000), typically occurring as laterally-continuous (over several meters or more) crusts or layers of calcite crystals that grew perpendicular to the seafloor (precipitate layers are typically < 2 cm-thick). The precipitate layers are commonly interbedded with cm-scale, tan, calcareous siltstone beds, likely deposited by turbidity currents. Some topographic variation appears to be present on the tops of the precipitate layers; however, well-developed fans or hemispheres have not been commonly observed at this locality. Growth as layers, as opposed to fans or hemispheres, suggests that oceanographic conditions differed between the Union Wash and Darwin Hills localities. Alternatively, the substrate at Union Wash may have been more suited for crystal growth over laterally extensive areas as opposed encouraging growth from nucleation points, which would lead to the formation of fans and hemispheres.

Precipitate growth is believed to be the result of unusual environmental conditions during the Early Triassic. Widespread anoxia and euxinia in the global oceans during the period are thought to have led to sulfate reduction of organic matter and the concomitant buildup of carbon dioxide in the deep ocean (Knoll et al., 1996; Woods et al., 1999). Upon mixing of anoxic, alkaline deep water with oxygenated surface waters, carbon dioxide degassing occurred, leading to supersaturation with respect to calcium carbonate and formation of seafloor precipitates. Growth of multiple precipitate layers at the Darwin Hills locality suggests that this process might not have been constant, but instead varied over time, becoming weaker or stronger, and perhaps even disappearing, as precipitates sometimes exhibit evidence of dissolution (Figure 1; Woods et al., 1999).

Strontium isotope stratigraphy demonstrates that the precipitate-bearing unit at the Darwin Hills locality correlates precisely with a widespread stromatolite occurrence from the Virgin Limestone of the Moenkopi Formation, the onshore equivalent to the Union Wash Formation (Corsetti, 2004). Stromatolites and seafloor fans are more common in Early Triassic strata than in the immediately preceding or succeeding strata. It seems possible that stromatolite growth during the Early Triassic may have been enhanced by the oceanographic phenomena that led to deposition of the inorganic seafloor precipitates, as the formation of both structures are ultimately linked to calcium carbonate supersaturation. Widespread stromatolite occurrences may have been fostered by persistent stressful environmental conditions that suppressed metazoan grazers and burrowers (Pruss and Bottjer 2004; also see below) and may have been further augmented by conditions favorable to widespread calcium carbonate precipitation.

The occurrence of inorganic calcium carbonate precipitates may signify increased levels of CO_2 in surface waters and the impingement of anoxic waters onto the continental shelf during the period (Woods, et al., 1999). Such conditions would have been stressful to marine biota, and may have acted to suppress biotic recovery from the Permian-Triassic mass extinction (*senso* Hallam, 1991). Wignall et al. (1998) note that the recovery from the Permian-Triassic crisis appears to commence earlier at high latitudes, and this observation suggests that the timing of the onset of the recovery may have been directly related to the retreat of stressful conditions; in those areas where environmental stresses persisted, the recovery was put on hold until they disappeared. Indeed, evidence from western North America supports this hypothesis: the Union Wash Formation contains the only known occurrence of inorganic seafloor precipitates from western Pangea; examination of laterally-equivalent North American strata (Dinwoody Formation and Thaynes Formation of southeastern Idaho, northwestern Nevada, eastern Wyoming and southwestern Montana, USA in addition to Lower Triassic rocks of the Western Canada Sedimentary Basin) has not revealed additional precipitate occurrences. Paleocommunities from the western United States remained in a post-extinction "mode" (i.e., low diversity, low complexity, dominated by generalists; Schubert and Bottjer, 1995) for the entire length of the Early Triassic while high-latitude paleocommunities in Spitsbergen (Wignall et al. 1998) and western Canada (C. M. Henderson and J. P. Zonneveld, pers. comm., 2004) recovered much sooner. Therefore, it appears that stressful environmental conditions played a strong role in determining the timing and shape of biotic recovery from the Permian-Triassic mass extinction.

Corsetti, F. A., 2004. Did enhanced lithification play a role in the Proliferation of Early Triassic stromatolites? A case study from the Virgin Limestone Member, Moenkopi Formation, western Nevada. Geological Society of America Abstracts with Programs, 36(5): 182.

Hallam, A., 1991. Why was there a delayed radiation after the end-Paleozoic extinctions? Historical Biology, 5: 257-262.

Knoll, A. H., Bambach, R. K., Canfield, D. E., Grotzinger, J. P., 1996. Comparative Earth history and the Late Permian mass extinction. Science, 273: 452-457.

Pruss, S. B., Bottjer, D. J., 2004. Late Early Triassic microbial reefs of the western United States; a description and model for their deposition in the aftermath of the end-Permian mass extinction. Palaeogeography, Palaeoclimatology, Palaeoecology, 211: 127-137.

Schubert, J. K., Bottjer, D. J., 1995. Aftermath of the Permian-Triassic mass extinction event: paleoecology of Lower Triassic carbonates in the western USA. Palaeogeography, Palaeoclimatology, Palaeoecology, 116: 1-39.

Stone, P., Stevens, C. H., Orchard, M. J., 1991. Stratigraphy of the Lower and Middle(?) Triassic Union Wash Formation, East-Central California. U.S.G.S. Bulletin 1928, Washington, D. C., 26 p.

Wignall, P. B., Morante, R., Newton, R., 1998. The Permo-Triassic transition in Spitsbergen: $\delta^{13}C_{org}$ chemostratigraphy, Fe and S geochemistry, facies, fauna, and trace fossils. Geological Magazine, 135: 47-62.

Woods, A. D., Bottjer, D. J., Mutti, M., Morrison, J., 1999. Lower Triassic large sea-floor carbonate cements: Their origin and a mechanism for the prolonged biotic recovery from the end-Permian mass extinction. Geology, 27: 645-648.

Woods, A. D., Bottjer, D. J., 2000. Distribution of ammonoids in the Lower Triassic Union Wash Formation (eastern California): Evidence for paleoceanographic conditions during recovery from the end-Permian mass extinction. PALAIOS, 15: 535-545.

Lower Triassic Bivalve Sequence of Chaohu, Anhui Province

Wu Shunbao, Li Zhiming, Guo Gang and Tong Jinnan*

*China University of Geosciences, Wuhan 430074, China; *jntong@cug.edu.cn*

10 genera and 25 species of bivalves are collected and identified from the Lower Triassic of Chaohu, Anhui Province in southeastern China. The bivalves are distributed throughout the Lower Triassic though they are much more common in the lower part, especially in mudrock and marl. In the upper Lower Triassic dominated by thick-bedded limestone they enrich some thin intercalated beds of shale. As in most areas of South China, the Lower Triassic bivalve assemblages are predominated by genera *Claraia* and *Eumorphotis*. However, *Claraia* dominates in the lower Induan Stage and *Claraia griesbachi*, *C. concentrica* and *C. hubeiensis* are the common forms in Chaohu. These species are characterized by a concentric sculpture. *Claraia radialis* with weak radial ornaments co-occurs occasionally. *Eumorphotis* is much commoner in the upper Induan and lower Olenekian and *E. inaequicostata* and *E. huancangensis* are the main species in Chaohu. In the middle and upper Olenekian *Claraia* and *Eumorphotis* become scarce and only very few *Claraia hubeiensis*, *Eumorphotis dafangensis* and *E. hinnitidea* are recognized, while *Guichiella* and *Periclaraia* enrich some beds in the middle and upper Olenekian.

Claraia and *Eumorphotis* are cosmopolitans and the commonest bivalves in the Lower Triassic of South China. They are characteristic disasters in the aftermath of the end-Permian mass extinction. *Posidonia* is a typical opportunistic form with small-sized shells in the Lower Triassic of Chaohu. They cluster in some beds of dark-colored shale or thin-bedded calcareous mudrock containing numerous fine grains of pyrite in the Olenekian, indicating a reductive condition. Both *Guichiella* and *Periclaraia* are endemic in Chaohu and its neighboring areas. Two species are recognized in *Guichiella*, *G. angulata* and *G. styliformis* and they are usually found in the lower Olenekian. *Periclaraia* has only one species, *P. circularis*, observed in Chaohu and it is yielded in the upper Olenekian.

Therefore, the Lower Triassic bivalve sequence is clear in Chaohu as follows:

***Periclaraia circularis* Zone**: corresponding with ammonoid *Subcolumbites* Zone and conodont *Neospathodus anhuiensis* Zone in the upper Olenekian (upper Spathian);

***Guichiella* Zone**: corresponding with ammonoid *Columbites—Tirolites* Zone and conodont *Neospathodus* sp. M Zone—*N. homeri* Zone in the middle Olenekian (lower Spathian);

***Eumorphotis inaequicostata-E. huancangensis* Zone**: corresponding with ammonoid *Gyronites—Prionolobus* Zone—*Flemingites-Euflemingites* Zone—*Anasibirites* Zone and conodont *Neospathodus* Zone—*N. kummeli* Zone—*N. waageni* Zone in the upper Induan (Dienerian) and lower Olenekian (Smithian);

***Claraia griesbachi-C. concentrica* Zone**: corresponding with ammonoid *Ophiceras—Lytophiceras* Zone and conodont upper *Hindeodus typicalis* Zone—*Neogondolella krystyni—N. planata* Zone in the lower Induan (Griesbachian).

Conodont Evolution During Permian-Triassic Transition in Mid-Low Latitudes: A Close-Up View

Wu Ya-Sheng

Institute of Geology and Geophysics, Chinese Academy of Science, Beijing 100029; wys@mail.igcas.ac.cn

During the Late Permian Lepinigian, three distinct conodont provinces had developed, referred to as the North Cool Water Province, the Equatorial Warm Water Province, and the Peri-Gondwana Cool Water Province (Mei et al., 2002). We found that conodonts of different provinces had different evolutionary trends during the Permian-Triassic transition. In this paper we discuss only the P-T transitional evolution of the conodonts in the Equatorial Warm Water Province, as exemplified by the Meishan sections (including Sections D, Z, A, B, C, E, F, AW) in Zhejiang province, east China, Shangsi section, in Sichuan province, south China, and the Kashmir section at Guryul Ravine, Kashmir.

Previous studies of Permian-Triassic conodont evolution are performed on time frame as large as geological time unit "Stage". In this paper P-T boundary conodont evolution is analyzed on time frame of litho-beds, with very much higher resolution. The P-T transition of Meishan section has been divided as litho-beds: 24e, 25, 26, 27a-

27b, 27c-27d, 28, in ascending order. Yin et al. (2001) divided them as 5 conodont faunas: 24e belonging to *Clarkina changxingensis yini* zone, 25 and 26 to *C. meishanensis* zone, 27a-27b to *Hindeodus typicalis* zone, 27c-27d to *H. parvus* zone, and 28 to *Isarcicella isarcica* zone.

We found that in previous document many conodonts from these sections were incorrectly identified, which would lead to incorrect understanding on conodont evolution during the P-T transition. We checked all conodonts which have been described from Meishan sections, Shangsi section and Kashmir section by previous researchers (e.g., Wang, 1995; Zhang et al., 1995, 1996; Li et al., 1989; Matsuda, 1981), and corrected those which have been incorrectly identified.

According to the revised conodont fauna composition, we revised the conodont zone division for the P-T transition. After revision, Bed 24e and 25 belong to *Clarkina yini* zone, 26 to *C. meishanensis* zone, 27a-b to *Hindeodus changxingensis* zone, 27c-d to *H. parvus* zone, and 28 to *I. staeschei* zone.

Based on the stratigraphic distribution of the revised conodonts, the followings evolutionary trends are found:

(1) From Beds 24e to 26, conodont fauna continued to develop, and the species diversity increased gradually; there was no mass extinction for conodonts during Beds 24 to 25;

(2) A mass extinction for conodonts occurred at between Beds 26 and 27a, where 83% of conodont species of Bed 26 disappeared;

(3) The conodonts of Bed 26 are mainly *Clarkina* components, except for one *Hindeodus* components, while the conodonts of Bed 27a are mainly *Hindeodus* components; only *C. paradeflecta* and *H. inflatus* lasted from 24e to 27a-b;

(4) The conodonts of Bed 27a are similar to those of Bed 27b;

(5) The conodonts with very large cusp occurred in Bed 27c, and the conodonts of Bed 27c had much higher species diversity than Bed 27b;

(6) The conodonts of Bed 27d mostly disappeared at between Beds 27d and 28; the conodonts of Bed 28 were new species, and components of *Isarcicella* and *Neospathodus* occurred in bed 28.

Then, three biotic boundaries of different scales formed in conodont evolution. The first one lies between Beds26 and 27a, of the largest scale, defined by the replacement of the *Clarkina*-dominated conodont fauna of Bed 26 by the *Hindeodus*-dominated conodont fauna of Bed 27a. The second boundary lies at between Bed 27b and Bed 27c, marked by the appearance of conodonts with very big (wider than denticles by more than 2~3 times) cusp. The third boundary lies at between Bed 27d and Bed 28, characterized by disappearance of most *Hindeodus* components of Bed 27d and appearance of *Isarcicella* and *Neospathodus* components in Bed 28.

The mass extinctions of many other marine groups occurred at between Beds 24e and 25, while conodonts had their mass extinctions much later, which probably indicates that it was caused by some more ruinous catastrophic events.

Acknowledgement: This study is supported by National Natural Scientific Foundation of China (Project Nos. 40172007 and 40472015)

Clark, D. J., Wang Chengyuan, Orth, C. J., Gilmore, J. S., 1986. Conodont survival and low Iridium abundances across the Permian-Triassic boundary in South China. Science, 233: 984-986.

Matsuda, T., 1981. Early Triassic conodonts from Kashmir, India, Part 1, *Hindeodus* and *Isarcicella*. Journal of Geosciences, Osaka City University 24(3): 75–108.

Mei, Shilong, Henderson, C. M., 2002. Evolution of Permian conodont provincialism and its significance in global correlation and paleoclimate implication. Palaeogeography, Palaeoclimatology, Palaeoecology, 180(1-3): 57-91.

Mei Shilong, Zhang Kexin, Wardlaw, B. R., 1998. A refined succession of Changhsingian and Griesbachian neogondolellid conodonts from the Meishan section, candidate of the global stratotype section and point of the Permian-Triassic boundary. Palaeogeography, paleoclimatology, Paleoecology 143: 213-226.

Nicoll, R. S., Metcalfe, I., Wang Chengyuan, 2002. New species of the conodont Genus *Hindeodus* and the conodont biostratigraphy of Permian-Triassic boundary interval. Journal of Asian Earth Sciences 20: 609-631.

Wang Chengyuan, 1995. Conodonts of Permian-Triassic boundary beds and biostratigraphic boundary. Acta Palaeontologica Sinica 34 (2),129-151.

Yin Hongfu, Zhang Kexin, Tong Jinnan, Yang Zunyi, Wu Shunbao, 2001. The Global Stratotype Section and Point (GSSP) of the Permian–Triassic Boundary. Episodes, 24(2): 102–114.

Chemical Composition of Seawater and Biotic Crisis Around the Paleozoic – Mesozoic Transition (PMT)

Yan Jiaxin

Faculty of Earth Sciences, China University of Geosciences, Wuhan 430074, P R China; jxyan@cug.edu.cn

Until the Mid-1990's it has been a common assumption of many sedimentologists that the major-ion chemistry of the global ocean has remained close to its present-day composition during the Phanerozoic. This classic concept conflicted with records of secular variations in the pre-

liminary mineralogy of marine carbonates and evaporites. Recent research suggests that major-ion composition of seawater changed significantly during the Phanerozoic. These secular variations in seawater composition, particularly with respect to Mg/Ca ratios driven mainly by changes in the spreading rates along mid-ocean ridges, govern synchronized oscillations in the mineralogical composition of potash evaporates and marine nonskeletal carbonate components, which correlate with previously proposed calcite and aragonite seas. It is also demonstrated that the secular variation in the Mg/Ca ratio of seawater has not only controlled Phanerozoic oscillations in hypercalcification by simple taxa, such as calcareous nannoplankton, sponges, and bryozoans, but has strongly influenced their skeletal evolution.

The mass extinction at the PTB constitutes the most devastating biotic crisis of the Phanerozoic, and punctuated the transition from Paleozoic to Mesozoic life. It seems unlikely that a change in the Mg/Ca ratio of seawater could contribute to such a sudden biotic change.

Nevertheless, following phenomena are worthy of attention. 1) The end-Permian mass extinction consists of two phases: end-Guadalupian and end-Changhsingian. Even for the end-Changhsingian phase, two extinctions were still hold by some researchers; 2) Severely influenced fauna around the transition were those with skeleton of (low-Mg) calcite. Most of them gradually reduced before its extinction at the PTB. For example, massive Wentzelellinae disappeared first in the Maokouan, followed by massive Waagenophyllinae and solitary forms. Fasciculate Waagenophyllinae and simple, non-dissepimented solitary rugosal corals survived to the latest Permian in South China. Such an extinction pattern of Rugosa reminds us of the "evolutionary osteoporosis" and subsequent extinction of Cenozoic *Discoaster*. Relatively slight affect was recorded for the genera with aragonite skeleton.

The recovery and radiation process after the PTB mass extinction last about 10 Ma, by no means a sudden process. Available data indicate that recovery firstly occurs in bivalves, ammonoids and gastropods, following by brachiopods, foraminifers and bryozoans. This pattern of recovery, calcite skeleton after aragonite skeleton, seems reflecting the decrease of Mg/Ca ratio of seawater after the PTB. That is fauna with skeleton of aragonite recovered first while the Mg/Ca ratio of seawater was relatively high, followed by fauna with skeleton of calcite as the Mg/Ca ratio falling.

Undoubtedly, comprehensive studies on the PMT will shed light not only on the chemical evolution of seawater, but also on the cause and process of the most devastating biotic crisis of the Phanerozoic.

Mid-Latitude Continental Climatic Variability Recorded in Permo-Triassic Fluvial-Lacustrine Sedimentary Rocks, Bogda Mountains, Northwestern China

Yang Wan[1], Liu Yiqun[2], Feng Qiao[2], Lin Jinyan[2] and Zhou Dingwu[2]

[1] Department of Geology, Wichita State University, Wichita, Kansas 67226, U.S.A; wan.yang@wichita.edu

[2] Department of Geology, Northwestern University, Xian, 710069, China

Mid-latitude continental climate variability is critical to understanding Pangean climate evolution and causes of end-Permian mass extinction. A 1209-m Permo-Triassic fluvial-lacustrine section in southern Bogda Mountains, NW China, measured at a cm-dm scale, was deposited in a rift-drift setting on the Junggar microplate at 45°N paleolatitude. Lithofacies, paleosols, fauna and flora, cycle stacking patterns, and TOC (total organic carbon) and type of organic matter were used in preliminary climate interpretation. Lower-Permian Taoxigou Group (328 m) consists of orthoconglomerate, sandstone, and non-calcareous paleosols, interpreted as braided stream deposits in a tectonically-active, sub-humid environment. Minor lacustrine limestones suggest periods of semi-arid conditions. Middle-Permian Daheyan Formation (104 m) contains similar facies but with upward-increasing Calcisols, suggesting a transition to a semi-arid strong-seasonality climate. This condition persisted upward, as indicated by lacustrine cycles composed of littoral sandstone, profundal organic-rich shale, limestone, and dolomitic shale of the Middle-Permian Luocaogou Formation (159 m) and abundant palustrine limestones and Calcisols of the Hongyanchi Formation (118 m). The condition culminated at base of Quanzhijie Formation (75 m, end-Guadalupian). Afterward, climate changed abruptly to sub-humid to humid with weak seasonality in Upper-Permian Quanzhijie, Wutonggou, and Guodiken formations (125 and 138 m, respectively), as indicated by abundant deltaic and meandering stream deposits containing highly-eluviated and oxidized Argillisols, hydromorphic paleosols, and coals. The sub-humid to humid conditions persisted into Lower-Triassic Jiuchaiyuan and Shaofanggou formations (116 and 46 m, respectively), without significant climatic changes across the Permo-Triassic boundary. Two higher-order climate fluctuations at a scale of 1-10s m also occur throughout the section.

In summary, the absence of abrupt climatic changes across Permo-Triassic boundary suggests that continental climate change was not a major cause of end-Permian terrestrial mass extinction.

Research on Conodont Biostratigraphy and Age Determination of the Lower-Middle Triassic Boundary in Southern Part of Guizhou Province, China

Yao Jianxin[1], Ji Zhansheng[1], Wang Yanbin[1], Liu Dunyi[1], Wang Liting[2] and Wu Guichun[1]

[1] Institute of Geology, Chinese Academy of Geological Sciences, Beijing 100037, China; yaojianin@ccsd.org.cn

[2] Bureau of Geological and Mineral Resources Survey of Guizhou Province, Guiyang 550004, China

The demarcation of the Lower-Middle Triassic boundary is a disputed problem in the stratigraphic research in the world (Yin Hongfu, 2000). Lower-Middle Triassic strata of different types, from platform facies to basin facies, are well developed in Southwest China. This is favorable for the research on Global Stratotype Section and Point (GSSP). According to research on conodonts in Ganheqiao section of Wangmo County and Qingyan section of Guiyang City, Guizhou Province, six conodont zones, which can be correlated with those in other regions, can be recognized (Fig. 1 and Fig. 2). They are in ascending order as follows: 1. *Neospathdus cristagalli* Interval-Zone; 2. *Neospathodus pakistanensis* Interval-Zone; 3. *Neospathodus waageni* Interval-Zone; 4. *Neospathodus homeri—N. triangularis* Assemblage-Zone; 5. *Chiosella timorensis* Interval-Zone; 6. *Neogongdolella regalis* Range-Zone. An evolutionary series of Early-Middle Triassic conodont *Neospathodus-Chiosella-Neogongdolella* (Bender, 1970; Kozur, 1989) occurs in the Ganheqiao section and Qingyan section. In this evolutionary series, intermediate type *Neospathodus qingyanensis* appears between *Neospathodus homeri* and *Chiosella timorensis,* in upper part of *Neospathodus homeri—N. triangularis* Zone. This shows an excellent evolutionary series of Early-Middle Triassic conodonts across the Lower-Middle Triassic boundary. The Lower-Middle Triassic boundary is located 1.5m below the top of Ziyun Formation, where *Chiosella timorensis* Zone first appears in the Qingyan section; while the Lower-Middle Triassic boundary is situated 0.5 m below the top of Ziyun Formation, where *Chiosella timorensis* Zone first appears in the Ganheqiao section.

The 5 m Lower-Middle Triassic boundary glassy tuff bed is located 0.5 m above the location where *Chiosella timorensis* Zone first appears at the Ganheqiao section. Zircons of the boundary glassy tuff from the Ganheqiao section have been analyzed using the SHRIMP ionprobe (Wang Yanbin et al., 2004). The zircons from the boundary glassy tuff in the Ganheqiao section have a weighted mean $^{206}Pb/^{238}U$ age of 239.0±2.9 Ma (2s) (Fig. 3 and Fig.

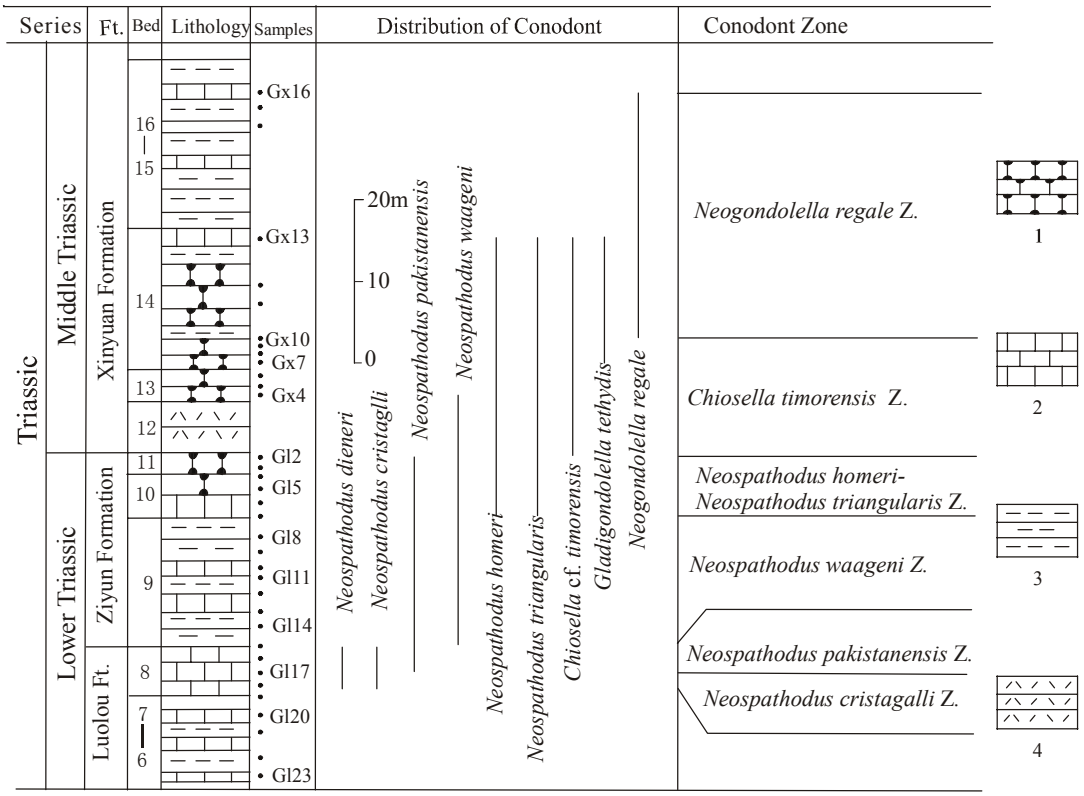

Figure 1. Range chart of important conodonts of the Lower Triassic and the lower part of the Middle Triassic at Ganheqiao section of Wangmo county, Guizhou province.
1. siliceous concretion limestone, 2. limestone, 3. mudstone, 4. vitric tuff

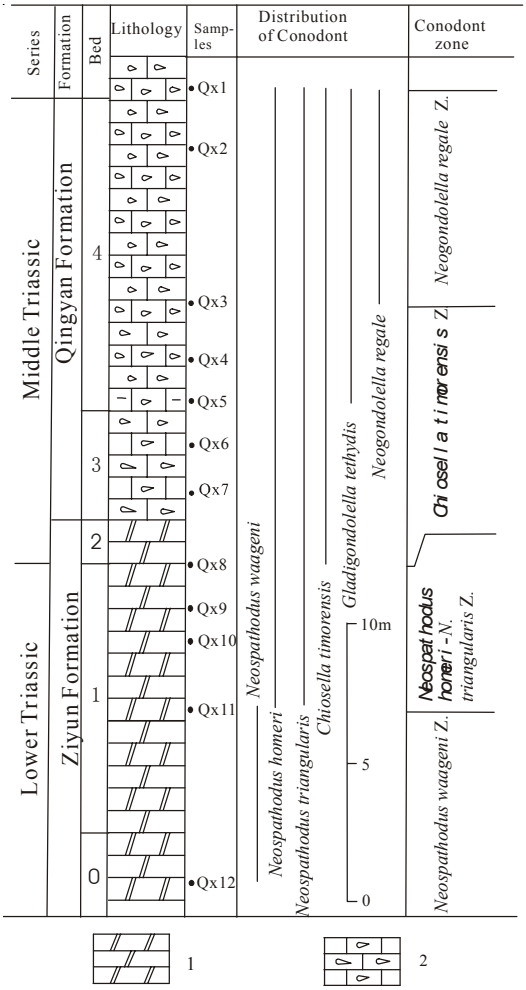

Figure 2. Range Chart of important conodonts of the upper part of the Lower Triassic and the lower part of the Middle Triassic at Qingyan section of Guiyang city, Guizhou Province. 1. brecciola, 2. dolomitic limestone

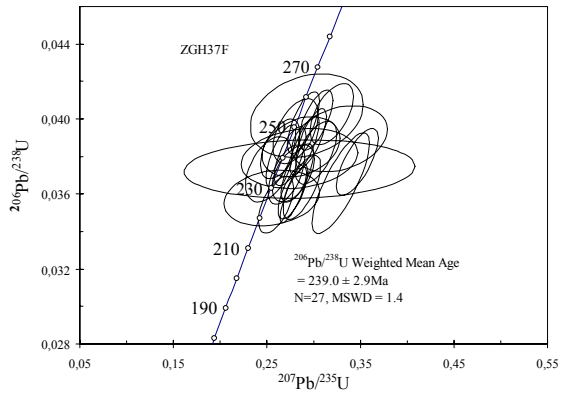

Figure 3. U-Pb Weatherill concordia diagrams showing SHRIMP data for ZGH37F sample

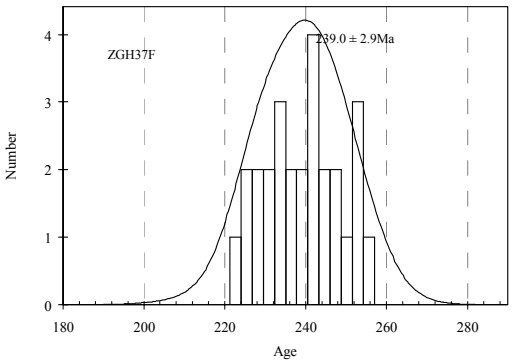

Figure 4. Cumulative probability plot of measured $^{206}Pb/^{238}U$ ages of glassy tuff sample zircons. Weighted by data point error mean age is 239.0±2.9Ma (95% CI), MSWD=1.

4). This is the direct constraint on the zircon U-Pb age of the Lower-Middle Triassic boundary. The SHRIMP zircon $^{206}Pb/^{238}U$ age is the same as the isochron age of 238.9±4.8 Ma obtained by $^{40}Ar/^{39}Ar$ dating of glassy tuff polished sections (Hu Shiling et al., 1996). This zircon U-Pb ages is accurate and comparable with other well-measured Phanerozoic ages. This age is interpreted as the age of eruption of the volcanic ash. Owing to the unique biostratigraphic position of the volcanic layer, the age of the boundary is exactly the age of the glassy tuff and thus extrapolation is not necessary.

Based on above-mentioned, authors suggest that the Ganheqiao and Qingyan sections are excellent sections regarded as a reference section of GSSP of the Lower-Middle Triassic boundary to compliment the Olenekian-Anisian boundary to be designated at the Desli Caira, Romanian for further necessary investigation.

Bender, H., 1970. Zur Gliederung der Mediterranen Trias II. Die Conodontenchronologie der Mediterranen Trias. Ann. Geol. Pavs Hell, 19: 465-540.

Hu Shiling, Li Yuejun, Dai Dongmo, Pu Zhiping,1996. The Laser mass-spectrometer ^{40}Ar-^{39}Ar age of green pisolites of Guizhou Province. Acta Petrologica Sinica, 12(3): 409-415.

Kozur, H., 1989. The taxonomy of the Gondolellid conodonts in the Permian and Triassic. Courier Forsch. Inst. Senckenberg, 117: 409-469.

Wang Yanbin, Liu Dunyi, Yao Jianxin, Ji Zhansheng, Wang Liting, Wu Guichun, 2004. Age determination of the Lower-Middle Triassic boundary at Ganheqiao, Wangmo, Guizhou Province. Acta Gewologica Sinica, 78(5): 586-590.

Yao Jianxin, Ji Zhansheng, Wang Yanbin, Wang Liting, Wu Guichun, 2004. Research on conodont biostratigraphy around bottom boundary of the Middle Triassic Qingyan Stage in southern part of Guizhou Province. Acta Geologica Sinica, 78(5): 577-585.

Yin Hongfu, Yang Zunyi, Tong Jinnan, 2000. On status of the international Triassic research. Journal of Stratigraphy, 24(2): 109-113.

A View on the Late Permian-Early Triassic Revolution

Yin Hongfu

China University of Geosciences, Wuhan 430074, China; hfyin@cug.edu.cn

The Late Permian-Early Triassic revolution, with its worldwide global changes and the macro mass extinction in geologic history, is a hotspot of geoscience, but is meanwhile becoming an endless controversy. More than a dozen hypotheses have been set forth, none of which so far have reached a consensus. In recent years, the hypothesis of a short-term mono-episode killing by a bolide impact prevails in some journals. It is based on findings of fullerenes with extraterrestrial helium ratios, Ni-Cr-Si particles at the boundary clay, "sudden" mass extinction and a possible crater in NW Australia. However it is too hurry to draw conclusion from these evidences. There are two lines of facts that constraint applying the impact hypothesis as the main cause of end-Permian mass extinction.

Firstly, a common fact about Late Permian—Early Triassic evolution is the long-term decline of all major organism taxa that irresistibly destined to their final extinction by the end of Permian. Such a preordained extinction commenced long before the possible bolide. The existence of a long-term biotic decline and recovery and the long-term fundamental global changes that spanned ten million years (Late Permian—Early Triassic) were consists of several phases—pre-Lopingian, end-Permian and early Triassic, thus must have been caused by certain long-term and repeatedly functioning factor. Any hypothesis on the end-Permian extinction should be put to the test of these facts.

Secondly, newly discovered evidences show that, during the Permian-Triassic boundary interval when many events—volcanism, anoxia, possible bolide—concentrically happened, the mass extinction was multi-episodic rather than mono-episodic (Xie et al., 2005). There are also evidences showing that, at the GSSP Meishan section, the biotic crisis initiated prior to the event beds (beds 25-26) where the proposed impact occurred. This earlier phase of biotic crisis was further documented at other sections in South China, Iran and Hungary. Its horizon is usually a few decimeters to meters below the acknowledged mass extinction at the event beds, and often coincides with the end-Permian sequence boundary (SB) or sea level fall caused by the great worldwide marine regression. Hence, this forefront extinction has no relationship with the presumed bolide impact at the event beds.

In our view, the Permian-Triassic global change and biotic revolution is better interpreted as a revolutionary stage of Earth's history consisting of relatively long-term environmental and biotic episodes during whole Late Permian-Early Triassic time and multi-phased global changes and mass extinctions during the main episode—the Permian-Triassic boundary episode. The revolution was caused by periodic acceleration of interactions among the Earth's spheres (such as the integration of Pangea during Permian) and strengthened by catastrophes evoked by intrinsic (e.g. volcanism) or possibly extraterrestrial factors (e.g. bolide).

Sporopollen Assemblages of Non-Marine Facies near PTB, Western Guizhou and Eastern Yunnan, South China and Their Significance

Yu Jianxin, Yang Fengqing, Peng Yuanqiao and Zhang Suxin

Faculty of Earth Sciences, China University of Geosciences, Wuhan 430074, Hubei Province, P.R. China; yujx_cug@yahoo.com.cn

Following the establishment of the Global Stratotype Section and Point (GSSP) of the Permian-Triassic boundary (PTB) (Yin et al, 2001), the definition of the Accessory Section and Point (ASP) of the non-marine PTB is now on the agenda for correlation of the PTB from marine to terrestrial environments. However, all good non-marines PTB sections so far known have the following shortcomings. Firstly, the exact non-marine PTB horizon is difficult to define with high-resolution by biostratigraphy. Secondly, correlation between marine and non-marine PTB sequences is hard to attain with accuracy because no fossils can be traced directly from marine facies to land, and the position of the non-marine PTB are usually uncertain. These, of course, hamper the understanding of the global life crisis from marine to terrestrial environments across the Paleozoic-Mesozoic transition.

Both marine and non-marine continuous PTB strata are well developed in western Guizhou and eastern Yunnan, south China (Fig.1), making this area a potential hotspot for the study of the PTB from marine to terrestrial environments and their relationships during the Permian-Triassic transition.

These boundary sections can be used as one of the high-resolution methods for the subdivision and correlation of the PTB from marine to land. Three clear palynological Assemblages are recognized across the PTBST at some terrestrial PTB sections in western Guizhou and eastern Yunnan, South China. Assemblage 1 (Xuanwei Formation) is dominated by a Late Permian palynological assemblage of ferns and pteridosperms, with a few gymnosperms. Most of them are Paleozoic types with the appearance of some typical Late Permian pollen such as *Lueckisporites*. Assemblage 2 (PTBST) is marked by an abrupt drop of palynomorphs and the appearance of fungi spores, though it is still dominated by a palynological assemblage of ferns and pteridosperms, with a few gymnosperms. A mixed flora containing both Late Permian and Early Triassic elements marks in this assemblage. Most

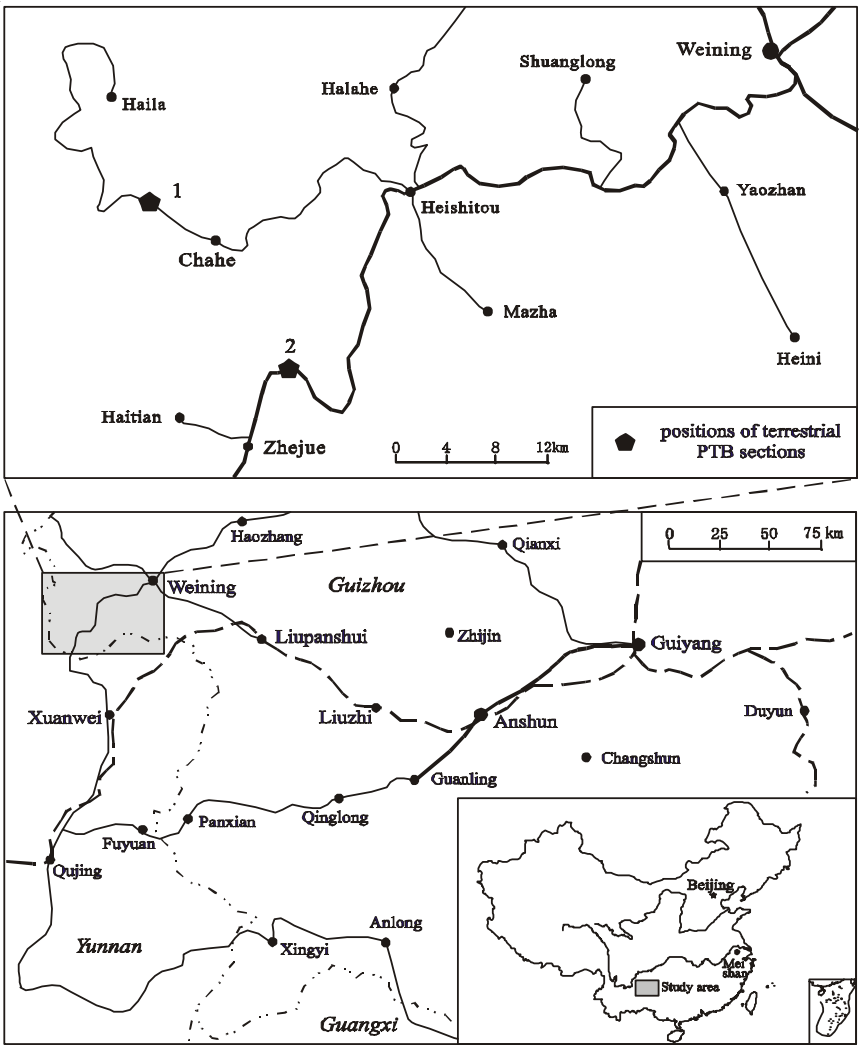

Figure 1. Locality map of terrestrial Sections

palynomorphs are still typical of the Late Permian types as found in Assemblage 1, however some palynomorphs of Early Triassic aspect (such as *Lundbladispora* and *Taeniaesporites*) already appeared. In Assemblage 3 (the top Xuanwei Formation and Kayitou Formation), the proportion of gymnosperm pollen increases rapidly, exceeds ferns and pteridosperms for the first time in western Guizhou and eastern Yunnan, although the content of palynomorphs was still very sparse. Some special palynomorphs of Early Triassic aspect (such as *Lundbladispora, Aratrisporites* and *Taeniaesporites*) were present in greater abundance in this Assemblage.

Thus according to palynomorphs the PTB should be located between Assemblage1 and 3, i.e., at the level of Assemblage 2. Similar palynomorph assemblages have been described in Fuyuan County of the adjacent Yunnan Province (Ouyang, 1986). Together they comprise a typical vegetation of the P/T interval of Sichuan-Yunnan Oldland. Palynomorphs of the Chahe Section are also correlated with those from the P/T transitional bed of the Junggar Basin, Xinjiang (Ouyang and Geoffrey, 1999).

Key words: Western Guizhou and eastern Yunnan, South China, Permian-Triassic boundary stratigraphic set (PTBST), Permian-Triassic boundary (PTB), Palynology

Significance of Caucasian Sections for the Working out of the Carbon-Isotope Standard for the Permian and Lower Triassic and Their Correlation with the Permian of North-Eastern Russia

Yuri D. Zakharov[1], Alexander S. Biakov[2], Aymon Baud[3] and Heinz Kozur[4]

[1] Far Eastern Geological Institute, Russian Academy of Sciences (Far Eastern Branch), Vladivostok, 690022, Russia; yurizakh@mail.ru

[2] North-East Interdisciplinary Scientific Research Institute, Russian Academy of Sciences (Far Eastern Branch), Magadan, 685000, Russia; stratigr@neisri.magadan.ru

[3] Musee de Geologie, BFSH2-UNI, 1015 Lausanne, Switzerland; aymon.baud@unil.ch

[4] Rézsü u. 83, H-1029 Budapest, Hungary; kozurh@helka.iif.hu

The eight anomalously high $\delta^{13}C$ values (2.8-3.8‰) were determined by A. Baud, W. Holser and M. Magaritz in samples of organogenic carbonates collected in the Sovetoshen section (Transcaucasia) in 1984 and published in 1989. These samples have been dated according to G. V. Kotlyar et al. (1983). This book contains some information, concerning mainly foraminifera, corals, brachiopods and ammonoids. Very important conodont material was obtained later by A.G. Grigoryan (1988a, b), but most significant paleontological part of his thesis has not been published. Recently we have possibility to copy some parts of his thesis, and H. Kozur made the revision of Grigoryan's paleontological determinations, using his own new data from Iran (Kozur, 2004). Together with the detailed carbon isotope data of the well dated sections Abadeh, Shahreza (Central Iran, Korte et al., 2004a, b), Jolfa and Zal (NW Iran, Korte et al., 2004c, Korte & Kozur, in press), the Sovetoshen section (with some data from other sections of Caucasus) yields a carbon-isotope standard for the uppermost Midian (Capitanian), Dzhulfian (Wuchiapingian), Dorashamian (Changhsingian) and Induan (Gangetian). The nine Middle-Late Permian and Early Triassic $\delta^{13}C$ events (positive anomalies) discovered in Caucasus were named by us as "A"-"I" (Figure 1).

Three anomalies ("A", "B" and "C") were recognized within the *Hemigordius irregulariformis–Orthotetina azarjani* and *Pseudodunbarula arpaensis – Araxilevis intermedius* Zones. The mentioned interval, with the exception of, apparently, its lowermost part characterized by big chert inclusions, corresponds to the Early Dzhulfian *Clarkina niuzhuangensis* and *Clarkina leveni* (lower part) Zones. Anomaly "C" is known also from the Vedi section in Transcaucasia, which good preserved Early Dzhulfian brachiopod shells were used for oxygen-isotope paleotemperature calculations (25.2-27.9°C) (Zakharov et al., 2000, 2001). Anomaly "D" was discovered from

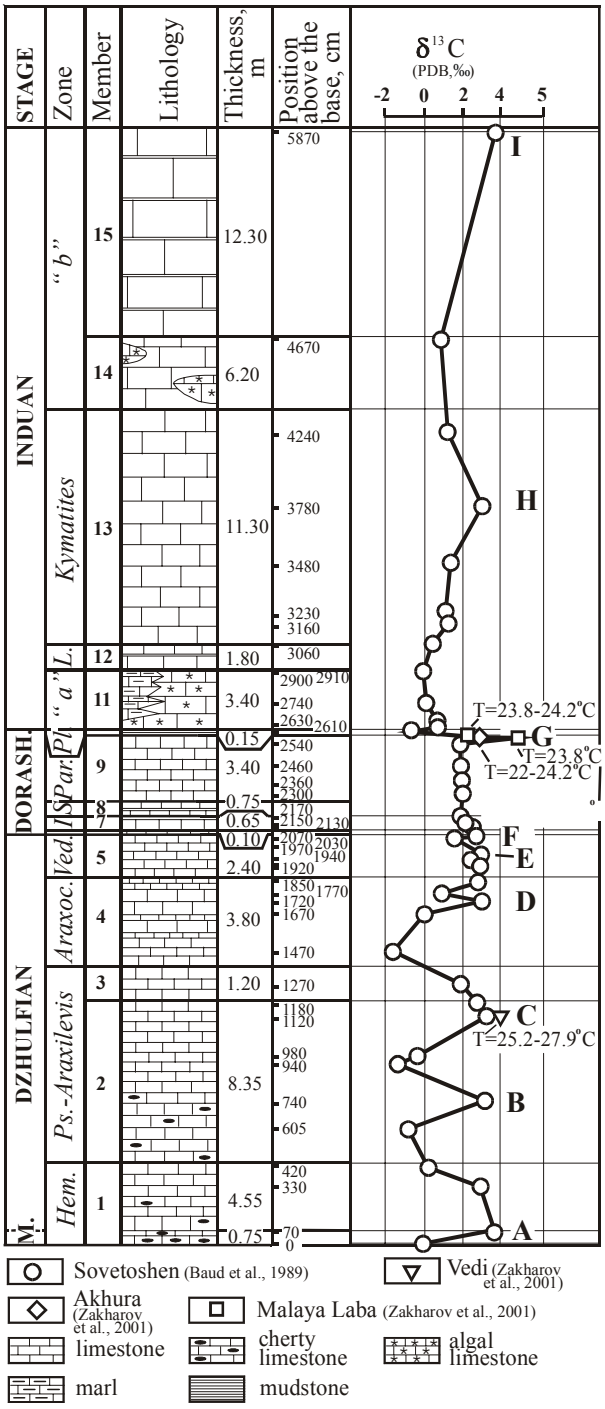

Figure 1. Carbon-isotope standard for the Middle-Upper Permian and Lower Triassic of the Caucasus area (Transcaucasia and North Caucasus) and Late Permian isotopic paleotemperatures. Abbreviatios: M. –Midian, Dorash. – Dorashamian, *Hem. – Hemigordius irregulariformis-Orthotetina azarjani, Ps.-Araxilevis – Pseudodunbarula arpaensis-Araxilevis intermedius, Araxoc. – Araxoceras latissimum, Ved. – Vedioceras ventrosulcatum, I. – Iranites transcaucasius, S. – Shevyrevites shevyrevi, Par. – Paratirolites kittli, Pl. – Pleuronodoceras occidentale-Xenodiscus jubilaearis,* "a" – Interval "a" without ammonoids, *L. – Lytophiceras* medium, "b" – Interval "b" without ammonoids.

the upper part of the Dzhulfian *Araxoceras latissimum* Zone (upper *Clarkina leveni* Zone). Anomalies "E" and "F" were determined in the Late Dzhulfian *Vedioceras ventrosulcatum* Zone (*Clarkina orientalis* and *Clarkina inflecta* Zones). Late Dorashamian positive anomaly "G" of the *Paratirolites kittli* Zone was found in Caucasus outside of the Sovetoshen section. *Paratirolites kittli* time is characterized by somewhat lower paleotemperatures than those calculated from Early Dzhulfian organogenic carbonates: 22.0-24.2°C (for the Akhura area in Transcaucasia) and 23.8°C (for Malaya Laba River, North Caucasus (Zakharov et al., 2000, 2001). In the uppermost Permian represented by the uppermost part of the *Paratirolites kittli* Zone (*Clarkina iranica* Zone) and *Pleuronodoceras occidentale–Xenodiscus jubilaearis* Zone (*Clarkina hauschkei to C. meishanensis–Hindeodus praeparvus* Zones) only negative $\delta^{13}C$ excursion was recognized (-0.8‰). The calculated paleotemperatures for the lower *Pleuronodoceras occidentale–Xenodiscus jubilaearis* Zone level in North Caucasus (23.8-24.2°C) are comparable with those for the *Paratirolites kittli* Zone. According to data on Ca/Mg ratio (Zakharov et al., 2000, Fig. 19), paleotemperatures in Transcaucasia became lower (in comparison with data from the uppermost Permian of Transcaucasia, North Caucasus and South China) only at the beginning of the Induan (interval 'a" without ammonoids and lowermost part of the *Lythopiceras medium* Zone). Somewhat warmer conditions seem to be appeared only at the end of the *Lythopiceras medium* time. The positive anomalies "H" (3.1‰) and "I" (3.8‰) of the Induan were recognized only in the middle part of the Lower Karabaglyar Formation in the Sovetoshen section. We obtained some new data on carbon-isotope composition of bivalve shells from the Permian of North-Eastern Russia (Omolon and Okhotsk) and used the Caucasus carbon-isotope standard for their correlation. In the Omolon area (Levyi Vodopadnyi and Pravyi Vodopadnyi Creeks, Gizhiga River basin), the two positive anomalies were discovered within the Upper Permian Khivach Formation (*Intomodesma costatum* Zone), which are correlated by us with the Late Dzhulfian "F" and Late Dorashamian "G". The latter is present in the Omolon area despite of some erosion recognized at the P/T boundary. Oxygen- isotope investigation of a good preserved bivalve shell shows the paleotemperature value comparable with those for the Late Dorashamian of Caucasus. The climate of the most part of the Late Permian seems to be somewhat warmer in comparison with the climate of the Wordian time (paleotemperature calculated from the isotopic composition of the good preserved bivalve shell from the Wordian *Kolymia multiformis* Zone of the Omolon Formation, Omolon area, is only 20.1°C). Another investigated Far Eastern section locates on the Okhotsk area (Titan Creek, Khuren River). The four positive anomalies were found there within the Upper Permian Khivach Formation (*Intomodesma costatum* Zone), fluctuating between 5.1 and 6.9‰. They are correlated by us with the Dzhulfian events "D", "E" and "F" and Late Dorashamian "G". New data confirm A. Biakov's idea, according which at least Wuchiapingian and the most part of Changhsingian sediments expose in the Omolon and Okhotsk areas.

The research was made under the financial support of a RFBR grant (05-05-64407), Russia.

Baud, A., Holser, W. T., Magaritz, M., 1989. Permian-Triassic of the Tethys: Carbon isotope studies: Geol. Rundschau, 78: 1-25.

Grigoryan, A. G., 1990a. Konodonty pogranichnykh otlozhenij permi i triasa Armyanskoj SSR (Conodonts from Permian-Triassic boundary sediments of Armenia). PhD Thesis abstract, Moscow University, Moscow, 18 pp. (in Russian).

Grigoryan, A. G., 1990b. Konodonty pogranichnykh otlozhenij permi i triasa Armyanskoj SSR (Conodonts from Permian-Triassic boundary sediments of Armenia). Dissertatsiya na soiskaniye uchenoi stepeni kandidata geologo-mineralogicheskikh nauk, Moscow University, Moscow, 210 pp., pls. 1-9 (in Russian).

Korte, C., Kozur, H. W., in press. Carbon isotope stratigraphy across the Permian-Triassic boundary at Jolfa (NW-Iran), Peitlerkofel (Sas de Pütia, Sass de Putia), Pufels (Bula, Bulla), Tesero (all three Suthern Alps, Italy) and Gerennavár (Bükk Mts., Hungary). Journ. Alpine Geol.

Korte, C., Kozur, H. W. Joachimski, M. M., Strauss, H., Veizer, J., Schwark, L., 2004a. Carbon, sulfur, oxygen and strontium isotope records, organic geochemistry and biostratigraphy across the Permian/Triassic boundary in Abadeh, Iran. Int. J. Earth Sci. (Geol. Rdsch.), 93: 565-581.

Korte, C., Kozur, H. W., Mohtat-Aghai, P., 2004b. Dzhulfian to lowermost Triassic delta 13 C record at the Permian/Triassic boundary section at Shahreza, Central Iran. Hallesches Jahrb. Geowiss., Reihe B, Beiheft 18: 73-78.

Korte, C., Kozur, H. W., Partoazar, H., 2004c. Negative carbon isotope excursion at the Permian/Triassic oundary section at Zal, NW-Iran. Hallesches Jahrb. Geowiss., Reihe B, Beiheft 18: 69 - 71.

Kotlyar, G. V., Zakharov, Y. D., Koczirkevicz, B. V., Kropatcheva, G. S., Rostovtsev, K. O., Chedija, I. O., Vuks, G. P., Guseva, E. A., 1983. Pozdnepermskij etap v evolutsii organicheskogo mira. Dzhulfinskij i Dorashamskij yarusy SSSR (Evolution of the Latest Permian biota. Dzhulfian and Dorashamian regional stages in the USSR). Nauka, Leningrad, 198 pp., pls. 1-16 (in Russian).

Kozur, H. W., 2004. Pelagic uppermost Permian and the Permian-Triassic boundary conodonts of Iran. Part 1. Taxonomy. Hallesches Jahrb. Geowiss., Reihe B, Beiheft 18: 39-68, pls. 1-6.

Zakharov, Y. D., Boriskina, N. G., Popov A. M. 2001. Rekonstruktsiya uslovij morskoi sredy pozdnego paleozoya i mezozoya po izotopnym dannym (na primere severa Evrazii) (The reconstruction of Late Paleozoic and Mesozoic marine envirionments from isotopic data). Dalnauka, Vladivostok, 111 pp. (in Rus-

sian).

Zakharov, Y. D., Ukhaneva, N. G., Ignatyev, A. V., Afanasyeva, T. B., Buryi, G. I., Panasenko, E. S., Popov, A. M., Punina, T. A., Cherbadzhi, A. K., 2000. Latest Permian carbonates of Russia: new palaeontological findings, stable isotopes, Ca-Mg ratio, and correlation. *in* Yin, H., Dickins, J. M., Shi, G. R., Tong, J. (eds.) Permian-Triassic Evolution and Western Circum-Pacific. Elsevier, Amsterdam, 141-171.

Unique Marine Olenekian-Anisian Boundary Section from South Primorye, Russian Far East

Yuri D. Zakharov[1], Alexander M. Popov[2] and Galina I. Buryi

Far Eastern Geological Institute, Russian Academy of Sciences (Far Eastern Branch), Stoletiya Prospect 159, Vladivostok, 690022 Russia; [1]yurizakh@mail.ru, [2]popov_alexander@list.ru

Late Olenekian and Anisian in South Primorye (Russian Far East) have been investigated by C. Diener (1895), A. Bittner (1899), P.V. Wittenburg (1910), L.D. Kiparisova (1961, 1972), I.V. Burij (1959), M.V. Korzh (1959), Y.D. Zakharov (1968, 1978, 1997), G.I. Buryi (1979), N.K. Zharnikova (1981) and some other workers. A review of a new data on the Upper Olenekian (*Neocolumbites insignis* and *Subcolumbites multiformis* Zones) and Lower Anisian (*Ussuriphyllites amurensis* and *Leiophyllites pradyumna* Zones) biostratigraphy of South Primorye is given on the basis of the five sections: Zhitkov Peninsula, Tchernyschew Bay, Golyi Cape, Petrovka River and Atlasov Cape, using new ammonoid, brachiopod and conodont findings. The most representative ammonoid assemblage at the base of the Anisian was discovered in the *Ussuriphyllites amurensis* Zone of the Atlasov Cape section (western Amur Gulf): *Parasageceras* sp. nov., Prionitidae gen. et sp. nov., *Ussuriphyllites amurensis* (Kiparisova) (dominant), *Megaphyllites atlasoviensis* Zakharov, *Leiophyllites praematurus* Kiparisova, *Leiophyllites* sp., *Ussurites* sp., *Paradanubites* sp. indet., *Paracrochordiceras* sp. nov., *Prohungarites popowi* Kiparisova, *Arctohungarites primoriensis* Zakharov, *A. solimani* (Toula), *Salterites* sp. indet. (gigantic shell), and *Tropigastrites sublachontanus* Zakharov. Conodonts *Neospathodus* cf. *homeri* (Bender) were found in the lower part of the *Ussuriphyllites amurensis* Zone (10.6 m thick). The Atlasov Cape seems to be one of most perspective sections in South Primorye. But research now needs to focus on the conodont succession of the Olenekian-Anisian boundary beds. If good results will be obtained, the unique Atlasov Cape section can be proposed as a candidate GSSP of the Olenekian-Anisian boundary.

This research was made under the financial support of a grant RFBR (Russia) (project 04-05-64061).

Bittner, A., 1899. Fossils from Triassic sediments of the South Ussuri area. Trudy Geol. Kom., 7(4): 1-35 (in Russian).

Burij, I.V., 1959. Triassic stratigraphy of South Primorye. Trudy Dalnevostochnogo Politekhnicheskogo Instituta, 54(1): 3-34 (in Russian).

Buryi, G. I., 1979. Lower Triassic conodonts in South Primorye. Nauka, Moscow, 144 pp., 14 pls. (in Russian).

Diener, C., 1895. Triadische Cephalopodenfaunen der Ostsibirischen Küstenprovinz. Mém. Com. Géol., 14(3): 1-59, 5 pls.

Kiparisova, L. D., 1961. Paleontological basis of Triassic stratigraphy of Primorye region. I. Cephalopods. Trudy VSEGEI, 48: 1-278, 38 pls. (in Russian).

Kiparisova, L. D., 1961. Paleontological basis of Triassic stratigraphy of Primorye region. II. Late Triassic mollusks and general stratigraphy. Trudy VSEGEI, 181: 1-246, 17 pls. (in Russian).

Korzh, M. V., 1959. Petrography of Triassic sediments of South Primorye and Triassic paleogeography. Izdat. AN SSSR, Moscow, 83 pp. (in Russian).

Wittenburg, P. V., 1910. Geological sketch on the Muravev-Amurskij Peninsula and Russian Island. S.-Peterburg, 44 pp. (in Russian).

Zharnikova, N. K., 1981. New Anisian ceratites of Acrochordiceratidae family of South Primorye. Paleont. Zhurn., 1981(1): 29-37, 1 pl. (in Russian).

Zakharov, Y. D., 1968. Biostratigraphy and ammonoids of the Lower Triassic of South Primorye. Nauka, Moscow, 175 pp., 31 pls. (in Russian).

Zakharov, Y. D., 1978. Early Triassic ammonoids of the East USSR. Nauka, Moscow, 224 pp., 19 pls. (in Russian).

Zakharov, Y. D., 1997. Ammonoid evolution and the problem of the stage and substage division of the Lower Triassic. Mém. Géologie (Lausanne), 1997(30): 121-132, 3 pls.

Lower Triassic and Carbon Isotope Excursion in West Guangxi, Southwest China

Zhang Haijun, Tong Jinnan* and Zuo Jingxun

*China University of Geosciences, Wuhan 430074, China; *jntong@cug.edu.cn*

The Permian-Triassic sequence of West Guangxi in the southwestern China is well known by covering various paleogeographic facies from deep basins to shallow carbonate buildups (Yang et al., 1987; Tong and Yin, 2002). The Zuodeng Section in Tiandong County is one of very typical and best-studied sequences well defined in biostratigraphy from the top of Upper Permian to the base of Middle Triassic. A very famous early study on the Lower Triassic ammonoids was by Chao (1959), who published a monograph of the Lower Triassic ammonoids from West Guangxi and established a Lower Triassic ammonoid sequence correlated with Spath's (1930, 1934) "standard" Triassic ammonoid zonation. The conodonts are also very common in the area and most Lower Triassic index fossils exist in the area (Yang et al., 1984, 1986; Zhang, 1990). At the Zuodeng Section the uppermost Permian is the Heshan Formation composed mainly of thick-bedded or massive limestone in shallow facies. A specific type of "knotted limestone", probably microbialite, occurs at the Permian-Triassic boundary. The overlying Luolou Formation is composed chiefly of medium- to thin-bedded micrite in deeper facies. The upper part of the Heshan Formation contains relatively poor fossils at the Zuodeng Section though bio-clasts are common and brachiopods and gastropods were observed. Even conodonts are very rare there, while fusulinids are frequently found. However, *Hindeodus parvus* was well developed at the section and it marks the Permian-Triassic boundary inside the "knotted limestone" about one meter below the top of the Heshan Formation. The Luolou Formation contains very rich ammonoids and conodonts while bivalves are relatively scarce. The ammonoids are commonly enriched as shelly beds. So the Lower Triassic ammonoid and conodont zonations are well recognized at the section. The Luolou Formation is overlaid with the Middle Triassic Baifeng Formation composed chiefly of mudrocks and siltstone with ammonoids and thin-shelled bivalves. The Lower and Middle Triassic boundary marked by the FAD of *Chiosella timoensis* is in the uppermost part of the Luolou Formation. Owing to a deep-water depositional sequence, the Lower Triassic in Zuodeng is only 120 m thick. In the meantime the Lower Triassic sequences on carbonate platforms or buildups are usually several hundred meters in thickness, which usually yield a very different conodont sequence though the Permian-Triassic boundary is still clearly indexed by *Hindeodus parvus* (Yang et al., 1999). Ammonoids are very scarce in the carbonate platform and buildup facies while bivalves are relatively common there.

141 carbonate samples were collected from the Zuodeng Section for the analysis of carbon and oxygen isotopes. The samples cover a sequence of about 130 m from the uppermost Changhsingian to the basal Anisian. At the same time 85 samples were collected from the Taiping Section, about 100 km to the east of the Zuodeng Section but in a platform facies, to cover a sequence of 60 m from upper Permian Heshan Formation (24 m) to the lower Triassic Majiaoling Formation (36 m). All the samples were analyzed for inorganic carbon and oxygen isotopes and the results are shown in Fig. 1 and Fig. 2.

The carbon isotopes from both Zuodeng and Taiping sections express a similar excursion across the Permian-Triassic boundary. The $\delta^{13}C$ is relatively high in the upper Permian while a decline occurs at the Permian-Triassic boundary. This excursion is the same as observed in many sections in South China and over the world. However, our study at both sections (basin and platform facies) shows a negative shift below the Permian-Triassic boundary is clearly gradual instead of a sharp drop as reported at the most sections. The results at the Taiping Section are somewhat similar to that reported by Wang et al. (2001). The values keep low around zero at the Permian-Triassic boundary till the lower Griesbachian while positive and clearly higher in the upper Griesbachian and Dienerian though a negative shift occurs around the Griesbachian and Dienerian boundary according to the data from the Zuodeng Section. A marked negative shift of $d^{13}C$ occurs in the Smithian though the values are not

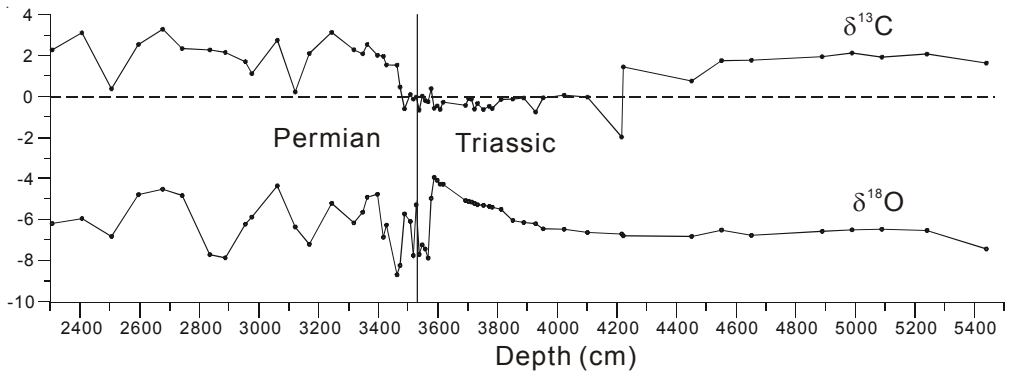

Figure 1. Lower Triassic sequence and carbon and oxygen isotopes excursion of Zuodeng Section, Tiandong, Guangxi

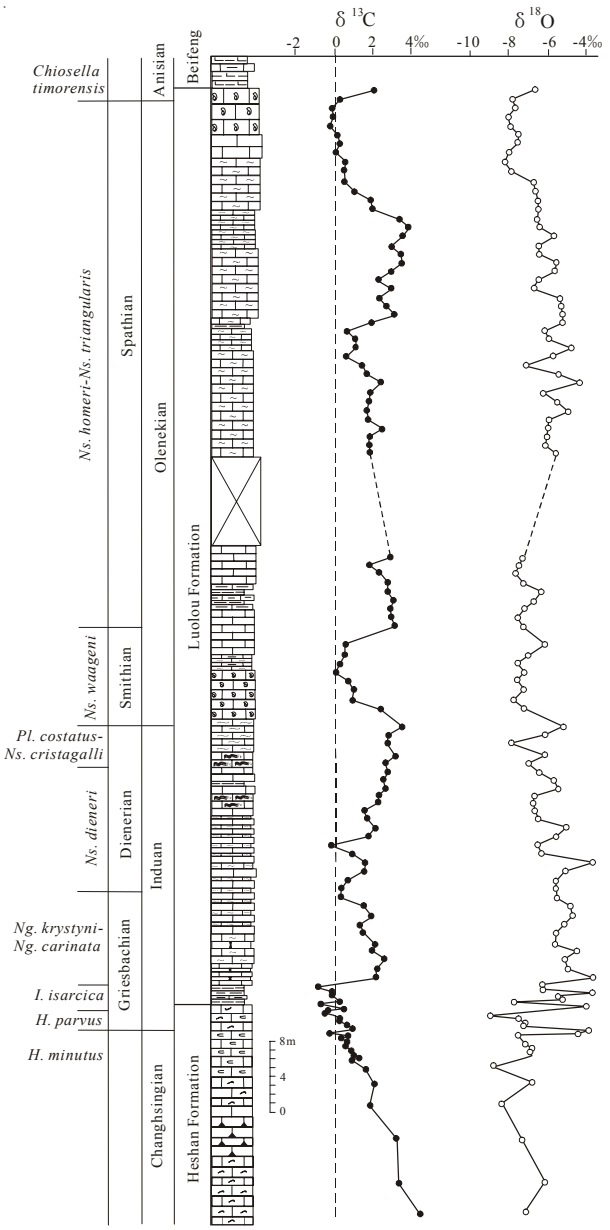

Figure 2. Lower Triassic carbon and oxygen isotopes excursions of Taiping Section, Pingguo, Guangxi

very negative. This excursion is quite similar to those observed in other areas of South China (Tong et al., 2002; Payne et al., 2004). Most $\delta^{13}C$ values are high in the Spathian except for an obvious decline at the top. A positive shift is at the Lower and Middle Triassic boundary as shown in many sections over the world.

The excursion of the carbon isotopes from the sections seems coincident with the biotic evolution and related events across the Paleozoic-Mesozoic transition. However, the gradual decline below the Permian-Triassic boundary and the negative shifts inside the Lower Triassic indicate the complexity of the events, which is hardly explained by a single rare trigger.

Chao Kingkoo, 1959. Lower Triassic Ammonoids from Western Kwangsi, China. Palaeontologia Sinica, New Ser. B, 9: 1-355. Science Press, Beijing.

Payne, J. L., Lehrmann, D. J., Wei, J., Orchard, M. J., Schrag, D. P., Knoll, A. H., 2004. Large perturbations of the carbon cycle during recovery from the end-Permian extinction. Science, 305: 506-509.

Spath, L. F., 1930. The Eo-Triassic invertebrate fauna of East Greenland. Medd. Om Gronland, 83: 1-90.

Spath, L. F., 1934. Catalogue of the fossil Cephalopoda in British Museum (Natural History). Part IV, The Ammonoidea of Trias. London, 1-521.

Tong Jinnan, Qiu Haiou, Zhao Laishi and Zuo Jingxun, 2002, Lower Triassic inorganic carbon isotope excursion in Chaohu, Anhui Province, China. Journal of China University of Geosciences, 13(2): 98-106.

Tong Jinnan, Yin Hongfu, 2002. The Lower Triassic of South China. Journal of Asian Earth Sciences, 20: 803-815.

Wang Darui, Wang Xinping and Sun Xiaoting, 2001. The anomaly of carbon and xytgen isotopic compositions across the Permian-Triassic boundary in northwest Guangxi, south China, and its significance. Geological Review, 47: 225-228.

Yang Shouren, Hao Weicheng and Wang Xingping, 1999. Triassic conodont sequences from different facies in China. In: Biotic and Geological Development of the Paleo-Tethys in China. p.97-112. Peking University Press, Beijing.

Yang Shouren, Wang Xingping and Hao Weicheng, 1984. New knowledge of the Lower Triassic of Zoudeng, Tiandong County of Guangxi Province. Selected Papers to Memorize Professor Le Senxun Engaged in Geological Research and Education for 60 Years, pp.105-118. Geological Publishing House, Beijing.

Yang Shouren, Wang Xingping and Hao Weicheng, 1986. Early Triassic bivalve assemblages of West Guangxi. Journal of Stratigraphy, 10(2): 88-97.

Yang Zunyi, Yin Hongfu, Wu Shunbao, Yang Fengqing, Ding Meihua and Xu Guirong, 1987. Permian-Triassic boundary stratigraphy and fauna of South China. Geological Publishing House, Beijing.

Zhang Shunxing, 1990. New knowledge on the Lower Triassic conodont sequence in West Guangxi. Modern Geology, 4(2): 1-15.

Early Triassic Sequence Stratigraphy and Sea Level Change at Meishan Section D of Changxing County, Zhejiang Province, South China

Zhang Kexin*, Tong Jinnan, Li Qixiang and Jin Yali

*Faculty of Earth Science, China University of Geosciences, Wuhan 430074, P. R. China;*kxzhang@vip.sina.com*

The Lower Triassic is well developed at Meishan Section D of Changxing County, Zhejiang Province, South China and composed of Yinkeng Fm, Helongshan Fm and lower part of Nanlinghu Fm in lithostratigraphy. The most part of Yinkeng Fm belongs to the Lower Triassic while the strata of 0.18 m at the base is the Upper Permian according to the definition of the GSSP of the Permian-Triassic boundary (Yin et al., 2001). The correlation of the lithostratigraphical "Formation" with the chronostratigraphical "Stage" at the Meishan Section is roughly as follows: Yinkeng Fm vs. lower substage of the Induan Stage (Griesbachian Substage); Helongshan Fm vs.upper substage of the Induan Stage (Dienerian Substage); lower part of Nanlinghu Fm vs. lower part of Olenekian Stage (Smithian Substage).

The Lower Triassic Yinkeng Fm, Helongshan Fm and lower part of Nanlinghu Fm at Section D are divided into five third-order sequences, each of which last about 1.5 Ma on average. Sequence one (T-Sq1) corresponds with the latest Changhsingian + early Griesbachian, Sequence two (T-Sq2) roughly with the middle Griesbachian, Sequence three (T-Sq3) roughly with the late Griesbachian +early Dienerian, Sequence four (T-Sq4) with the late Dienerian, and Sequence five (T-Sq5) roughly with the Smithian.

Sequence 1 (T-Sq1): It is type II sequence, composed of the SMST, TST and HST, covering the conodont zones in an ascending order: *Clarkina changxingensis yini* Zone, *Hindeodus latidentatus–Clarkina meishanensis* Zone, *Hindeodus parvus* Zone, *Isarcicella isarcica* Zone and the lower part of the *Clarkina carinata* Zone. The SMST is the slightly progradational – aggradational deposition system on shelf ramp, which is a starved deposition in a slightly dysoxic condition. But both benthos and planktons are common. The TST is predominated by calcareous mudrocks, which were slowly deposited in poor biological activity after the Permian–Triassic mass extinction. The lower HST is characteristic of grayish black and grayish green mudrock and calcareous mudrock, in which the grayish green calcareous mudrock is predominant. The sedimentation was starved, occasionally with bioturbation. The upper HST has evidently more limestone. The depositional rate increased and the parasequences were well developed. The limestone beds that are a regressive progradational filling sequence became more and thicker upwards while the mudrock decreased rapidly.

Sequence 2 (T-S1-2): It is type II sequence, and only the TST and HST recognized, including the conodont zones in an ascending order: upper *Clarkina carinata* Zone and lower *Neospathodus kummeli* Zone. The basal surface of T-Sq2, SB_2, locates nearly at the base of the Lower Mb of the Helongshan Fm at Meishan Section D. The intermittent exposure marks such as the mud cracks occur around the surface. The mfs is situated in the base of Bed 68 of the Lower Mb of the Helongshan Fm. Beds 62–67 are the TST, composed of the retrogradational parasequence set. According to the conodont fauna, the lower TST contains the forms common in the shallow water, such as *Pachycladina obliqua* Staesche, *Parachirognathus* cf. *newadensis* (Mueller); the upper TST has the forms rich in the relatively deep facies, such as *Neohindeodella triassica* (Mueller). The HST has relatively big thickness. The lower HST is relatively thinner bedded, colored dark and developed in horizontal bedding, indicating relatively deeper water. The upper HST is bedded relatively thicker and colored lighter with low-angular crossing bedding in the top part, indicating the gradual shallowing upward. In the areas controlled by the previous paleotectonic geography and at the margins of the basin, such as Niutoushan of Guangde and Taihu of Suzhou around the Jiangyin – Guangde Oldland at the end of the Permian, the carbonate depositional filling was very active, thus the thickness of T-Sq2 is relatively big. In the Meishan area close to the basin, the depositional rate was relatively slow.

Sequence 3 (T-Sq3): It is type II sequence, composed of the TST and HST and covering the conodont zones of the upper *Neospathodus kummeli* Zone and the *Neospathodus dieneri* Zone from lower to upper. The base of this sequence contains lenticular thick-bedded calcirudite. The basal surface of the calcirudite is wavy scouring surface, which becomes low-angular crossing bedding upwards, showing that with the beginning of a new transgression a tidal channel sedimentary bed occurred on the transgressive onlap surface of the sequence. The TST totally consists of the upward deepening retrogradational parasequences though the upward shallowing progradational sequences occasionally occur in the middle part, in which some large-scale low-angular crossing bedding or large-scale scouring crossing bedding was formed. Gray thin-bedded micrite exists at the transitional surface between the TST and HST, indicating the low-energy deep water to form well-developed horizontal bedding. As a whole, T-Sq3 was formed in the relatively deep part on the shallow open shelf carbonate platform.

Sequence 4 (T-Sq4): It is type II sequence composed of the TST and HST, corresponding the conodont *Neospathodus cristagalli* Zone. The TST consists of the upward-deepening retrogradational parasequence set. Lower part of the parasequence is composed of medium bedding limestone in relatively thicker bedding. The upper part is thin-bedded limestone in relatively thinner bedding. The horizontal bedding becomes marked upwards. The lower part in the HST is mainly the thin-bedded limestone with horizontal bedding, composed of aggradational parasequence set, while the upper part consists of upward-

shallowing progradational sequence set. The scouring occurs at the top of the HST. The bedding becomes thicker and the grading beds and scouring structures occur, showing that the sea level fell considerably so that the area turned from the lower upper shallow sea to the upper upper shallow sea and shoreface, then at the top of the HST a stage of scouring without deposition appeared.

Sequence 5 (T-Sq5): It is type II sequence that is composed of the TST and HST, covering the conodont *Neospathodus waageni* Zone of the Smithian. The TST of T-Sq5 is not evident, composed of a faintly retrogradational parasequence set. Because during T-Sq5 deposited, the Lower Yangtze sea was relatively shallow epicontinental sea as a whole and the studying area located in the shallow bank of epicontinental shoreface. Therefore, the high-stand systems tract(HST) is well-developed in the T-Sq5 in which the parasequence sets have big thickness and the high-energy shallow bank facies deposits are common.

Study on Claystone at Permian-Triassic Boundary of Daxiakou Section in Xingshan, Hubei Province

Zhang Suxin*, Tong Jinnan, Yang Fengqing and Yang Hao

Faculty of Earth Science, China University of Geosciences, Wuhan 430074, China;
**sxzhang@cug.edu.cn*

Several clay beds exist in the strata around the Permian-Triassic boundary throughout South China, whether it was marine or terrestrial facies. Studies have been done on the boundary clay beds at the Meishan Section of Changxing, Zhejiang, the Ermeng Section of Huangshi, Hubei, the Zhongliangshan Section of Chongqing, and the Gaowo Section of Puding, Guizhou, which are shallow marine facies, at the Zhongzhai Section of Langdai, Guizhou in a littoral facies, and at the Chahe Section of Weining, Guizhou in a paralic or terrestrial facies. These clay beds well yield such minerals as high-temperature quartz, apatite, zircon, and microspheres and some tuffaceous structures are observed, indicating that the clay beds were originated from some volcanic events and they are the mixture of volcanic ash and normal sediments (He et al., 1988; Yin et al., 1989; Wu et al., 1990; Huang, 1993; Wang and Yin, 2002; Zhang et al., 2004a, b). Since the volcanic events recorded by these clay beds are believed to result in the mass extinction at the end of the Permian and, meanwhile, the event beds are regarded as an accessory mark to identify and correlate the Permian-Triassic boundary, the study on these clay beds becomes crucial (Yang et al., 1991; Yin, 1996; Yin et al., 2001; Peng et al., 2005).

Seeking for the correlation of the Lower Triassic Induan-Olenekian boundary, we studied the Lower Triassic in Daxiakou, Xingshan, Hubei Province recently and collected some samples from the clay beds aroung the Permian-Triassic boundary at the Daxiakou Section. This paper presents the study on these clay beds and tries to provide an interpretation on the origin of the rocks as well as the relation to the mass extinction.

Samples and methods

Eight samples were collected from strata around the Daxiakou Section, including one from the top of the Changhsingian, the "boundary clay bed", and six samples from the lower part of the Induan, separately numbered HXD-9, HXD-10, HXD-12, HXD-14, HXD-14+30, HXD-21, HXD-23 and HXD-23+140. All the samples are elutriated in door to separate clay and clastic materials at the State Key Laboratory of Geo-Processes and Mineral Resources in Wuhan. The clay is detected by an X-ray diffractometer for the identification and quantification of clay minerals. The clastic materials are for the selection and observation of special minerals. Most well-shaped minerals are carefully sought and picked out under a stereomicroscope for further study in an environmental scanning electron microscope.

The clay is detected by a D/max-3B mineral powder

Table 1 Minerals in the clay rocks from the Permian-Triassic boundary strata at the Daxiakou Section, Xingshan

Sample No.	Minerals and contents (%)
HXD-23+140	Illite-montmorillonite mixed-layer mineral (60)+ gypsum (30) + quartz (5) + calcite (5)
HXD-23	Illite-montmorillonite mixed-layer mineral (80) +gypsum (20)
HXD-21	Illite-montmorillonite mixed-layer mineral (80) +gypsum (0) +quartz (5) +calcite (5) + kaolinite (10)
HXD-14+30	Illite-montmorillonite mixed-layer mineral (20) + gypsum (45) + quartz (5) +calcite (30)
HXD-14	Illite-montmorillonite mixed-layer mineral (80) + gypsum (15) + quartz (5)
HXD-12	Illite-montmorillonite mixed-layer mineral (30) + gypsum (40) + quartz (10) + illite (20)
HXD-10 (boundary clay)	Illite-/montmorillonite mixed-layer mineral (80) + gypsum (20)
HXD-9	Illite-montmorillonite mixed-layer mineral (80) + gypsum (15) + quartz (5)

diffractometer under a condition: tubing voltage 30Kv, tubing current 30mA, Cu barn, Ni filtering, and scanning speed 5^0/min. The clastic minerals are observed and scanned by a Quanta200 environmental scanning electron microscope under a condition: accelerating voltage 20Kv, filament current 2.54A and beam spot size 3.0.

Clay minerals

Table 1 lists the results for the initial clay samples detected by the X-ray mineral powder diffractometer.

It can be seen that the all the clay rocks are predominated by illite-montmorillonite mixed-layer mineral. In addition, there is a small quantity of illite in Bed 12 and some kaolinite in Bed 21. The other minerals are gypsum, quartz and calcite. The content of illite-montmorillonite mixed-layer mineral is about 80% in most samples, and between 20%~30% in few samples. Sample from Bed 12 also contains 20% illite and Bed 21 has 10% kaolinite.

Clastic materials

The residual clastic materials extracted from the samples are firstly observed under a stereomicroscope to seek and pick out the better shaped minerals. The selected clastics are then scanned by the environmental scanning electron microscope to determine the shape, size and mineral species.

The study indicates that a hexagonal bipyramid quartz is quite common in Bed 10 and Bed 21. Such a hexagonal bipyramid quartz is a b-quartz mineral originated in a condition of normal pressure and high temperature of 573-870ºC. It is an uncolored and transparent crystal in a hexagonal bipyramid shape, sized between 150~200˜m. There are also a lot of clay balls found in the samples from Bed 12. They are silicate microspheres, determined by an energy spectrometer. They are in a spherical or water-drop globular shape, sized in about 200˜m.

Origination of the clay rocks

According to the above results, it would be believable that the origination of these clay beds is closely related to volcanic activities. The hexagonal bipyramid quartz common in Bed 10 and Bed 21 were formed in a temperature higher up to 573-867ºC. With slow cooling, the high temperature ˜-quartz will be transformed to low temperature ˜-quartz. If the cooling is rapid, the morphology of the hexagonal bipyramid remains. So the ˜-quartz in morphology of hexagonal bipyramid is common in a rapidly cooling volcanic rock. Therefore, these two clay beds can be believed to be a volcanic origination. There are two possibilities for the origination of the silicate microspheres in Bed 12. One is that they are the products of volcanic eruption and the other explanation is that they are probably resulted from some impact events. In the other five clay beds no clastic minerals clearly showing a volcanic origination have been collected yet, but the clay beds contain a certain content of illite-montmorillonite mixed-layer mineral, which still indicates a volcanic origination. The explanation for these clay beds might be that the eruption centers were far from the depositional area and no hexagonal bipyramid quartzes formed in high temperature fall except for the volcanic ash deposited along with normal sediments at the section. In the sea, the neutral-acidic volcanic ash is transformed to montmorillonite, the Ca^{++} and H_2O in montmorillonite crystal lattice are replaced by K^+, and so the illite-montmorillonite mixed-layer mineral is formed. As a result, these clay beds may also have an origination of volcanic events. The content of illite-montmorillonite mixed-layer mineral in the clay beds is related to the intensity of the volcanic eruption and the distance of the eruption center. It can be seen that the volcanic activity was very frequent in the area or in the neighboring areas during the Permian-Triassic transition though the intensity of the eruptions and position of the eruption centers might be different during the period.

Conclusions

The following preliminary conclusions can be reached based upon the analysis for the clay samples from the Permian-Triassic boundary strata at the Daxiakou Section in the Three-Gorge area, central China.

1. All the samples from the eight clay beds contain evidence indicating synchronous volcanic activity.

2. During the Permian-Triassic transition the volcanic events were very frequent in the area or in the neighboring areas, but the intensity and position of the volcanic eruption were different. However, the volcanic events recorded in Beds 10 and 12 impacted this area much stronger.

3. The frequent volcanic activities should be at least one of leading events to cause the momentous turnover of biota and ecosystem during the Permian-Triassic transition.

Acknowledgement: This study is supported by the National Natural Science Foundation of China (Nos. 40325004, 40232025).

He Jinwen, Chai Zhifang, Ma Shulan, 1988. Discovery and signification of hexagonal dipyramid quartz at the Permian-Triassic boundary section from Changxing, Zhejiang. Bulletin of Science and Technology, 33(14): 1088-1091.

Huang Sijing, 1993. Microspherulitic and Clastic Mineral in the Clay Rock Near the Permian-Triassic Interface of Zhonglianshan Mountain, Chongqing. Acta Sedimentologica Sinice, 11(3): 105-113.

Peng Yuanqiao, Zhang Suxin, Yu Jianxin et al., 2005. High-resolution terrestrial Permian-Triassic eventostratigraphic boundary in western Guizhou and eastern Yunnan, southwestern China. Palaeogeography, Palaeoclimatology, Palaeoecology. 215: 285-295.

Wang Shangyan, Yin Hongfu, 2002. Characteristics of claystone at the continental Permian-Triassic Boundary in the eastern Yunnan-Western Guizhou region, Geology of China, 29 (2): 155-160.

Wu Shunbao, Ren Yingxing, Bi Xianmei, 1990. Volcanic Material and Origin of Clay Rock Near the Permian-Triassic Boundary from Huangshi, Hubei and Meishan of Changxing, Zhejiang. Earth Science –Journal of China University of Geosciences, 15(6): 589-595.

Yang Zunyi,Wu Shunbao,Yin Hongfu et al., 1991. Permo-Triassic Events of South China. Geological Publishing House, Beijing.

Yin Hongfu (ed.), 1996. The Palaeozoic-Mesozoic Boundary-Candidates of Global Stratotype Section and Point of the Permian-Triassic Boundary. China University of Geosciences Press, Wuhan. 135pp.

Yin Hongfu, Huang Siji, Zhang Kexing et al., 1989. Volcanism at the Permian-Triassic boundary in South China and its effects on mass extinction. Acta Geological Sinica, 63(2): 167-181.

Yin Hongfu, Zhang Kexin, Tong Jinnan et al., 2001. The Global Stratotype Section and Point (GSSP) of the Permian-Triassic boundary. Episodes, 24(2): 102-114.

Zhang Suxin, Peng Yuanqiao, Yu Jianxin et al., 2004a. Claystones of the Permian-Triassic boundary of Chahe Section, Weining, western Guizhou Province, South China. Geological Science and Technology Information, 23(1): 21-26.

Zhang Suxin, Yu Jianxin, Yang Fengqing et al., 2004b. Study on claystones across the neritic, shore-based, alternating of sea and terrene Permian-Triassic boundary at area of eastern Yunnan and western Guizhou, South China. Journal of Mineralogy and Petrology, 24(4): 81-86.

Conodont Sequences and its Global Correlation of the Induan-Olenekian Boundary in West Pingdingshan Section, Chaohu, Anhui Province

Zhao Laishi[1], Mike Orchard[2] and Tong Jinnan[1]

[1] State Key Laboratory of Geological Processes and Mineral Resources, China University of Geosciences, Wuhan 430074, China

[2] Geological Survey of Canada, 101-605 Robson Street, Vancouver B. C., V6B 5J3, Canada

The conodont and ammonoid biostratigraphical sequences have been basically established (Ding, 1983, Tong et al., 2003, Zhao et al., 2003, 2004). The ammonoid fossils have received more studies (e.g. Guo and Xu, 1980; Guo, 1982a, 1982b; Tong et al., 2004a, 2004b). To confirm the FADs of some key taxa in the boundary interval strata, continuous stratigraphic column samples were collected across the Induan-Olenekian boundary at the West Pingdingshan Section to precisely identify the conodont sequence at the boundary interval strata. Bed 25 is 2.41m thick and subdivided into 33 subbeds; Bed 24 is 1.62m thick and subdivided into 22 subbeds; Bed 23 is 1.73m thick and subdivided into 14 subbeds at the West Pingdingshan section. Based on the detailed study of the conodont fauna sequence at the Induan-Olenekian boundary interval strata of the West Pingdingshan Section, the candian of the global stratotype section (Tong et al., 2003), two conodont zones are established. In ascending order they are as follows: (1) *Neospathodus dieneri* zone; (2) *Neospathodus waageni* zone. Furthermore, three conodont subzones have been recognized from the *Neospathodus dieneri* zone, in ascending order they are: (1) *Neospathodus dieneri* Morphotype 3 Subzone; (2) *Neospathodus dieneri* Morphotype 2 Subzone; (3) *Neospathodus dieneri* Morphotype 1 Subzone. In addition, the *Neospathodus waageni* zone is divided into three subzones in ascending order based on the first successive appearances of *N. waageni* n.subsp.A, *N. waageni* n.subsp.B, and *N. w. waageni*, the nominal subspecies of three successive subzones. The development of these subspecies involves a progressive morphological change in the configuration of the blade elements (basal margin-basal cavity-outline). These three subspecies clearly occur in succession at the section. The conodont biozones proposed here are well correlated with those conodont zones throughout the world (Table 1).

1. *Neospathodus dieneri* Zone is marked by the last occurrence of *N. kummeli* and the top by the first occurrence of *N. waageni* n.subsp.A. It contains common *N. dieneri*, *N. cristagalli*, *N. novaehollandiae*, *and N. kummeli* in association with the ammonoids *Lytophiceras*, *Gyronites*, *Kymatites* and the bivalves *Claraia griesbachi*, *Eumorphotis huancangensis*, and *E.* cf.*venetina*. The nominate species, however, ranges upward into the Smithian, where it is associated with *N. w. waageni* Sweet. This zone is divided into three subzones in ascending order: Subzone *Neospathodus dieneri* Type1 is defined by the last disappearance of the *N. kummeli*, and upper limit is marked by the first occurrence of the *N. dieneri* Type 2. Subzone *N. dieneri* Type 2 is marked by the first appearance of *N. dieneri* Type 2, and the upper limit is defined by the first occurrence of *N. dieneri* Type 3. Subzone *N. dieneri* Type 3 is marked by the first appearance of *N. dieneri* Type 3, and the top by the first occurrence of *N. waageni* n.subsp.A. The three morphotypes of *N. dieneri* appear successively, but all range upward into higher zones. At West Pingdingshan section, dominant type of this species change vertically. Specimens from Bed19, 20 are mainly *N. dieneri* Type 1. Specimens from Beds 21, 22, 23, 24 are mainly *N. dieneri* Type2 with a number of *N. dieneri* Type 1 and small numbers of *N. dieneri* Type 3; Specimens from Beds 25, 26, 27, 28, 29 are mainly *N. dieneri* Type 3 with abundant *Neospathodus* n. sp. D, and fewer *N. dieneri* Type 1 and *N. dieneri* Type 2.

The range chart shows *N. dieneri* in samples from 28.11m to 57.38m at the West Pingdingshan Section. The *N. dieneri* Zone corresponds to the strata interval from Bed 20 (sample C20-4) to Bed 24-15 (sample CP24-6-1) and

a 6.52m-thick interval from 38 samples. An additional 0.27m thick interval underlying Bed 23 (sample CP23-2) has been searched and proved barren, and is added to the thickness of *N. dieneri* Zone. Other authors have not differentiated specimens assigned to *N. dieneri* even though they vary greatly in morphology. Mainly the length of the cusp and adjacent denticle distinguishes the three morph types introduced here.

2. *Neospathodus waageni* zone is divided into three subzones in ascending order based on the first successive appearances of *N. waageni* n.subsp.A, *N. waageni* n.subsp.B, and *N. w. waageni*, the nominal subspecies of three successive subzones. The development of these subspecies involves a progressive morphological change in the configuration of the blade elements (basal margin-basal cavity-outline). These three subspecies clearly occur in succession at the section, thus they are taken as three subzones of the *N. waageni* Zone.

(1) The *N. waageni* n.subsp.A Subzone is defined by the first occurrence of *N. waageni* n.subsp.A, and the upper limit is marked by the first appearance of *N. waageni* n.subsp.B. The *N. waageni* n.subsp.A Subzone corresponds to the strata interval from Bed 24-16 (sample CP24-6-2) to Bed 24-19 (sample 6), that is a 0.28m-thick interval represented by 2 samples. This subzone is characterized by all the three morphotypes of *N. dieneri*, and rich ramiform elements; *N. waageni* n.subsp.A has a superficial resemblance to the *N. w. waageni* except for the basal margin, which is straight throughout. The specimens of *N. waageni* n.subsp.A were found from 10 samples ranging from throughout the subzones of *N. waageni.* The base of the *Flemingites* zone is 0.26m above the base of the *N. waageni* n.subsp.A.

(2) The lower boundary of the *N. waageni* n.subsp.B Subzone is marked by the first occurrence of *N. waageni* n.subsp.B, and the upper boundary of the subzone is defined by the first occurrence of *N. w. waageni* (the specimen of *N. w. waageni* is the holotype of *N. waageni*, originally described by Sweet, 1970). *N. waageni* n.subsp.B has a superficial resemblance to the *N. w. waageni*, but the former has an elongated blade element, rectangular in lateral view and with the basal margin is upturned posteriorly. The specimens of *N. waageni* n.subsp.B were found from 6 samples in the subzones of *N. waageni* n.subsp.B and *N. w. waageni*. The associated conodonts include abundant *N. dieneri* Type 1, *N. dieneri* Type 2, a few *N. dieneri* Type 3, *N.* n. sp. B, *Neospathodus* n. sp. E, *Neospathodus*n. n. sp. F, *N. waageni* n.subsp.A and abundant ramiform elements. *Neospathodus dieneri* Type 2 reached its peak abundance in this interval. The *N. waageni* n.subsp.B Subzone corresponds to the strata interval from Bed 24-20 (sample CP24-7) to Bed CP25-9 (sample CP25-2) and a 0.52m-thick interval represented by 12 samples. This *N. waageni* n.subsp.B Subzone is associated with ammonoids *Flemingites* sp., and *Euflemingites* sp. in four samples (number 14, C8, C7, CP24-8) from 40.08 to 41.15m. *Koninckites* sp. is recovered in a sample (C9) from 40.94 to 40.99m, *Paranorites* cf. *ovalis* was found in 3 samples from 40.89 to 41.04m, and *Pseudosageceras tsotengense* in a sample from 40.94 to 40.99m. The base of the *Flemingites – Euflemingites* zone is 0.03m above the base of the conodont *N. waageni* n.subsp.B.

(3) The base of *Neospathodus w.waageni* Subzone is determined by the first occurrence of *N. w. waageni* and the top marked by the first occurrence of *N.* n. sp. M; The *N. w. waageni* Subzone corresponds to the strata interval from Bed 25-10 (sample (CP25-2) to Bed 52-1 (sample CP52-2) and a 52.14m-thick interval from 69 samples. The *N.*

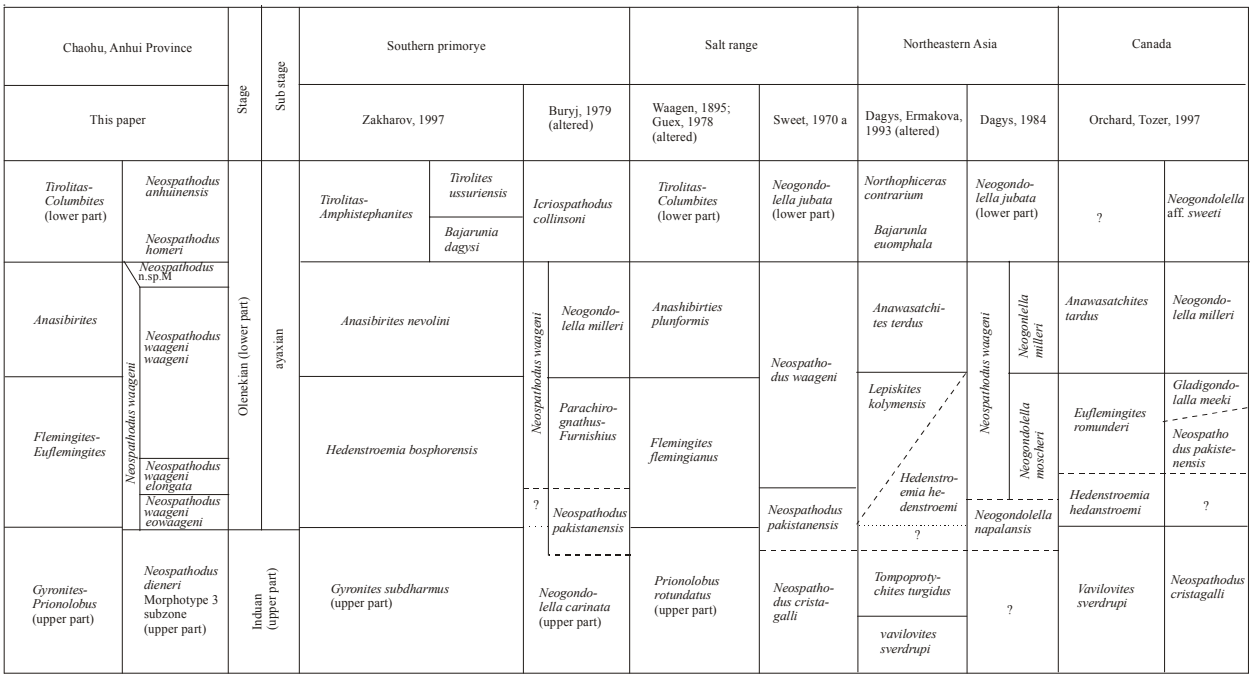

Table 1. Correlation of the upper Induan and lower Olenekian ammonoid and conodont zones in the Tethys and Boreal realms

w. waageni Subzone is characterized by the association with *N. waageni* n.subsp.A, *N. waageni* n.subsp.B, *N. w. waageni*, *N. cristagalli*, all the three morphotypes of *N. dieneri*, *N. spitiensis*, *N.* aff. *discretus*, *N. conservativus*, *N. novahollandiae*, *N. peculiaris*, *N.* n. sp. L, *N.* aff. *waageni*, *Platyvillosus costatus*, *Platyvillosus hamadai*, *Parachirognathus* sp., *Pachycladina* sp. , *Aduncodina unicosta*, and numerous ramiform elements. Zonal fossils and *N. dieneri* Type 3 and *N. cristagalli* reached their peak abundance in this interval. The specimens of *N. w. waageni* are fairly abundant and common The conodont *N.* n. sp L was found from the three samples (CP25-6, CP25-7, CP25-11) and reached its peak abundance from sample CP25-7 from 42.61 to 42.66m above the base of the Yinkeng Formation**.** Bony fishes were found in Bed 52 from 93.43m above the base of the Yinkeng Formation. The species of *Platyvillosus* were found in 8 samples from 42.38 to 43.3 m and reached their peak abundance in samples CP25-6, which is a rhyolitic clay.

The specimens of *N. conservativus* were recovered from 3 samples (CP25-13, CP26-1, CP26-4) but are not well preserved. The species is fairly common in the *Meekoceras* bed in Dinner Spring Canyon, Nevada (Muller, 1956), and the lower part of the Thaynes Formation, Utah (Solien, 1979). Subsequently the species was reported from the limestone in Kelantan, Malaya (Igo et al, 1965), the lower part of the Taho Limestone (Koike, 1979) and the lower part of the Kamura Limestone (Watanbe et al, 1979) in Japan, the Locker Shale of the Carnarvon Basin, western Australia (McTavish, 1973), Central Dolpo, Nepal (Nicora, 1991), and lower Smithian limestone in Kotal-e-Tela, Afghanistan (Matsuda, 1985). This form is known from Zone 7 and Zone 8 of the Smithian (Solien, 1979) and the marker of Zone 8 (Sweet et al., 1971). Well preserved specimens of *N. novaehollandiae* were found from 5 samples (32, CP25-7, CP25-10, CP25-11, CP25-13). This species is commonly found in Smithian strata in western Austria (McTavish, 1973), and Khar, Spiti (Geol, 1977). It is worthy of mention that the specimen of *Aduncodina unicosta* is found at Bed 31 and Bed 39 from 2 samples (CPX31, C39-2), about 57.88 to 75.93m above the base of the Yinkeng Formation,along with the ammonoid *Owenites* sp., *Koninckites* sp., and *Anasibirites kingianus*. Based on the associated ammonoids, we are of the opinion that the age of *Aduncodina unicosta* is upper Smithian, older than its previously supposed age of Spathian (Koike, 1996). In Chaohu section, some specimens resembling *N. cristagalli* first occur at the base of the *N. w. waageni* subzone, but they differ from the holotype material described by Sweet (1970) from Salt Range and Kashmir by possessing entirely discrete denticles. In Chaohu, the associated ammonoids *Flemingites* sp., and *Euflemingites* sp., were recognized in 2 samples from 41.31 to 41.51m, *Flemingites* cf. *ellipticus* and *Koninckites lolowensis*, from 43.9 to 43.94m, *Preflorienites* cf. *strongi* from 41.31 to 41.41m, *Paranorites* cf. *ovalis* from 42.38 to 42.48m, *Pseudosageceras tstoengense*, *Xenodiscoides* sp., and *Owenites* sp., from 41.41 to 41.51m. *Owenites pakungensis*, *Arctoceras* aff. *lolouensis*, and *Pseoudoceltites* sp., from 62.89m. *Wasachite*s sp., *Hemiprionites* sp., *Juvenites orientalis*, from 68.38m. *Dieneroceras* sp., from beds 36 to 40. *Anassibirites* cf. *kwangstana* was found in bed 51.

Acknowledgments: The work was made under the financial support of the National Natural Science Foundation of China (Nos. 40325004, 4023025), the ministry of education (No. 03033), the Chinese "973 Program" (No. G2000077705), the State Key Laboratory of Geological Processes and Mineral Resources (MGMR2002-22), and the Geological Survey of Canada Project GK4700.

Bhatt, D. K., Joshi, V. K., Arora, R. K., 1999. Conodont biostratigraphy of the Lower Triassic in Spiti Himalaya, India. Journal Geological Society of India, 54: 153-167.

Buryi, G. L., 1979. Lower Triassic Conodonts of South Primorye. Moskva, Nauka, 143: 1-21.

Dagys, A. S., Kazakov, A. M., 1984. Stratigraphy, Lithology and Cyclic of Triassic Sediments in the North Middle Siberia. Moskva: Nauka. 177 (in Russian).

Ding Meihua, 1983. Lower Triassic conodonts from the Mountain Majiashan in Anhui Province and their stratigraphic significance. Earth Science—Journal of Wuhan College of Geology, (2):37-48 (in Chinese with English abstract).

Guo Peixia, 1982. On the occurrence of late Lower Triassic ammonoids from Anhui and Jiangsu. Acta Palaeontologica Sinica, 21(5): 560-568. (in Chinese with English abstract).

Guo Peixia, Xu Jiacong, 1980. Knowledge on the age of the Qinglong Group in Chaoxian, Anhui Province. Journal of Stratigraphy, 4(4): 310-315 (in Chinese).

Koike, T., 1982. Triassic conodont biostratigraphy in Kedah, West Malaysia. Geol. Paleont. Southeast Asia, 23: 9-51.

Matsuda, T., 1982. Early Triassic conodonts from Kashmir, India. Part II: *Neospathodus* 1. Jour. Geosci. Osaka City Univ., 25: 87-102.

Mosher, L. C., 1973. Triassic conodonts from British Columbia and the Northern Islands. Geol. Surv. Canada, Bull., 222: 141-193.

Nicora, A., 1992. Conodonts from the Lower Triassic sequence of Central Dolpo, Nepal. Riv. It. Paleont. Strat., 97: 239-268.

Orchard, M. J., 1995. Taxonomy and correlation of Lower Triassic (Spathian) segminate conodonts from Oman and revision of some species of *Neospathodus*. J. Paleont., 69: 110-122

Orchard, M. J., Krystyn, L., 1998. Conodonts of the lowermost Triassic of Spiti, and new zonation based on *Neogondolella* successions. Revista Italiana di Paleontologia e Strstigrafia, 104 (3): 341-368.

Orchard, M. J., Nassichuk, W. W., Rui Lin, 1994. Conodonts from the Lower Griesbachian Otoceras latilobatum bed of Selong, Tibet and the position of the Permian-Triassic boundary. Canadian Society of Petroleum Geologists, Memoir, 17: 823-843

Orchard, M. J., Tozer, E. T., 1997. Triassic conodont biochronology, its calibration with the ammonoid standard, and a biostratigraphic summary for the western Canada sedimentary basin. Bull Can Petrol Geol, 45: 675-692.

Sweet, W. C., 1970a. Uppermost Permian and Lower Triassic conodonts of the Salt Range and Trans-Indus Ranges, West Pakistan. *in* Kummel, B., Teichert, C. (eds.) Stratigraphic boundary problems: Permian and Triassic of West Pakistan. Univ. Kansas, Dept. Geol. Spec. Publ., 4: 207-275.

Sweet, W. C., 1970b. Permian and Triassic conodonts from a section at Guryul Ravine, Vihi District, Kashmir. Univ. Kansas Paleont., Contr., Paper, 49: 1-11.

Sweet, W. C., Mosherm, L. C., Clark, D. L. et al., 1971. Conodont biostratigraphy of the Triassic. *in* Sweet, W. C., Bergstroem, S. M. (eds.) Symposium on Conodont Biostratigraphy. GSA Memoir, 127: 441-465.

Tong Jinnan, Zakharov, Y. D., Orchard, M. J., Yin Hongfu, Hansen, H. J., 2003. A candidate of the Induan-Olenekian boundary stratotype in the Tethyan region. Science in China (Series D), 46(11): 1182-1200.

Tong Jinnan, Zakharov, Y. D., Wu Shunbao, 2004a. Early Triassic ammonoid succession in Chaohu, Anhui Province. Acta Palaeontologica Sinica, 43(2): 192-204.

Tong Jinnan, Zakharov, Y. D., 2004b. Lower Triassic ammonoid zonation in Chaohu, Anhui Province, China. Albertiana.

Wang, C. Y., Wang, Z. H., 1976. Triassic conodonts from the Mount Julmo Lungma Region. In: A report of Scientific Expedition in the Mount Jolmo Lungma Region 1966-1968, Paleontology Fasc. 2: 387-424, Science Press, Beijing (in Chinese).

Yin Hongfu, Wu Shunbao, Du Yuanshen, Peng Yuanqiao, 1999. South China defined as part of Tethyan archipelagic ocean system. Earth Science — Journal of China University of Geosciences, 24: 1-12 (in Chinese).

Yin Hongfu, Zhang Kexin, Tong Jinnan, Yang Zunyi, Wu Shunbao, 2001. The Global Stratotype Section and Point (GSSP) of the Permian-Triassic boundary. Episodes, 24(2): 102-114.

Zakharov, Y. D,. 1996. The Induan-Olenekian boundary in the Tethys and Boreal realm. Ann Mus Civ Rovereto Sec Arch St Sc Nat, 11(Suppl): 133-156.

Zakharov, Y. D., 1997. Ammonoid evolution and the problem of the stage and substage division of the Lower Triassic. Mem. Geologie (Lausanne), 30: 121-136.

Zakharov, Y. D., Shigeta, Y., Popov, A. M., Buryi, G. I., Oleinikov, A. V., Era, A., 2002. Triassic Ammonoid Succession in South Primorye: 1 Lower Olenekian *Hedenstroemia Bosphorensis* and *Anasibirites Nevolini* Zones. Albertiana 27: 42-64.

Zhao Laishi**,** Orchard, M. J., Tong Jinnan, 2004. Lower Triassic conodont biostratigraphy and speciation of *Neospathodus waageni* around the Induan-Olenekian boundary of Chaohu, Anhui Province, China. Albertiana, 29: 41-43

Zhao Laishi, Tong Jinnan, Orchard, M. J., 2003. Morphological variation of the conodonts *Platyvillosus* from the Yinkeng Formation in Chaohu, Anhui Province, China. Journal of China University of Geosciences, 19(4): 358-366.

Zhao Laishi, Tong Jinnan, Zuo Jingxun, et al., 2002. Discussion on the Induan-Olenekian boundary in Chaohu, Anhui Province, China. Journal of China University of Geosciences, 13(2): 141-150.

An Intercalibrated Biostratigraphy of the Uppermost Permian and Lower Triassic of the Guimenguan Section, South Chaohu, Anhui Province

Zhao Laishi[1*], Tong Jinnan[1], Mike Orchard[2], Chen Bing[1] and Huang Xiaogang[1]

[1] State Key Laboratory of Geological Processes and Mineral Resources, China University of Geosciences, Wuhan 430074, China; [*]lszhao@cug.edu.cn

[2] Geological Survey of Canada, 101-605 Robson Street, Vancouver B. C., V6B 5J3, Canada

Through detailed field and laboratory investigations of the well developed and abundantly fossiliferous Upper Permian and Lower Triassic of the Guimenguan section, South Chaohu, Anhui province, five conodont zones, five ammonoid zones and three bivalve assemblages zones were recognized and their mutual correlation is made.

1. Lithostratigraphy

In the Guimenguan section, strata from the Permian-Triassic boundary to the Induan-Olenekian boundary are continuously exposed and easily studied. The latest Permian Dalong Formation is overlain in ascending order by the Lower Triassic Yinkeng, Helongshan and Nanlinghu formations. Their features are as follows.

1.1 Dalong Formation: Lithologically, this Formation is dominated by, siliceous mudstones intercalated with marls, which are coeval with the Changhsing Formation but in different facies. The thickness is about 32.7 m and contains ammonites *Pleuronodoceras attenuatum*, *Pleuronodoceras* sp., *Pseudogastrioceras* sp., *Sinoceltites* sp.; brachiopods *Neochonetes convexa, Neochonetes* sp., *Cathaysia chonetoids* and conodonts, Clarkina *changxingensis* and *C. deflecta*. Dalong Formation contacts underlying Longtan Formation and overlying Yinkeng Formation with conformity. Although the index conodont *Hindeodus parvus* has been found at the Guimenguan section, the Permian - Triassic boundary can be definitely defined through the correlation of the "lithologic boundary sequence" with the Meishan section (Peng and Tong, 1999).

1.2 Yinkeng Formation: The lower part of the Yinkeng

Formation is composed of grayish green, thin-bedded calcareous mudstone, a few interbeds of thin-bedded argillaceous mudstone, and gray thin-bedded argillaceous limestone. The middle part is gray thin-bedded nodular argillaceous limestone. The upper part is grayish green-brown medium-bedded nodular calcareous limestone, intercalated by a few beds of gray thin-bedded lenticular argillaceous limestone, about 63.05 m thick. These beds yield such Induan and Olenekian ammonoids as *Ophiceras demissum*, *Ophiceras* sp., *Prionolobus* sp., *Paranorites* cf. *ovalis*, *Dieneroceras* sp., *Flemingites muthensis, Flemingites* sp., *Paranotites* sp., *Lytophiceras*, together with various species of *Claraia*, such as *Claraia stachei*, *C. griesbachi, C. concentrica, C. pingxiangensis*, as well as *Eumorphotis inaequicostata*, *Bakevellia* sp., *Guichiella angulata* and *Guichiella styliformis* in association with abundant conodonts, such as *Hindeodus typicalis*, *Neogondolella planata*, *Neospathodus dieneri*, *N. cristagalli*, *N. waageni*, and *Platyvillosus costatus*.

1.3 Helongshan Formation: The lower part of the Helongshan Formation is composed of intercalated grayish brown shale and argillaceous limestone, the upper part of this formation is grayish green thin-bedded nodular limestone, intercalated by grayish brown argillaceous mudstone, altogether about 74.45m thick. It contains ammonoids such as *Dieneroceras* sp., *D.* cf. *pakungense*, *Flemingites* sp., etc., together with conodonts such as *Neospathodus dieneri*, *N. cristagalli*, *N. waageni*, etc., in association with bivalves *Posidonia* sp., *Guichiella* sp.

1.4 Nanlinghu Formation: The lower part of the Nanlinghu Formation is composed of grayish green thick-bedded limestone, intercalated by a few beds of gray thin-bedded argillaceous mudstone and black shale. The middle part of this formation is grayish green thick-bedded limestone, intercalated by a few beds of gray medium-bedded argillaceous limestone and grayish green shale. The upper part of the formation is gray medium-bedded vermiculate limestone, intercalated by a few beds of gray shale, altogether about 326 m thick. It contains conodonts such as *Neospathodus homeri* and *N. brevissimus.*

2. Biostratigraphy

The fossils in this section are abundant, and most were found in Yinkeng Formation and Helongshan Formation. There are brachiopods, bivalves, ammonoids and conodonts. These fossils are very important in dividing and correlating the strata, and reconstructing the palaeo-environment and palaeogeography.

2.1 Ammonoids: 17 species (including species indeterminate) of 10 genera of ammonoids were found in this section, lying in 17 horizons. The ammonoids of the late Permian are few, only 4 genera, namely *Pseudogastrioceras*, *Laibinnoceras*, *Sinoceltites*, *Pleuronodoceras*. The fossils are badly broken, only *Pleuronodoceras* can be identified to species (*Pleuronodoceras attenuatum*). The Lower Triassic ammonoids are more common but are preserved as mold without shells. The ammonoid assemblage is typical and similar to that of the platform in South China. Five ammonoid zones are recognized from the upper Permian to lower Olenekian, they are *Pleuronodoceras* zone, *Ophiceras-Lytophiceras* zone, *Prionolobus* zone, *Flemingites* zone, and *Anasibirites* zone. The ammonoid biozones proposed here are well correlated with those erected by Guo (1982) and Tong and Zakaharov (2004), and are directly correlated with conodont and bivalve zones of the same section.

2.2 Conodonts: 36 species (including species indeterminate) assigned to 13 genera of conodonts were found in this section, which appeared in 21 horizons. The conodonts are abundant and well preserved. The conodont zonation of the Upper Permian *Neogondolella changxingensis-Ng. deflecta* Zone is similar to that at the Meishan section where Zhang et al. (1995) divided the *changxingensis-deflcta* Zone into three faunas on the basis of the range of *Neogondolella subcarinata, Ng. meishanensis* and *Ng. deflecta*. However, this subdivision is not recognized in this section. The conodonts in the Lower Triassic are quite abundant, four conodont zones are recognized: *Neogondolella krystyni-Neogondolella planata* zone, *Neospathodus dieneri* zone, *Neospathodus waageni* zone and *Neospathodus homeri* zone. Three morphotypes of *Neospathodus dieneri* can be recognized, *Neospathodus waageni* zone includes the elements of *N. waageni* n.subsp.A and *N. waageni* n.subsp. B. The samples were collected with an average sampling interval of 2-3 m. The zones of *N. kummeli* and *N.* n. sp. M were not found. The conodont biozones proposed here are well correlated with those erected by Zhao et al. (2004), and are directly correlated with ammonoid and bivalve zones of the same section.

2.3 Bivalves: 13 species (including species indeterminate) in 6 genera of bivalves were found in this section, lying in 19 horizons, mostly in argillaceous mudstone. The bivalves contained in this section are similar with those of the other places in South China. *Claraia* is the most abundant. These bivalve zones were found in ascending order: *Claraia griesbachi-Claraia concentrica* zone, *Eumorphotis inaequicostata* zone, and *Guichiella angulata* zone. The bivalve biozones proposed here are well correlated with those erected by Tong and Zakharov (2004).

Acknowledgments: The work was made under the financial support of the National Natural Science Foundation of China (Nos. 40325004, 4023025), the Ministry of Education (No. 03033), the Chinese "973 Program" (No. G2000077705), the State Key Laboratory of Geological Processes and Mineral Resources (MGMR2002-22), and the Geological Survey of Canada Project GK4700.

Guo Peixia, Xu Jiacong, 1980. Knowledge on the age of the Qinglong Group in Chaoxian, Anhui Province. Journal of Stratigraphy, 4(4): 310-315.

Orchard, M. J., 1995. Taxonomy and correlation of Lower

Triassic (Spathian) segminate conodonts from Oman and revision of some species of *Neospathodus*. J. Paleont, 69: 110-122

Orchard, M. J., Krystyn, L., 1998. Conodonts of the lowermost Triassic of Spiti, and new zonation based on *Neogondolella* successions. Revista Italiana di Paleontologia e Strstigrafia. 104 (3): 341-368

Peng Yuanqiao, Tong Jinnan, 1999. Integrated study on the Boundary Bed of the Permian-Triassic boundary in Yangtze platform. Earth Sciences- Journal of China University of Geosciences, 24(1): 39-48.

Sweet, W. C., 1970a. Uppermost Permian and Lower Triassic conodonts of the Salt Range and Trans-Indus Ranges, West Pakistan. *in* Kummel, B., Teichert, C. (eds.) Stratigraphic boundary problems: Permian and Triassic of West Pakistan. Univ. Kansas, Dept. Geol. Spec. Publ., 4: 207-275.

Tong Jinnan, Zakharov, Y. D., Wu Shunbao, 2004. Early Triassic ammonoid succession in Chaohu, Anhui Province. Acta Palaeontologica Sinica, 43(2): 192-204.

Tong Jinnan, Zakharov, Y. D., Orchard, M. J., Yin Hongfu, Hansen, H. J., 2003. A candidate of the Induan-Olenekian boundary stratotype in the Tethyan region. Science in China (Series D), 46(11): 1182-1200.

Yin Hongfu, Zhang Kexin, Tong Jinnan, Yang Zunyi, Wu Shunbao, 2001. The Global Stratotype Section and Point (GSSP) of the Permian-Triassic boundary. Episodes, 24(2): 102-114

Zakharov, Y. D., Shigeta, Y., Popov, A. M., Buryi, G. I., Oleinikov, A. V., Era, A., 2002. Triassic Ammonoid Succession in South Primorye: 1 Lower Olenekian *Hedenstroemia Bosphorensis* and *Anasibirites Nevolini* Zones. Albertiana 27: 42-64.

Zhang Kexin, Lai Xulong, Ding Meihua et al., 1995. Conodont sequence and its global correlation of Permian-Triassic boundary in Meishan Section, Changxing, Zhejiang Province. Earth Sciences- Journal of China University of Geosciences, 20(6): 670-676.

Zhao Laishi**,** Orchard, M. J., Tong Jinnan, 2004. Lower Triassic conodont biostratigraphy and speciation of *Neospathodus waageni* around the Induan-Olenekian boundary of Chaohu, Anhui Province, China. Albertiana, 29: 41-43.

Zhao Laishi, Tong Jinnan, Zuo Jingxun et al., 2002. Discussion on the Induan-Olenekian boundary in Chaohu, Anhui Province, China. Journal of China University of Geosciences, 13(2): 141-150.

Zhao Laishi, Tong Jinnan, Zuo Jingxun, 2003. Lower Triassic conodonts of West Pingdingshan Section in at Chaohu, Anhui Province, China. Journal of China University of Geosciences, 28(3): 414-418.

Conodonts from the Lower Triassic in the Nantuowan Section of Daxiakou, Xingshan Country, Hubei Province

Zhao Laishi[1], Xiong Xinqi[2,] Yang Fengqing[3,] Wang Zhiping[3], and He Weihong[3]

[1] State Key Laboratory of Geological Processes and Mineral Resources, China University of Geosciences, Wuhan 430074, China; lszhao@cug.edu.cn

[2] China University of Geosciences Museum, Wuhan 430074, China

[3] Faculty of Earth Sciences, China University of Geosciences, Wuhan 430074, China

Introduction

The Lower Triassic in the Three Gorges on the Yangtze Block is mainly composed of carbonate rocks and argillaceous components, yielding rich fossils and relatively complete biostratigraphical sequences. It is one of the classic Lower Triassic sequences in South China and received considerable studies in early years (Chen et al., 1979; Feng et al; 1984; Zhang et al., 1979, 1987; Wang et al., 2002). The conodont biostratigraphy has, however, poorly been described because of a limited number of conodonts recovered, a limited number of conodonts- bearing horizons studied, and samples often from scattered localities. To better understand the detailed sequence and the biota marker of *Neospathodus waageni* as the index for the basal Olenekian in West Pingdingshan section, which is proposed as the candidate of the Induan-Olenekian boundary stratotype, with a various paleogeographical distribution, several sections, including Permian-Triassic boundary to the Induan-Olenekian boundary, are investigated in the Three Gorges.

We examined some well-exposed Lower Triassic sections in the area, which were excavated by road building. The Permian-Triassic boundary beds and Lower Triassic at the Nantuowan Section of Daxiakou, Xingshan Country, 70 km away from Northwest Yichang city, Hubei Province, has been studied here. The latest Permian is the Baoan Formation. The Lower Triassic is subdivided into two formations: Daye Formation and Jialingjiang Formation. Preliminary study shows that the Daye Formation at the Nantuowan Section contains not only all the Induan-Olenekian boundary conodont zones found in Chaohu, but also the lowest conodont zone of the Induan.

More than 1200 conodont elements have been recovered from the Permian-Triassic boundary up to the Induan-Olenekian boundary samples collected by Chinese Lower Triassic Working Group from the Nantuowan Section. All the conodonts are well preserved with high diversity. Especially conodonts from the lower Induan include the *Neogondolella* pectiniform (45%) elements with specimens of *Hindeodus-Isarcicella* (40%) and fewer ramiform elements (<15%). The *Neogondolella* elements gradually increase in quantity from the bottom to upper part. Paleoecological controls on the P-T boundary conodont distri-

bution have been discussed by Kozur (1996), who suggested very specific controls to explain observed anomalies. Orchard (1996) pointed out that, in general, the relative abundances of *Hindeodus* and *Neogondolella* varied in an onshore-off-shore relationship, with the former more common in shallower water habitats. Conodont faunas of the section yielding *Neogondolella* and *Hindeodus-Isarcicella-Neospathodus* indicate a deeper carbonate ramp area.

Conodont successions

In the Nantuowan Section, the samples were collected from beds 11-121, with an average sampling interval of 0.5m and 1m above 121, continuous stratigraphic column samples were collected across the Induan-Olenekian boundary. Each sample weighed 1kg, crushed and disaggregated by applying a 10% to 12% solution acetic acid treatment for removal of carbonates, a few fish teeth were also encountered in the residues. 70% of the rock samples produced conodonts. The conodonts biostratigraphy is based on the most abundant elements, which are also *Neogondolella* and *Hindeodus-Isarcicella-Neospathodus*. Their ranges and evolution in the Daye Formation define 6 conodont zones, based on the first occurrences of the nominal species. These zones are briefly described in the ascending order as follows:

1. *Hindeodu parvus* zone: This zone *ranges* from bed 11c to the top of bed 38. The associated conodonts are *H. praeparvus, H. typicalis*, *H. latidentus, Neogondolella tulongensis, Ng. orchardi*, *Ng. changxingensis*, *Ng. carinata*, *Ng. planata*, *Ellisonia* sp., and ramiforms.

2. *Neogondolella krystyni* zone: This zone ranges from the base of bed 39 to the top of the bed 61. The associated conodonts are *H. praeparvus*, *H. parvus*, *H. typicalis*, *H. latidentus, H. anterodentatus, Ng. orchardi*, *Ng. tylorae*, *Ng. tulongensis*, *Ng. carinata*, *Ng. planata*, *Isarcicella* sp., *Ellisonia* sp., and ramiforms.

3. *Neogondolella discreta* zone: This zone ranges from the base of bed 62 to the top of the bed 66. The associated conodonts are *Ng. carinata*, *Ng. Planata, Ng. tulongensis , Ellisonia* sp., and ramiforms.

4. *Neospathodus kummeli* zone: This zone ranges from the base of bed 67 to the top of the bed 68b. The associated conodonts are *Ng. carinata, Ellisonia* sp., and ramiforms.

5. *Neospathodus dieneri* zone: This zone ranges from the base of bed 68c to the top of the bed 85c. This zone is divided into three subzones in ascending order, subzone *Neospathodus dieneri* Type1, subzone *Neospathodus dieneri* Type2, subzone *Neospathodus dieneri* Type3. The associated conodonts are *Neospathodus dieneri*, *N.novaehollandiae*, *N. cristagalli*, *N.* sp. B (nov.), *Ellisonia* sp., and ramiforms.

6. *Neospathodus waageni* zone: This zone ranges from the base of bed 86a to possible top of the bed 104. But top range has not yet been determined. This zone is divided into three subzones in ascending order, subzone *Neospathodus waageni eowaageni,* subzone *Neospathodus waageni elongata*, subzone *Neospathodus waageni waageni*. The associated conodonts are *N. dieneri* Type 1, *N. dieneri* Type 2, *N. dieneri* Type 3, *N. novaehollandiae, N. cristagalli, N.* sp. L (nov.), *N.* aff. *waageni*, *Pltyvillosus costatus, Pl. hamadai, Parachirognathus sp., Ellisonia* sp., and ramiforms.

The marked changeover in faunas from those dominated by *N. dieneri* Type 3 in the *Neospathodus dieneri* zone to those dominated by *N. waageni eowaageni* appears to dictate the best horizon for drawing the Induan- Olenekian boundary in accordance with high diversity.

Summary

Abundant conodonts have been recovered from the lowermost Triassic up to Induan-Olenekian boundary at Nantuowan Section of Daxiakou, Xingshan Country. The first appearance of *Hindeodu parvus* may serve in P-T boundary definition. Two new *Neogondolella*-based zones are differentiated, *Neogondolella krystyni* zone and *Neogondolella discreta* zone, which are equivalent to those defined by Orchard and Krystyn (1998) in Spiti. Other zones here have been reported at the Chaohu sections and these conodont biozones proposed are well correlated with those erected by Zhao et al. (2004).

Acknowledgments: The work was made under the financial support of the National Natural Science Foundation of China (Nos. 40325004, 4023025), the Ministry of Education (No.03033), the Chinese “973 Program”(No. G2000077705), the State Key Laboratory of Geological Processes and Mineral Resources (MGMR2002-22).

Chen Chuzheng, Lin Wenben et al., 1979. Triassic System of Southwest, China, Science Press, Beijing, 289-336.

Feng Shaonan, Xu Shouyong, Lin Jiaxin et al., 1984. Biostratigraphy of the Yangtze Gorges Ares (3), Late Paleozoic Era. Geological Publishing House, Beijing, 1-109.

Kozur, K. 1996. The conodonts *Hindeodus-Isarcicella* and Sweetohindeodus in the Uppermost Permian and Lowermost Triassic. Geol. Croat., 49(1): 81-115.

Orchard, M. J., 1996. Conodont fauna from the Permian-Triassic boundary: observations and reservations. Permophiles. 28: 36-39.

Orchard, M. J., Krystyn, L., 1998. Conodonts of the lowermost Triassic of Spiti, and new zonation based on *Neogondolella* successions. Revista Italiana di Paleontologia e Strstigrafia. 104 (3): 341-368

Tong Jinnan, Zakharov, Y. D., Orchard, M. J., Yin Hongfu, Hansen, H. J., 2003. A candidate of the Induan-Olenekian boundary stratotype in the Tethyan region. Science in China (Series D), 46(11): 1182-1200.

Wang Xiaofeng, Chen Xiaohong et al., 2002. Protection of Precise Geological Remains in the Yangtze Georges Area, China with the study of the Archean-Mesozoic Multiple Stratigraphic Subdivision and Sea-Level Chang. Geological Publishing House, Beijing, 231-291.

Zhang Zhenlai, Meng Fansong et al., 1987. Biostratigraphy of the Yangtze Gorges Ares (4), Triassic and Juras-

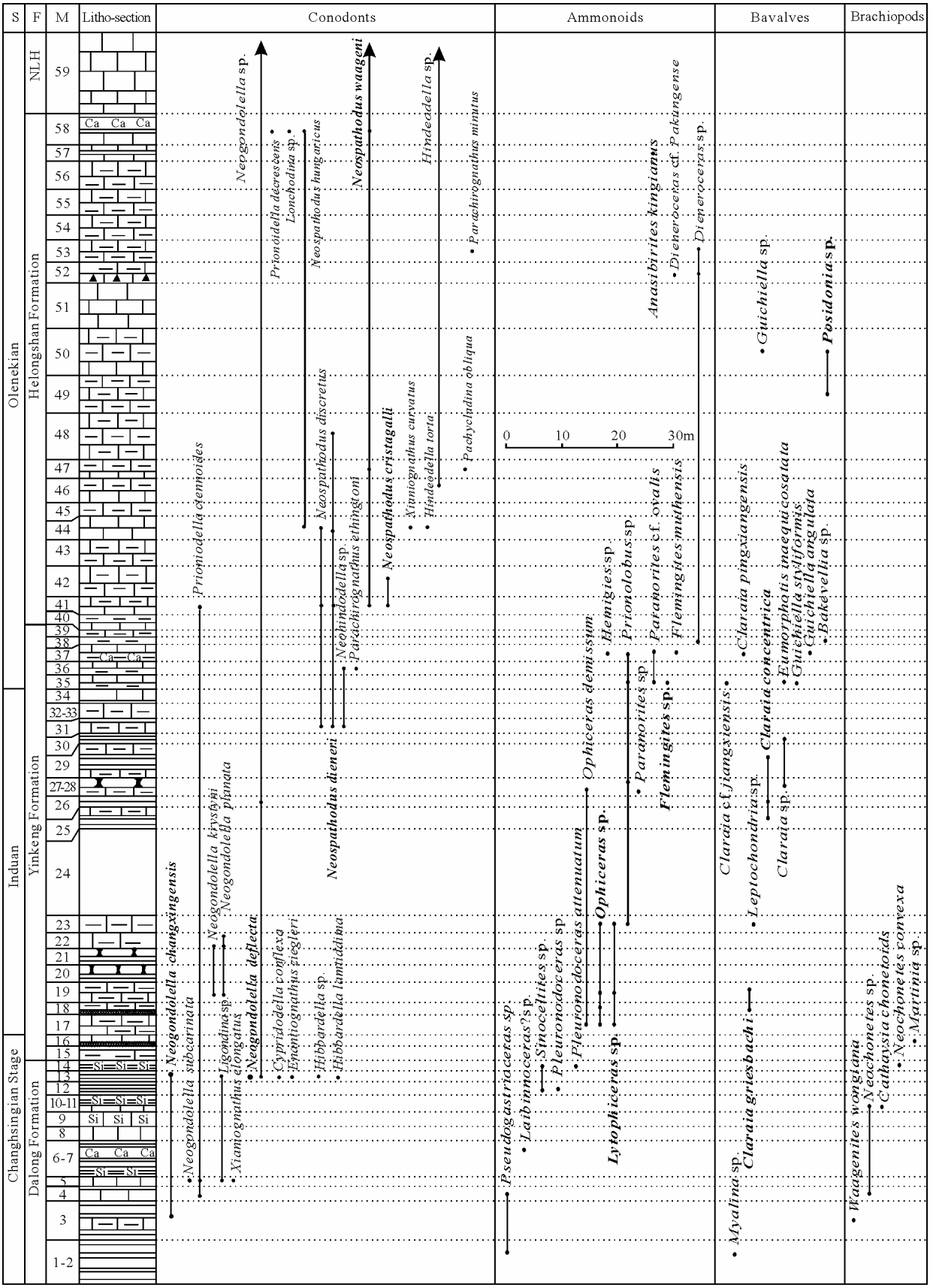

S, Stage; F, Formation; M, Member; NLH, Nanlinghu Formation.

Figure 1. Stratigraphic column and fossil distribution around the Permian-Triassic and the Induan-Olenekian boundary at Guimengguan Section.

Subcommission on Triassic Stratigraphy

STS Chairman

Dr. Mike Orchard, Geological Survey of Canada, 101-605 Robson Street, Vancouver, British Columbia, Canada.

Vice Chairman

Dr. Marco Balini Professore associato, Paleontology Dipartimento di Scienze della Terra "Ardito Desio" Universita' degli Studi di Milano Via Mangiagalli 34, 20133 Milano, Italy

Vice Chairman

Dr. Ying Hongfu, Office of the President, China University of Geosciences, Yujiashan, Wuhan, Hubei, 430074, People's Republic of China

STS Secretary General

Dr Chris McRoberts Department of Geology State University of New York at Cortland P.O. Box 2000 Cortland, New York 13045 USA

ALBERTIANA is published twice a year by the Subcommission on Triassic Stratigraphy. Individuals can obtain ALBERTIANA for the sum of US $ 20,- or EURO 20,- per year. Readers are kindly requested to pay their annual contribution timely.
European readers can send a Eurocheque made payable in Euro to Dr. Zwier Smeenk, Laboratory of Palaeobotany and Palynology, Utrecht University, Budapestlaan 4, 3584 CD Utrecht, The Netherlands. Everyone else is kindly requested to send cash in a closed non-transparent envelope to the above Utrecht adress. Because of the high provision costs of other cheques/currencies, other methods of payment cannot be accepted. Institutions can receive ALBERTIANA on an exchange basis.

All correspondence regarding the distribution of ALBERTIANA should be sent to Dr. Z. Smeenk.